

A SEQUENTIAL APPROACH OF SOLVING
SECOND ORDER AC-DC LOAD FLOW AND
STATE ESTIMATION PROBLEM



*A thesis submitted in fulfilment of
the requirements for the degree of*

DOCTOR OF PHILOSOPHY



by
Md. Zahidul Haque
B.Sc., M.Sc. Engg. (Electrical & Electronic)

in the
Department of Electrical and Electronic Engineering
Faculty of Engineering
Victoria University of Technology
Australia, October 1996.

FTS THESIS

621.31915 HAQ

30001005050655

Haque, Md. Zahidul

A sequential approach of
solving second order AC-DC
load flow and state

*Dedicated to my
Parents*



Late Md. Shamsul Haque and Mrs. Ranu Begum

Declaration

I hereby declare that the following thesis entitled, “**A Sequential Approach of Solving Second Order AC-DC Load Flow and State Estimation Problem**”, which is being submitted by myself, in fulfilment of the requirements for the award of the Degree of Doctor of Philosophy in Electrical and Electronic Engineering, Victoria University of Technology, Australia. The matter embodied in this thesis has not been submitted in part or full to any other University or Institute for award of any degree.

(Md. Zahidul Haque)

Acknowledgements

The author wishes to express his heartfelt gratitude and sincere thanks to his principal supervisor, Dr. A. Kalam, Associate Professor of the Department of Electrical and Electronic Engineering, Victoria University of Technology, Australia, for his kind guidance, invaluable support, constant encouragement and supervision throughout the course of this research.

The author would like to express his gratitude to his co-supervisor Dr. Qin Jiang for her support during this research.

The author is profoundly grateful to Associate Professor Wally Evans, Head of the Department of Electrical and Electronic Engineering for providing me with the necessary facilities in order to successfully complete this research.

The author would like to express his sincere gratitude to Mr. Richard Jacewicz, System Support Engineer, the Department of Computer and Mathematical Science, VUT for his help and kind permission for the use of Cyber where some computations were performed.

The author is thankful to the people who have helped him directly or indirectly during the course of study.

It is a distinct pleasure for the author to acknowledge and his heartfelt gratitude to his wife Shafia Firoja Haque for her moral support, inspiration, patience and bearing with him in the moments of frustration. The author is

also grateful to his daughter Zakia Haque and son Shafiul Haque for the time they had to miss their father.

Finally the author would express his thanks to all staff member in the Department of Electrical and Electronic Engineering for their help and assistance.

1.3.1	Characteristics of second order and decoupled second order algorithms13
1.3.2	Characteristics of the proposed methods in comparison with FDLF method15
1.4	AC-DC power system state estimation16
1.4.1	Definition16
1.4.2	Review of ac-dc state estimation16
1.4.3	Limitations of WLS and FD estimators and scope of further investigation20
1.4.4	Characteristics of the proposed method21
1.5	Scope and objective22
1.6	Originality of the thesis23
1.7	Development of thesis24

PART - I Load Flow

CHAPTER 2: INTEGRATED AC-DC LOAD FLOW IN RECTANGULAR CO-ORDINATES

2.1	Introduction29
2.2	Development of mathematical model30
2.2.1	DC converter model30
2.2.2	Mathematical model for rectangular co-ordinates32
2.2.3	AC network model37
2.3	First order ac-dc load flow method38
2.3.1	Mathematical model39
2.3.2	Solution steps42
2.4	Conclusions43

CHAPTER 3: SECOND AND DECOUPLED SECOND ORDER AC-DC LOAD FLOW IN RECTANGULAR CO-ORDINATES

3.1	Introduction	46
3.2	second order ac-dc load flow method	49
3.2.1	Mathematical model	50
3.2.2	Salient features of SRLF algorithm	54
3.2.3	Solution steps	55
3.3	Decoupled second order ac-dc load flow method	57
3.3.1	Mathematical model	59
3.3.2	Distinguishing features of the DSRLF algorithm	62
3.3.3	Solution steps	63
3.4	Conclusions	65

CHAPTER 4: SIMULATION STUDIES

4.1	Introduction	67
4.2	Parameters selection	68
4.2.1	Initialisation	68
4.3	Modification of standard test systems (load flow)	69
4.4	Ill-conditioned system	71
4.4.1	High values of branch resistance	71
4.4.2	High value of R/X ratio	72
4.5	Loading conditions	73
4.6	Test results	74
4.7	Analysis of simulation results	85
4.8	Conclusions	94

PART - II State Estimation

CHAPTER 5: INTEGRATED AC-DC STATE ESTIMATION IN RECTANGULAR CO-ORDINATES

5.1	Introduction	95
5.2	Mathematical modelling	97
5.2.1	AC system measurements	98
5.2.2	DC system measurements	98
5.2.3	Interface system measurements	98
5.3	Basic formulation	98
5.3.1	Formulation of $h(x)$	100
5.4	First order ac-dc state estimator	104
5.4.1	Solution steps	105
5.4.2	Characteristics of H and G matrices	107
5.4	Conclusions	107

CHAPTER 6: SECOND AND DECOUPLED SECOND ORDER AC-DC STATE ESTIMATOR IN RECTANGULAR CO-ORDINATES

6.1	Introduction	109
6.2	Second order ac-dc state estimator	110
6.2.1	Algorithmic development	113
6.2.2	Characteristics of SRSE	116
6.2.3	Solution steps	117
6.3	Decoupled second order ac-dc state estimator	117
6.3.1	Algorithmic development	119
6.3.2	Advantages	125
6.3.3	Characteristics of DSRSE	125
6.3.4	Solution steps	126

6.4	Conclusions129
-----	-------------	----------

CHAPTER 7: SIMULATION STUDIES

7.1	Introduction130
7.2	Initialisation131
7.3	Modification of standard test system (state estimation)132
7.4	Performance indices133
7.5	State estimation under ill-conditioned system134
7.6	State estimation in case of missing data135
7.7	State estimation under abnormal reference voltage136
7.8	Test results136
7.9	Analysis of simulation results177
7.10	Conclusions186

PART - III General Conclusions

CHAPTER 8: GENERAL CONCLUSION AND SUGGESTIONS FOR FUTURE WORK

8.1	Conclusions188
8.2	Future work195

REFERENCES197
-------------------	----------

APPENDICES

Appendix - A	: Per-unit system208
Appendix - B	: First and second order derivatives209
Appendix - C	: Benefits of rectangular co-ordinates formulation	

	and basic mathematical model for ac system217
Appendix - D	: System data234
Appendix - E	: Bus diagram and dc link, mesh, mesh-link configuration270
Appendix - F	: Load flow and line flow solutions of different bus system280

List of Tables

4.1	Effect of control specifications on convergence and solution time for 14 bus system with dc link 75
4.2	Effect of control specifications on convergence and solution time for 14 bus system with dc mesh 75
4.3	Effect of control specifications on convergence and solution time for 30 bus system with dc link 76
4.4	Effect of control specifications on convergence and solution time for 30 bus system with dc mesh 76
4.5	Effect of control specifications on convergence and solution time for 57 bus system with dc link 77
4.6	Effect of control specifications on convergence and solution time for 57 bus system with dc mesh 77
4.7	Number of iterations and solution time comparison of different methods 78
4.8	Percentage of solution time comparison of different method at different iterative stage 79
4.9	Effect of increasing R on convergence 80
4.10	Effect on convergence of increasing R/X ratio 81
4.11	Effect of convergence for high value of reactive power loading 82
4.12	Effect of convergence under different loading condition 83
4.13	Effect on convergence for different R/X ratios under different loading conditions84
7.1	Jacobian matrix [H] of a 3 busbar ac-dc system137
7.2	Gain matrix $[G] = [H]^T [W][H]$ of a three busbar ac-dc system140

7.3	State estimation results of 14 bus ac-dc link system 143
7.4	State estimation results of 30 bus ac-dc link system 145
7.5	State estimation results of 57 bus ac-dc link system 147
7.6	State estimation results of 107 bus ac-dc link system 148
7.7	State estimation results of 14 bus ac-dc mesh system 149
7.8	State estimation results of 30 bus ac-dc mesh system 151
7.9	State estimation results of 57 bus ac-dc mesh system 154
7.10	True values, estimated values and percentage of error of 14 busbar system using DSRSE 156
7.11	True values, estimated values and percentage of error of 14 busbar ac-dc mesh system using DSRSE 157
7.12	True values, estimated values and percentage of error of 30 busbar ac-dc link system using DSRSE 158
7.13	True values, estimated values and percentage of error of 57 busbar ac-dc link system using DSRSE 160
7.14	Maximum and average percentage of error compared to true values 161
7.15	Computing time comparison of different methods 162
7.16	Percentage of saving in solution time with FRSE method as reference 162
7.17	Comparison of performance indices 163
7.18	Comparison of performance indices using DSRSE method.....	163
7.19	Missing data of 5 nodes, namely 2, 3, 4, 5, 6 for 14 bus dc link 164
7.20	Missing data of 5 nodes, namely 1, 4, 9, 12, 19 for 30 bus dc link 165
7.21	State estimation solution of 14 bus ac-dc mesh system under abnormal reference voltage (0.85) 167
7.22	State estimation solution of 30 bus ac-dc mesh system under	

	abnormal reference voltage (1.15)169
7.23	Power flow accuracy comparison of 30 bus ac-dc system under abnormal reference voltage (0.85)171
7.24	Power flow accuracy comparison of 30 bus ac-dc system under abnormal reference voltage (1.15)173
7.25	Effect of increasing R/X ratio on convergence175
7.26	Effect of convergence under different loading condition176
D.1	System data for 14 bus system234
D.1.1	Bus data234
D.1.2	Line data235
D.1.3	Transformer data236
D.1.4	Shunt capacitance data236
D.1.5	DC link system236
D.1.5.1	Bus data236
D.1.5.2	Line data236
D.1.6	DC mesh system237
D.1.6.1	Bus data237
D.1.6.2	Line data237
D.1.7	DC mesh-link system238
D.1.7.1	Bus data238
D.1.7.2	Line data238
D.2	System data for 30 bus system239
D.2.1	Bus data239
D.2.2	Line data240
D.2.3	Transformer data242
D.2.4	Shunt capacitance data242
D.2.5	DC link system243
D.2.5.1	Bus data243
D.2.5.2	Line data243

D.2.6	DC mesh system243
D.2.6.1	Bus data243
D.2.6.2	Line data244
D.2.7	DC mesh-link system244
D.2.7.1	Bus data244
D.2.7.2	Line data244
D.3	System data for 57 bus system245
D.3.1	Bus data245
D.3.2	Line data248
D.3.3	Transformer data251
D.3.4	Shunt capacitance data252
D.3.5	DC link system252
D.3.5.1	Bus data252
D.3.5.2	Line data252
D.3.6	DC mesh system253
D.3.6.1	Bus data253
D.3.6.2	Line data253
D.3.7	DC mesh-link system254
D.3.7.1	Bus data254
D.3.7.2	Line data254
D.4	System data for 107 bus system255
D.4.1	Bus data255
D.4.2	Line data260
D.4.3	Transformer data267
D.4.4	DC link system268
D.4.4.1	Bus data268
D.4.4.2	Line data269
F.1	Load flow solution of 14 bus system with dc link280
F.2	Load flow solution of 30 bus system with dc link281

F.3	Load flow solution of 57 bus system with dc link283
F.4	load flow solution of 107 bus system with dc link284
F.5	Load flow solution of 14 bus system with dc mesh286
F.6	Load flow solution of 30 bus system with dc mesh288
F.7	Load flow solution of 57 bus system with dc mesh290
F.8	Load flow solution of 14 bus system with dc mesh-link291
F.9	load flow solution of 30 bus system with dc mesh-link293
F.10	Load flow solution of 57 bus system with dc mesh-link296
F.11	Line flow of 14 bus system with dc link297
F.12	Line flow of 30 bus system with dc link298
F.13	Line flow of 57 bus system with dc link300
F.14	Line flow of 107 bus system with dc link303
F.15	Line flow of 14 bus system with dc mesh304
F.16	Line flow of 30 bus system with dc mesh305
F.17	Line flow solution of 57 bus system with dc mesh307
F.18	Line flow of 14 bus system with dc mesh-link311
F.19	Line flow of 30 bus system with dc mesh-link312
F.20	Line flow of 57 bus system with dc mesh-link314

List of Figures

2.1	HVDC converter model31
2.2	Thevenin's equivalent of the HVDC model31
2.3	Flow chart for FRLF44
3.1	Flow chart for SRLF58
3.2	Flow chart for DSRLF66
4.1	Convergence characteristics of 14 bus system with dc link 89
4.2	Convergence characteristics of 14 bus system with dc mesh 89
4.3	Convergence characteristics of 14 bus system with dc mesh-link 90
4.4	Convergence characteristics of 30 bus system with dc link 90
4.5	Convergence characteristics of 30 bus system with dc mesh 91
4.6	Convergence characteristics of 30 bus system with dc mesh-link 91
4.7	Convergence characteristics of 57 bus system with dc mesh 92
4.8	Convergence characteristics of 107 bus system with dc link 92
5.1	Flow chart for FRSE method106
6.1	Flow chart for SRSE method118
6.2	Flow chart for DSRSE method128
7.1	Convergence characteristics of 14 bus system with dc link179
7.2	Convergence characteristics of 14 bus system with dc	

	mesh179
7.3	Convergence characteristics of 14 bus system with dc mesh-link180
7.4	Convergence characteristics of 30 bus system with dc link180
7.5	Convergence characteristics of 30 bus system with dc mesh181
7.6	Convergence characteristics of 30 bus system with dc mesh-link181
7.7	Convergence characteristics of 30 bus system with dc link182
7.8	Convergence characteristics of 57 bus system with dc mesh182
7.9	Convergence characteristics of 57 bus system with dc mesh-link183
E.1	IEEE 14 bus system270
E.1.1	14 bus dc link system271
E.1.2	14 bus dc mesh system271
E.1.1	14 bus dc link-mesh system272
E.2	IEEE 30 bus system273
E.2.1	30 bus dc link system274
E.2.2	30 bus dc mesh system274
E.2.1	30 bus dc link-mesh system275
E.3	IEEE 57 bus system276
E.3.1	57 bus dc link system277
E.3.2	57 bus dc mesh system277
E.3.1	57 bus dc link-mesh system278
E.4.1	107 bus dc link system279

Nomenclature

N_{ac}	= Number of ac busbars
N_{dc}	= Number of dc busbars
NL	= Number of lines in ac networks
NDL	= Number of lines in dc networks
X	= State vector
\tilde{X}	= Estimated value of state vector
k	= Measurement errors or noise
μ	= Overlap angle
R	= Residuals
L	= Second order term
Z	= Measurement vector
J	= Jacobian matrix
n	= Number of state variables
m	= Number of measurements
e_p	= Real ac busbar voltage at busbar 'p' (pu)
f_p	= Imaginary ac busbar voltage at buabar 'p' (pu)
G_{pq}	= p,q element of ac network admittance matrix (pu)
B_{pq}	= p,q element of ac network susceptance matrix (pu)
P_p	= Real ac power injection at busbar 'p' (pu)
Q_p	= Reactive ac power injection at busbar 'p' (pu)
ΔP_p	= Mismatch function of real power at busbar 'p' (pu)
ΔQ_p	= Mismatch function of reactive power at busbar 'p' (pu)
P_{ij}	= Real ac power flow in line i,j (pu)
Q_{ij}	= Reactive ac power flow in line i,j (pu)

ΔP_{ij}	= Mismatch function of real power flow in line i,j (pu)
ΔQ_{ij}	= Mismatch function of reactive power flow in line i,j (pu)
ΔR	= Residual for dc network and interface
$\Delta V $	= Error in nodal voltage
Vd_i	= Direct voltage at busbar 'i' (pu)
Id_i	= Direct current injection at dc busbar 'i' (pu)
a_i	= Off-nominal converter transformer tap position for transformer connected to converter at dc busbar 'i'
C_i	= Real part of ac current on the secondary side of converter transformer at dc busbar 'i' (pu)
d_i	= Imaginary part of ac current on the secondary side of converter transformer at dc busbar 'i' (pu)
$\theta_i = \alpha_i$	= Ignition delay angle of the rectifier
$\quad = \gamma_i$	= Extinction advance angle of the inverter
R_{dc}	= DC resistance
Gdc_{ij}	= i,j th element of the dc network conductance matrix (pu)
Pd_i	= DC power injected at dc busbar 'i' (pu)
Pd_{ij}	= DC power flow in line connecting dc busbars 'i' & 'j'(pu)
Xc_i	= Commutating reactance of converter at dc busbar 'i' (pu)
ϕ_i	= Power factor angle at converter at dc busbar 'i'
k_1	= $\frac{3\sqrt{2}}{\pi}$
k_2	= $\frac{3}{\pi}$
S_i	= 0 , for ac busbar 'p' with no converter connected to it

	= +1, for rectifier connected to ac busbar 'p' and dc busbar 'i'
	= -1, for inverter connected to ac busbar 'p' and dc busbar 'i'
t_i	= 0, for ac busbar 'p' with no converter connected to it = +1, for ac busbar 'p' with converter connected to it
$E(vv^T)$	= Covariance matrix of v
$[W]$	= Weighting matrix
$[W^{-1}]$	= Weighting matrix inverse
σ_{ii}^2	= Variance of i th measurements
$H(x)$	= Jacobian matrix
$H(x)^T W H(x)$	= Information matrix
ΔZ	= Mismatch vector
λ	= Resistance multiplication factor
ω	= Value of R/X ratio
β	= Reactive load multiplication factor
η	= Real power multiplication factor
τ	= Reactive power multiplication factor
	= Specified tolerance
**	= Fail to converge
AC	= Alternating current
CPU	= Central processing unit
DC	= Direct current
DSRLF	= Decoupled second order rectangular co-ordinate ac-dc load flow
DSO	= Decoupled second order
DSRSE	= Decoupled second order rectangular co-ordinate ac-dc state estimator

ESO	= Exact second order
FD	= Fast decoupled
FDLF	= Fast decoupled ac-dc load flow
FDSE	= Fast decoupled ac-dc state estimator
FO	= First order
FRLF	= First order rectangular co-ordinate ac-dc load flow
FRSE	= First order rectangular co-ordinate ac-dc state estimator
GS	= Gauss-Seidel
HVDC	= High voltage direct current
LFC	= Load frequency control
NR	= Newton-Raphson
NRLF	= Newton-Raphson load flow
PU	= Per unit
SO	= Second order
SRLF	= Second order rectangular co-ordinate ac-dc load flow
SRSE	= Second order rectangular co-ordinate ac-dc state estimator
WLS	= Weighted least square
WLSE	= Weighted least square state estimator

Subscripts

i, j, p, q	= Busbar index
ij, pq	= Line connection busbars, i and j or p and q
P	= Real power index
q	= Reactive power index
d	= DC quantities index
b	= base value
E	= Estimated value
M	= Measured value

av	= Average value
max	= Maximum value

Superscripts

m	= Measurement variables
k	= Iteration count
~	= Estimated quantity
T	= Transpose of a matrix or vector
t	= True values
sp	= Specified value
min	= Minimum value
0	= Initial value
*	= Final value

Abstract

Load flow and state estimation problems are solved for an economic and efficient operation, and an effective and stable control of the power system. Several methods are available to solve these problems, yet new ones are developed with a view to enhance the computational efficiency and convergence stability. Three new methods each for the ac-dc load flow and the ac-dc state estimation are developed and experimented in this thesis. These methods are based on formulating ac, dc and ac-dc (interface) performance equations in the rectangular form. Most of these equations are completely expressible in the Taylor series, and contain terms upto the second order derivatives, other higher order terms being zero. The solution process that are based on the first order derivatives of the Taylor series are called first order rectangular co-ordinate ac-dc load flow (FRLF) and the first order rectangular co-ordinate ac-dc state estimation (FRSE) algorithms. These algorithms are found to have characteristics similar to the polar coordinate Newton-Raphson (NR) and weighted least square (WLS) algorithms. In the former methods the derivatives higher than second order are neglected in developing the solution algorithms. The second order terms which are not insignificant can be included in the solution algorithm without increasing the computer memory. In addition to this, it is possible to keep the Jacobian and gain matrices constant during the solution process, which makes the method several times faster than the conventional NR and WLS methods. As there is no major approximation, the mathematical models are exact. Resulting solution algorithms are called second order rectangular co-ordinate ac-dc load flow (SRLF) and second order rectangular co-ordinate ac-dc state estimation (SRSE) methods. The Jacobian and gain matrices

remain constant in the recursive process. The nonlinearity of the network equations is retained. This contrasts sharply to the existing ac-dc load flow and state estimation algorithms which are based on the linearised relationship between the residual and error vectors. Digital solution studies indicate that the SRLF and SRSE are respectively superior to the NR and WLS methods.

The mathematical models of the SRLF and SRSE possess a number of desirable features. An exploitation of these features without introducing any approximation results in the faster versions of the SRLF and SRSE algorithms. These faster versions are referred to as decoupled second order rectangular co-ordinate ac-dc load flow (DSRLF) and decoupled second order rectangular co-ordinate ac-dc state estimator (DSRSE) respectively. Numerical experimentations reveal that the convergence characteristics and the computing time of DSRLF and DSRSE are superior than the fast decoupled ac-dc load flow (FDLF) and fast decoupled ac-dc state estimator (FDSE).

Preface

This thesis contains three new mathematical models for ac-dc load flow and state estimation. The algorithms were tested under various operating conditions. Digital simulation results indicate that the proposed methods are superior than the conventional ac-dc load flow and state estimation method. A listing of all the relevant publications related to this thesis are provided below.

- [1] M.Z. Haque & A. Kalam, "*A comparative study of AC-DC load flow with the development of new algorithm*" **International Conference on Modelling and Simulation**, Vol.1, July 12-14,1993, pp. 356-374.
 - [2] M.Z. Haque & A. Kalam, "*Second order dynamic state estimation using cartesian co-ordinate algorithm*", **International Conference on Modelling and Simulation**, Vol. 2, July 12-14,1993, pp-707-716.
 - [3] A.Kalam & M.Z. Haque, "*A new version of exact decoupled second order AC-DC load flow solution in rectangular co-ordinates*", **IEE APSCOM-93**, Hong Kong, Vol.1, Dec. 1993, pp. 262-267.
 - [4] M.Z. Haque & A. Kalam, "*Exact decoupled second order AC-DC load solution under loading and ill-conditioned networks*", **AUPEC'94**, Adelaide, Vol. 3, Sept. 1994, pp. 603-608.
 - [5] M.Z. Haque & A.Kalam, "*A new method of solving AC-DC power system state estimation problem*" **ICEE '96**, Beijing, China, Vol. 2, Aug. 12-15, pp. 983-987.
 - [6] A. Kalam, M.Z. Haque & J. Nanda," *An exact second order load flow solution under loading and ill-conditioned networks*", **International Journal of Power and Energy Systems**, Vol. 16, Issue 3, September 1996, pp. 150-156.
-

- [7] M.Z. Haque & A.Kalam, "*A comparative study of first and second order AC-DC state estimator*" **UPEC '96**, Greece, Vol. 2, Sept. 18-20, pp. 578-581.
 - [8] M.Z. Haque & A.Kalam, "*Exact decoupled Second order AC-DC power system state estimator*" **11 CEPSI '96**, Malaysia, Vol. 3, Oct. 21-25, pp. 134-143.
 - [9] M.Z. Haque & A.Kalam, "*Novel decouple AC-DC state estimator*" **AUPEC '96**, Melbourne, Vol. 3, Oct. 2-4, pp. 599-604.
 - [10] M.Z. Haque, A. Kalam & L. Roy ,"*Second order ac-dc power system state estimator*", **International Journal of Power and Energy Systems**, Vol. 17, Issue 2, April 1997, pp. (in press).
-

PART - I

LOAD FLOW

Chapter 1

INTRODUCTION AND REVIEW

1.1 INTRODUCTION

In the modern age of science and technology, the necessity of electricity is increasing day by day. In view of rapid growth in demand and supply of electricity, electric power system is becoming increasingly large and more complex. Moreover, regular electric supply is the sheer necessity for growing industry and other fields of life. The power industry planners are demanding stronger trend towards supplying electric power of higher quality by improving the system security and its impact on environment in parallel with pursuit of economy. In real life situation, the criterion of perfection is never met, because there are deviations between the model and reality. Load flow and state estimation analysis are an important tool for stable operation and control of power system as well as future planning of power systems. High voltage ac-dc technology has made considerable advances in recent years. Engineers are now considering dc multi-terminal network as a feasible option. Therefore, the load flow and state estimation techniques have to be extended to deal with such mixed ac-dc systems. Multi-terminal dc network integrated into an existing system can improve ac equipment loading and stability, participate in load frequency control (LFC) and voltage

regulation, increase interchange capacity, limit short circuit capacity and contribute to the economy of electric power transmission. Multi-terminal dc network as well as two-terminal dc links require communication between converter terminals and control of dc system start-up and shutdown, for coordination of operating set points, and for dc system structure changes such as line or terminal outages. Link or meshed dc multi-terminal network integrated to ac systems is feasible and can be advantageous in certain applications such as bulk power transmission, ac networks interconnection and reinforcing ac networks.

1.1.1 AC-DC Power System Load Flow

Under normal operating conditions electric transmission systems operate in their steady-state mode and the basic calculations required to determine the characteristics of this state are termed as load flow or power flow [95]. The main objective of load flow calculations is to determine the steady state operating characteristics of the power generation/transmission system for a given set of busbar loads. The load flow calculations provide voltages, power flows and power losses for a specified power system subject to the regulating capabilities of the generators, condensers and on-load tap changing transformers as well as the net power exchange between the individual power system. This information is essential for continuously evaluating the operating performance of a power system and analysing the effectiveness of alternative plans for system expansion to meet the increasing load demand. The load flow studies are also necessary for the power system stability assessment, contingency evaluation and economic operation. The significance of these studies has become more relevant

in modern times due to the control and operation of the interconnected large size power systems in a real-time environment.

Imposing a dc network between ac generators and load or between two ac systems offer several technical and economical advantages which are described in the next section. The growing number of schemes in existence and under consideration demands corresponding modelling facilities for planning and operational purposes. In recent years, great advantages have been made in converter technology which has resulted in cheaper and more reliable power utilisation. The basic load flow has to be substantially modified to be capable of modelling the operating state of the combined ac and dc systems under the specified conditions of load, generation and dc system control strategies.

1.2 REVIEW OF AC-DC LOAD FLOW

Load flow calculation has a very important role in power system research and power industry. Although many methods have been proposed, further development of load flow method for the purpose of obtaining greater computational speed, lower storage requirements, more reliable and better convergence pattern and especially for loading and ill-conditioned systems, is still a very significant field of study.

The load flow calculation is one of the most commonly used tools in power system engineering. For this reason, the history of load flow calculation is a relatively long one. The initial work of load flow studies has been carried

out by many investigators. Different types of algorithms have been proposed [1-6]. However, most of these studies have been carried out on ac systems [7], and not much work have been reported on the ac-dc systems. The options of dc line linking to ac systems are used as they are better technical alternative and are financially beneficial in certain occasions such as:

- to facilitate the operation of interconnected ac systems at different frequencies;
- to enhance the operation of ac systems with incompatible frequency control techniques;
- to transmits power in underground and submarine cables;
- to transfer bulk power over long distances more economically;
- to reduce the short circuit level in an interconnected ac system;
- to increase the transient stability margin;
- to improve dynamic stability.

Earlier digital solution of the power flow in ac-dc systems is the work done by Horigome *et al.* [17], Gavrilovic *et al.* [18], Hingorani *et al.* [19], Barker *et al.* [20], Brever *et al.* [21], Sato *et al.* [22], Sheble *et al.* [23] and others. Additional characteristics of the cartesian coordinate formulation for ac load flows were investigated by El-Hawary *et al.* [14], Rao *et al.* [15], Krishnaparandhama *et al.* [16] and Cory *et al.* [89]. However, their works were limited upto the first order derivatives of the

Taylor series. The third and other higher order terms which are not zero, were neglected.

1.2.1 Gauss-Seidel Method

The Gauss-Seidel (GS) method is an iterative algorithm for solving a set of non-linear algebraic equations. In this method the solution vector is assumed, based on guidance from practical experience in a physical situation. One of the equations is then used to obtain the revised value of a particular variable by substituting in it the present value of the remaining variables. The solution vector is immediately updated in respect of this variable. The process is then repeated for all the variables thereby completing one iteration. The iterative process is then repeated till the solution vector converges within prescribed accuracy.

The initial effort in the digital solution of the load flows was based on the GS method. The method was extensively used by Ward *et al.* [1], Laughton [94], Clair *et al.* [2], Glimn *et al.* [5] and many others. Therefore, the initial algorithms developed for ac-dc load flow problems were also based on the GS technique in the sequential framework [17-22]. In the sequential approach, dc parameters are estimated first and then holding these parameters constant, ac parameters are solved. Next, the ac parameters are used to readjust the dc parameters. The process is continued until a solution with the specified accuracy is obtained. An extensive investigation indicated that solving the dc link at every GS iteration increases the total computing time. However, this feature was absent in other methods [22]. It was also observed that there is no need to have the full

convergence for the ac load flows at each stage, rather a partial convergence scheme needs less overall solution time. The chief advantage of the GS method is the ease of programming and most utilisation of core memory. Also the GS method performs satisfactorily on small and well conditioned networks. However, on some large systems it encounters convergence problems. Further evidence is the fairly well known fact that the convergence of the GS method is poor for system having lines with large R/X ratios.

1.2.2 Newton-Raphson Method

Newton-Raphson (NR) method is an iterative solution algorithm for solving a set of simultaneous non-linear equations in an equal number of unknowns. At each iteration the non-linear problem is approximated by the linear matrix equation. The linearising approximation can be visualised in the case of a single-variable problem. The NR algorithm will converge quadratically if the functions have continuous first derivatives in the neighbourhood of the solution. The Jacobian matrix is non-singular, and the initial approximations of the state vectors are close to the actual solutions. The method is sensitive to the behaviour of the functions i.e. the more linear they are, the more rapidly and reliably the method converges.

The NR method along with its companion techniques of sparsity and optimal ordering is successful in the ac load flow [8,9]. Stott [87] combined the dc link solution technique of Sato *et al.* [22] with the NR ac load flow programme and solved the ac-dc load flow problem in the sequential framework. The method works quite well for most of the system. The NR method, though accurate and reliable for most of the

system, is not very fast. Also, the method does not work well under heavy loading condition. However, there appears to be several drawbacks with this approach :

- the convergence characteristics are quadratic in nature;
- speed advantage of the NR method in solving the ac part of the system - particularly for large systems is not fully realised;
- link calculation is time consuming and involves complex logic;
- the algorithm is relatively inflexible for adopting control specifications;
- convergence is of arbitrary nature and not fully reliable;
- the method does not perform well under ill-conditioned situation.

The problems outlined above were mitigated by combining the ac load flow and dc link solution in an integrated NR solution process [24,27,87]. Some modified version of ac-dc load flow methods have been proposed [31-33,44,48,86]. This approach was claimed to be faster and more stable than the sequential one using the NR technique.

1.2.3 Advantages of NR Method Over GS Method

The rate of convergence of GS method is slow, requiring a considerably greater number of iterations to obtain a solution, particularly for large

system. Whereas, with sparse programming techniques and optimally ordered triangular factorisation, the NR method for solving load flow has become faster than GS method and the number of iterations is virtually independent of system size due to the quadratic characteristic of convergence. One NR iteration is equivalent to about seven GS iterations [95]. For a 500 bus system, the conventional GS method takes about 500 iteration and the speed advantage of the NR method is about 15:1 [95]. The time per iteration in both these methods increases almost directly as the number of buses of the network. In the GS method the convergence is affected by choice of slack bus and the presence of series capacitors. On the other hand, the NR method is very reliable in system solving, given good starting approximations. The method is readily extended to include tap-changing transformers, variable constants on bus voltages, and reactive and optimal power scheduling. Therefore, for small and large systems the NR method is faster, more accurate and more reliable.

1.2.4 Fast Decoupled Method

The fast decoupled (FD) load flow method is actually an extension of NR formulated in the polar coordinates with certain approximations. These approximations are assumed to be valid due to the fact that any practical electric power transmission system operation in the steady-state condition has strong interdependence between active powers (P) and voltage angles (δ), and between reactive powers (Q) and voltage magnitudes (V). So, the coupling between the P - δ and Q - V components of the problem is relatively weak. The Jacobians of the decoupled Newton load flow can be made constant. This means that they need to be triangularised only once per iterative solution.

The loose coupling between $P-\delta$ and $Q-V$ equations was exploited in the FD method for ac load flows [10,46]. The method was characterised by minimal computing time and computer memory requirements. The FD method developed by introducing few approximations into the NR model, though generally is very efficient, is known to have the disadvantage of poor convergence characteristic for systems having lines with large R/X ratios. The FD method was extended to the ac-dc load flow by Arrillaga *et al.* [25], Reeve *et al.* [28], Arrillaga *et al.* [26,39] El-Marsafawy *et al.* [29], Fudeh *et al.* [30], De Silva *et al.* [91] and many others. A large number of algorithms with varying degree of sophistication and versatility are available in the literature for the ac-dc load flow using the FD technique. Among them, the algorithms proposed by Arrillaga *et al.* [25,26] and El-Marsafawy *et al.* [29] using the simultaneous solution scheme are computationally superior, particularly viable and technically versatile.

1.2.5 Advantages of FD Method Over NR Method

In case of FD method the convergence characteristics is geometric in nature, whereas in NR method the convergence characteristics is quadratic. Though FD method requires five-six iterations to obtain required convergence but the total solution time is far better than NR method. The speed per iteration of the FD method is about five times than that of formal NR method and the storage requirements are about 60 percent of the formal NR method [95]. The FD load flow can be used in optimisation studies for a network and is particularly useful for accurate information of both real and reactive power

for multiple load flow studies, as in contingency evaluation for system security assessment.

1.2.6 Limitations of NR and FD Methods

An inspection of the available literature indicates that practically adopted ac-dc load flow algorithms are based on either the NR technique or the FD technique. These algorithms are reported to be successful. However, they have got some limitations. Some investigators [35-40] have shown that the NR technique encounters convergence problem on the ill-conditioned networks. On the other hand, the FD technique does not perform well if the decoupling assumptions are not valid. It also has the disadvantage of poor convergence characteristic for the systems having lines with large R/X ratios.

It can be noted from the above that the NR method requires large computing time and encounters convergence problems for the ill-conditioned systems [36]. Mention has also been made [34-38] that the FD technique does not perform well for all the systems and under all the operating modes, the limitations of the FD load flow method are:

- slow or oscillatory convergence is encountered at buses connected to branches with R/X ratios exceed from unity or higher values;
- convergence rate of P- δ and Q-V decoupled algorithms are determined by how well the coefficient matrices approximate to the slope of the function $\partial P/\partial \delta$ and $\partial Q/\partial V$, respectively. These approximations are excellent

around $\delta = 0$ and $V = 1$ pu. At high system active or reactive power loadings (large δ 's and poor V's) the approximations deteriorate;

- the rate of convergence are strongly influenced by the coupling between P- δ and Q-V mathematical models. This coupling decreases with system loading levels and branches R/X ratios and consequently the convergence rate decreases;
- on the ill-conditioned power systems the method often encounters oscillatory convergence;
- also on loading conditioned system the method some times take long time to converge;
- the method also fails with most of the load flow equivalencing techniques, due to the large value of shunt and series admittances contributed by an equivalent of the external parts of the inter-connected power system.

Ghonem *et al.* [90] proposed a new version of the decoupled load flow method, which is claimed to be superior to the original version of the FD algorithm. However, the method is not examined under ill-conditioned and different loading conditions. Also the method can be applied on ac system only. Nanda *et al.* [97] proposed a decoupled power flow model with some justifiable network assumptions. The model exhibits stable convergence behaviour for both well behaved and ill-conditioned situations. However, the algorithm is in polar coordinate formulation and there is no provision for dc networks. Haque [96] developed a decoupled load flow algorithm without ignoring the coupling sub-Jacobians and the method performs well

under ill-conditioned networks. Also the method reduces the computing time as compared to the other methods, but his study was confined to ac systems.

1.3 Cartesian Co-ordinate Second Order Method

In this thesis, a second order method was suggested, so as to achieve a more accurate model, by considering the first three terms of the Taylor series expansion of the load flow equations [11,45,47,88]. Iwamoto *et al.* [12] proposed a second order method using rectangular co-ordinate formulation and showed that no terms of the Taylor series expansion need be neglected in this method. From the Iwamoto's method it is observed that though the results show considerably reduced computing time as compared to the NR method, it is quite inferior to the FD method from the point of view both memory and time as clearly brought in the discussion of reference 40. Even Roy's [11] method is not superior to FD method on this ground. Rao *et al.* [40] developed an exact second order load flow model in rectangular co-ordinate and claim to have faster and requiring less computer storage than any other existing second order method. The memory requirement of their method is comparable to that of the FD method and is more reliable than the FD method for ill-conditioned system.

All the above discussions however, are pertinent to ac load flow only. An inspection of the available literature indicates that practically adopted ac-dc load flow algorithms are based on either the NR technique or the FD technique. Some investigations have shown that the NR technique encounters convergence problems on the ill-conditioned networks

[34,36,42,43]. On the other hand, the FD techniques do not perform well if the decoupling assumption are not valid. Though FD methods have been used for ac-dc system their convergence for different loading condition and ill-conditioned situation have not been examined so far. The usual assumptions and approximations in FD model when applied to ac-dc system may meet convergence problem while dealing with ill-conditioned system, represented by system having lines of large R/X ratios, presence of capacitive series branches etc. In such a situation it may be worthy to use an exact model based on the concept of second order ac-dc system and then examining in details the performance of this model as compared to that of FD model, not only for well behaved system but also for ill-conditioned system.

Literature survey reveals that till date, second order load flow model for ac-dc system does not exist. The main objective of the present work is to develop a model for ac-dc system based on the concept of second order load flow technique and compare its performance with FD model for different loading condition and ill-conditioned situation. While developing the second order load flow for the ac-dc system attempt has been made to explain the desirable feature of co-efficient matrix which leads to the development of faster version of the model.

1.3.1 Characteristics of the Second Order and Decoupled Second Order Algorithms

The attractive features of the second order (SO) and decoupled second order (DSO) algorithms are:

- ac network equations are completely expressible in the Taylor series involving terms upto the second order only;
- Jacobian matrix is constant and thereby needs to be computed and triangularised once only in the iterative scheme;
- second order derivatives are not required to be stored in the matrix form;
- SO method is faster than the NR method and requires comparable memory;
- SO method needs more computing time and computer storage than the FD method;
- DSO method is faster than the NR and SO methods and requires less storage;
- computational requirements (storage and computing time) of the DSO method are comparable with those of the FD method;
- SO and DSO methods are computationally more stable than the NR and FD methods, as no assumptions or linearisations have been used in the formulation of these methods.

1.3.2 Characteristics of the Proposed Methods in Comparison with FD Method

The characteristics of the proposed methods are ascertained and compared with those of the FD algorithm. The main observations are summarised below:

- cartesian co-ordinate formulation of the ac-dc load flow problem is feasible;
- omission of some higher order derivatives of the Taylor series associated with dc converter buses and inclusion of the second order derivatives lead to a viable ac-dc load flow solution method;
- solution time of the SO algorithm is less compared to the first order (FO) ac-dc method. However, the storage requirement is similar;
- solution time and computer storage of the DSO ac-dc load flow algorithm are comparable to those of the FD ac-dc method;
- convergence characteristics are moderately influenced by the nature of the control specifications; the method performs well on some ill-conditioned networks where the FD method some time fails to converge;
- the proposed methods performs well under different loading condition where the FD method does not perform well;
- for some control specifications, the proposed methods seem to perform better than the FD ac-dc method.

1.4 AC-DC POWER SYSTEM STATE ESTIMATION

1.4.1 Definition

State estimation is defined as a statistical procedure for deriving from a set of measurements, a 'best' estimate of the system state. State estimation is a digital processing schedule of scheme which provides a real time data base for many of the central and dispatch functions in a power system. In the field of power system, the objective is to provide a reliable and consistent data base for security monitoring, contingency analysis, economic operation and system control. The estimator processes the imperfect information available and produces the best estimate of the true state of the system.

1.4.2 Review of Ac-Dc State Estimation

The work towards state estimation or real time monitoring of power system started in early seventies. A number of methods are available in the literature for the state estimation of electric power systems. Schweppe *et al.* [51] and Dopazo *et al.* [49] formulated on-line power system state estimation algorithms using the weighted least square (WLS) and independent equations. The contribution was supplemented and extended by a number of researchers, including Smith [50], Schweppe *et al.* [54], Larson *et al.* [52], and Dopazo *et al.* [53]. Among these solution techniques, the WLS approach has gained widespread applications in the power industry. The popularity of the WLS method can be attributed to the fact that, it provides a best fit of the complex nodal voltage, gives a set of redundant nodal power injections and line flow measurements while

handling input data errors. A problem associated with this approach is that the statistical characteristic of the errors must be known a priori to determine the proper values for the weighting factors. Another numerical difficulty encountered is that, if sufficient redundancy is not included, ill-conditioning of system equations may lead to poor convergence. Further, the computer storage and time requirements are relatively large.

The real time monitoring using independent equations (real time load flow) is based on the node injections as input data, but utilises independent line flows as redundant information for correction of erroneous/missing data. It however, does not make use of the P-Q busbar voltage measurements. Further, it requires a high level of accuracy in the input data to ensure the detection of bad data. The chief merit of this approach is that, unlike the basic WLS method, it does not require a large number of redundant data, thereby, reducing the cost of metering and communication facilities.

To overcome the large computational requirement associated with the basic WLS approach, a number of alternative algorithms [55-58,85] have been suggested. One such modification involves the application of the P- δ and Q-V decoupling technique used in the conventional fast decoupled load flow approach [59-63,93]. This algorithm referred to as the fast decoupled state estimator (FDSE) has been demonstrated to be computationally very efficient, and seems to enjoy wide acceptance. Tripathy *et al.* [84] developed a state estimator algorithm using Newton's method, the algorithm performs well on ill-conditioned networks but it can

only be applied to ac networks. Monticelli *et al.* [92] proposed a decoupled state estimator without zeroing the coupling submatrices and the method performs well under ill-conditioned networks but no provision is made for dc system. Habiballah *et al.* [98] proposed a decoupled state estimation algorithm with efficient data structure management, which substantially reduced the computing time. However, the algorithm has not been tested under loaded and ill-conditioned network, also their study was confined to ac system. Abou El-Ela [99] proposed a state estimation technique based on the exact linearisation of the cartesian co-ordinate formulation of nodal load flow equations. The technique reduces the computing time and is also suitable for solving ill-conditioned network which have large bad-data points. However, the algorithm can only be applied on the ac system.

Dopazo *et al.* [53] proposed a method based on the line flow measurements only for the evaluation of the nodal voltages. The technique was shown to be efficient. It has a number of limitations, such as:

- it does not make use of nodal measurements;
- it involves a special type of metering and communication strategy.

Subsequent developments involved extending and enlarging the range of the application of the available techniques to encompass the bad data [64-68], tracking [69-72] and dynamic [73-74] aspect of the state estimation. Some investigators using linear programming technique in order to reduce the computing time [13,85]. An interesting comparisons of the state estimation techniques are available in references 75 and 76 . The

comparison can be useful in the selection of a suitable method for a particular power system. It is observed that since early seventies many papers have been published on the state estimation of the power systems [93]. Different types of algorithms - static, tracking and dynamic have been proposed. These studies, however, were mostly confined to ac system.

Realising the existence of ac-dc electric networks, attempts were made to extend the ac system state estimation algorithms to accommodate dc links and multi-terminal network. Sirisena *et al.* [77] presented an algorithm for the mixed system involving only the dc links. No provision was made for multi-terminal dc networks. Glover *et al.* [78] devised an algorithm for the multi-terminal dc networks and was confined to the dc network state estimation. The ac-dc interconnected system (converter system) was not included in the study. Leita da Silva *et al.* [79] presented a more general state estimator capable of handling dc multi-terminal networks embedded in an ac system. The limitations of the Sirisena *et al.* [77] and Glover *et al.* [78] algorithms were overcome to a great extent. The FD state estimation technique originally applied on the ac systems [58] was extended by Jagatheesan *et al.* [63] to the ac-dc systems and a sequential scheme was proposed. All these algorithms [56-81] are based on the polar formulation and the first order derivatives of the Taylor series. Roy *et al.* [41] proposed a second order state estimation by using the conventional load flow equations. The algorithm is not very fast and it can only apply to ac system. The proposed state estimation algorithms is based on the rectangular formulation, and the first and second order derivatives of the Taylor series. The algorithm is capable of

handling the ac system, the dc system and the interconnection system simultaneously. The ac, dc and converter networks are modelled in the rectangular form. AC-DC performance equations are completely expressible in the Taylor series and terminate after the second order derivatives. However, the interconnection system equations contain terms upto the sixth order derivatives in the Taylor series. The fact that the ac, dc and converter equations are completely expressible in the Taylor series and the Taylor series is exact was hitherto, not reported. The proposed method is more general and free from many limitations.

1.4.3 Limitations of WLS and FD Estimators and Scope of Further Investigation

Most of the commercial state estimation programmes are based on the FD technique. However, the success of these programmes are subject to satisfying the underlying assumptions, viz :

- voltage magnitudes are near unity;
- angular differences between the adjacent nodal voltages are small;
- shunt connection to ground is small;
- X/R ratios of the lines are large;

Some investigations revealed that the FD estimator performs satisfactorily so long as the underlying decoupling and associated assumptions are satisfied [56-81]. However, where the assumptions are not valid, convergence problems are encountered and the solution process generally diverges. As such, the FD estimator although simple and efficient is not

versatile. Thus, there exists a need to develop new methods for the state estimation of ac-dc power systems which should possess the desirable features of the FD estimator, but be free from its limitations. An attempt is made in this thesis to develop and test such methods.

One of the objectives of the thesis is to develop new algorithms for the state estimation of ac-dc power systems, that are both efficient and stable. The algorithms used for the state estimation of ac-dc power systems are based on the polar co-ordinate formulation of the network performance equations. The network equations are expanded in the Taylor series, and the first order derivatives are used in developing the solution model.

Effects of the cartesian co-ordinate formulation of the network performance equations were studied for the state estimation of ac networks [81-83]. Details of the benefits of cartesian co-ordinate formulation for load flow and state estimation are given in Appendix - C. No such attempt seems to have been made for ac-dc systems. As such, the aim of the thesis is to develop new methods for the state estimation of ac-dc systems, that are based on the rectangular co-ordinate formulation of the network equations.

1.4.4 Characteristics Of the Proposed Method

The method is characterised by the following :

- ac system, dc system and ac-dc interconnection system are modelled separately and independently. Essentially, an

integrated ac-dc system is partitioned into three independent subsystems;

- state of three parts is estimated separately. The state estimation problem is split into three number of smaller sub-problems. This introduces interface errors;
- objective (cost) function is broken into three parts. The objective function of each part is minimised independently. The cost function of the total system is not minimised. The sum of the local minima need not be the global minimum;
- Coupling sub-matrices among the ac system, the dc system and the interconnection system are ignored. This introduces a major approximation.

1.4 SCOPE AND OBJECTIVE

From the literature survey it is clear that the FD ac-dc method does not appear to be suitable for all kind of power systems under all operating conditions. On the other hand computational requirements of the NR ac-dc method are large. So there is a need for developing new methods for the ac-dc load flow that are devoid of the limitations of the FD and NR methods.

The main objectives of the thesis are:

- to develop a new mathematical model which is more exact and requires smaller time for computation. Hence, the

second order load flow model in rectangular co-ordinates is chosen as the basic tool;

- to develop a mathematical model which can operate ac system, dc system and the ac-dc (interface) system independently;
- to formulate a new model which is highly reliable and provide solutions for a number of ill-conditioned systems;
- to apply SO and DSO techniques for solving the load flow and state estimation problems of ac-dc power systems.

1.6 ORIGINALITY OF THE THESIS

The work presented in this thesis is based on the presentation of the ac-dc network equations in the cartesian co-ordinate form for the solution of the load flow and state estimation problems. The option of dc link on ac system has got some advantages. The power system engineers are more concerned about dc system. Though many paper has been published in order to solve the ac-dc load flow and state estimation problems but new ones high lights more reliable and attractive features. Literature survey reveals that till date algorithms for second order ac-dc load flow and state estimation does not exist. The original contributions of this thesis are summarised as follows:

1. A mathematical model has been developed for ac-dc load flow and state estimator based on the concept of second order technique.
2. A new mathematical model of decoupled second order ac-dc load flow and state estimator has been investigated without

ignoring the coupling sub-Jacobians. As there are no major approximation on the model, the solutions are more accurate and reliable.

3. The proposed algorithms have an interesting aspect that, the ac and dc part of the networks can be handled separately without modification to the program.
4. The proposed algorithms perform well under different converter control specifications and under various operating modes.
5. The performance characteristic of the proposed algorithms are comparable to the NR load flow & state estimation and FD load flow & state estimation and it appears that the proposed algorithms are far superior than the conventional load flow and state estimation algorithms.
6. The proposed algorithms can faithfully be applied to the low voltage distribution system where the line resistance, R or R/X ratios are very high.
7. The proposed algorithms have been tested under different loading conditions and abnormal reference voltages and it performs well.

1.7 DEVELOPMENT OF THESIS

The development of the subject matter of the investigation reported in the thesis is on the following lines :

Chapter 1 : The first chapter introduces the problem of ac-dc load flow and state estimation. The ac-dc load flow and state estimation are briefly

reviewed. The limitations of the popular methods are described and the scope of further investigations outlined.

Chapter 2 : The ac-dc load flow problem is formulated in the cartesian co-ordinate. The equations are expanded in the Taylor series. A new mathematical models for ac-dc load flow in rectangular co-ordinate is developed. The mathematical model are based on the first order derivatives of the Taylor series and is called the first order rectangular co-ordinate load flow (FRLF). In this formulation the other second and higher order terms which are not zero but neglected which causes small errors in network solutions.

Chapter 3 : In this chapter an exact method based on full Taylor series expansion of load flow equations in cartesian co-ordinates has been proposed. The method is called the exact second order (ESO) method perform better than the NR i.e., fast order (FO) method, but do not stack up well against the state of art FD method. This method is called the second order rectangular co-ordinate ac-dc load flow (SRLF), both the first and second order derivatives are used in developing the model. The third and higher order terms in the Taylor series are found to be zero except for only a few equations associated with the dc converter busbars. The omission of these few higher order terms in a second order mathematical model in which the coefficient matrix remains constant, a new mathematical model has been developed. Therefore, like in the FD load flow it needs to be computed and triangularised once only at the beginning of the iterative scheme, making the solution process extremely fast.

The structure of the coefficient matrix of the SRLF method is found to contain certain desirable features. Exploitation of these features result in a faster version called decoupled second order rectangular ac-dc load flow (DSRLF) method. The coefficient matrix of the DSRLF method is comparable in size and structure with that of the fast decoupled ac-dc load flow (FDLF) method and hence, is characterised by comparable computational requirements.

Chapter 4 : In this chapter detail simulation results are provided. Load flow and line flow solution of IEEE 14, 30, 57 and 107 bus system are given in this chapter. The algorithm is tested under different control specifications and under different degree of ill-condition. The convergence characteristics, the cpu time and the solution accuracy of the different methods are compared not only for well behaved system but also for the ill-conditioned and heavily loaded networks.

Chapter 5 : This chapter presents a new solution algorithm for the state estimation of the ac-dc power systems. The ac, dc and converter equations are formulated in the cartesian co-ordinate. The rectangular co-ordinate version of the nodal and line flow equations for the ac busbars with no converter connected to them are completely expressible in Taylor series that contains terms up to the second order derivatives. Only a few of the equations at the converter busbars and interface involve terms higher than the second order in the Taylor series. The first solution algorithm is based on the linearised relationship between the residual and the error vectors, and uses only the first order derivatives of the Taylor series. This algorithm is basically the weighted least square state estimation (WLSE) in

the rectangular co-ordinate form, and is called the first order rectangular co-ordinate ac-dc state estimator (FRSE).

Chapter 6 : In this chapter two new algorithms for the second order ac-dc state estimation has been developed. In the solution, algorithm uses both the first and second order derivatives of the Taylor series. In this version, the non-linearity of the ac network equations is completely retained. The resulting mathematical model involves a constant coefficient matrix subject to the approximation outlined as before. The constant Jacobian matrix results in a constant gain matrix. As the gain matrix is constant, it needs to be calculated and triangularised once only in the iterative process. The WLSE type procedure is employed to obtain a solution. The method is known as the second order rectangular co-ordinate ac-dc state estimator (SRSE).

An inspection of the structure of the gain matrix of the SRSE reveals a number of desirable features. Exploiting these features a new version of the SRSE, called the decoupled second order rectangular co-ordinate ac-dc state estimator (DSRSE) is developed.

Chapter 7 : Exhaustive numerical experimentation is required to validate the findings. Experimentation of the new methods for the state estimation of ac-dc power systems are examined in this chapter. Detail simulation results of IEEE 14, 30, 57 and 107 are provided. Different test results are compared. The characteristics of the new algorithms have been investigated and compared with those of the basic FRSE and FDSE algorithms.

Chapter 8 : This chapter provides the overall conclusions of the research done. Both, the contribution and utilisation of the multi-objective mathematical modelling in ac-dc load flow and state estimation studies are systematically presented and summarised. Some new directions for further research efforts are also highlighted.

Chapter 2

INTEGRATED AC-DC LOAD FLOW IN RECTANGULAR CO-ORDINATES

2.1 INTRODUCTION

Load flow analysis is an important tool for the planning, operation and control of power system. However, high voltage direct current (HVDC) transmission is now gaining considerable importance not only for long distance but also for underground and submarine transmission, and it becomes necessary to develop a method for carrying out the load flow analysis of an integrated ac-dc power system. The basic load flow has to be substantially modified to be capable of modelling the operating state of the combined ac and dc systems under the specified conditions of load, generation and dc system control strategies. This chapter deals with the development of an ac-dc load flow program based on rectangular co-ordinates. Variables of the dc link which have been chosen for the problem formulation are the converter terminal dc voltage, the real and imaginary component of the transformer secondary current, converter transformer tap ratios, firing angle of the rectifier and current in the dc link. Equations relating these six variables and their solution strategy have been discussed. The model developed is independent of a particular control mode of the dc link. Also, the ac and dc link equations are solved separately and thus the

integration into standard load flow program is carried out without significant modifications of the ac load flow algorithm. For the ac system iterations, each converter is simply modelled as a complex power load at the ac terminal bus bar. The dc link equations are solved using the latest update value of the ac bus bar voltage. This gives full recognition to the interdependence between the ac and dc system equations and requires solving the ac and dc system equations simultaneously.

2.2 DEVELOPMENT OF MATHEMATICAL MODEL

In this section a mathematical model for the integrated operation of ac-dc systems is developed. An integrated ac-dc system consists of ac network, dc network and ac-dc interface (converter) system. For the purpose of the load flow analysis, ac network components connected to a converter are considered as part of the converter system. The advantage of this approach is that the ac network admittance matrix remains unaffected due to converter transformer tap variations or due to reactive power changes caused by switching of the capacitor banks at the converter terminal busbars.

2.2.1 DC Converter Model

For the purpose of the load flow analysis of ac-dc power systems, HVDC converters have, so far, been modelled in the polar co-ordinate form. In this chapter, the HVDC converters are modelled in the rectangular co-ordinate form.

A HVDC converter connected to an ac busbar 'P' and a dc busbar 'i' is shown in Fig. 2.1 and its Thevenin's equivalent is shown in Fig. 2.2. For

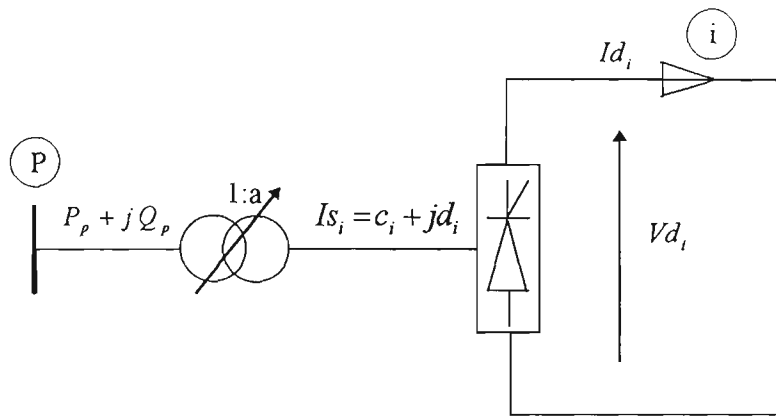


Fig. 2.1 HVDC converter model

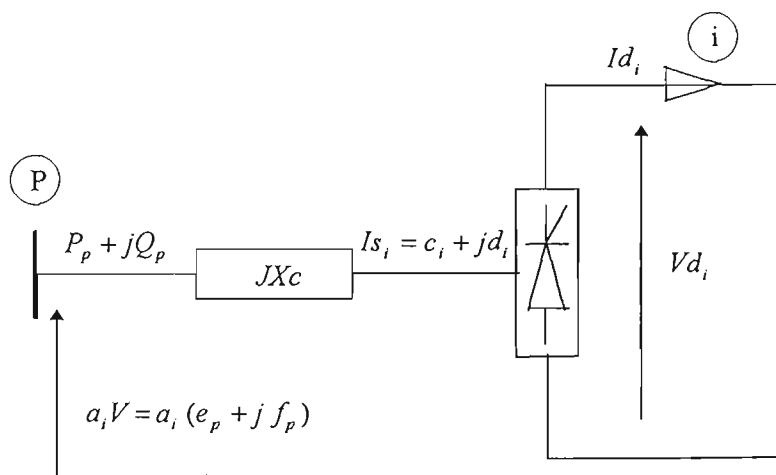


Fig. 2.2 Thevenin's equivalent of the HVDC model

the purpose of mathematical model the following simple assumptions are made:

- The three phase voltage at a converter terminal busbar is balanced and sinusoidal at system frequency.
- Converter valves are ideal (no voltage drop) and converter operation is balanced.
- Converter transformer is lossless and its magnetising admittance is negligible.
- DC voltages and currents are smooth (ripple free).
- Effect of the overlap angle (μ) whilst establishing a relationship between the secondary current of the converter transformer and converter current is neglected.

The above assumptions are reasonable and made for the polar co-ordinate formulation as well.

2.2.2 Mathematical Model for Rectangular Co-ordinates

The performance equations using the converter variables in the rectangular coordinates are derived. The variables are expressed in the per-unit system (Appendix A).

The dc voltage Vd_i at the converter terminal 'i' is

$$Vd_i = k_1 a_i \cos \theta_i |V_p| - S_i k_2 Xc_i Id_i \quad (2.1)$$

where

$$V_p = \text{ac terminal voltage}$$

a_i = converter transformer tap

Xc_i = commutating reactance

Id_i = dc current

k_1 = $3 \sqrt{2/\pi}$

k_2 = $3/\pi$

S_i = 0 if no converter at ac busbar

= 1 if converter at ac busbar 'P' is a rectifier

= -1 if converter at ac busbar 'P' is an inverter

θ_i = converter control angle

= α_i for rectifier operation

= γ_i for inverter operation.

Expressing V_p in the rectangular co-ordinates

$$Vd_i = k_1 a_i \cos \theta_i (e_p^2 + f_p^2)^{1/2} - S_i k_2 Xc_i Id_i \quad (2.2)$$

Squaring both sides and after rearranging the above equation can be written as

$$(k_1 a_i \cos \theta_i)^2 (e_p^2 + f_p^2) - (Vd_i + S_i k_2 Xc_i Id_i)^2 = 0 \quad (2.3)$$

where

$$V_p = e_p + j f_p$$

The complex power injection $(P_p + jQ_p)$ in to the HVDC converter at ac terminal busbar 'P' is

$$P_p + jQ_p = S_i V_p I_p^* = S_i a_i V_p Is_i^* \quad (2.4)$$

Expressing V_p and Is_i in the rectangular co-ordinates

$$P_p + jQ_p = S_i a_i (e_p + jf_p)(c_i + jd_i)$$

or

$$P_p + jQ_p = S_i a_i [(e_p c_i - f_p d_i) + j(e_p d_i + f_p c_i)] \quad (2.5)$$

where

I_p = primary side current

$I_{s_i} = (c_i + jd_i)$ = secondary side current.

The real power P_p from equation (2.5)

$$P_p = S_i a_i (e_p c_i - f_p d_i) \quad (2.6)$$

Neglecting losses in the converter and converter transformer the following relationship hold good

$$P_{ac} = P_{dc} \quad (2.7)$$

Therefore, the real power injection into the HVDC converter in terms of the dc voltage and current is

$$P_p = Vd_i Id_i \quad (2.8)$$

From equations (2.6) and (2.8)

$$Vd_i Id_i - S_i a_i (e_p c_i - f_p d_i) = 0 \quad (2.9)$$

The dc current injection at the dc busbar 'i' in terms of dc network conductance and dc busbar voltage is

$$Id_i = \sum_{j=1}^{N_{dc}} Gdc_{ij} Vd_j \quad (2.10)$$

where

Gdc_{ij} = i,jth element of dc network conductance matrix

N_{dc} = number of dc busbars.

Rearranging equation (2.10)

$$Id_i - \sum_{j=1}^{N_{dc}} G_{dc_{ij}} Vd_j = 0 \quad (2.11)$$

The secondary current of the converter transformer is related to the dc current as shown in equation (2.12) is

$$k_1 Id_i = |Is_i| = (c_i^2 + d_i^2)^{1/2} \quad (2.12)$$

Squaring both sides of equation (2.12) and after rearranging

$$(k_1 Id_i)^2 - (c_i^2 + d_i^2) = 0 \quad (2.13)$$

For a HVDC converter operating under the balanced condition from a known ac terminal voltage, only two independent variables Vd and Id are sufficient. However, the control requirements of the converter involve additional variables. In the rectangular co-ordinate formulation, a set of six variables $[Vd, Id, a, c, d, \cos\theta]$ are required for the modelling of the HVDC converter. Whereas, in the polar coordinate formulation, five variables $[Vd, Id, a, \phi, \cos\theta]$ are sufficient. In the latter case the converter secondary current angle is taken as the reference [5]. The choice of $\cos\theta$ instead of θ as a primary dc variable removes the trigonometric non-linearity from the system equations.

The evaluation of the six variables of the converter model in the rectangular co-ordinate requires six independent equations. Of the six, four equations are characterised by the mathematical model as expressed in equations (2.3), (2.9), (2.11) and (2.13). The other two independent

equations are obtained from the specified control strategy for the converter operation.

The converter controls normally specified are :

$$\text{i) Specified dc voltage } Vd_i - Vd_i^{sp} = 0 \quad (2.14)$$

$$\text{ii) Specified dc current } Id_i - Id_i^{sp} = 0 \quad (2.15)$$

$$\text{iii) Specified dc power } Pd_i - Pd_i^{sp} = 0 \quad (2.16)$$

$$\text{iv) Specified firing angle } \theta \quad \cos\theta_i - \cos\theta_i^{sp} = 0 \quad (2.17)$$

v) Specified converter transformer tap position

$$a_i - a_i^{sp} = 0 \quad (2.18)$$

vi) Specified converter reactive power

$$a_i (e_p d_i + f_p c_i) - Q_i^{sp} = 0 \quad (2.19)$$

These control equations are simple and easily incorporated into the solution algorithm.

The P-V, P-I and V-I controls being over specified are normally not used. For the load flow analysis, the mathematical model of a HVDC converter is written in the residual form. The residual in the concise form is

$$\bar{R}_{ik} [\bar{X}d, \bar{e}, \bar{f}] = 0 \quad (2.20)$$

where

$$\Delta R_{i1} = (k_1 a_i \cos\theta_i)^2 (e_p^2 + f_p^2) - (Vd_i + S_i k_2 Xc_i Id_i)^2 \quad \text{from eqn.(2.3)}$$

$$\Delta R_{i2} = Vd_i Id_i - S_i a_i (e_p c_i - f_p d_i) \quad \text{from eqn.(2.9)}$$

$$\Delta R_{i3} = Id_i - \sum_{j=1}^{Nac} Gdc_{ij} Vd_j \quad \text{from eqn.(2.11)} \quad (2.21)$$

$$\Delta R_{i4} = (k_i Id_i)^2 - (c_i^2 + d_i^2) \quad \text{from eqn.(2.13)}$$

$$\Delta R_{i5} = \text{control equation}$$

$$\Delta R_{i6} = \text{control equation.}$$

Six equations similar to equation (2.21) are written for each converter. Such equations for all converters characterise the mathematical model of a dc system.

2.2.3 AC Network Model

In the rectangular co-ordinate formulation, the expressions for the real and reactive power injections at a busbar 'P' are given as follows :

For busbar 'P' without converter connection

$$P_P = \sum_{q=1}^{Nac} \{e_P (e_q G_{Pq} + f_q B_{Pq}) + f_P (f_q G_{Pq} - e_q B_{Pq})\} \quad (2.22)$$

and

$$Q_P = \sum_{q=1}^{Nac} \{f_P (e_q G_{Pq} + f_q B_{Pq}) - e_P (f_q G_{Pq} - e_q B_{Pq})\} \quad (2.23)$$

For busbar 'P' with converter 'i' connected to it

$$P_P = \sum_{q=1}^{Nac} \{e_P (e_q G_{Pq} + f_q B_{Pq}) + f_P (f_q G_{Pq} - e_q B_{Pq})\} \\ + a_i S_i (e_P c_i - f_P d_i) \quad (2.24)$$

and

$$Q_P = \sum_{q=1}^{Nac} \{ f_P (e_q G_{Pq} + f_q B_{Pq}) - e_P (f_q G_{Pq} - e_q B_{Pq}) \} + a_i t_i (f_P c_i + e_P d_i) \quad (2.25)$$

From equation (2.5) it is seen that the term $a_i S_i (e_P c_i - f_P d_i)$ is the real power injection into the converter 'i' and the term $a_i t_i (f_P c_i + e_P d_i)$ is the reactive power injection into the converter 'i'.

For all busbar the following relationship holds good

$$V_P^2 = e_P^2 + f_P^2 \quad (2.26)$$

The load flow model of the ac network is characterised by equations (2.22), (2.23) and (2.26).

2.3 FIRST ORDER AC-DC LOAD FLOW METHOD

One of the most recognised ac load flow method for the past few years is the NR method with the sparsity techniques and sub-optimal ordering. The method is popular due to its accuracy and convergence behaviour. The NR algorithm converges quadratically if the function has continuous first order derivatives in the neighbourhood of the solution. The technique which has been used to make NR method competitive with other load flow methods involve the solution of the Jacobian matrix equation and the preservation of the sparsity of the matrix by ordered triangular factorisation. Most of the conventional NR methods were used to solve load flow problems in ac system. However, in this thesis modified form of NR method has been developed in order to solve ac-dc load flow problem.

2.3.1 Mathematical Model

The load flow equations corresponding to a converter terminal ac busbar 'P' connected to a dc busbar 'i' is an ac-dc system are given by equations (2.21), (2.24) and (2.25). Expanding these equations in the Taylor series around the initial estimate $[e^0, f^0, Xd^0]^T$ one can obtain the followings:

From equation (2.24) it can be written

$$\begin{aligned}
 P_p - P_p^0 = \Delta P_p = & \sum_{q=1}^{Nac} \frac{\partial P_p}{\partial e_q} \Delta e_q + \sum_{q=1}^{Nac} \frac{\partial P_p}{\partial f_q} \Delta f_q + \sum_{j=1}^6 \frac{\partial P_p}{\partial Xd_{ij}} \Delta Xd_{ij} \\
 & + \frac{1}{2} \sum_{q=1}^{Nac} \frac{\partial^2 P_p}{\partial e_q^2} (\Delta e_q)^2 + \frac{1}{2} \sum_{q=1}^{Nac} \frac{\partial^2 P_p}{\partial f_q^2} (\Delta f_q)^2 \\
 & + \sum_{j=1}^6 \frac{\partial^2 P_p}{\partial Xd_{ij}^2} (\Delta Xd_{ij})^2 + \sum_{q=1}^{Nac-1} \sum_{r=q+1}^{Nac} \frac{\partial^2 P_p}{\partial e_q \partial e_r} \Delta e_q \Delta e_r \\
 & + \sum_{q=1}^{Nac} \sum_{r=1}^{Nac} \frac{\partial^2 P_p}{\partial e_q \partial f_r} \Delta e_q \Delta f_r + \sum_{q=1}^{Nac-1} \sum_{r=q+1}^{Nac} \frac{\partial^2 P_p}{\partial f_q \partial f_r} \Delta f_q \Delta f_r \\
 & + \sum_{q=1}^{Nac} \sum_{j=1}^6 \frac{\partial^2 P_p}{\partial e_q \partial Xd_{ij}} \Delta e_q \Delta Xd_{ij} + \sum_{q=1}^{Nac} \sum_{j=1}^6 \frac{\partial^2 P_p}{\partial f_q \partial Xd_{ij}} \Delta f_q \Delta Xd_{ij} \\
 & + \sum_{j=1}^5 \sum_{k=j+1}^6 \frac{\partial^2 P_p}{\partial Xd_{ij} \partial Xd_{ik}} \Delta Xd_{ij} \Delta Xd_{ik} + \text{higher order terms}
 \end{aligned} \tag{2.27}$$

From Equation (2.25) it can be written

$$\begin{aligned}
 Q_p - Q_p^0 = \Delta Q_p = & \sum_{q=1}^{Nac} \frac{\partial Q_p}{\partial e_q} \Delta e_q + \sum_{q=1}^{Nac} \frac{\partial Q_p}{\partial f_q} \Delta f_q + \sum_{j=1}^6 \frac{\partial Q_p}{\partial Xd_{ij}} \Delta Xd_{ij} \\
 & + \frac{1}{2} \sum_{q=1}^{Nac} \frac{\partial^2 Q_p}{\partial e_q^2} (\Delta e_q)^2 + \frac{1}{2} \sum_{q=1}^{Nac} \frac{\partial^2 Q_p}{\partial f_q^2} (\Delta f_q)^2
 \end{aligned}$$

$$\begin{aligned}
& + \sum_{j=1}^6 \frac{\partial^2 Q_p}{\partial X d_{ij}^2} (\Delta X d_{ij})^2 + \sum_{q=1}^{Nac-1} \sum_{r=q+1}^{Nac} \frac{\partial^2 Q_p}{\partial e_q \partial e_r} \Delta e_q \Delta e_r \\
& + \sum_{q=1}^{Nac} \sum_{r=1}^{Nac} \frac{\partial^2 Q_p}{\partial e_q \partial f_r} \Delta e_q \Delta f_r + \sum_{q=1}^{Nac-1} \sum_{r=q+1}^{Nac} \frac{\partial^2 Q_p}{\partial f_q \partial f_r} \Delta f_q \Delta f_r \\
& + \sum_{q=1}^{Nac} \sum_{j=1}^6 \frac{\partial^2 Q_p}{\partial e_q \partial X d_{ij}} \Delta e_q \Delta X d_{ij} + \sum_{q=1}^{Nac} \sum_{j=1}^6 \frac{\partial^2 Q_p}{\partial f_q \partial X d_{ij}} \Delta f_q \Delta X d_{ij} \\
& + \sum_{j=1}^5 \sum_{k=j+1}^6 \frac{\partial^2 Q_p}{\partial X d_{ij} \partial X d_{ik}} \Delta X d_{ij} \Delta X d_{ik} + \text{higher order terms}
\end{aligned} \tag{2.28}$$

From equation (2.26)

$$\begin{aligned}
V_p^2 - (V_p^0)^2 = \Delta V_p^2 = \frac{\partial (V_p)^2}{\partial e_q} \Delta e_q + \frac{\partial (V_p)^2}{\partial f_q} \Delta f_q + \frac{1}{2} \frac{\partial^2 (V_p)^2}{\partial e_p^2} \Delta e_p^2 \\
+ \frac{1}{2} \frac{\partial^2 (V_p)^2}{\partial f_p^2} \Delta f_p^2
\end{aligned} \tag{2.29}$$

From equation (2.21)

$$\begin{aligned}
R_{ij} - R_{ij}^0 = \Delta R_{ij} = \sum_{q=1}^6 \frac{\partial R_{ij}}{\partial e_p} \Delta e_p + \sum_{q=1}^6 \frac{\partial R_{ij}}{\partial f_p} \Delta f_p + \sum_{j=1}^6 \sum_{k=1}^6 \frac{\partial R_{ij}}{\partial X d_{ik}} \Delta X d_{ik} \\
+ \frac{1}{2} \sum_{j=1}^6 \frac{\partial^2 R_{ij}}{\partial e_p^2} (\Delta e_p)^2 + \frac{1}{2} \sum_{j=1}^6 \frac{\partial^2 R_{ij}}{\partial f_p^2} (\Delta f_p)^2 \\
+ \frac{1}{2} \sum_{j=1}^6 \sum_{k=1}^6 \frac{\partial^2 R_{ij}}{\partial X d_{ik}^2} (\Delta X d_{ik})^2 + \sum_{j=1}^6 \frac{\partial^2 R_{ij}}{\partial e_p \partial f_p} \Delta e_p \Delta f_p \\
+ \sum_{j=1}^6 \sum_{k=1}^6 \frac{\partial^2 R_{ij}}{\partial e_p \partial X d_{ik}} \Delta e_p \Delta X d_{ik} + \sum_{j=1}^6 \sum_{l=1}^6 \frac{\partial^2 R_{ij}}{\partial f_p \partial X d_{il}} \Delta f_p \Delta X d_{il} \\
+ \sum_{j=1}^6 \sum_{k=1}^6 \sum_{l=k+1}^6 \frac{\partial^2 R_{ij}}{\partial X d_{ik} \partial X d_{il}} \Delta X d_{ik} \Delta X d_{il} + \text{higher order terms}
\end{aligned} \tag{2.30}$$

Truncating the Taylor series as given by equations (2.28) to (2.30) after the first order derivatives, a linearised relationship between the residuals and errors can be written as:

$$\begin{bmatrix} \Delta P \\ \Delta Q \\ |\Delta V|^2 \\ \Delta R \end{bmatrix} = \begin{bmatrix} J \end{bmatrix} \begin{bmatrix} \Delta e \\ \Delta f \\ \Delta Xd \end{bmatrix} \quad (2.31)$$

Equation (2.31) in an iterative scheme

$$\begin{bmatrix} \Delta P \\ \Delta Q \\ |\Delta V|^2 \\ \Delta R \end{bmatrix}^{(k)} = \begin{bmatrix} J \end{bmatrix}^{(k)} \begin{bmatrix} \Delta e \\ \Delta f \\ \Delta Xd \end{bmatrix}^{(k+1)} \quad (2.32)$$

where

J = Jacobian matrix (first order derivatives of the Taylor series)

ΔP = real power mismatch

ΔQ = reactive power mismatch

ΔV = error in nodal voltage

ΔR = residual for dc network and interface

k = iteration count.

The elements of the Jacobian matrix 'J' are derived in Appendix - B. It is square, sparse and real matrix. Equation (2.32) is solved using Gaussian forward elimination and backward substitution method. Alternative schemes involving factorised form of 'J' or bi-factorisation of 'J' are also possible. 'J' is extremely sparse, so the sparsity technique can be employed to conserve

the memory and enhance the computational efficiency.

2.3.2 Solution Steps

- Step 1 : Read system data and converter control specifications.
- Step 2 : Initialise state vector $[X^0] = [e^0, f^0, Xd^0]^T$.
- Step 3 : Compute the elements of the ac and dc network admittance matrices $(G_{ij} + jB_{ij})$ and Gdc_{ij} .
- Step 4 : Set iteration count, $k = 0$.
- Step 5 : Compute the Jacobian matrix $[J]^k$. Triangularise and store the factors of 'J' using sparsity technique.
- Step 6 : Compute the mismatch vector $[\Delta P, \Delta Q, |\Delta V|^2, \Delta R]^k$.
- Step 7 : Perform forward and backward operations on the mismatch vector to obtain new values of changes in state vector $[\Delta e, \Delta f, \Delta R]^{(k+1)}$.
- Step 8 : Update new values of the state vector
- $$e^{(k+1)} = e^{(k)} + \Delta e^{(k+1)} ; f^{(k+1)} = f^{(k)} + \Delta f^{(k+1)}$$
- $$\text{and } Xd^{(k+1)} = Xd^{(k)} + \Delta Xd^{(k+1)}$$
- Step 9 : Check for convergence

$$\begin{vmatrix} \Delta P^{(k)} \\ \Delta Q^{(k)} \\ |\Delta V^2|^{(k)} \\ \Delta R^{(k)} \end{vmatrix} \leq \text{(the specified tolerance)}$$

or

$$\begin{vmatrix} \Delta e^{(k+1)} \\ \Delta f^{(k+1)} \\ \Delta Xd^{(k+1)} \end{vmatrix} \leq \epsilon \quad (\text{the specified tolerance})$$

If converged go to step 11. Otherwise, go to step 10.

Step 10 : Set $k = k+1$ and go to step 5.

Step 11 : Compute slack bus power line flows etc. Output results and stop.

The flow chart of the algorithm is shown in Fig. 2.3.

2.4 CONCLUSIONS

In this chapter a new mathematical model for ac-dc load flow has been developed. In this formulation the first order derivatives of the Taylor series are considered to develop the mathematical model. The second, third and other higher order terms which are not zero are neglected in this formulation. The ac, dc and converter (interface) system equations are formulated in the cartesian coordinate. This method is actually the conventional NR technique with some modification. The method offers an uniquely attractive combination of advantages over the established methods, including NR, in terms of speed, reliability, simplicity and storage, for conventional ac-dc load flow solutions. The basic algorithm remains unchanged for a variety of different applications. Given a set of good ordered elimination routines, the basic program is easy to code efficiently, and its speed and storage requirements are roughly proportional to system size. The method can be faithfully applied to a number of power system

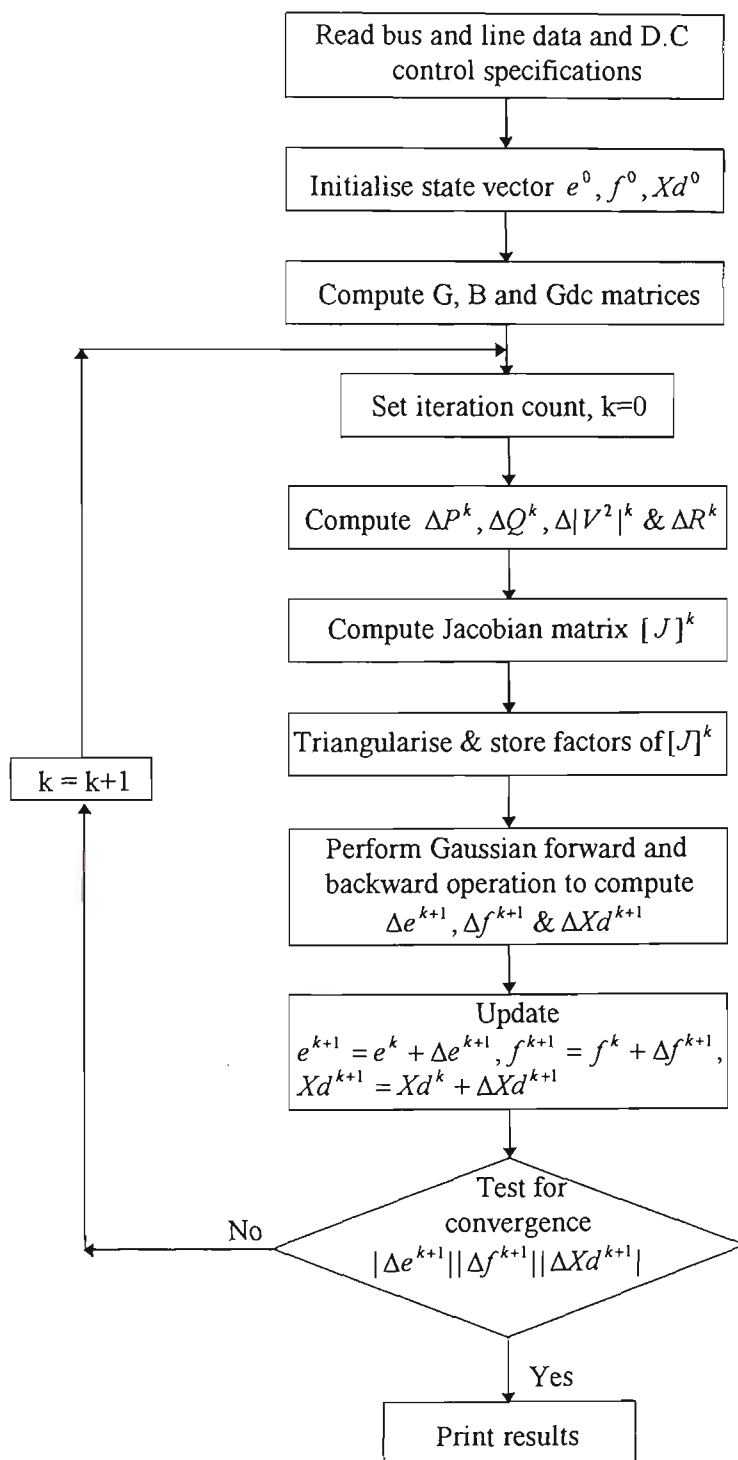


Fig. 2.3 Flow chart for FRLF

cases where the other methods do not perform satisfactorily.

Chapter 3

SECOND AND DECOUPLED SECOND ORDER AC-DC LOAD FLOW IN RECTANGULAR CO-ORDINATES

3.1 INTRODUCTION

The solution of load flow problems is one of the most essential issues in power system operation and planning. Hundreds of contributions have been offered in the literature to overcome these problems [7]. The main properties that are required of a load flow solution method are high computational speed, low computer storage, reliability of solution, versatility and simplicity. Over the last few decades, the Newton-Raphson (NR) method has emerged as the most prominent load flow algorithm. Therefore, most of the researchers in this field have centred on the NR algorithm for the past many years. With sparse programming techniques and optimally ordered triangular factorisation, the NR method for solving load flow problem has become faster. However, the computer storage requirements of this method are greater and the time per iteration rises nearly linearly with the number of system buses. Another problem of this approach is that it can diverge very rapidly or converge to the wrong solution if the equations are not well behaved or if the starting voltages are badly chosen [95].

One of the algorithms that has attracted considerable attention in the past few years is the second order load flow. This approach transforms the non-linear load flow equation to a linear form before a solution is attempted. It is also possible to formulate the load flow problem by using the first three terms of the Taylor series. Sachdev *et al.* [100] have tried to improve the convergence properties and reliability of NR method by retaining the second order terms in the Taylor series expansion. However, the formulation is in polar co-ordinate. In polar co-ordinate formulation also involves neglecting all the higher order terms in the series expansion. Furthermore, when this method is compared with the NR and fast decoupled (FD) load flow methods, it does not offer any advantage from the point of view of either memory or computing time. El-Hawary *et al.* [14] have proposed an alpha modified quasi second order NR load flow technique in rectangular co-ordinates. However, both these second order load flow methods employ variable Jacobians. Rectangular co-ordinate formulation has the advantage that the Taylor series expansion of the load flow equations contains terms up to the second order derivatives only. Realising this feature, Iwamoto *et al.* [12], Roy [11] and Rao *et al.* [40] have developed constant matrix second order load flow algorithms. The Jacobian matrix in Iwamoto's model is unsymmetric, whereas it is symmetric in Roy and Rao's methods. Though these methods considerably reduce the solution time as compared with the NR method, however they are quite inferior as compared to the FD load flow method from the point of view of both memory and computing time.

Another distinctly different class of algorithms which have gained popularity in the last few years is the decoupled NR algorithm. This method utilises some justifiable network assumptions, the weak coupling between active powers and bus voltage angles, and between reactive powers and bus voltage magnitudes,

such as, $\cos(\delta_p - \delta_q) \cong 1$, $G_{pq} \sin(\delta_p - \delta_q) \ll B_{pq}$ and $Q_p \ll B_{pp} E_p^2$. These assumptions are valid for ideal conditions. Among the decoupled versions, the fast decoupled load flow method suggested by Stott *et al.* [10] is possibly the most popular method and most widely used by the power industries because of its simplicity and computational efficiency. Though FD load flow method is efficient but it exhibits poor convergence specially with ill-conditioned networks. The presence of lines with high R/X ratios in power networks poses a serious limitation to FD load flow algorithms. Moreover, when a line is overloaded the angular differences between the two adjacent nodes may not be neglected. In order to overcome these difficulties Haque [96], Monticelli *et al.* [101] proposed a decoupled load flow method without ignoring the coupling sub-Jacobians but their algorithm was in polar co-ordinates. Their methods considerably reduces the solution time and it performs well under ill-conditioned networks. However, one obvious disadvantage with the algorithms in polar co-ordinates is that the power calculations during the iterative process becomes time consuming, due to the involved computations of the trigonometric functions. Also, Nanda *et al.* [45] developed a decoupled load flow algorithm without neglecting the coupling sub-jacobians in rectangular co-ordinate. The method performs well under ill-conditioned networks as well as it reduces the computing time. However, all the above discussions are pertinent to ac load flow only.

It was stated in Chapter 2 that the simultaneous solution of the ac-dc load flow equations increases the programming complexity; and is somewhat less flexible but computationally more efficient than the sequential approach which requires a repeat solution of both ac and dc system equations in order to match the ac-dc interface conditions. It was also stated that second order (SO) algorithms for the ac system load flow are computationally more efficient and reliable than the

NR and the computing time and convergence characteristics of decoupled second order (DSO) algorithms are comparable to the FD load flow algorithms. So far, the SO and DSO techniques have not been applied to ac-dc systems. The main objective of this chapter is to develop a load flow algorithms for the ac-dc systems based on the SO and DSO techniques. The new method is based on the cartesian co-ordinate formulation of network performance equations and a complete Taylor series representation of these equations, without involving any major approximation. As there is no major approximation involved in the development of the method, the new algorithm is exact, and performs quite well on different kinds of power system. Digital simulation studies on a number of tests and real power systems indicate that the algorithms are not only superior to the NR method, but their performance is even better than the FD method.

3.2 SECOND ORDER AC-DC LOAD FLOW METHOD

An ac-dc load flow problem consists of solving a set of quadratic algebraic equations. Upon taking Taylor series expansion of these equations, it is seen that the equations are expressed completely up to the third order terms (except some converter equation) which has the same form but different variables as the first order terms. In other words, it is possible to formulate the ac-dc load flow problem by using the first three terms of the Taylor series. The advantage of full Taylor series expansion is that, it is possible to keep the elements of the Jacobian matrix as constant and needs to be computed once in the iterative process, which reduces the computing time drastically. As there is no major approximation in the mathematical model the solution is more exact and it performs well under different operating conditions.

3.2.1 Mathematical Model

An inspection of the load flow equations (2.22) to (2.26) indicate that they are quadratic in 'e' and 'f'. As such their Taylor series expansion contain terms upto the second order derivatives only. However, for the converter busbars, the Taylor series expansion of these equations contain terms upto the third order derivatives. The number of converter busbars in any practical system will be very few compared to the ac busbars, resulting in very few equations containing the third order terms. There are six equations in equation (2.21). Out of the six, the Taylor series expansion of the first two (R_{i1} and R_{i2}) contains derivatives beyond the second order. However, the Taylor series expansion of (R_{i3} , R_{i4} , R_{i5} and R_{i6}) terminates within the second order terms.

It is observed that except two converter equations, rest of the equations have terms upto the second order derivatives in their Taylor series. Therefore, a new mathematical model for ac-dc load flow including the second order derivatives is developed. The new method inspite of exact, in some cases perform better than FD load flow method.

Considering the second order derivatives the relationship between the residuals and errors in the concise matrix form is :

$$\begin{bmatrix} \Delta P \\ \Delta Q \\ |\Delta V|^2 \\ \Delta R \end{bmatrix} = \begin{bmatrix} J \end{bmatrix} \begin{bmatrix} \Delta e \\ \Delta f \\ \Delta Xd \end{bmatrix} + \frac{1}{2} [L] \begin{bmatrix} \Delta e \ \Delta e \\ \Delta e \ \Delta f \\ \Delta f \ \Delta e \\ \Delta f \ \Delta f \\ \Delta e \ \Delta Xd \\ \Delta f \ \Delta Xd \\ \Delta Xd \ \Delta e \\ \Delta Xd \ \Delta f \\ \Delta Xd \ \Delta Xd \end{bmatrix} \quad (3.1)$$

Equation (3.1) in the reorganised form is

$$\begin{bmatrix} \Delta P \\ \Delta Q \\ |\Delta V|^2 \\ \Delta R \end{bmatrix} = \begin{bmatrix} J_1 & J_2 & J_3 \\ J_4 & J_5 & J_6 \\ J_7 & J_8 & J_9 \\ J_{10} & J_{11} & J_{12} \end{bmatrix} \begin{bmatrix} \Delta e \\ \Delta f \\ \Delta Xd \end{bmatrix} + \begin{bmatrix} S_P \\ S_Q \\ S_V \\ S_R \end{bmatrix} \quad (3.2)$$

where S_P , S_Q , S_V and S_R contain the second order terms in the concise form.

A further reorganisation of equation (3.2) yields

$$\begin{bmatrix} J \end{bmatrix} \begin{bmatrix} \Delta e \\ \Delta f \\ \Delta Xd \end{bmatrix} = \begin{bmatrix} \Delta P \\ \Delta Q \\ |\Delta V|^2 \\ \Delta R \end{bmatrix} - \begin{bmatrix} S_P \\ S_Q \\ S_V \\ S_R \end{bmatrix} \quad (3.3)$$

or,

$$\begin{bmatrix} J \end{bmatrix} \begin{bmatrix} \Delta e \\ \Delta f \\ \Delta Xd \end{bmatrix} = \begin{bmatrix} \Delta P' \\ \Delta Q' \\ \Delta V' \\ \Delta R' \end{bmatrix} \quad (3.4)$$

where

$$\begin{aligned}
\Delta P' &= \Delta P - S_P \\
\Delta Q' &= \Delta Q - S_Q \\
\Delta V' &= |\Delta V|^2 - S_V \\
\Delta R' &= \Delta R - S_R
\end{aligned} \tag{3.5}$$

Equation (3.4) in an iterative scheme is

$$\begin{bmatrix} \Delta P' \\ \Delta Q' \\ \Delta V' \\ \Delta R' \end{bmatrix}^{(k)} = \begin{bmatrix} J^0 \end{bmatrix} \begin{bmatrix} \Delta e \\ \Delta f \\ \Delta Xd \end{bmatrix}^{(k+1)} \tag{3.6}$$

where

k = iteration count, and

$$\begin{bmatrix} \Delta P' \\ \Delta Q' \\ \Delta V' \\ \Delta R' \end{bmatrix}^{(k)} = \begin{bmatrix} \Delta P^0 - S_P^k \\ \Delta Q^0 - S_Q^k \\ |\Delta V^0|^2 - S_V^k \\ \Delta R^0 - S_R^k \end{bmatrix} \tag{3.7}$$

J^0 is the Jacobian matrix evaluated using the initial estimated values of the vectors e^0 , f^0 and Xd^0 . J^0 remains constant in the iterative solution process. It is well known that if a function is quadratic in unknowns and if the first and second order derivatives of the Taylor series are included in the solution model, then the solution is obtained in one iteration for the quadratic function. However, if the function is non-linear, an iterative scheme is needed. In both the cases the first order derivatives (Jacobian matrix) is evaluated at the initial estimate and remains constant. The second notable difference between the proposed and previously presented methods is that in the present case Δe , Δf

and ΔXd are updated in the iterative solution scheme. In the existing methods e , f and Xd are updated in the recursive scheme.

The correction in the state vectors Δe , Δf , and ΔXd are obtained from

$$\begin{bmatrix} \Delta e \\ \Delta f \\ \Delta Xd \end{bmatrix}^{(k+1)} = \begin{bmatrix} J^0 \end{bmatrix}^{-1} \begin{bmatrix} \Delta P' \\ \Delta Q' \\ \Delta V' \\ \Delta R' \end{bmatrix}^k \quad (3.8)$$

The iteration is counted until the changes in $[\Delta e, \Delta f, \Delta Xd]^T$ or the mismatch vectors $[\Delta P', \Delta Q', \Delta R']^T$ between the consecutive iterations become less than a specified tolerance.

That is if

$$\begin{aligned} |\Delta P'|^{(k+1)} - |\Delta P'|^{(k)} \\ |\Delta Q'|^{(k+1)} - |\Delta Q'|^{(k)} &\leq \epsilon \\ |\Delta V'|^{(k+1)} - |\Delta V'|^{(k)} \\ |\Delta R'|^{(k+1)} - |\Delta R'|^{(k)} \end{aligned} \quad (3.9)$$

or

$$\begin{aligned} |\Delta e|^{(k+1)} - |\Delta e|^{(k)} \\ |\Delta f|^{(k+1)} - |\Delta f|^{(k)} &\leq \epsilon \\ |\Delta Xd|^{(k+1)} - |\Delta Xd|^{(k)} \end{aligned} \quad (3.10)$$

The mathematical model characterised by equation (3.8) denotes the proposed second order rectangular co-ordinate ac-dc load flow (SRLF) method.

3.2.2 Salient Features of SRLF Algorithm

The salient features of the SRLF ac-dc load flow algorithm are as follows:

- The Jacobian matrix remains constant in the iterative solution scheme. This contrasts sharply with the FRLF algorithm in which the Jacobian matrix is evaluated and factorised in each iteration.
- The first iteration of the SRLF and FRLF algorithms is similar because for the first iteration the incremental values of all the variables are zero. Therefore, the second order terms S_P , S_Q , S_V and S_R are also zero.
- For the second and subsequent iterations the modified mismatch vector $[\Delta P', \Delta Q', \Delta V', \Delta R']^T$ are computed using equation (3.7). This requires the calculation of the second order terms only. The calculation of ΔP_P , ΔQ_P , $|\Delta V_P|^2$, and ΔR_{ij} is not required in each iteration. The second order terms are neither calculated nor stored in the matrix form. Each element of S_P , S_Q , S_V and S_R is computed using the network matrix elements and errors Δe , Δf , and ΔXd . This eliminates the need to store the second order terms in the matrix form.
- Since the Jacobian matrix is neither calculated nor triangularised after the first iteration, the computational burden in the second and subsequent iterations become considerably less. Hence, the second and subsequent iterations are termed as

sub-iterations, in order to differentiate this from the first iteration.

- The use of constant Jacobian matrix in the SRLF algorithm implies that its convergence is no longer quadratic. Therefore, the SRLF algorithm is expected to require a few more sub-iterations than the number of iterations in the FRLF algorithm.
- The use of constant Jacobian matrix in the SRLF algorithm considerably reduces the computational burden, making it faster than the FRLF method even though the SRLF method requires more sub-iterations to obtain a converged solution.
- The computer memory requirement of the SRLF method is similar to that in the FRLF method. However, it is more than in the fast decoupled method.
- The SRLF seems to be faster than the FRLF but not so than the FDLF.

3.2.3 Solution Steps

The sequence of steps for the SRLF algorithm are given below:

- Step 1 : Read system data and converter control specifications.
- Step 2 : Initialise the state vector $[e^0, f^0, Xd^0]^T$ and set $\Delta e^0 = 0$, $\Delta f^0 = 0$ and $\Delta Xd^0 = 0$.
- Step 3 : Compute the elements of the ac and dc network admittance matrices $(G_{ij} + jB_{ij})$ and Gdc_{ij} .

Step 4 : Compute the elements of the Jacobian matrix $[J^0]$ using initial state. Triangularise and store the factors of J^0 .

Step 5 : Compute the mismatch and residual vectors $[\Delta P, \Delta Q, |\Delta V|^2 \text{ \& } \Delta R]^{(0)}$.

Step 6 : Solve

$$\begin{bmatrix} J^0 \end{bmatrix} \begin{bmatrix} \Delta e \\ \Delta f \\ \Delta Xd \end{bmatrix} = \begin{bmatrix} \Delta P' \\ \Delta Q' \\ \Delta V' \\ \Delta R' \end{bmatrix}^{(0)}$$

for Δe , Δf , and ΔXd .

Step 7 : Set iteration count $k = 0$.

Step 8 : Compute the $\Delta P'^{(k)}$, $\Delta Q'^{(k)}$, $\Delta V'^{(k)}$ and $\Delta R'^{(k)}$ using latest values of Δe , Δf , and ΔXd .

Step 9 : Solve
$$\begin{bmatrix} J \end{bmatrix}^0 \begin{bmatrix} \Delta e \\ \Delta f \\ \Delta Xd \end{bmatrix}^{(k+1)} = \begin{bmatrix} \Delta P' \\ \Delta Q' \\ \Delta V' \\ \Delta R' \end{bmatrix}^k$$

for $\Delta e^{(k+1)}$, $\Delta f^{(k+1)}$, and $\Delta Xd^{(k+1)}$.

Step 10 : Check for convergence using

$$\begin{aligned} |\Delta e|^{(k+1)} - |\Delta e|^{(k)} \\ |\Delta f|^{(k+1)} - |\Delta f|^{(k)} \\ |\Delta Xd|^{(k+1)} - |\Delta Xd|^{(k)} \end{aligned} \leq \epsilon$$

or

$$\begin{aligned}
|\Delta P'|^{(k+1)} - |\Delta P'|^{(k)} \\
|\Delta Q'|^{(k+1)} - |\Delta Q'|^{(k)} &\leq \epsilon \\
|\Delta V'|^{(k+1)} - |\Delta V'|^{(k)} \\
|\Delta R'|^{(k+1)} - |\Delta R'|^{(k)}
\end{aligned}$$

Step 11 : Repeat steps 8 through 10, until convergence criteria are satisfied .

Step 12 : Update values of state vector are

$$\begin{aligned}
e &= e^0 + \Delta e^{(k+1)} \\
f &= f^0 + \Delta f^{(k+1)} \\
Xd &= Xd^0 + \Delta Xd^{(k+1)}
\end{aligned}$$

Step 13: Compute the slack bus power and the line flows for ac and dc networks.

The flow chart of the SRLF algorithm is given in Fig. 3.1

3.3 DECOUPLED SECOND ORDER AC-DC LOAD FLOW METHOD

Since SRLF method is superior than conventional NR method in terms of computing time and it gives solutions for a number of networks whereas NR method takes longer time and FD method sometimes fail. However, the computing time of SRLF method is not superior than FD load flow method. Most of the reported FD load flow methods are derived from the Newton method by neglecting the coupling sub-Jacobians. For a system having high R/X ratio of all branches, the convergence pattern of decoupled load flow methods may be directed by the coupling sub-Jacobians rather than the

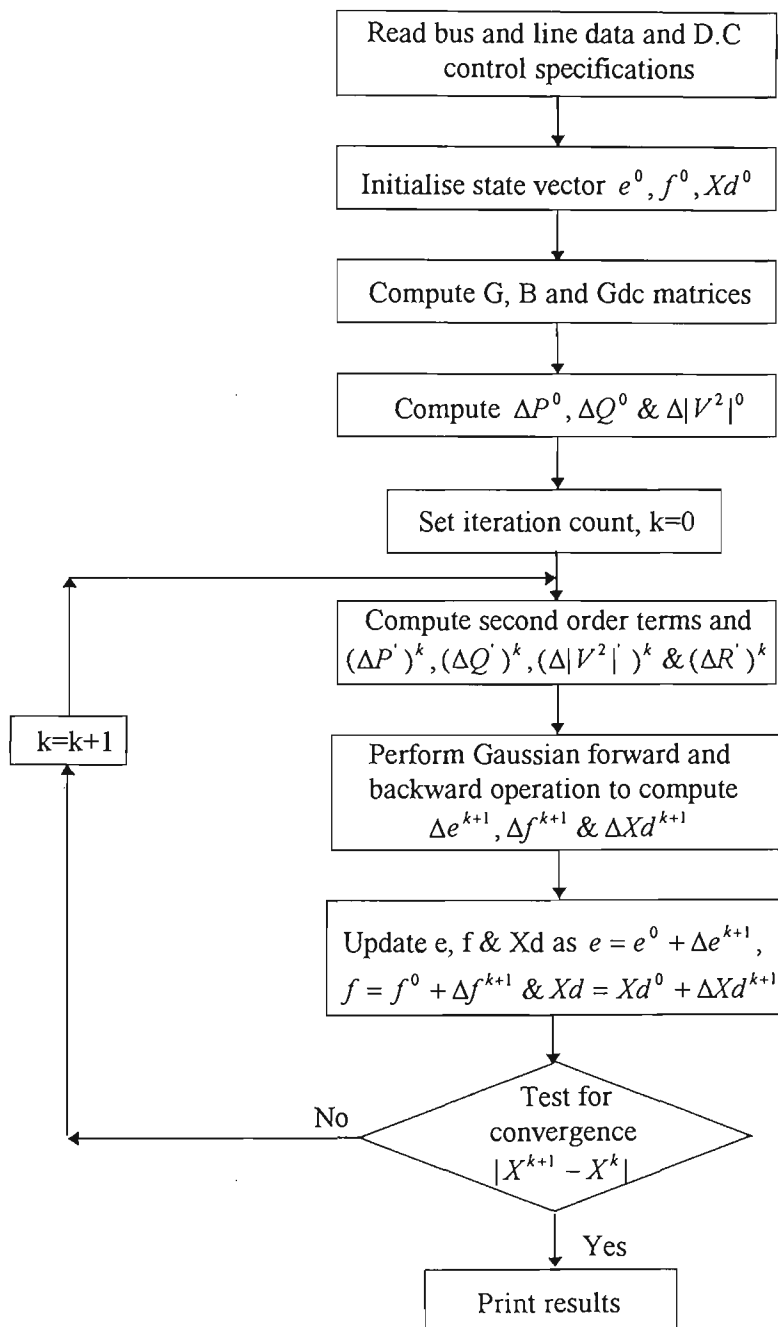


Fig. 3.1 Flow chart for SRLF

diagonal sub-Jacobians. A practical power system may not consist of such high R/X ratio branches. However, any decoupled ac-dc load flow equations derived from the Newton method, taking into account the effects of all sub-Jacobians, will offer a good convergence pattern, especially for systems having relatively high R/X ratio branches. In the proposed technique, decoupling is done by the SRLF method with some intelligent technique rather than ignoring most of the coupling sub-Jacobians. This results saving in solution time and computer storage.

3.4 Mathematical Model

A careful examination of the structure of the SRLF mathematical model of section (3.2) reveals the following features :

1. The elements of the submatrix J_2 are much larger than the corresponding elements of the submatrices J_1 and J_3 .
2. The elements of the submatrix J_4 are much larger than the corresponding elements of the submatrices J_5 and J_6 .
3. The elements of the submatrix J_7 are much larger than the corresponding elements of the submatrices J_8 and J_9 .
4. The elements of the submatrix J_{12} are much larger than the corresponding elements of the submatrices J_{10} and J_{11} .

This implies that

- Submatrix $J_2 = [\partial P / \partial f]$ dominates the relationship for the ac busbar real power injections.
- Submatrix $J_4 = [\partial Q / \partial e]$ dominates the relationship for the busbar reactive power injections.

- Submatrix $J_7 = [\partial V^2 / \partial e]$ dominates the relationship for the ac busbar voltage magnitudes.
- Submatrix $J_{12} = [\partial R / \partial Xd]$ dominates the relationship for the dc residuals.

Exploiting the above features, an improved faster version of the SRLF ac-dc load flow, known as decoupled second order rectangular coordinate ac-dc load flow (DSRLF) has been developed.

The SRLF ac-dc load flow model given by equations (3.4) and (3.8) can be written as:

$$\begin{bmatrix} \Delta P' \\ \Delta Q' \\ \Delta V' \\ \Delta R' \end{bmatrix} = \begin{bmatrix} J_1 & J_2 & J_3 \\ J_4 & J_5 & J_6 \\ J_7 & J_8 & J_9 \\ J_{10} & J_{11} & J_{12} \end{bmatrix} \begin{bmatrix} \Delta e \\ \Delta f \\ \Delta Xd \end{bmatrix} \quad (3.11)$$

Equation (3.11) can be written in decoupled form

$$\Delta P' = J_1 \Delta e + J_2 \Delta f + J_3 \Delta Xd$$

$$\Delta Q' = J_4 \Delta e + J_5 \Delta f + J_6 \Delta Xd \quad (3.12)$$

$$\Delta V' = J_7 \Delta e + J_8 \Delta f + J_9 \Delta Xd$$

$$\Delta R' = J_{10} \Delta e + J_{11} \Delta f + J_{12} \Delta Xd$$

Rearranging the above equations, one can get

$$\Delta P' - J_1 \Delta e - J_3 \Delta Xd = J_2 \Delta f \quad (3.13)$$

$$\Delta Q' - J_5 \Delta f - J_6 \Delta Xd = J_4 \Delta e \quad (3.14)$$

$$\Delta V' - J_8 \Delta f - J_9 \Delta Xd = J_7 \Delta e \quad (3.15)$$

$$\Delta R' - J_{10} \Delta e - J_{11} \Delta f = J_{12} \Delta Xd \quad (3.16)$$

Equations (3.14) and (3.15) are combined together and the resulting equation can be written as

$$\Delta QV' - J_{14} \Delta f - J_{15} \Delta Xd = J_{13} \Delta e \quad (3.17)$$

where

$$\Delta QV' = [\Delta Q' \Delta V']^T$$

$$J_{13} = \begin{bmatrix} J_4 \\ J_7 \end{bmatrix}; \quad J_{14} = \begin{bmatrix} J_5 \\ J_8 \end{bmatrix}; \quad J_{15} = \begin{bmatrix} J_6 \\ J_9 \end{bmatrix} \quad \text{and}$$

T = transpose.

Equations (3.13) to (3.16) can be written in an iterative scheme

$$\Delta P' - J_1^0 \Delta e - J_3^0 \Delta Xd = J_2^0 \Delta f^{(k+1)} \quad (3.18)$$

$$\Delta QV' - J_{14}^0 \Delta f - J_{15}^0 \Delta Xd = J_{13}^0 \Delta e^{(k+1)} \quad (3.19)$$

$$\Delta R' - J_{10}^0 \Delta e - J_{11}^0 \Delta f = J_{12}^0 \Delta Xd^{(k+1)} \quad (3.20)$$

And in concise form it is

$$(\Delta P'')^k = J_2^0 \Delta f^{(k+1)} \quad (3.21)$$

$$(\Delta Q'')^k = J_{13}^0 \Delta e^{(k+1)} \quad (3.22)$$

$$(\Delta R'')^k = J_{12}^0 \Delta Xd^{(k+1)} \quad (3.23)$$

where

$$(\Delta P'')^k = (\Delta P')^k - J_1^0 \Delta e^k - J_3^0 \Delta Xd^k \quad (3.24)$$

$$(\Delta Q'')^k = (\Delta QV')^k - J_{14}^0 \Delta f^k - J_{15}^0 \Delta Xd^k \quad (3.25)$$

$$(\Delta R'')^k = (\Delta R')^k - J_{10}^0 \Delta e^k - J_{11}^0 \Delta f^k \quad (3.26)$$

Equations (3.21) to (3.23) are solved sequentially using the Gaussian forward and backward substitution method in order to evaluate the state vectors $\Delta f^{(k+1)}$, $\Delta e^{(k+1)}$ and $\Delta Xd^{(k+1)}$.

The mathematical model characterised by equations (3.21) to (3.23) represent decoupled second order rectangular co-ordinate ac-dc load flow (DSRLF) method.

3.3.2 Distinguishing Features of the DSRLF Algorithm

The distinguishing features of the DSRLF ac-dc load flow algorithm are outlined below:

- Submatrices J_2^0 , J_{13}^0 and J_{12}^0 are evaluated using the system parameters G , B and Gdc and the initial estimated values Δe , Δf , and ΔXd . Hence, these submatrices remain constant in the iterative solution scheme.
- Submatrices J_2^0 , J_{13}^0 and J_{12}^0 are much smaller in size as compared to the J^0 matrix of equation (3.8). Hence the triangularisation and back substitution process involve much less computational burden (time and storage).
- The elements of the submatrices J_1^0 , J_3^0 , J_{14}^0 , J_{15}^0 , J_{10}^0 and J_{11}^0 are stored in a matrix form. Similarly the second order terms S_P^k , S_Q^k , S_V^k and S_R^k are not stored in the computer memory. While solving the equations (3.24) to (3.26) each element of $[P^*]^k$, $[Q^*]^k$ and $[R^*]^k$ is evaluated one at a

time using G , B and Gdc , Δe , Δf , and ΔXd and the error vectors Δe^k , Δf^k and ΔXd^k .

3.3.3 Solution Steps

The solution steps of the DSRLF algorithm are given below:

- Step 1 : Read system data and converter control specifications.
- Step 2 : Initialise state vector $X^0 = [e^0, f^0, Xd^0]$ and set $\Delta e^0 = 0$, $\Delta f^0 = 0$ and $\Delta Xd^0 = 0$.
- Step 3 : Compute elements of ac and dc network matrices $[G_{ij} + jB_{ij}]$ and $[Gdc_{ij}]$.
- Step 4 : Computes elements of submatrices J_2^0 , $[J_{12}]^0$ and $[J_{13}]^0$ using the initial state. Triangularise and store factors of J_2^0 , J_{12}^0 and J_{13}^0 .
- Step 5 : Compute and store elements of mismatch vectors ΔP^0 , ΔQ^0 , $|\Delta V^2|^0$ and ΔR^0 using initial estimate.
- Step 6 : Set iteration count $k = 0$.
- Step 7 : Compute new mismatch $\Delta P^{(k)} = \Delta P^0 - S_p^k$ using Δe^k , Δf^k , ΔXd^k , G and B one at a time.
- Step 8 : Compute modified mismatch
 $(\Delta P')^k = (\Delta P)^k - J_1^0 \Delta e^k - J_3^0 \Delta Xd^k$.
- Step 9 : Solve equation (3.21) for $\Delta f]^{(k+1)}$ using forward and backward operations.
- Step 10 : Compute new mismatch

$$\Delta QV']^k = \begin{bmatrix} \Delta Q \\ \Delta V^2 \end{bmatrix}^{(0)} - \begin{bmatrix} S_Q \\ S_V \end{bmatrix}^{(k)}$$

using $\Delta e^k, \Delta f^k, \Delta Xd^k$.

Step 11: Compute modified mismatch

$$(\Delta Q^*)^k = (\Delta QV')^k - J_{14}^0 \Delta f^k - J_{15}^0 \Delta Xd^k.$$

Step 12: Solve equation (3.22) for $[\Delta e]^{(k+1)}$ using forward and backward operations.

Step 13: Compute new residual

$$\Delta R'^{(k)} = \Delta R^0 - S_R^{(k)} \text{ using } [\Delta e]^{(k+1)}, [\Delta f]^{(k+1)} \text{ and } \Delta Xd^{(k+1)}.$$

Step 14: Compute modified residual

$$(\Delta R^*)^k = (\Delta R')^k - [J_{10}^0][\Delta e^{(k+1)}] - [J_{11}^0]\Delta f^{(k+1)}$$

Step 15: Solve equation (3.23) for $\Delta Xd]^{(k+1)}$ using forward and backward operations.

Step 16: Test for convergence

$$\begin{aligned} |\Delta e|^{(k+1)} - |\Delta e|^{(k)} \\ |\Delta f|^{(k+1)} - |\Delta f|^{(k)} &\leq \epsilon \\ |\Delta Xd|^{(k+1)} - |\Delta Xd|^{(k)} \end{aligned}$$

or

$$\begin{aligned} |\Delta P^{*(k+1)} - \Delta P^{*(k)}| \\ |\Delta Q^{*(k+1)} - \Delta Q^{*(k)}| &\leq \epsilon \\ |\Delta R^{*(k+1)} - \Delta R^{*(k)}| \end{aligned}$$

Step 17: If convergence criteria are satisfied, the iterative process is terminated, otherwise next iteration starts commencing with step 7.

Step 18: Obtain the values of ac and dc states from

$$e = e^0 + \Delta e^{(k+1)}$$

$$f = f^0 + \Delta f^{(k+1)}$$

$$Xd = Xd^0 + \Delta Xd^{(k+1)}$$

Step 19 : Compute the slack bus power and the ac and dc network line flows.

The flow chart of the DSRLF algorithm is shown in Fig. 3.2.

3.4 CONCLUSIONS

Two new methods have been developed and presented in this chapter for the load flow study of the ac-dc power systems. Compared to the FRLF method with the sparsity techniques and sub-optimal ordering, the proposed methods has the same mathematical complexity, accuracy and with less memory requirement, and is much faster. The methods are based on the rectangular co-ordinate formulation of full Taylor series of the ac-dc system performance equations. A full Taylor series expansion of the ac system equations in the rectangular co-ordinate form terminate after the second order derivatives. Similarly, the four of the six equations per converter also terminate after the second order derivatives. Two equations per converter have derivatives higher than the second order terms. Omission of the terms beyond the second order of these equations and inclusion of full Taylor series of the remaining equations results in the SRLF method. A further reorganisation of the SRLF method in decoupled form without introducing any approximation results in a faster version, called the DSRLF method. The primary difference between the SRLF and DSRLF is that the latter is faster than the former one and uses less computer storage.

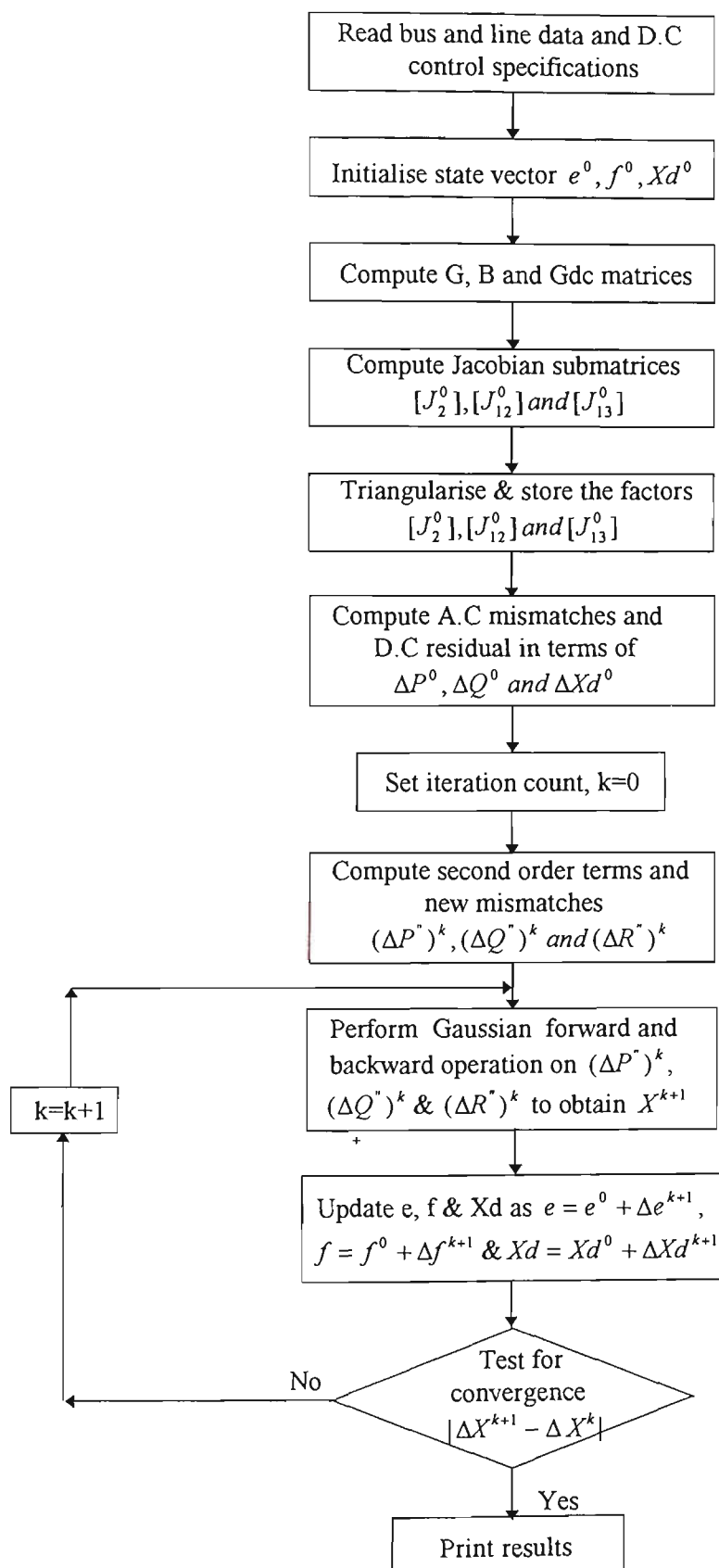


Fig. 3.2 Flow chart for DSRLF

Chapter 4

SIMULATION STUDIES

4.1 INTRODUCTION

In Chapters 2 and 3 detail derivatives of the different types of algorithm has been derived. The methods are claimed to be superior than any conventional Newton-Raphson (NR) and fast decoupled (FD) ac-dc load flow method in terms of accuracy and computational speed. Also the methods perform well under different types of network conditions where other methods cannot give satisfactory results. In this chapter detailed simulation study of IEEE 14, 30, 57 and 107 bus system has been carried out. The standard bus system have been modified in to Mesh, Link and Mesh-Link system in order to solve ac, dc and ac-dc system independently. The simulation studies has also been carried out under different control specifications. Also, detailed tests has been carried out on ac system under different degree of ill-conditioning and loading conditions. Most of the decoupled load flow methods are derived from the Newton method by neglecting the coupling sub-Jacobians. This is probably one of the main reason FD method sometimes diverge under ill-conditioned situations. For a system having high R/X ratio of all branches, the convergence pattern of the conventional decoupled load flow methods are divergence in nature. A practical power

system may not consist of such high R/X ratio of all branches. The high R/X ratio branches can be found for the low-voltage distribution networks where the branch resistances are relatively high. For all conventional FDLF methods it is assumed that $R \ll X$. So a significant change in the convergence pattern occurs when the branch resistance R or R/X ratio is increased. Moreover, the proposed algorithm has also been tested under different loading conditions and loading with different R/X ratios and it gives satisfactory results.

4.2 PARAMETERS SELECTION

4.2.1 Initialisation

The initial values of the ac and dc variables e^0 , f^0 and Xd^0 are assigned as outlined below:

AC system variables (e^0 , f^0):

$$e^0 = 1.0 ; \text{ for all P-Q busbars}$$

$$e^0 = V^{sp} ; \text{ for all P-V busbars and slack busbar}$$

$$f^0 = 0.0 ; \text{ for all busbars.}$$

DC system variables (Xd^0):

- Converter transformer tap position (a_i) $a_i^0 = 1.0$ or a_i^{SP} ; if a_i is specified.
- Converter firing angle (θ_i) $\theta_i = \theta_i^{\min}$; if converter firing angle is not specified.

- Converter terminal voltage $d_i = Vd_i^{sp}$; if Vd is specified, or $d_i = k_1 \alpha_i \cos \theta_i - k_2 Xc_i Id_i$; if Id_i and θ_i are specified. If only Id_i is specified then θ_i is replaced by θ_i^{\min} ; the minimum firing angle is allowed for converter operation. If Id_i is not specified, then $Vd_i = 1.3$ pu.
- Converter current $Id_i = Id_i^{sp}$; if converter current is specified, or $Id_i = Pd_i^{sp} / Vd_i$; if converter power is specified. If Id_i or Pd_i are not specified, then Id_i can be calculated by using

$$Id_i = \frac{k_1 \alpha_i V_p \cos \theta_i - Vd_i}{k_2 Xc_i}$$

- Converter transformer secondary current ($c_i - j d_i$)

$$\begin{aligned} c_i &= 1.2 Id_i \\ d_i &= 0.6 Id_i \end{aligned}$$

These correspond to $\cos \phi = 0.9$ (lagging) power factor for the converter.

The characteristics of the three methods (FRLF, SRLF and DSRLF) developed in Chapters 2 and 3 are ascertained on a number of power systems. A brief description of these systems are outlined below.

4.3 MODIFICATION OF STANDARD TEST SYSTEMS (Load flow analysis)

IEEE 14-busbar system:

Case I : ac line between busbars 4 and 5 is replaced by a dc link.

Case II : ac lines between busbars 2-4, busbars 2-5 and busbars 4-5 are replaced by dc links and a three terminal dc mesh systems is

obtained between busbars 2, 4 and 5.

Case III : system in Case II is further modified by replacing the ac lines between busbars 9 and 10 by a dc link. It results in a 5 terminal dc link-mesh system.

IEEE 30-busbar system:

Case I : ac line between busbars 2 and 5 is replaced by a dc link.

Case II: a three terminal dc mesh system is formed between busbars 2, and 7 by placing ac line connecting busbars 2 and 5 by a dc link and introducing dc links between busbars 2 and 7 and busbars 5 and 7.

Case III: the system in Case II is further modified by replacing the ac line between busbars 15 and 18 by a dc link to form a dc link-mesh system.

IEEE 57-busbar system:

Case I : ac line between busbars 8 and 9 is replaced by a dc link.

Case II: a three terminal dc mesh system is formed between busbars 6, 8 and 9 by replacing ac line between busbars 8 & 9 and 6 & 8, and introducing dc links between busbars 6 and 9.

Case III: a five terminal dc link-mesh system is formed by replacing the ac line between busbars 44 and 45 in Case II by a dc link.

107 - busbar system

Case I: A double circuit ac line out of the two double circuit ac lines between busbars 60 and 99 is replaced by a dc link.

Detailed circuit configurations for Link, Mesh and Mesh-link system are given in Appendix - E and the bus data are provided in Appendix - D.

4.4 ILL-CONDITIONED SYSTEM

It is well known that GS method is unstable for both large and ill-conditioned systems. On the other hand though NR method is very reliable and accurate for most of the system, but it is not very fast. Also it involves considerable complex programming logic. The fast decoupled load flow method is possibly the most popular method and widely used by the power industry because of its simplicity and computational efficiency. The method is derived from the NR method by neglecting the coupling sub-Jacobians. The final load flow equations of this method are then obtained with some other justifiable network assumptions. For most of the high voltage power networks, the standard FD load flow method has an excellent convergence pattern. However, the method has convergence difficulties in solving the load flow problem of some networks having relatively high R or R/X ratio branches. High R or R/X ratio branches can be found in the low voltage networks or in certain types of power system equivalent. In addition, it is found that the presence of capacitive series branches in a system could also result in the failure or slow convergence of the FD load flow method.

4.4.1 High Values of Branch Resistance

It was mentioned earlier that FD load flow method possesses an excellent convergence pattern when the decoupling assumptions are valid. For most of the conventional FD load flow methods, it is assumed that the elements of

the coupling sub-Jacobians are negligible when the condition $R \ll X$ is satisfied for all branches in the system. Also, the branch resistances, transformer off-nominal tap settings and shunt admittances are neglected while the coefficient matrix of the $P-\delta$ problem is formed. However, the omission of the branch resistances while the coefficient matrix of the $P-\delta$ problem is formed plays an important role in the convergence pattern of the FD load flow method. In the proposed decoupled ac-dc load flow method, the effects of the branch resistance, and hence of the coupling sub-Jacobians are carefully taken into consideration. The resistance (R) of all the branches was multiplied by a factor λ ($\lambda \geq 1$), while the same value of branch reactances X was kept. A brief summary of the results are shown in Table 4.9.

4.4.2 High Values Of R/X Ratio

In any practical high voltage transmission system the line resistances are very small as compared to its inductive reactance. This is why, the R/X ratios of the high voltage transmission lines are extremely small. Most of the FD load flow algorithms are derived from the NR method in which the R/X ratio of all branches are neglected, such that $\cos \delta_{pq} = 1.0$ and $G_{pq} \sin \delta_{pq} \ll B_{pq}$. However, some low voltage distribution networks have some lines with high value of R/X ratio. Also IEEE bus system have certain lines with large R/X ratios (greater than unity). FD method have some convergence problem of the system having lines with R/X ratio greater than unity. The convergence behaviour of the proposed methods were tested for various values of R/X ratio of the branches. To do this, the R/X ratio of all branches is increased by a factor ω ($0.25 \leq \omega \leq 3.0$). The R/X ratio of

branches having zero resistance was not changed. Details results are summarised in Table 4.10.

4.5 LOADING CONDITIONS

Some algorithms perform well under lightly loaded conditions but does not perform well under heavy loading conditions. In addition, under heavy line loading conditions, the angle difference between the two adjacent nodes may not be small. In the conventional FD load flow method it is assumed that the busbar reactive powers are very small in comparison to the corresponding diagonal elements of the B matrix; i.e., $Q_p \ll B_{pp} V_p^2$. This assumption is valid under ideal operating conditions. However, in certain cases the above assumption is not valid, which may cause failure of the FD method to converge. To verify the convergence characteristics of the proposed methods in comparison with the FD method under different loading conditions, all the reactive load is multiplied by a factor β ($\beta \geq 1$). A summary of the results is shown in Table 4.11. The test systems were then modified by changing the real and reactive power at different values. If $(P_p + jQ_p)$ represents the base loading condition, then $(\eta.P_p + j\tau.Q_p)$ will represent the change in loadings. A comparison of the convergence characteristics of different methods for the different values of η and τ are given in Table 4.12. The test systems were then extended by changing the R/X ratio under different loading. A summary of the results are given in Table 4.13.

4.6 TEST RESULTS

A number of sample systems are studied through the proposed methods and its performance were compared with the FD ac-dc load flow. The standard bus system has been modified to link, mesh and mesh-link configuration in order to solve ac-dc load flow simultaneously. The maximum number of iterations fixed at 50.0. Several case studies for load flow analysis were performed and are provided in Appendix - F. Other test results are given in Tables 4.1 to 4.13 and Figs. 4.1 to 4.8.

Table 4.1 Effect of control specifications on convergence and solution time for 14 bus system with dc link.

Conv. 1 Rectifier Specified control	Conv. 2 Inverter Specified control	Conv. 3 Rectifier Specified control	Methods							
			FRLF		SRLF		DSRLF		FDLF	
			Soln. time	No.of itn.	Soln. time	No.of itn.	Soln. time	No.of itn.	Soln. time	No.of itn.
α, P_d	γ, V_d	a, P_d	1.34	3	.68	4	.36	5	.41	6
α, P_d	γ, V_d	α, I_d	1.34	3	.68	4	.36	5	.53	8
a, P_d	γ, V_d	α, I_d	1.34	3	.68	4	.36	5	.41	6
α, P_d	γ, I_d	α, I_d	1.34	3	.68	4	.36	5	.53	8
a, P_d	γ, I_d	a, I_d	1.34	3	.68	4	.36	5	.41	6
a, α	γ, I_d	α, P_d	1.34	3	.68	4	.36	5	.66	10

Table 4.2 Effect of control specifications on convergence and solution time for 14 bus system with dc mesh.

Rectifier Specified control	Inverter Specified control	Methods							
		FRLF		SRLF		DSRLF		FDLF	
		Soln. time	No. of itn.						
a, P_d	γ, I_d	1.34	3	.68	4	.36	5	.41	6
α, P_d	γ, V_d	1.34	3	.68	4	.36	5	.53	8
α, I_d	γ, V_d	1.34	3	.68	4	.36	5	.41	6
a, P_d	γ, V_d	1.34	3	.68	4	.36	5	.53	8
α, P_d	γ, I_d	1.34	3	.68	4	.36	5	.41	6
a, V_d	γ, I_d	1.34	3	.68	4	.36	5	.66	10

Table 4.3 Effect of control specifications on convergence and solution time for 30 bus system with dc link.

Conv. 1 Rectifier Specifid control	Conv. 2 Inverter Specified control	Conv. 3 Rectifier Specified control	Methods							
			FRLF		SRLF		DSRLF		FDLF	
			Soln. time	No. of itn.						
α, P_d	γ, V_d	a, P_d	1.62	3	.76	4	.47	5	.52	6
α, P_d	γ, V_d	α, I_d	1.62	3	.76	4	.47	5	.67	8
a, P_d	γ, V_d	α, I_d	1.62	3	.76	4	.47	5	.52	6
α, P_d	γ, I_d	α, I_d	1.62	3	.76	4	.47	5	.76	10
a, P_d	γ, I_d	a, I_d	1.62	3	.76	4	.47	5	.52	6
a, α	γ, I_d	α, P_d	1.62	3	.76	4	.47	5	.96	12

Table 4.4 Effect of control specifications on convergence and solution time for 30 bus system with dc mesh.

Rectifier Specified control	Inverter Specified control	Methods							
		FRLF		SRLF		DSRLF		FDLF	
		Soln. time	No. of itn.						
a, P_d	γ, I_d	1.62	3	.76	4	.47	5	.52	6
α, P_d	γ, V_d	1.62	3	.76	4	.47	5	.67	8
α, I_d	γ, V_d	1.62	3	.76	4	.47	5	.52	6
a, P_d	γ, V_d	1.62	3	.76	4	.47	5	.76	10
α, P_d	γ, I_d	1.62	3	.76	4	.47	5	.52	6
a, V_d	γ, I_d	1.62	3	.76	4	.47	5	.96	12

Table 4.5 Effect of control specifications on convergence and solution time for 57 bus system with dc link.

Conv. 1 Rectifier Specified control	Conv. 2 Inverter Specified control	Conv. 3 Rectifier Specified control	Methods							
			FRLF		SRLF		DSRLF		FDLF	
			Soln. time	No. of itn.						
α, P_d	γ, V_d	α, P_d	2.12	3	.88	4	.53	5	.58	6
α, P_d	γ, V_d	α, I_d	2.12	3	.88	4	.53	5	.90	10
α, P_d	γ, V_d	α, I_d	2.12	3	.88	4	.53	5	.58	6
α, P_d	γ, I_d	α, I_d	2.12	3	.88	4	.53	5	1.06	12
α, P_d	γ, I_d	α, I_d	2.12	3	.88	4	.53	5	.58	6
α, α	γ, I_d	α, P_d	2.12	3	.88	4	.53	5	1.22	14

Table 4.6 Effect of control specifications on convergence and solution time for 57 bus system with dc mesh.

Rectifier Specified control	Inverter Specified control	Methods							
		FRLF		SRLF		DSRLF		FDLF	
		Soln. time	No. of itn.						
α, P_d	γ, I_d	2.12	3	.88	4	.53	5	.58	6
α, P_d	γ, V_d	2.12	3	.88	4	.53	5	.90	10
α, I_d	γ, V_d	2.12	3	.88	4	.53	5	.58	6
α, P_d	γ, V_d	2.12	3	.88	4	.53	5	1.06	12
α, P_d	γ, I_d	2.12	3	.88	4	.53	5	.58	6
α, V_d	γ, I_d	2.12	3	.88	4	.53	5	1.22	14

Table 4.7 Number of iterations and solution time comparison of different methods.

System Studied	FRLF		SRLF		DSRLF		FDLF	
	CPU time (s)	No. of itn.						
14 Bus dc link	1.34	3	.68	4	.36	5	.41	6
14 Bus dc mesh	1.34	3	.68	4	.36	5	.41	6
14 Bus dc mesh-link	1.34	3	.68	4	.36	5	.41	6
30 Bus dc link	1.62	3	.76	4	.47	5	.52	6
30 Bus dc mesh	1.62	3	.76	4	.47	5	.52	6
30 Bus dc mesh-link	1.62	3	.76	4	.47	5	.52	6
57 Bus dc link	2.12	3	.88	4	.53	5	.58	6
57 Bus dc mesh	2.12	3	.88	4	.53	5	.58	6
57 Bus dc mesh-link	2.12	3	.88	4	.53	5	.58	6
107 Bus dc link	3.42	3	1.12	4	.65	5	.70	6

Table 4.8 Solution time comparison of different methods at different iterative stage.

System Studied	FRLF		SRLF		DSRLF		FDLF	
	<u>CPU time</u>		<u>CPU time</u>		<u>CPU time</u>		<u>CPU time</u>	
	T1	T2	T1	T2	T1	T2	T1	T2
14 Bus dc link	.56	.39	.32	.12	.16	.05	.10	.062
14 Bus dc mesh	.56	.39	.32	.12	.16	.05	.10	.062
14 Bus dc mesh-link	.56	.39	.32	.12	.16	.05	.10	.062
30 Bus dc link	.72	.45	.37	.13	.23	.06	.15	.074
30 Bus dc mesh	.72	.45	.37	.13	.23	.06	.15	.074
30 Bus dc mesh-link	.72	.45	.37	.13	.23	.06	.15	.074
57 Bus dc link	.88	.62	.46	.14	.25	.07	.18	.080
57 Bus dc mesh	.88	.62	.46	.14	.25	.07	.18	.080
57 Bus dc mesh-link	.88	.62	.46	.14	.25	.07	.18	.080
107 Bus dc link	1.46	.98	.67	.15	.33	.08	.25	.090

T1 = Time for first iteration; T2 = Time for second or next subsequent iterations.

Table 4.9 Effect of increasing R on convergence.

System Studied	Value of λ	FRLF	SRLF	DSRLF	FDLF
		No. of itn.	No. of itn.	No. of itn.	No. of itn.
14 Bus	1.0	3	4	5	6
Mesh-Link	1.5	3	4	5	6
	2.0	3	4	5	8
	2.5	3	4	5	8
	2.75	3	4	5	10
	3.0	3	4	5	13
	3.25	4	5	5	18
	3.5	4	5	5	24
	3.75	4	5	5	36
	4.0	4	5	5	**
30 Bus	1.5	3	4	5	6
Mesh-Link	1.5	3	4	5	6
	2.0	3	4	5	10
	2.5	3	4	5	10
	2.75	3	4	5	12
	3.0	3	4	5	15
	3.25	4	5	5	25
	3.5	4	5	5	47
	3.75	4	5	5	**
	4.0	4	5	5	**
57 Bus	1.0	3	4	5	6
Mesh-Link	1.5	3	4	5	6
	2.0	3	4	5	8
	2.5	3	4	5	9
	2.75	3	4	5	12
	3.0	3	4	5	15
	3.25	4	5	5	32
	3.5	4	5	5	**
	3.75	4	5	5	**
	4.0	4	5	5	**

Table 4.10 Effect on convergence of increasing R/X ratio.

System Studied	Value of ω	FRLF	SRLF	DSRLF	FDLF
		No. of itn.	No. of itn.	No. of itn.	No. of itn.
14 Bus	0.25	3	4	5	6
Mesh-Link	0.50	3	4	5	6
	0.75	3	4	5	8
	1.00	3	4	5	15
	1.25	3	4	5	22
	1.50	3	4	5	36
	1.75	4	5	6	**
	2.00	4	5	6	**
	2.50	5	5	6	**
	3.00	**	5	6	**
30 Bus	0.25	3	4	5	6
Mesh-Link	0.50	3	4	5	6
	0.75	3	4	5	10
	1.00	3	4	5	17
	1.25	3	4	5	29
	1.50	4	4	5	47
	1.75	4	5	6	**
	2.00	5	5	6	**
	2.50	**	5	6	**
	3.00	**	6	6	**
57 Bus	0.25	3	4	5	6
Mesh-Link	0.50	3	4	5	8
	0.75	3	4	5	16
	1.00	3	4	5	30
	1.25	3	4	5	48
	1.50	4	4	5	**
	1.75	4	5	6	**
	2.00	**	5	6	**
	2.50	**	5	6	**
	3.00	**	6	6	**

Table 4.11 Effect of convergence for high value of reactive power loading

System Studied	Value of β	FRLF	SRLF	DSRLF	FDLF
		No. of itn.	No. of itn.	No. of itn.	No. of itn.
14 Bus	1.0	3	4	5	6
Mesh-Link	1.5	3	4	5	6
	2.0	3	4	5	6
	2.5	4	4	5	8
	3.0	5	4	5	11
	3.5	5	4	5	14
30 Bus	1.0	3	4	5	6
Mesh-Link	1.5	3	4	5	6
	2.0	3	4	5	10
	2.5	5	4	5	12
	3.0	5	4	5	15
	3.5	6	4	5	18
57 Bus	1.0	3	4	5	6
Mesh-Link	1.5	3	4	5	6
	2.0	3	4	5	10
	2.5	5	4	5	13
	3.0	5	4	5	16
	3.5	6	4	5	18

Table 4.12 Effect of convergence under different loading condition

System Studied	$\eta P_p + j\tau Q_p$	FRLF	SRLF	DSRLF	FDLF
		No. of itn.	No. of itn.	No. of itn.	No. of itn.
14 Bus	$\eta = 1, \tau = 1$	3	4	5	6
Mesh-Link	$\eta = .5, \tau = .5$	3	4	5	6
	$\eta = 1.5, \tau = 1$	3	4	5	6
	$\eta = 1, \tau = 1.5$	3	4	5	6
	$\eta = 2, \tau = 2$	3	4	5	7
	$\eta = 3, \tau = 3$	3	4	5	13
30 Bus	$\eta = 1, \tau = 1$	3	4	5	6
Mesh-Link	$\eta = .5, \tau = .5$	3	4	5	6
	$\eta = 1.5, \tau = 1$	3	4	5	6
	$\eta = 1, \tau = 1.5$	3	4	5	7
	$\eta = 2, \tau = 2$	3	4	5	11
	$\eta = 3, \tau = 3$	3	4	5	16
57 Bus	$\eta = 1, \tau = 1$	3	4	5	6
Mesh-Link	$\eta = .5, \tau = .5$	3	4	5	6
	$\eta = 1.5, \tau = 1$	3	4	5	6
	$\eta = 1, \tau = 1.5$	3	4	5	7
	$\eta = 2, \tau = 2$	3	4	5	12
	$\eta = 3, \tau = 3$	3	4	5	17

Table 4.13 Effect on convergence for different R/X ratios under different loading conditions.

System Studied	Value of ω	FRLF				DSRLF				FDLF			
		No. of iteration for $\beta = 1$ 1.5 2.0 2.5				No. of iteration for $\beta = 1$ 1.5 2.0 2.5				No. of iteration for $\beta = 1$ 1.5 2.0 2.5			
14 Bus Mesh-Link	0.25	3	3	3	3	5	5	5	5	6	6	6	8
	0.50	3	3	3	3	5	5	5	5	6	8	10	10
	0.75	3	3	3	3	5	5	5	5	12	12	12	14
	1.00	3	3	3	4	5	5	5	5	16	16	16	27
	1.25	3	3	4	6	5	5	5	5	25	25	35	**
	1.50	3	3	4	6	5	5	5	5	**	**	**	**
	1.75	4	4	6	11	6	6	6	6	**	**	**	**
	2.00	4	4	6	11	6	6	6	6	**	**	**	**
	2.50	5	5	7	15	6	6	6	6	**	**	**	**
3.00	**	**	**	**	6	6	6	6	**	**	**	**	
30 Bus Mesh-Link	0.25	3	3	3	3	5	5	5	5	6	6	8	8
	0.50	3	3	3	3	5	5	5	5	6	8	10	12
	0.75	3	3	3	3	5	5	5	5	15	15	18	28
	1.00	3	3	3	4	5	5	5	5	23	23	36	**
	1.25	3	3	4	6	5	5	5	5	**	**	**	**
	1.50	3	3	4	8	5	5	5	5	**	**	**	**
	1.75	4	4	8	12	6	6	6	6	**	**	**	**
	2.00	4	4	8	15	6	6	6	6	**	**	**	**
	2.50	5	5	10	**	6	6	6	6	**	**	**	**
3.00	**	**	**	**	6	6	6	6	**	**	**	**	
57 Bus Mesh-Link	0.25	3	3	3	3	5	5	5	5	6	6	6	10
	0.50	3	3	3	3	5	5	5	5	8	8	12	15
	0.75	3	3	3	3	5	5	5	5	18	18	28	35
	1.00	3	3	3	4	5	5	5	5	36	**	**	**
	1.25	3	3	4	6	5	5	5	5	**	**	**	**
	1.50	3	3	4	12	5	5	5	5	**	**	**	**
	1.75	4	4	9	18	6	6	6	6	**	**	**	**
	2.00	**	**	**	**	6	6	6	6	**	**	**	**
	2.50	**	**	**	**	6	6	6	6	**	**	**	**

4.7 ANALYSIS OF SIMULATION RESULTS

An inspection of Tables F.1 to F.4 (In Appendix - F) indicates that the results obtained from the FRLF, SRLF, DSRLF and fast decoupled ac-dc load flow (FDLF) methods are in good agreement on all the systems with a dc link. This has been found true for the dc mesh-link configurations also as evident from Tables F.5 to F.10.

The power flow results are provided in Tables F.11 to F.14. As the voltage results are found to be in good agreement, so are the results for the power flows. Therefore, in order to avoid a repetition of similar results, the power flow results using only the DSRLF method on 14, 30, 57 and 107 busbar system with the dc mesh and dc mesh-link are provided for illustration.

Since first order ac-dc load flow method based on the NR technique (FRLF in this case) provides accurate results despite a linearisation of the relationship between the mismatches and errors. It is also known that the FDLF method yields accurate results when the decoupling and other assumptions are complied with. Since the solutions have been obtained with the flat voltage start and normal mode of operation, the FDLF method is expected to give correct results. This is confirmed by the digital solutions provided in Tables F.1 to F.10.

In the proposed second and decoupled second order methods all the ac system equations in the rectangular co-ordinates terminate after the second order derivatives in the Taylor series. There are six equations per converter at the ac-dc busbar. Among the six, four terminate after the second order

derivatives in the Taylor series like the ac equations. However, the other two equations do not terminate after the second order. So the terms after the second order for these equations were neglected in the mathematical modelling of the SRLF and DSRLF methods. It is interesting to note that this approximation has almost negligible effect over the accuracy of the solution. A comparison of the results obtained using the FRLF and FDLF methods confirms it.

Actual ac-dc power systems may have link, mesh or mesh-link configurations for the dc portion. As such, to evaluate the performance of the proposed methods, number of cases were studied in which the dc system had link, mesh and mesh-link configurations. Results of these studies are provided in Tables F.1 to F.10. These investigations indicate that the proposed methods work well for these configurations.

An economic and effective operation of the ac-dc power systems necessitate operation of the converters under different control specifications. A load flow method is acceptable only when it performs satisfactorily under various realistic operating modes. To examine the suitability of the proposed methods the 14, 30 and 57 busbar systems with six different converter control combinations were studied. The results are presented in Tables 4.1-4.6 respectively. It is seen from these tables that the results obtained from the four methods are in good agreement. However, it is also observed that in some cases FDLF method produces oscillatory convergence and increases slightly with the system size. This indicates that the proposed method work well for different combinations of converter control specifications.

Table 4.7 shows the solution time comparison taking FRLF method as a reference. It is observed from the table that the overall solution time in the case of the SRLF method is less than that for the FRLF method. This is attributed to the fact that in the FRLF method, the Jacobian matrix is calculated and factorised in each iteration. On the other hand, in the SRLF method the Jacobian matrix is calculated and factorised once only in the iterative scheme.

It is also observed that the solution time for the SRLF method is more than that for the DSRLF method. This is due to the fact that the size of the coefficient matrix is much smaller for the DSRLF as compared to the SRLF. It is also observed that the solution time for the DSRLF and FDLF methods are comparable. From Table 4.7 it is also observed that the CPU time of the DSRLF method is much less than the FDLF method but from Table 4.8 it is seen that though the CPU time for the first iteration of the proposed method is greater, however, the times for the next iterations become less. Thus the total solution time of the proposed method becomes less. It may be concluded that in terms of computational speed and number of iteration required, the DSRLF method is better than FDLF method.

To check and compare the convergence behaviours and CPU time of the various load flow methods for different degree of ill-conditioning, the test systems were modified by (i) the resistance of all branches which is increased by a factor $\lambda (\lambda \geq 1)$, while the same or original value of branch reactances X was kept and (ii) the R/X ratio of all branches is increased by a factor $\omega (0.25 \leq \omega \leq 3.0)$. In this case the resistance is kept constant and the reactances of all line were decreased. The load flow problems were

solved in the modified systems. Tables 4.9 and 4.10 give a comparison of number of iterations and solution times of different load flow methods for various degree of ill-conditioning. It is observed from the tables that the number of iterations required by the FDLF method increases rapidly as the resistance multiplier factor λ is increased. On the other hand, the iterations required by the proposed method remains unchanged. Though the iterations required by the FRLF and SRLF methods become less than the proposed method but the CPU time is large. The test systems were then modified by changing the R/X ratio of all branches. The R/X ratio of branches having zero resistance was not changed. Table 4.10 shows the number of iterations required by various methods for different values of the R/X ratio. It can be observed in the table that the iterations required by the FDLF method increased rapidly as the R/X ratio of branches is increased and fails to converge (does not converge within 50 iteration) when R/X ratio exceeds 1.75 for 14, 30 bus and 1.5 for 57 bus system. Also, it is observed that the convergence characteristics of the proposed method is independent of system size. It is apparent from the tables that, for high values of R or R/X ratio the performance of the proposed method becomes significantly better than that of the conventional FDLF method.

It was mentioned earlier during heavy line loading conditions, the angle difference between the adjacent nodes cannot be negligible. In most FD load flow methods this angle difference is neglected, which may cause convergence problem in FD method. Tables 4.11 to 4.13 shows a comparison of the convergence characteristics of the various methods under different loading conditions. In this case all the reactive load is multiplied by a factor β , $\beta \geq 1.0$. From Table 4.11 it is observed that FDLF method takes some more iteration when the system is overloaded.

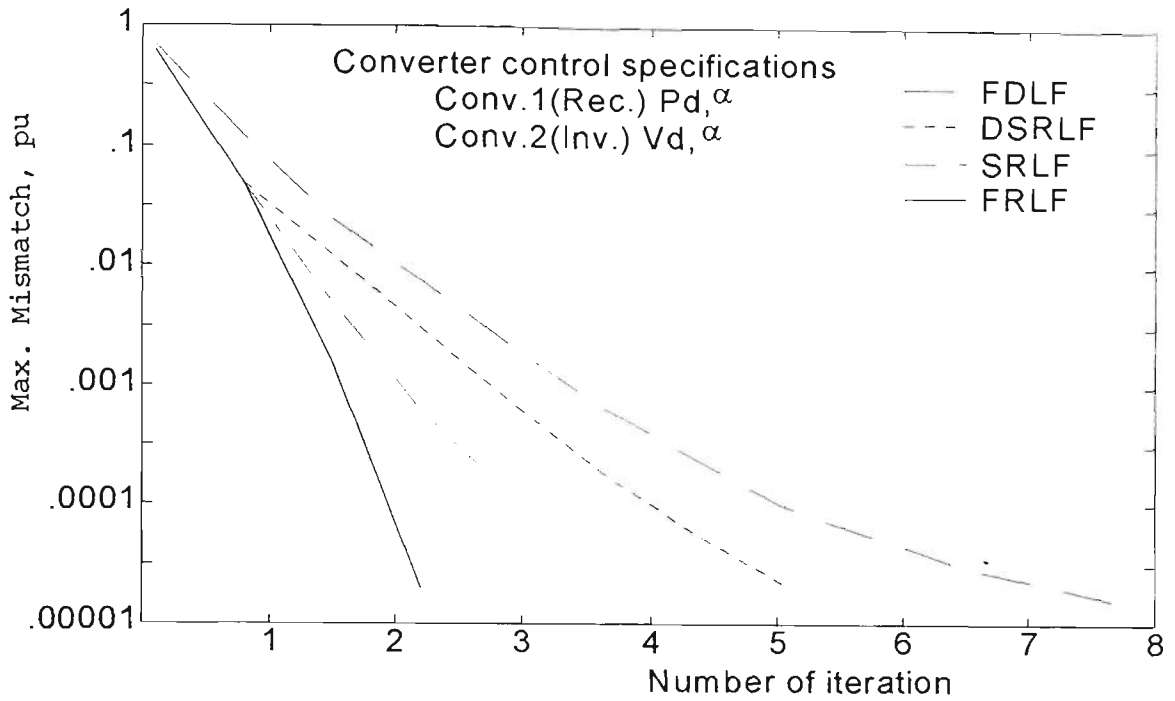


Fig. 4.1 Convergence characteristics of 14 bus system with dc link.

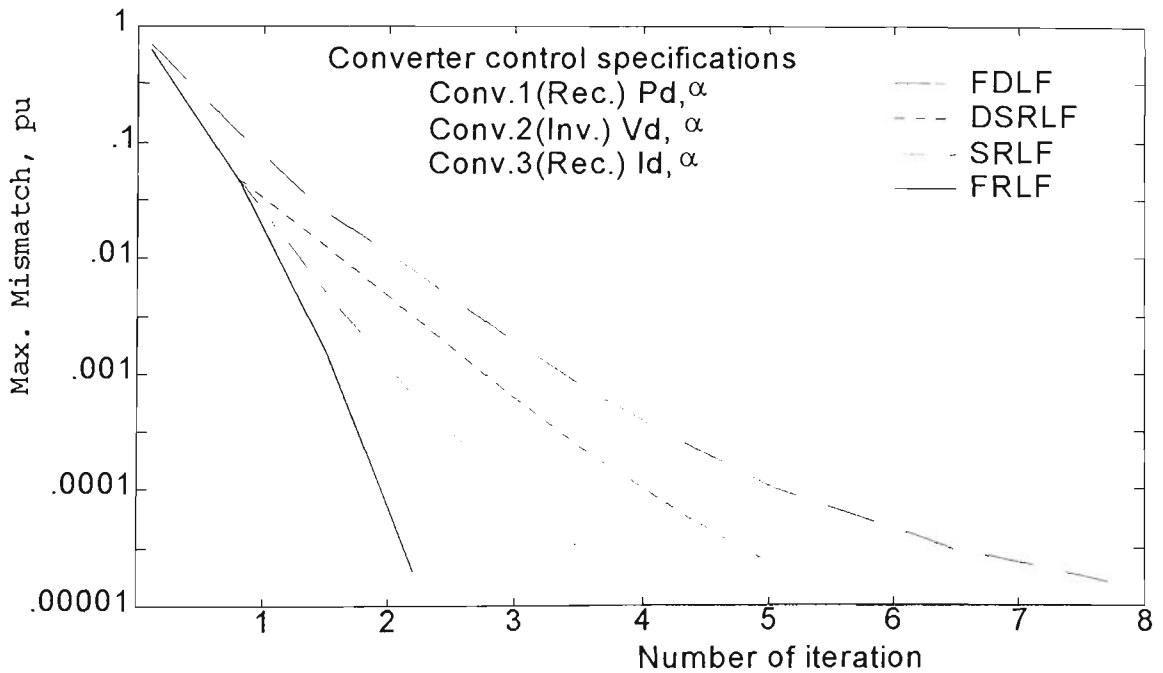


Fig. 4.2 Convergence characteristics of 14 bus system with dc mesh.

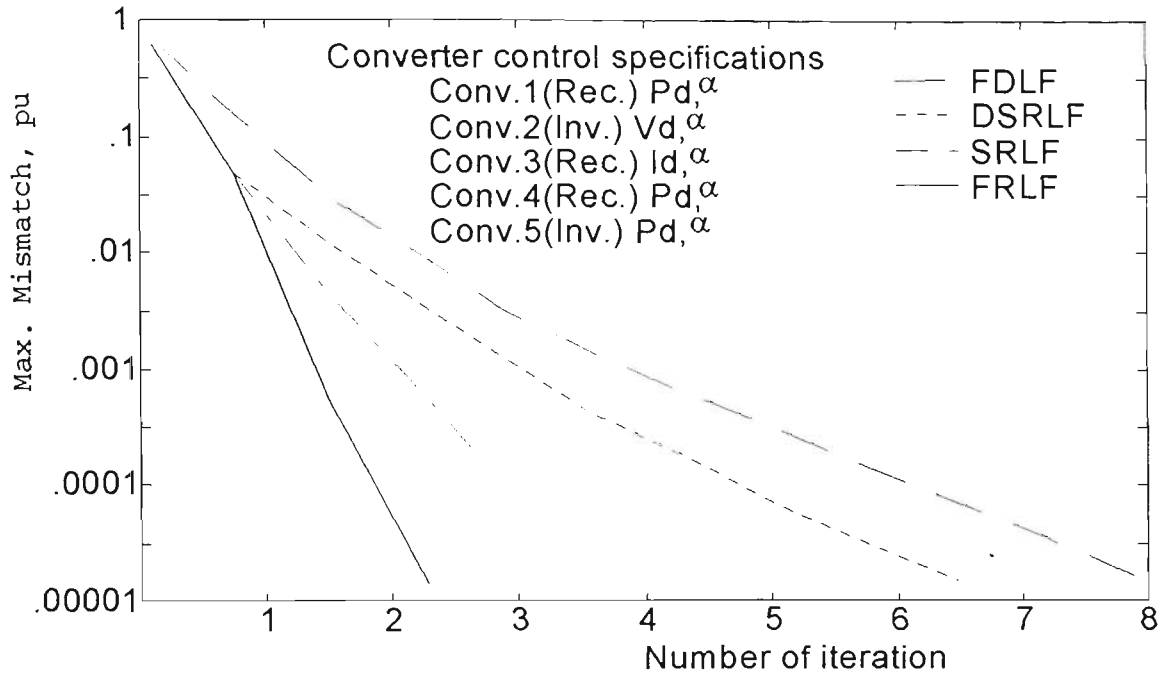


Fig. 4.3 Convergence characteristics of 14 bus system with dc mesh-link.

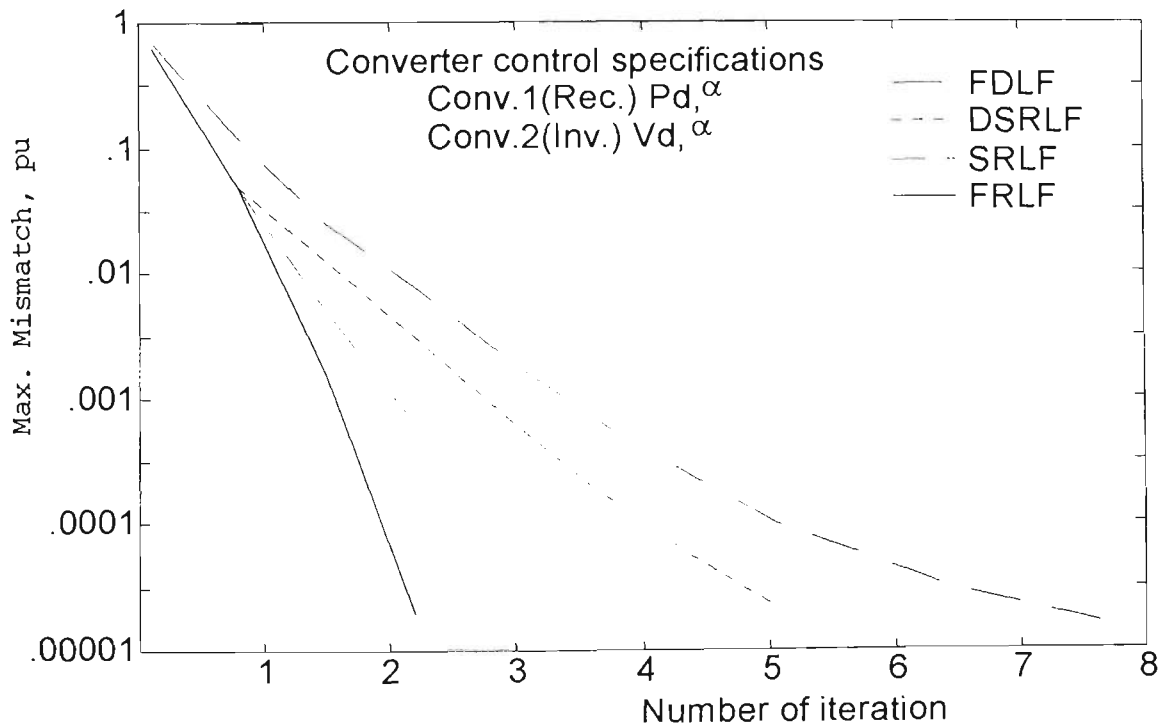


Fig. 4.4 Convergence characteristics of 30 bus system with dc link.

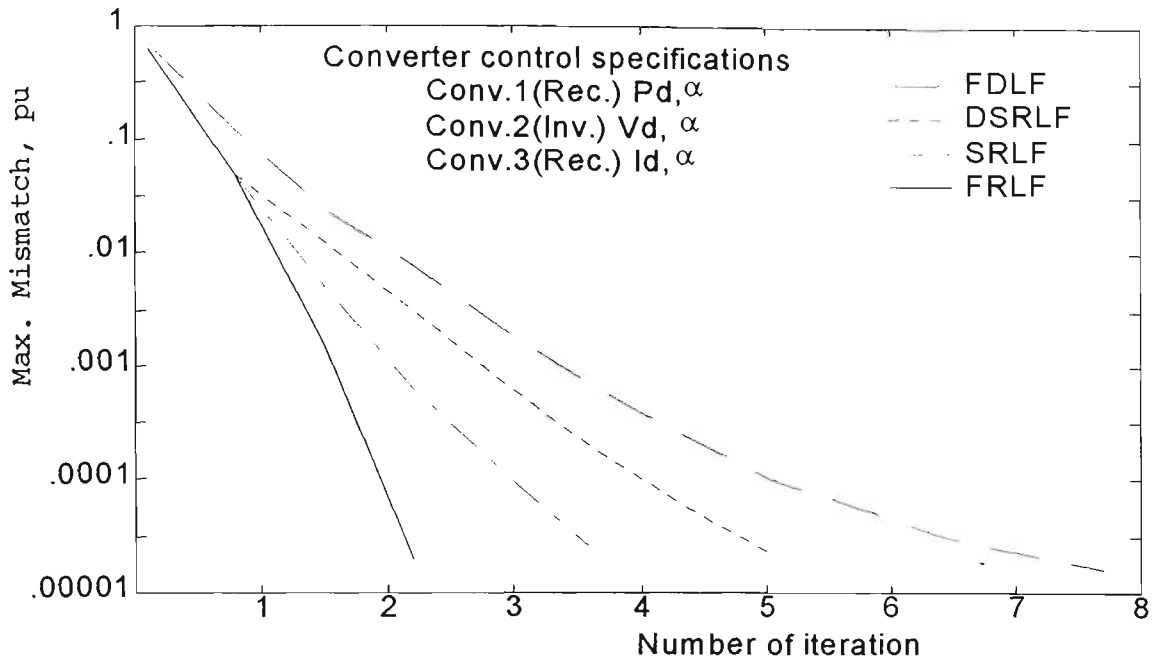


Fig. 4.5 Convergence characteristics of 30 bus system with dc mesh.

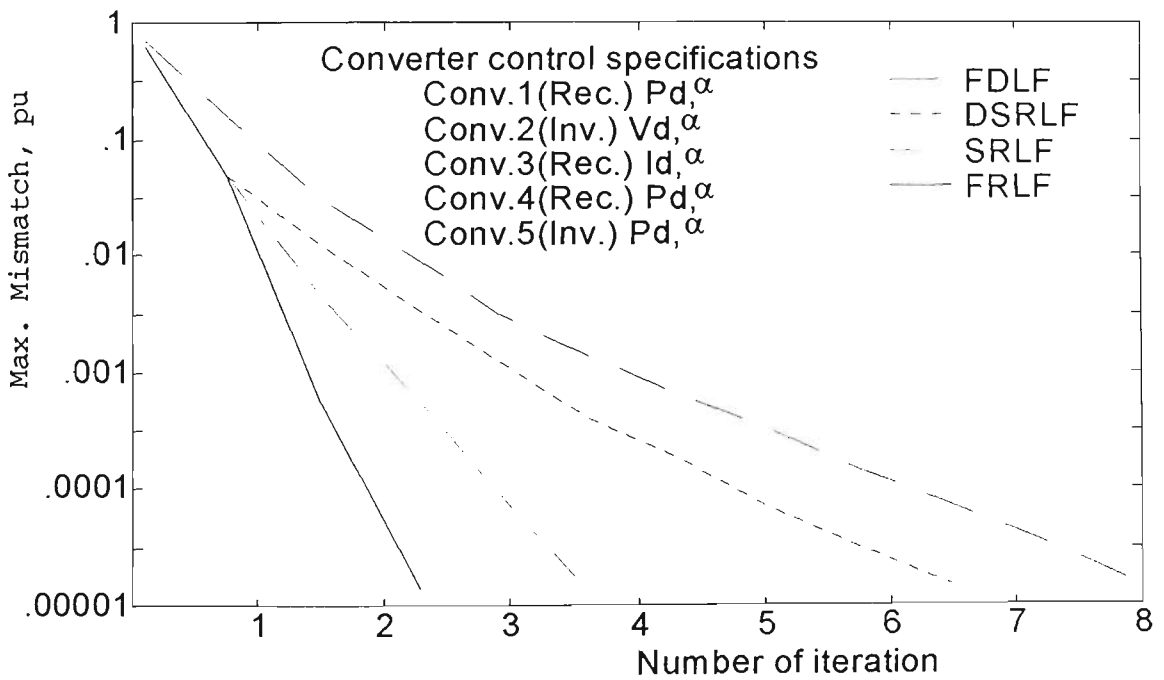


Fig. 4.6 Convergence characteristics of 30 bus system with dc mesh-link.

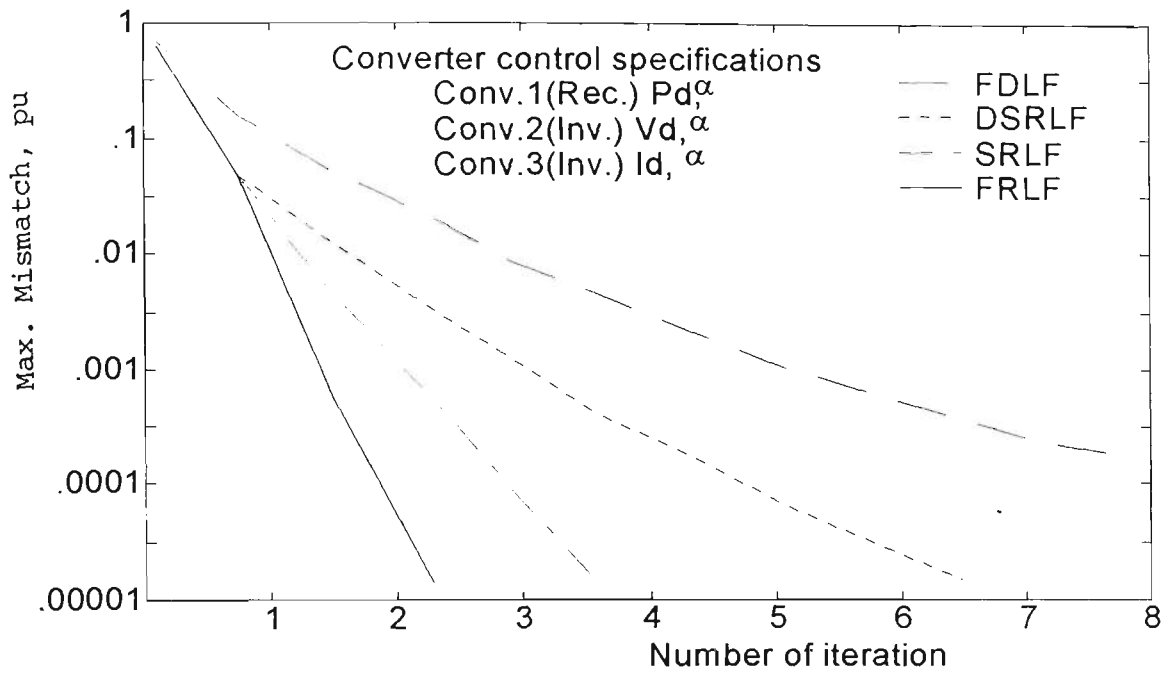


Fig. 4.7 Convergence characteristics of 57 bus system with dc mesh.

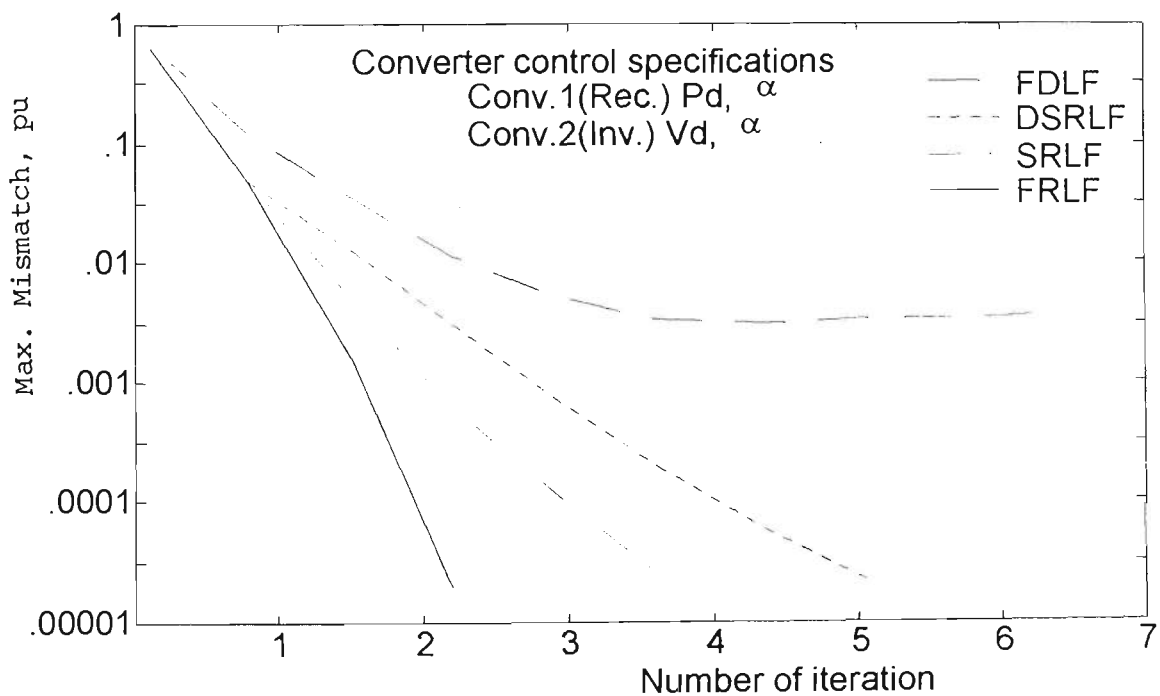


Fig. 4.8 Convergence characteristics of 107 bus system with dc link.

However, the number of iterations remains unchanged in the case of proposed method when the system is overloaded. The same conclusion may be drawn in the case of FRLF and SRLF methods. The test system was then modified by changing the R/X ratio under different loadings. The convergence characteristics of the proposed methods are compared with FRLF, SRLF and FDLF method by increasing the R/X ratio to a value of 3.00 for different loading of the systems. Table 4.13 shows number of iterations required by various methods for different values of R/X ratio under different loading. It can be observed from the table that the iterations required by the FDLF method increases as the R/X ratio increased and it takes some more iterations when the system is overloaded. FRLF method sometimes take some more iterations when the system is overloaded. However, in case of proposed method the number of iteration is independent of R/X ratio and also independent of system loading.

An inspection of Figs. 4.1 to 4.8 shows that the convergence characteristics of the SRLF method is inferior to those of the FRLF method but better than those of the DSRLF and FDLF methods. On the other hand, the convergence of the DSRLF and FDLF methods are comparable in most of the cases. However, in certain cases some convergence difficulties are encountered with the FDLF method but the DSRLF methods provides satisfactory solution. This could be attributed to the fact that the FDLF method is based on a number of approximations. Also, the convergence of the FRLF method is quadratic, since it is basically the NR method whose convergence is quadratic in nature.

4.8 CONCLUSIONS

Three methods to include dc system in load flow calculations have been tested and the test results are provided in this chapter. The procedure uses all ac-dc equations simultaneously and fully exploits the sparsity techniques. The dc system is formulated in a most general way such that any multi-terminal system of any configuration can be easily accommodated. The choice of the dc system variables and equations makes the calculation procedure very systematic. The proposed solution technique for the dc system is faster as compared to other known procedures. The six variable model for the converter enables to account for the losses in the interface converter system. From the analysis of the simulation results it appears that the proposed methods exhibit better convergence pattern, more accuracy and more stable characteristics than the existing first, second and decoupled second order ac-dc models. Though FDLF method is computationally faster than the FRLF and SRLF methods but its convergence pattern deteriorates on ill-conditioned system. However, for ill-conditioned systems having line with large R/X ratio the proposed models have much better reliability and convergence properties than the FDLF method. The convergence of the proposed methods are also found to be better than the FDLF method for varying system loading conditions. In many situations where the FDLF method diverges, the proposed methods converge. It is envisaged that the proposed methods will appeal to the practising engineers as it is preferable over the FDLF method for obtaining ac-dc load flow solutions of ill-conditioned and loaded conditioned systems. Also in some cases the FDLF method requires a large number of iterations or fails to provide a solution.

PART - II

STATE ESTIMATION

Chapter 5

INTEGRATED AC-DC STATE ESTIMATION IN RECTANGULAR CO-ORDINATES

5.1 INTRODUCTION

Selective monitoring of the generation and transmission system has been providing the data needed for economic dispatch and load frequency control. However, interconnected power networks have become more complex and the task of securely operating the system has become more difficult. To avoid major system failures and regional power blackouts, electric utilities have installed more extensive supervisory control and data acquisition throughout the network to support computer based systems at the energy control centre. Before any security assessment or control actions can be taken, a reliable estimate of the existing state of the system must be determined. For this purpose, the number of physical measurements can not be restricted to only those which are quantities required to support conventional power flow calculations. The inputs to the conventional power flow program are confined to the P, Q injections at load buses and P, |V| values at voltage controlled buses. Even if one of these inputs are unavailable, the conventional power flow solution cannot be obtained. Moreover, gross errors in one or more of the input quantities can cause the

power flow results to become useless. These limitations can be removed by state estimation.

The electric power transmission system uses various measuring devices like wattmeters, varmeters, voltmeters, ammeters etc. These continuous or analog quantities are monitored by current and potential transformers installed on the lines and on transformers and buses of the power plants and substations of the system. They pass through transducers and analog-to-digital converters and the digital outputs are then telemetered to the energy control centre over various communication links. The data received at the energy control centre is processed by computer to inform the system operators of the present state of the system. The acquired data always contain inaccuracies which is unavoidable, since physical measurements cannot be entirely free of random errors or noise. Because of noise, the true values of physical quantities are never known and one has to consider how to calculate the best possible estimates of these unknown quantities. In practical state estimation the number of actual measurements is far greater than the number of data inputs required by the planning type power flow. As a result, there are many more equations to solve the unknown state variables. This redundancy is necessary, as mentioned earlier, because measurements are sometimes grossly erroneous or unavailable owing to malfunctions in the data gathering system. Direct use of the raw measurements is not advisable, and some of data filtering is needed before the raw data are used in computers. State estimation performs this filtering function by processing the set of measurements as a whole so as to obtain a mean or average value estimate of all the system state variables.

Power system reliability and optimal operation require accurate measurements of current, voltage and real and reactive power. Several hundreds of these measurements are telemetered to the control centre for monitoring control and for use in various computer applications. There is a need for an efficient and economic approach for state estimation to calibrate the measurements and to identify defective instruments. The weighted least square state estimator (WLSE) method has been widely used to solve the power system state estimation problem [93]. The popularity of this method can be attributed to the fact that it provides a best fit for the complex nodal voltages and works well with a large amount of redundant data, such as nodal injections and line measurements. Some of these measurements produce more errors. The weights of the different measurements are proportional to the squares of their residuals.

Most of the WLSE methods are based on the polar co-ordinate formulation of performance equations and can apply on ac systems. However, this chapter provides an estimator based on the rectangular co-ordinate formulation of the performance equations and which can be applied in ac-dc systems.

5.2 MATHEMATICAL MODELLING

The measurement vector 'Z' of a multi-terminal ac-dc power system consists of the telemetered measurements of the followings:

- (i) AC system
- (ii) DC system
- (iii) AC-DC interface (converter) system.

In addition, the ac and dc pseudo measurements can also be used, if needed.

5.2.1 AC System Measurements (Z_{ac})

The following measurements are considered:

- (a) Real & reactive power injections at ac busbars (P_p^m, Q_p^m)
- (b) Real & reactive power flows in lines of ac system (P_{ij}^m, Q_{ij}^m)
- (c) Voltage at ac busbars (V_p^m).

5.2.2 DC System Measurements (Z_{dc})

The dc system measurement set includes the following:

- (a) DC power flow from busbar 'i' to busbar 'j' (Pd_{ij}^m)
- (b) DC current flow from busbar 'i' to busbar 'j' (Id_{ij}^m)
- (c) DC power injection at busbar 'i' (Pd_i^m)
- (d) DC current injection at busbar 'i' (Id_i^m).

5.2.3 Interface System Measurements (Z_{in})

The interface measurement set includes the following:

- (a) AC current into converter 'i' (Is_i^m)
- (b) DC current into converter 'i' (Id_i^m)
- (c) Off-nominal converter transformer tap ratio (a_i^m)
- (d) Firing angle (α_i^m).

5.3 BASIC FORMULATION

Let the measurement vector 'Z' consists of Z_p, Z_q and Z_d where

Z_p = active power measurement

Z_q = reactive power measurement

Z_d = dc parameter measurement

The measurement vector 'Z' is related to the state vector 'X' by

$$Z = h(x) + \mathcal{G} \quad (5.1)$$

where

Z = 'm' dimension vector of measurements (voltages, currents, watts, vars, taps, firing angle etc.)

X = 'n' dimension vector of variables (voltage magnitude & angle at all ac busbars, dc systems and interface state variables)

$h(X)$ = function involving X

\mathcal{G} = 'm' dimension vector of measurement errors or noise; $m > n$

Z = $[Z_p, Z_q, Z_d]^T$

m = number of measurements

n = state variables.

It is assumed that \mathcal{G} is Gaussian, so that $E(\mathcal{G}) = 0$, and

$E(\mathcal{G}\mathcal{G}^T) =$ covariance matrix of \mathcal{G}

= weighting inverse matrix

= $[W^{-1}]$

If the measurement errors \mathcal{G} are assumed to be uncorrelated, then $[W]$ is a diagonal matrix with diagonal elements $W_{ii} = 1/\sigma_{ii}^2$, where σ_{ii}^2 is the variance of the i th measurement.

The method of weighted least square (WLS) technique is used to solve 'm' equations and 'n' unknowns, where 'm' is greater than 'n'.

With the WLS approach, the estimated state \tilde{X} is defined as the value of 'X' which minimises the weighted square residuals

$$r(X) = Z - h(X) \quad (5.2)$$

The least square method which consists of finding the values of the independent variables that minimises the following objective functions:

$$J(X) = [Z - h(X)]^T [W] [Z - h(X)] \quad (5.3)$$

At the estimated value of state vector change of this objective function with respect to the change of state vector should be equal to zero, i.e.;

$$\left. \frac{\partial J(X)}{\partial X} \right|_{x=\bar{x}} = 0 = -2[H(X)]^T [W][Z - h(X)] = 0 \quad (5.4)$$

where

$$H(X) = \frac{\partial h(X)}{\partial X} = \text{is the Jacobian matrix.} \quad (5.5)$$

One of the methods of solving equation (5.4) is based on the Taylor series expansion of $h(X)$ around a nominal point X^0 .

5.3.1 Formulation of $h(x)$

The following equations in the rectangular co-ordinate for the real and reactive nodal power at busbar 'P' can be derived from equation 5.1.

$$P_P^m = \sum_{q=1}^{Nac} \{e_p (e_q G_{pq} + f_q B_{pq}) + f_p (f_q G_{pq} - e_q B_{pq})\} + S_i \alpha_i (e_p c_i - f_p d_i) + k_{p1} \quad (5.6)$$

and

$$Q_P^m = \sum_{q=1}^{Nac} \{f_p (e_q G_{pq} + f_q B_{pq}) - e_p (f_q G_{pq} - e_q B_{pq})\} + t_i \alpha_i (f_p c_i + e_p d_i) + k_{p2} \quad (5.7)$$

The line flow equations in the rectangular coordinates for real and reactive powers in the line 'ij' are

$$P_{ij}^m = \sum e_i \{G_{ij} (e_j - e_i) + f_i B_{ij}\} + f_i \{G_{ij}' (f_j - f_i) - e_j B_{ij}'\} + (e_i^2 + f_i^2) G_{ij}' + k_{p3} \quad (5.8)$$

and

$$Q_{ij}^m = \sum f_i \{G_{ij} e_j + B_{ij}' (f_j - f_i)\} - e_i \{G_{ij}' f_j - B_{ij} (e_j - e_i)\} + (e_i^2 + f_i^2) B_{ij}' + k_{p4} \quad (5.9)$$

where

k_{p1}, k_{p2}, k_{p3} and k_{p4} are measurement errors or noise

e_p = real power components of voltage at busbar 'p'

f_p = imaginary components of voltage at busbar 'p'

$Y_{pq} = G_{pq} + jB_{pq}$ = (p,q)th element of nodal admittance matrix

$Y_{ij}' = G_{ij}' + jB_{ij}' = 1/2 X$ (line charging admittance for line ij).

From inspection of Figs. 2.1 and 2.2 (Chapter 2) the dc voltage of a converter terminal 'i' may be written as

$$V_{di}^2 = k_1^2 \alpha_i^2 (e_p^2 + f_p^2) \cos^2 \alpha_i - k_2^2 Xc_i^2 Id_i^2 - 2S_i k_2 Xc_i Id_i Vd_i \quad (5.10)$$

The power injected into the dc converter 'i' is

$$P_{di} + jQ_{di} = a_i S_i (e_p + jf_p) I_{si}^* \quad (5.11)$$

The real power of equation (5.11) is

$$P_{di} = a_i S_i (e_p c_i - f_p d_i) \quad (5.12)$$

The dc power is also given by

$$P_{di} = V_{di} I_{di} \quad (5.13)$$

From equations (5.12) and (5.13) one can derive

$$V_{di} I_{di} = S_i a_i (e_p c_i - f_p d_i) \quad (5.14)$$

The dc current injection at the dc busbar 'i' in terms of dc network conductance and dc busbar voltage is

$$I_{di} = \sum_{j=1}^{N_{dc}} G_{dc_{ij}} V_{dj} \quad (5.15)$$

The rms alternating current I_{si} is given by

$$I_{si}^2 = c_i^2 + d_i^2 = (k_1 I_{di})^2 \quad (5.16)$$

Writing equations (5.10), (5.14) to (5.16) in the form of equation (5.1):

$$R_1 = (k_1 a_i \cos \alpha_i)^2 (e_p^2 + f_p^2) - (V_{di} + S_i k_2 x_{ci} I_{di})^2 + k_{d5} \quad (5.17)$$

$$R_2 = V_{di} I_{di} - S_i a_i (e_p c_i - f_p d_i) + k_{d6} \quad (5.18)$$

$$R_3 = I_{di} - \sum_{j=1}^{N_{dc}} G_{dc_{ij}} V_{dj} + k_{d7} \quad (5.19)$$

$$R_4 = (k_1 I_{di})^2 - (c_i^2 + d_i^2) + k_{d8} \quad (5.20)$$

Equations from (5.17) to (5.20) form the pseudo measurement equations for each converter.

The equation (5.1) in the residual form for the dc system is:

for nodal voltage at the busbar 'i'

$$R_5 = P_i^m - V_{di} I_{di} + k_{d9} \quad (5.21)$$

Similarly, the nodal voltage at the busbar 'i'

$$R_6 = Vd_i^m - Vd_i + \kappa_{d10} \quad (5.22)$$

The following relationship holds good for power flow and current from busbar 'i' to busbar 'j'

$$R_7 = Pd_{ij}^m - Vd_i Gdc_{ij} (Vd_j - Vd_i) + k_{d11} \quad (5.23)$$

$$R_8 = Id_{ij}^m - Gdc_{ij} (Vd_j - Vd_i) + k_{d12} \quad (5.24)$$

The ac side current $Is_i = (c_i - jd_i)$ can be expressed in terms of the dc side current Id_i as

$$R_9 = (k_1 Id_i^m)^2 - (c_i^2 + d_i^2) + k_{d13} \quad (5.25)$$

Similarly, the following relations may be written for the transformer taps and firing angles

$$R_{10} = a_i^m - a_i + k_{d14} \quad (5.26)$$

$$R_{11} = \cos \alpha_i^m - \cos \alpha_i + k_{d15} \quad (5.27)$$

Equations (5.6) to (5.9) and (5.17) to (5.27) constitute $h(X)$.

Differentiating $h(X)$ with respect to state vector X , and writing in the concise matrix form gives equation (5.28).

$$\frac{\partial h(x)}{\partial x} = \begin{bmatrix} \frac{\partial P}{\partial e} & \frac{\partial P}{\partial f} & \frac{\partial P}{\partial Xd} \\ \frac{\partial Q}{\partial e} & \frac{\partial Q}{\partial f} & \frac{\partial Q}{\partial Xd} \\ \frac{\partial R}{\partial e} & \frac{\partial R}{\partial f} & \frac{\partial R}{\partial Xd} \end{bmatrix} \quad (5.28)$$

The R.H.S. of equation (5.28) is known as the Jacobian matrix $[H]$. The elements of the Jacobian matrix are derived in Appendix - B.

5.4 FIRST ORDER AC-DC STATE ESTIMATOR

The WLSE is based on the first order derivatives of $h(X)$, where $h(X)$ is expressed in the polar co-ordinate. In this section the WLSE has been formulated in such a way that $h(X)$ is expressed in the rectangular co-ordinate. This version of the WLSE is called the first order rectangular co-ordinate ac-dc state estimator (FRSE). Hence, the FRSE is essentially the WLSE in the rectangular form.

From the Taylor series expansion of $h(X)$ around a nominal value X^0 one can write

$$h(X) = h(X^0) + H(X^0) \Delta X + 1/2 L \Delta X^2 + \text{Higher order derivatives} \quad (5.29)$$

Consider only the first order terms

$$h(X) = h(X^0) + H(X^0) \Delta X \quad (5.30)$$

However, from equation (5.4)

$$[H(X)]^T [W] [Z - h(X)] = 0 \quad (5.31)$$

$$\text{or, } [H(X)]^T [W] [Z - h(X^0) - H(X^0) \Delta X] = 0 \quad (5.32)$$

$$\text{or, } [H(X)]^T [W] [H(X^0) \Delta X] = H(X^0)^T [W] [Z - h(X^0)] \quad (5.31)$$

In concise form it is

$$G \Delta X = H(X^0)^T W [Z - h(X^0)] \quad (5.32)$$

The above equation can be written as iterative form

$$\Delta X^{k+1} = G^{-1} H(X^0)^T W \Delta Z^k \quad (5.33)$$

where

$$G = \text{information matrix} = H(X)^T W H(X)$$

$\Delta Z^k = [Z - h(X^k)]$ is the residual in k th iteration.

The equation (5.33) is referred to as proposed FRSE. Equation (5.33) is solved using the Gaussain forward elimination & backward substitution method.

5.4.1 Solution Steps

Step 1 : Read system data and measurements

Step 2 : Initalise state vector $[X^0] = [e^0, f^0, Xd^0]^T$

Step 3 : Set iteration count $k = 0$

Step 4 : Compute Jacobian matrix $[H(X^k)]$

Step 5 : Compute gain matrix $[G(X^k)] = [H(X^k)]^T [W][H(X^k)]$

Triangularise and store factors of $[G(X^k)]$

Step 6 : Compute residual vector $[\Delta Z^k] = [Z - h(X^k)]$

Step 7 : Compute $[H(X^k)]^T [W][\Delta Z^k]$ and solve for $[\Delta X^{(k+1)}]$

using forward and backward operations

Step 8 : Test for convergence. If $\Delta X^{(k+1)} \leq \varepsilon$, then go to step 9. otherwise

set $k=k+1$ and update $X^{(k+1)} = X^k + \Delta X^{(k+1)}$ and go to step 4

Step 9 : Output state vector $X^{(k+1)}$ and stop.

The solution steps are depicted in the flow chart given in Fig. 5.1.

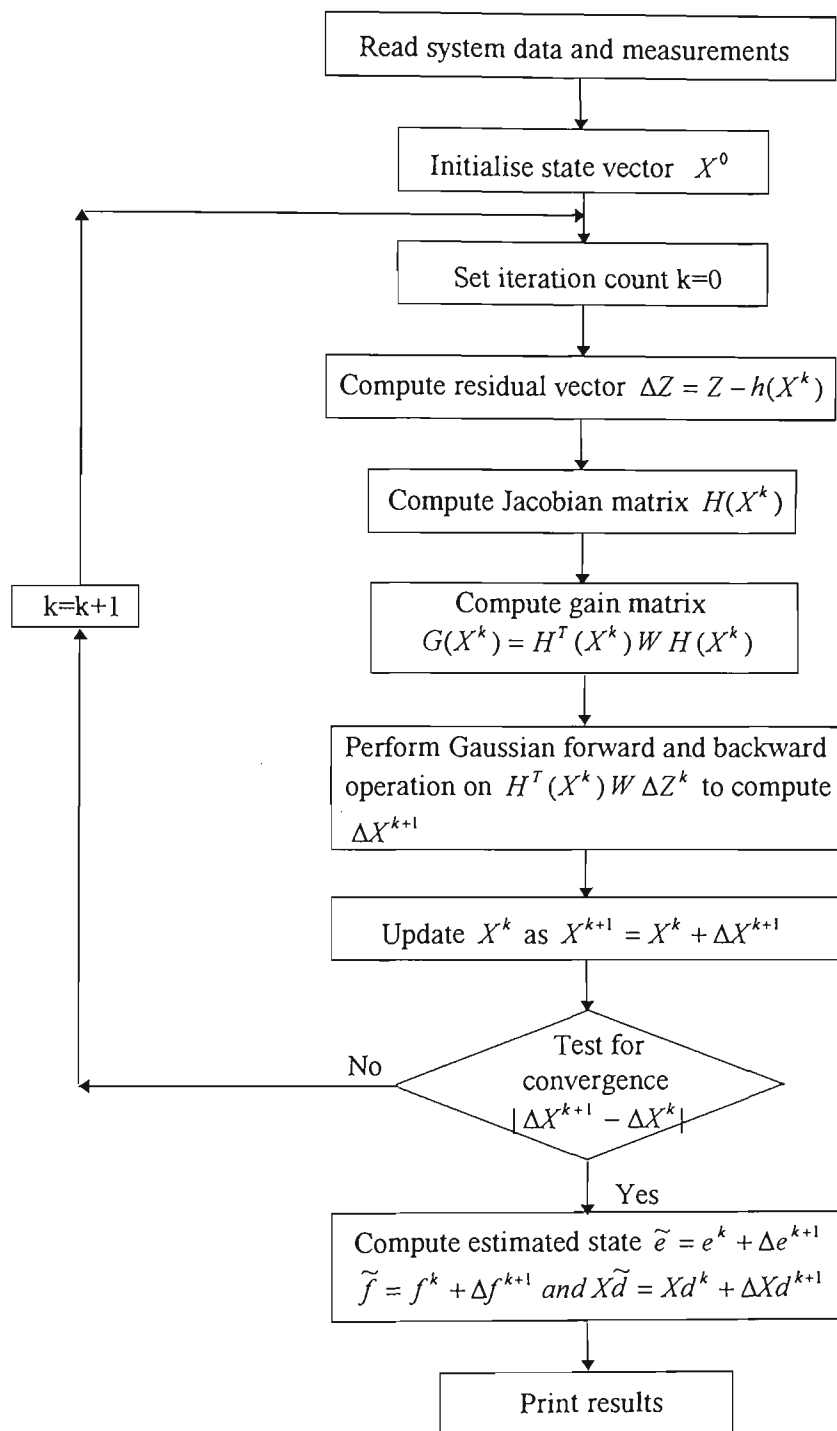


Fig. 5.1 Flow chart for FRSE method

5.4.2. Characteristics of H and G Matrices

The Jacobian matrix is non-symmetrical, diagonally non-dominant, positive and sparse. In the normal form, even some of the diagonal elements are zero. The structure of the H matrix for a 3-busbar network is shown in Chapter -7 (Table 7.1).

The matrix is extremely sparse and so sparsity technique can be employed to conserve the computer memory requirement.

The gain matrix is symmetrical, diagonally dominant, positive - definite and sparse. Diagonals are normally non-zero and so pivoting strategy need not be employed. The sparsity technique can be used in reducing the memory requirement. Table 7.2 (Chapter -7) illustrates the structure of the gain matrix G of a 3-busbar system.

The convergence and computational characteristics of the FRSE are expected to be the same as those of the WLSE.

5.5 CONCLUSIONS

A method called FRSE for assessing the state of ac-dc power systems in the simultaneous framework is developed and presented in this chapter. The method uses the first order derivatives of the ac-dc system equations. The second and other higher order terms which are not insignificant are neglected in this formulation. The proposed state estimation process is performed independently for ac system, the dc system and for the interconnected system. In practice, the computational requirement of dc state estimation is minor in comparison to the ac state estimation. DC state

estimation has all the advantages of ac state estimation including high accuracy during data losses, bad data detection capability and computational efficiency. The control and operation of multi-terminal dc networks during meter and communication outages are enhanced by the proposed method for handling redundant measurements. The computational procedure of the proposed algorithm is highly stable and rapidly convergent. The method performs well under loaded and ill-conditioned networks whereas other methods do not.

Chapter 6

SECOND AND DECOUPLED SECOND ORDER AC-DC STATE ESTIMATOR IN RECTANGULAR CO-ORDINATES

6.1 INTRODUCTION

Two of the important tasks of the modern electrical utility energy control centre are the measurements of real-time data and the estimate of an error-free data base from the measurements. A number of methods are available in the literature [49-85] for the state estimation of electric power systems. Among them, the weighted least square (WLSE) and fast decoupled (FD) state estimator have gained wide spread recognition in the power industry [93]. Though the polar formulation of the full WLSE is an accurate and reliable method for power system state estimation. However, this method is found to be unreliable in many control centres [93]. The FD state estimator method is regarded as the bench mark technique due to its computational superiority. It performs quite well so long as the decoupling and other assumptions are valid. Otherwise, convergence problems are encountered in some ill-conditioned networks.

Methods proposed by Roy (11) and Iwamoto *et al.* (12) involve cartesian coordinate formulation of the load flow equations and a complete repre-

sensation of these equations in a Taylor series. These methods will, hereafter, be referred to an exact second order (ESO) method, perform better than the NR method and do not stack up well against the state of the art FD method.

Using the same formulation as in the ESO method, two new mathematical models for ac-dc state estimation has been developed and experimented in this Chapter. These estimators are called second order rectangular co-ordinate ac-dc state estimator (SRSE) and decoupled second order rectangular co-ordinate ac-dc state estimator (DSRSE). The primary difference between the two estimators is that the latter is faster than the former. The new estimators are based on a complete Taylor series expansion of the nodal and line-flow equations in cartesian coordinate. The capability of the proposed methods to serve as a real-time monitor is demonstrated by digital simulation studies on a number of sample power systems, the results being comparable to those utilising the FD state estimator method. This comparison reveals that, owing to its exact formulation, lower computational requirements, and the ability to provide a reliable system state even during unusual operating conditions, the proposed method is practically viable and preferred analytically as a tool for real-time monitoring of power system.

6.2 SECOND ORDER AC-DC STATE ESTIMATOR

It was mentioned in Chapter 5 that the classical WLSE method has been widely used to solve the power system state estimation problem. The method performs well for most of the systems. However, the numerical

problem associated with this approach is that the statistical characteristic of the errors must be known to determine proper values for the weighting factors. Another numerical difficulty encountered is that, if sufficient redundancy is not included ill-conditioning of system equations may lead to poor convergence. Furthermore, the computer memory and time requirements are relatively high. To overcome these difficulties, a number of alternative algorithms, including modifications and refinements of the basic WLSE approach have been proposed [55-62]. One such modification involves the application of the P- δ and Q-V decoupling technique used in the fast decoupled load flow method [10] and is called the FD state estimator. The FD state estimator has been demonstrated to be computationally very efficient and seems to enjoy wide acceptance as a result. However, since the FD state estimator is based on the underlying decoupling assumptions of the FD load flow, there are number of limitations of this method.

- The FD state estimator is dependent on the initial flat voltage, which in some systems has a large δ and a poor V.
- The rate of convergence are strongly influenced by the coupling between the P- δ and Q-V mathematical models. This coupling increases with system loading levels and branch with high R/X ratios.
- On ill-conditioned power systems, the decoupled method either fails to provide a solution or results in oscillatory convergence.

From the above discussion it is clear that FD state estimator does not appear

to be suitable for real-time monitoring of power system under all conditions and the computational requirements of the basic WLSE are large. Hence, there is a need for developing new method for state estimation that are devoid of the limitations of WLSE and FD state estimator.

A method based on full Taylor series expansion of load flow equations in cartesian co-ordinates has been proposed [81]. The fact that in rectangular co-ordinate version the network performance equations are completely expressible in a Taylor series and contains terms up to the second order derivatives only, results into an estimator called second order state estimator (SOSE). In this estimator, the Jacobian and information matrices are constant, and hence need to be computed only once in the iterative scheme. This results in considerable saving of computation and storage requirements, making the algorithm more attractive than the FD state estimator, although keeping it free from the limitations of the latter. The exact formulation of the algorithm enables it to perform well even during unusual operating conditions, when the metered reference voltage is not close to 1.0 pu. The method is also found to be advantageous when the R/X ratios of the line is large.

The above formulation is based on ac system only. In this section a new state estimation algorithm for ac-dc system which is based on the rectangular co-ordinate and first and second order derivatives of the Taylor series has been developed. The algorithm is capable of handling the ac system, the dc system and the interconnection system simultaneously. The ac, dc and converter networks are modelled in the rectangular form. The ac and dc equations in the Taylor series terminate after the second order derivatives.

However, some interconnection system equations contain terms up to the sixth order derivatives in the Taylor series. An approximation is made for two converter equations that contain higher than second order derivatives. In the proposed method the Jacobian matrix, H and the information matrix, G need to be computed once only. These desirable features lead to considerable saving in the solution time, making the method faster than the basic WLSE, while keeping the memory requirements comparable both for well-conditioned and ill-conditioned network.

The first order rectangular co-ordinate state estimator is based on the first order derivatives of the function $h(x)$. In first order method, the mathematical model is based on the truncated Taylor series and linearisation. The Jacobian matrix, H and the information matrix, G need to be computed in every iteration. As such, the method is expected to take large computing time.

To minimise the limitations of fast order and FD state estimator, an entirely new method, called the second order rectangular co-ordinate ac-dc state estimator has been developed.

6.2.1 Algorithmic Development

The function $h(x)$ involves equations (5.6) to (5.9) and (5.17) to (5.27). An inspection of equations (5.6) to (5.9) reveals that they are quadratic in e and f for the ac busbars. As such, the first order derivatives, $\frac{\partial h}{\partial e}$ and $\frac{\partial h}{\partial f}$ contain e and f , but the second order derivatives $\frac{\partial^2 h}{\partial e^2}$, $\frac{\partial^2 h}{\partial f^2}$, $\frac{\partial^2 h}{\partial e \partial f}$ and

$\frac{\partial^2 h}{\partial f \partial e}$ do not contain e and f . The second order network constants G , B , G' and B' and they are constant. Consequently, the third and higher order derivatives of the function $h(x)$ with respect to ' e ' and ' f ' are zero. However, for the converter busbars, the Taylor series expansion of the performance equation contains third order derivatives also.

Similarly, the Taylor series expansion of equations (5.19) to (5.27) terminate after the second order derivatives. Only equations (5.17) and (5.18) do not terminate after the second order derivatives. An approximation is made and the derivatives higher than second orders are neglected in the mathematical formulation.

Consider the Taylor series expansion around a nominal point X^0 , equation (6.1) is obtained.

$$h(X) = h(X^0) + \frac{\partial h}{\partial X^0} \Delta X + \frac{1}{2} \frac{\partial^2 h}{\partial (X^0)^2} \Delta X^2 + \text{higher order derivatives} \quad (6.1)$$

It has already been mentioned that the third and higher order derivatives of $h(X)$ corresponding to equations (5.6) to (5.9) and (5.19) to (5.27) are zero. However, the higher order derivatives (higher than the second order) corresponding to equations (5.17) and (5.18) and (5.6) and (5.7) for converter busbars are not zero, and are present in equation (6.1).

Neglecting the third and higher order derivatives, equation (6.1) reduces to

$$h(x) = h(X^0) + \frac{\partial h}{\partial X^0} \Delta X + \frac{1}{2} \frac{\partial^2 h}{\partial (X^0)^2} \Delta X^2 \quad (6.2)$$

$$= h(X^0) + H(X^0)\Delta X + \frac{1}{2}L\Delta X^2 \quad (6.3)$$

where L is the second order derivatives.

Substituting equation (6.3) in equation (5.4) and after reorganising the resulting equation is

$$H(X^0)^T W H(X^0)\Delta X = H(X^0)^T W [Z - h(X^0) - \frac{1}{2}L\Delta X^2] \quad (6.4)$$

In concise form it is

$$G(X^0)\Delta X = H(X^0)^T W [Z - h(X^0) - \frac{1}{2}L\Delta X^2] \quad (6.5)$$

The above equation can be written in iterative form

$$G(X^0)\Delta X^{(k+1)} = K(X^0)\Delta Z^{(k)} \quad (6.6)$$

where

$$\Delta Z = Z - h(X^0) - \frac{1}{2}L(\Delta X^k)^2$$

$$G = H(X^0)^T W H(X^0)$$

$$K = H(X^0)^T W$$

$$\Delta Z = Z - h(X^0)$$

The matrices G and K are calculated using the initial assumed value of $X = X^0 (e^0, f^0, Xd^0)$. Both G and K remain constant in the recursive solution of equation (6.5). They change whenever there is any change in the network configuration. The initial estimate X^0 remains constant in the iterative scheme but the error vector ΔX is updated recursively.

In fact G and K remain constant in the iterative solution leading to

considerable reduction in the solution time making the proposed procedure faster. The mathematical model characterised by equation (6.5) is the proposed second order rectangular co-ordinate ac-dc state estimator (SRSE).

Equation (6.5) is solved using Gaussian forward elimination and backward substitution procedures. H and G are sparse and sparsity technique may be used to advantage. L is not stored in the matrix form. L involves constant of the network that are available in the memory. Element by element calculation is made for ΔZ and the relevant network constants.

6.2.2 Characteristics of SRSE

A comparison of equations (5.33) and (6.6) reveals that the size of the information matrix H^TWH and that of gain matrix is the same. Also, the size of the H^TW matrix is equal to that of the K matrix. As described earlier, L does not require additional memory. Therefore, the computer memory requirement of the FRSE and SRSE is almost the same. Unlike the computation of H^TWH and H^TW of the FRSE approach in each iteration, whereas G and K of the SRSE are evaluated once only. The mathematical operations required to compute $[Z-h(X)]$ in the FRSE are comparable to those to compute $\Delta Z'$ in the SRSE. Thus the convergence characteristic of the SRSE method is similar to that of FRSE method, but the former method can be expected to require less computation time. Consequently, the SRSE method turns out to be faster than the FRSE method. The SRSE method is not only exact and computationally superior than the FRSE, but also it does not stack up against ill-conditioned networks where the FD state estimator requires some more iterations and some time it fails.

6.2.3 Solution Steps

Step 1 : Read system data and measurements

Step 2 : Initialise the state vector $[X^0] = [e^0, f^0, Xd^0]^T$

Step 3 : Compute the Jacobian matrix $[H(X^0)]$

Step 4 : Compute the gain matrix $[G(X^{(0)})] = [H(X^{(0)})]^T [W][H(X^{(0)})]$
and triangularise and store factors of $[G(X^{(0)})]$

Step 5 : Set iteration count $K=0$

Step 6 : Compute the residual vector

$$\Delta Z' = [Z - h(X^{(0)}) - \frac{1}{2} [L(X^{(0)})[\Delta X^k]^2]$$

Step 7 : Compute $[H(X^{(0)})]^T [W][\Delta Z'^{(k)}]$ and perform forward and backward operations to solve for $\Delta X^{(k+1)}$

Step 8 : Test for convergence. If $|\Delta X^{(k+1)} - \Delta X^{(k)}| \leq \varepsilon$, go to step 9.

Otherwise, set $k = k+1$, go to step 6

Step 9 : Update the state vector $X = X^{(0)} + \Delta X^{(k+1)}$ and output the state vector X .

The flow chart of SRSE is given in Fig. 6.2

6.3 DECOUPLED SECOND ORDER AC-DC STATE ESTIMATOR

The SRSE method is computationally superior than the methods based on the FRSE approach and its CPU time is comparable to the fast decoupled ac-dc state estimator (FDSE). Also the convergence characteristics of the SRSE is linear which is found to be quadratic in nature for FRSE

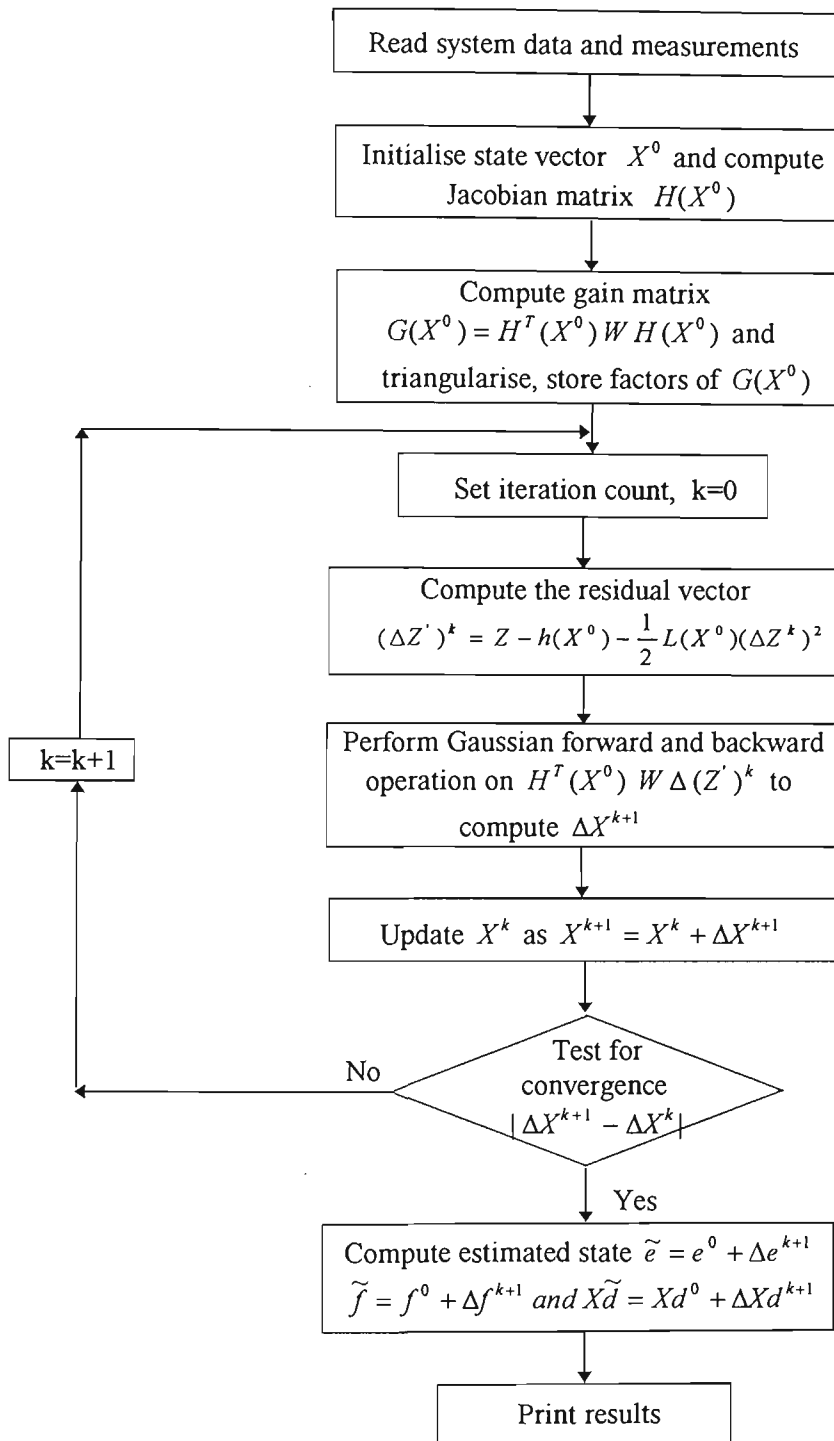


Fig. 6.1 Flow chart for SRSE method

method. Though SRSE performs well under ill-conditioned and heavily loaded conditioned networks whereas the FDSE takes more iterations and in some cases it fails to converge but its computational efficiency is inferior than FDSE method. Therefore, a faster version of the SRSE is developed. This version is called, decoupled second order rectangular ac-dc state estimator. In the proposed method the first and second order derivatives of the ac, dc and converter equations in the rectangular form are used to develop the decoupled algorithm. Decoupling is not done by zeroing the off-diagonal submatrices of the Jacobian and gain matrices but by shifting them to the other side. The mathematical model involves both the first and second order derivatives of the performance equations. The diagonal blocks of the gain matrix are required to be factorised in the iterative scheme. Their size and structure are similar to those in the fast decoupled state estimator which is based on the linearised version of the Taylor series equations. These desirable features lead to considerable saving in solution time making the method little bit faster than FDSE method. As there is no major approximation in the mathematical model, so the solution is exact. The proposed method in spite of being exact and little bit faster than the FDSE, does not stack up against ill-conditioned and heavily loaded conditioned networks.

6.3.1 Algorithmic Development

The measurement vector 'Z' can be partitioned into three parts

$$Z = \begin{bmatrix} Z_p \\ Z_q \\ Z_d \end{bmatrix} = \begin{bmatrix} f_1(e, f, Xd) \\ f_2(e, f, Xd) \\ f_3(e, f, Xd) \end{bmatrix} + v = h(e, f, Xd) + v \quad (6.7)$$

where

Z_p = Set of real power line flow and injection measurements.

Z_q = Set of reactive power line flow and injection and voltage magnitude measurements.

Z_d = Measurements involving set of dc line current, dc voltage, firing angle, transformer tap, converter transformer secondary current, converter dc voltage, converter dc power, converter dc current, converter reactive power etc.

Accordingly, the change in the state and measurement vectors can be expressed as

$$\Delta X = \begin{bmatrix} \Delta X_p \\ \Delta X_q \\ \Delta X_d \end{bmatrix} = \begin{bmatrix} \Delta e \\ \Delta f \\ \Delta Xd \end{bmatrix} \quad (6.8)$$

$$\Delta Z = \begin{bmatrix} \Delta Z_p \\ \Delta Z_q \\ \Delta Z_d \end{bmatrix} = \begin{bmatrix} \Delta P \\ \Delta Q \\ \Delta Zd \end{bmatrix} \quad (6.9)$$

With the above definition, equation (6.5) can be expressed in the expanded form

$$\begin{bmatrix} G_1 & G_2 & G_3 \\ G_4 & G_5 & G_6 \\ G_7 & G_8 & G_9 \end{bmatrix} \begin{bmatrix} \Delta e \\ \Delta f \\ \Delta Xd \end{bmatrix} = \begin{bmatrix} K_1 & K_2 & K_3 \\ K_4 & K_5 & K_6 \\ K_7 & K_8 & K_9 \end{bmatrix} \begin{bmatrix} \Delta Z_p \\ \Delta Z_q \\ \Delta Z_d \end{bmatrix} - 1/2 \begin{bmatrix} L \end{bmatrix} \begin{bmatrix} \Delta e^2 \\ \Delta f^2 \\ \Delta Xd^2 \end{bmatrix} \quad (6.10)$$

In concise form it is

$$\begin{bmatrix} G_1 & G_2 & G_3 \\ G_4 & G_5 & G_6 \\ G_7 & G_8 & G_9 \end{bmatrix} \begin{bmatrix} \Delta e \\ \Delta f \\ \Delta Xd \end{bmatrix} = \begin{bmatrix} K_1 & K_2 & K_3 \\ K_4 & K_5 & K_6 \\ K_7 & K_8 & K_9 \end{bmatrix} \begin{bmatrix} \Delta Z_p \\ \Delta Z_q \\ \Delta Z_d \end{bmatrix} - \begin{bmatrix} S_p \\ S_q \\ S_d \end{bmatrix} \quad (6.11)$$

In shorter form

$$\begin{bmatrix} G_1 & G_2 & G_3 \\ G_4 & G_5 & G_6 \\ G_7 & G_8 & G_9 \end{bmatrix} \begin{bmatrix} \Delta e \\ \Delta f \\ \Delta Xd \end{bmatrix} = \begin{bmatrix} K_1 & K_2 & K_3 \\ K_4 & K_5 & K_6 \\ K_7 & K_8 & K_9 \end{bmatrix} \begin{bmatrix} \Delta Z'_p \\ \Delta Z'_q \\ \Delta Z'_d \end{bmatrix} \quad (6.12)$$

where G and K are partitioned into nine blocks. Each block is a submatrix.

$$G_1 = H_{11}^T W_p H_{11} + H_{21}^T W_q H_{21} + H_{31}^T W_d H_{31}$$

$$G_2 = H_{11}^T W_p H_{12} + H_{21}^T W_q H_{22} + H_{31}^T W_d H_{32}$$

$$G_3 = H_{11}^T W_p H_{13} + H_{21}^T W_q H_{23} + H_{31}^T W_d H_{33}$$

$$G_4 = H_{12}^T W_p H_{11} + H_{22}^T W_q H_{21} + H_{32}^T W_d H_{31}$$

$$G_5 = H_{12}^T W_p H_{12} + H_{22}^T W_q H_{22} + H_{32}^T W_d H_{32}$$

$$G_6 = H_{12}^T W_p H_{13} + H_{22}^T W_q H_{23} + H_{32}^T W_d H_{33}$$

$$G_7 = H_{13}^T W_p H_{11} + H_{23}^T W_q H_{21} + H_{33}^T W_d H_{31}$$

$$G_8 = H_{13}^T W_p H_{12} + H_{23}^T W_q H_{22} + H_{33}^T W_d H_{32}$$

$$G_9 = H_{13}^T W_p H_{13} + H_{23}^T W_q H_{23} + H_{33}^T W_d H_{33}$$

$$K_1 = H_{11}^T W_p; \quad K_2 = H_{21}^T W_p; \quad K_3 = H_{31}^T W_p$$

$$K_4 = H_{12}^T W_q; \quad K_5 = H_{22}^T W_q; \quad K_6 = H_{32}^T W_q$$

$$K_7 = H_{13}^T W_d; \quad K_8 = H_{23}^T W_d; \quad K_9 = H_{33}^T W_d$$

$$[W] = \begin{bmatrix} W_p & 0 & 0 \\ 0 & W_q & 0 \\ 0 & 0 & W_d \end{bmatrix}$$

$$[H] = \begin{bmatrix} \frac{\partial h_p}{\partial e} & \frac{\partial h_p}{\partial f} & \frac{\partial h_p}{\partial Xd} \\ \frac{\partial h_q}{\partial e} & \frac{\partial h_q}{\partial f} & \frac{\partial h_q}{\partial Xd} \\ \frac{\partial h_d}{\partial e} & \frac{\partial h_d}{\partial f} & \frac{\partial h_d}{\partial Xd} \end{bmatrix} = \begin{bmatrix} H_{11} & H_{12} & H_{13} \\ H_{21} & H_{22} & H_{23} \\ H_{31} & H_{32} & H_{33} \end{bmatrix}$$

and

$$\Delta Z'_p = \Delta Z_p - S_p; \quad \Delta Z'_q = \Delta Z_q - S_q; \quad \Delta Z'_d = \Delta Z_d - S_d$$

where

S_p, S_q and S_d are second order terms in concise form.

A reorganisation of equation (6.12) yields

$$\begin{bmatrix} G_1 & 0 & 0 \\ 0 & G_5 & 0 \\ 0 & 0 & G_9 \end{bmatrix} \begin{bmatrix} \Delta e \\ \Delta f \\ \Delta Xd \end{bmatrix} = \begin{bmatrix} K_1 & K_2 & K_3 \\ K_4 & K_5 & K_6 \\ K_7 & K_8 & K_9 \end{bmatrix} \begin{bmatrix} \Delta Z'_p \\ \Delta Z'_q \\ \Delta Z'_d \end{bmatrix} - \begin{bmatrix} 0 & G_2 & G_3 \\ G_4 & 0 & G_6 \\ G_7 & G_8 & 0 \end{bmatrix} \begin{bmatrix} \Delta e \\ \Delta f \\ \Delta Xd \end{bmatrix} \quad (6.13)$$

After decoupling,

$$G_1 \Delta e = [K_1 \ K_2 \ K_3] \begin{bmatrix} \Delta Z'_p \\ \Delta Z'_q \\ \Delta Z'_d \end{bmatrix} - [G_2 \ G_3] \begin{bmatrix} \Delta f \\ \Delta Xd \end{bmatrix} \quad (6.14)$$

$$G_5 \Delta f = [K_4 \ K_5 \ K_6] \begin{bmatrix} \Delta Z'_p \\ \Delta Z'_q \\ \Delta Z'_d \end{bmatrix} - [G_4 \ G_5] \begin{bmatrix} \Delta e \\ \Delta Xd \end{bmatrix} \quad (6.15)$$

$$G_9 \Delta Xd = [K_7 \ K_8 \ K_9] \begin{bmatrix} \Delta Z'_p \\ \Delta Z'_q \\ \Delta Z'_d \end{bmatrix} - [G_7 \ G_8] \begin{bmatrix} \Delta e \\ \Delta f \end{bmatrix} \quad (6.16)$$

Equations (6.14 to 6.16) can be written in concise form

$$G_1 \Delta e = K_p \Delta Z' - G_p \Delta X_p \quad (6.17)$$

$$G_5 \Delta f = K_q \Delta Z' - G_q \Delta X_q \quad (6.18)$$

$$G_9 \Delta Xd = K_d \Delta Z' - G_d \Delta Xd \quad (6.19)$$

And in an iterative form it is

$$G_1 \Delta e^{(k+1)} = K_p \Delta Z'^{(k)} - G_p \Delta X_p^{(k)} = Y_1^{(k)} \quad (6.20)$$

$$G_5 \Delta f^{(k+1)} = K_q \Delta Z'^{(k)} - G_q \Delta X_q^{(k)} = Y_2^{(k)} \quad (6.21)$$

$$G_9 \Delta Xd^{(k+1)} = K_d \Delta Z'^{(k)} - G_d \Delta Xd^{(k)} = Y_3^{(k)} \quad (6.22)$$

where k = iteration count, and

$$K_p = [K_1 \ K_2 \ K_3]; \ K_q = [K_4 \ K_5 \ K_6]; \ K_d = [K_7 \ K_8 \ K_9]$$

$$G_p = [G_2 \ G_3]; \ G_q = [G_4 \ G_6]; \ G_d = [G_7 \ G_8]$$

$$[\Delta X_p]^k = [\Delta f^k \ \Delta Xd^k]$$

$$[\Delta X_q]^k = [\Delta e^{k+1} \ \Delta Xd^k]$$

$$[\Delta Xd]^k = [\Delta e^{k+1} \ \Delta f^{k+1}]$$

Equations (6.20 to 6.22) are solved sequentially using the Gaussian forward elimination and backward substitution method, and denote the decoupled second order rectangular co-ordinate ac-dc state estimator (DSRSE).

In equations (6.20 to 6.22) $G_1, G_5, G_9, K_p, K_q, K_d, G_p, G_q,$ and G_d are calculated at $X = X^0$, and remain constant in the recursive solution. G_1, G_5 and G_9 are extremely sparse and their factored form should fully exploit symmetry and sparsity.

For the evaluation of $\Delta Z^{(k)}$, a particular row of L is multiplied by $\Delta X^{2(k)}$, where again the sparsity structure of L is exploited. The second order terms are neither calculated nor stored in the matrix form.

Each element of Y_1 is calculated using the corresponding row of K_p and G_p in each iteration. Y_2 and Y_3 are calculated in the similar manner. The sparsity and structure are fully exploited.

Iterations are terminated if $|\Delta e^{(k+1)} - \Delta e^{(k)}|, |\Delta f^{(k+1)} - \Delta f^{(k)}|$ & $|\Delta Xd^{(k+1)} - \Delta Xd^{(k)}|$ are less than the specified tolerance.

6.3.2 Advantages

Several advantages occur from embedding the decoupled technique into the state estimation algorithm.

- The Jacobian submatrices are constant, which in turn, produce constant information submatrices.
- The computer memory requirement is considerably reduced by the e , f and Xd decouplings.
- The number of multiplications are considerably reduced because of the block diagonal structure of the Jacobian and information matrices in the decoupled algorithm.
- Since only one factorisation of the constant information submatrices is necessary, the DSRSE is considerably faster than the basic FRSE and SRSE methods.

Accordingly, although the quadratic nature of the convergence is degraded in the decoupled estimator, the total solution time is far less in view of the factors as aforementioned.

6.3.3 Characteristics of DSRSE

The set of matrix equations (6.20) to (6.22) constitute the proposed DSRSE method. As the solution algorithm has been developed from the SRSE mathematical model without involving any major approximation, the proposed DSRSE is also exact. It may be recalled that FDSE method consists of two co-efficient matrices $I_{P\delta}$ and I_{QV} , each are equal in size and one fourth of the full information matrix. Similarly, each of G_1, G_5 and G_9 ,

are equal in size and one fourth of information matrix. Further, matrix K is calculated once only and remain constant in the iteration scheme. In contrast, matrix H are computed in each iteration. Otherwise, the accuracy of the solution is degraded as the objective function is then not actually minimised. The weighting matrix W and the elements of the nodal admittance matrix G_p, G_q and G_d are available in the computer. G_p, G_q and G_d are computed in each iteration and are not stored explicitly in the matrix form. This avoids the need for extra computer memory but increases the computational time. It is also noted that L involve the elements of the nodal admittance matrix and hence are constant and do not require additional memory. Also, $\Delta Z'_p, \Delta Z'_q$ and $\Delta Z'_d$ are constant as they are computed at the initial estimate state. On the other hand, ΔZ in the FDSE method is computed in each iteration. From the above comparative estimates, it is evident that the computer memory and unit time requirements of the proposed DSRSE and the conventional FDSE are of the same order. The beauty of the proposed algorithm is that it performs well under all circumstances and all operating modes whereas the FDSE does not converge under certain conditions.

6.3.4 Solution Steps

Step 1 : Read the system data and measurements

Step 2 : Initialise the state vector $[X^0] = [e^0, f^0, Xd^0]^T$

Step 3 : Set $[\Delta e] = [0]$; $[\Delta f] = [0]$; $[\Delta Xd] = [0]$

Step 4 : Compute the Jacobian matrix $H(X^0)$; using e^0, f^0, Xd^0, G, B and Gdc

Step 5 : Compute Gain matrices $[G_1(X^0)], [G_5(X^0)],$ and $[G_9(X^0)]$

Step 6 : Triangularise and store factors of

$$[G_1(X^0)], [G_5(X^0)], \text{ and } [G_9(X^0)]$$

Step 7 : Compute the residual measurements $\Delta Z_p, \Delta Z_q$ and ΔZ_d using e^o, f^o, Xd^o, G, B and Gdc and the measurements $\Delta Z_p, \Delta Z_q$ and ΔZ_d

Step 8 : Set iteration count $k = 0$

Step 9 : Compute the second order terms and new residuals

$$\Delta Z_p'^{(k)} = \Delta Z_p - S_p^{(k)}; \Delta Z_q'^{(k)} = \Delta Z_q - S_q^{(k)}; \Delta Z_d'^{(k)} = \Delta Z_d - S_d^{(k)}$$

Step 10 : Compute $Y_1^{(k)}$ using $\Delta e^{(k)}, \Delta f^{(k)}$ and $\Delta Xd^{(k)}$

Step 11 : Obtain $\Delta e^{(k+1)}$

Step 12 : Compute $Y_2^{(k)}$ using $\Delta e^{(k+1)}, \Delta f^{(k)}$ and $\Delta Xd^{(k)}$

Step 13 : Obtain $\Delta f^{(k+1)}$

Step 14 : Compute $Y_3^{(k)}$ using $\Delta e^{(k+1)}, \Delta f^{(k+1)}$ and $\Delta Xd^{(k)}$

Step 15 : Obtain $\Delta Xd^{(k+1)}$

Step 16 : Check the convergence

$$|\Delta e^{(k+1)} - \Delta e^{(k)}| \leq \varepsilon$$

$$|\Delta f^{(k+1)} - \Delta f^{(k)}| \leq \varepsilon$$

$$|\Delta Xd^{(k+1)} - \Delta Xd^{(k)}| \leq \varepsilon.$$

If converged go to step 17. Otherwise, set $k = k+1$ and go to step 9.

Step 17 : System states are obtained from

$$\tilde{e} = e^{(0)} + \Delta e^{(k+1)}$$

$$\tilde{f} = f^{(0)} + \Delta f^{(k+1)}$$

$$\tilde{Xd} = Xd^{(0)} + \Delta Xd^{(k+1)}.$$

The flow chart of DSRSE algorithm is given in Fig. 6.2

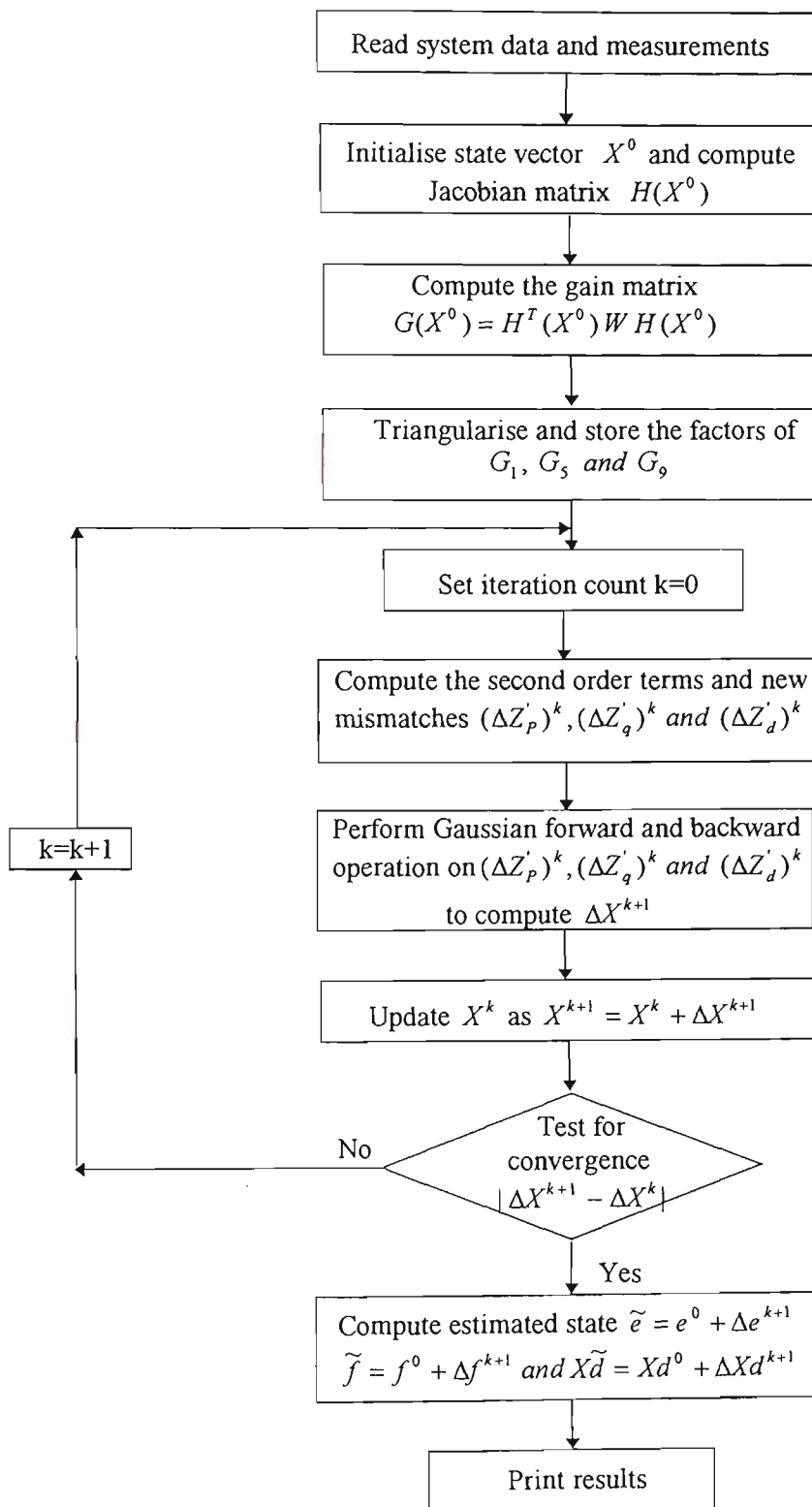


Fig. 6.2 Flow chart for SRSE method

6.6 CONCLUSIONS

Two new mathematical models for ac-dc state estimator have been developed without any major approximation of the Taylor series. The algorithms are more exact. It is assumed that SRSE method, in spite of being exact and faster than the FRSE method, does not perform well against the most popular FDSE method in terms of computational efficiency but does not stack up against ill-conditioned networks whereas the FDSE takes longer time and sometime fails. The new methods are based on the cartesian coordinate formulation of network performance equations and a complete Taylor series representation of these equations, without involving major approximation. The mathematical model of the DSRSE is of the same size as that of the FDSE method, and hence characterised by comparable computational requirements. Its performance is comparable to that of the FDSE method on well-conditioned networks, but decidedly superior on ill-conditioned and heavily loaded conditioned networks.

Chapter 7

SIMULATION STUDIES

7.1 INTRODUCTION

Chapters 5 & 6 dealt with the development of first and second order ac-dc state estimation in rectangular co-ordinate. First order rectangular co-ordinate ac-dc state estimator (FRSE) is basically the weighted least square state estimator (WLSE) with some dc network connected to the ac system. Second order rectangular co-ordinate ac-dc state estimator (SRSE) is derived from the full Taylor series expansion of the system equations without involving any major approximations on the converter equations. Decoupled second order rectangular co-ordinate ac-dc state estimator (DSRSE) is derived from the SRSE without any approximation in order to reduce the CPU time and to obtain better convergence pattern. In this chapter the computational efficiency, convergence characteristics, solution accuracy and real time monitoring of the proposed estimators have been examined by digital simulation studies on a number of sample power systems. The proposed algorithms have been tested on well behaved ac-dc networks in order to get normal state estimation solution. Also the proposed algorithms have been tested on some ill-conditioned power systems and some loaded conditioned networks where the fast decoupled (FD) state estimators fail to

converge or produce oscillatory convergence. The proposed algorithms are also tested on well behaved networks with unusual operating conditions and its results are compared with FD state estimator. Since the DSRSE is basically derived from the SRSE algorithm without involving any approximations this is the reason it is more exact and is computationally more efficient than its parent version. The fast decoupled state estimator is used in simulation studies for comparative purpose. Performance characteristics of the ac-dc state estimator are investigated incorporating with a link, mesh and mesh-link connected dc networks on IEEE 14, 30, 57 and 107 bus system.

7.2 INITIALISATION

Appropriate weighting factors are calculated from the following considerations:

(1) For ac network

$$\sigma = 0.02 \mid \text{meter readings} \mid + 0.0035 \mid \text{fullscale} \mid$$

(ii) For dc network

$$\sigma = 0.01 \mid \text{meter readings} \mid + 0.002 \mid \text{fullscale} \mid$$

(iii) For dc voltage, current, tap ratio and firing angle

$$\sigma = 0.01 \mid \text{meter readings} \mid + 0.0035 \mid \text{fullscale} \mid$$

The full scale value for all meters are assumed 1.0 pu. Initial values assumed for the other variables are: $e = 1.0$; $f = 0.0$; $\alpha_i = 1.0$; $Vd_i = 1.3$; $c_i = 1.2 Id_i$; $d_i = 0.6 Id_i$; $Id_i = Pd_i / Vd_i$; $\cos \alpha_i = \cos \alpha_{i \min}$.

The above assumed values can be replaced by the available measured ones, if available or desired.

7.3 MODIFICATION OF STANDARD TEST SYSTEM (State Estimation analysis)

The ac-dc system are formed by replacing some of the ac lines by dc links with dc power flow in the links set equal to the real power flow in the replaced ac lines. A brief description of the systems used for testing proposed algorithms are given below:

IEEE 14-busbar system:

- Case I ac line between busbars 4 and 5 is replaced by a dc link.
- Case II ac lines between busbars 2-4, busbars 2-5 and busbars 4-5 are replaced by dc links and a three terminal dc mesh systems is obtained between busbars 2,4 and 5.
- Case III the system in Case II is further modified by replacing the ac lines between busbars 9 and 10 by a dc link. It results in a 5 terminal dc link-mesh system.

IEEE 30-busbar system:

- Case I ac line between busbars 2 and 5 is replaced by a dc link.
- Case II a three terminal dc mesh system is formed between busbars 2 and 7 by placing ac line connecting busbars 2 and 5 by a dc link and introducing dc links between busbars 2 and 7 and busbars 5 and 7.
- Case III the system in Case II is further modified by replacing the ac line between busbars 15 and 18 by a dc link to form a dc link mesh system.

IEEE 57-busbar system:

- Case I ac line between busbars 8 and 9 is replaced by a dc link.
- Case II a three terminal dc mesh system is formed between busbars 6, 8 and 9 by replacing ac line between busbars 8 and 9 and 6 and 8, and introducing dc links between busbars 6 and 9.
- Case III a five terminal dc link-mesh system is formed by replacing the ac line between busbars 44 and 45 in case II by a dc link.

107 - busbar system

- A double circuit ac line out of the two double circuit ac lines between busbars 60 and 99 is replaced by a dc link.

Detailed circuit configurations for Link, Mesh and Mesh-link system are given in Appendix - E and the bus data are provided in Appendix - D.

7.4 PERFORMANCE INDICES

The performance of the algorithm in the simulation studies is assessed by comparing the estimated value \tilde{Z} and the measured value Z with the true value Z^t . The following indices are used for this comparison.

$$J_E = \frac{1}{m} \sum_{i=1}^m \{(\tilde{Z}_i - Z_i^t) / \sigma_i\}^2$$

$$J_M = \frac{1}{m} \sum_{i=1}^m \{(Z_i - Z_i^t) / \sigma_i\}^2$$

$$R_{av} = \frac{1}{m} \sum_{i=1}^m (|\tilde{Z}_i - Z_i^t| / \sigma_i)$$

$$R_{\max} = \max \sum_{i=1}^m (|\tilde{Z}_i - Z_i'|/\sigma_i)$$

The performance index J_M indicates the level of uncertainty in the measurements. The index J_E shows how close are the estimated values to the true ones. The effectiveness of the filtering process is indicated by a value of J_E less than the corresponding value of the J_M . The R_{av} and R_{\max} indicates the average and the maximum values of weighted residuals from the true values to complement the general information of the indicators J_M and J_E .

The true and estimated values of the state variables are compared by $\varepsilon_\lambda = \frac{\tilde{X} - X^t}{X^t} 100$. The average and maximum values of ε_λ are also computed.

7.5 STATE ESTIMATION UNDER ILL-CONDITIONED SYSTEM

The basic approaches to solve the state estimation problem involves the solution of set of quadratic equations using the conventional load flow techniques. Amongst the load flow methods, fast decoupled (FD) load flow is found to be the most popular due to its computational speed and convergence characteristics. The superiority of the FD method is primarily attributed to its decoupling assumptions. These assumptions are not valid under all operating modes, especially in real time environment and the results provided by the FD load flow may be unreliable. Since the FD state estimator is based on the same underlying decoupling assumptions of the FD

load flow. It was mentioned earlier that, in FD technique the rates of convergence are strongly influenced by the coupling between the P- δ and Q-V mathematical models. This coupling increases with the system loading and high value of branch R/X ratios and consequently the convergence rates decrease. The high value of R/X ratio branches are found in low voltage distribution systems where the line resistances are relatively large, which causes the FD state estimator fails to converge or produces slow or oscillatory convergence, depending upon the degree of ill-conditioning. In addition, it is found that the presence of capacitive series branches in a system could also result in ill-conditioning which causes failure or slow convergence of the FD state estimator. However, the proposed methods very much converge for high value of R/X ratio. A summary of the results are provided in Table 7.23.

7.6 STATE ESTIMATION IN CASE OF MISSING DATA

In the real-time environment, data is transported via the telemetry network to the main frame central computer. Occasionally, some data gets lost. Often noises corrupt the data and so the received data may be erroneous. Under such a condition, a state estimator must be capable of providing an acceptable estimate. To examine the suitability of the proposed state estimators, measurements were assumed missing at five nodes both in 14 busbar and 30 busbar systems. In the case of 14 busbar system data is missing on busbars 2, 3, 4, 5 and 6 and on 30 busbar system missing data is at nodes 1, 4, 9, 12 and 19. Under the missing data cases, results were obtained using the FRSE, SRSE and DSRSE methods. The results are given in Tables 7.19 and 7.20.

7.7 STATE ESTIMATION UNDER ABNORMAL REFERENCE VOLTAGE

A state estimator assumes one of the nodal voltage measurements as the reference. Under abnormal situations, such as tripping of a generator, rejection of a large load, snapping of the bulk power carrying line etc, the reference signal undergoes wide fluctuations. Under these circumstances, a state estimator estimates the state with the reference signal much different from the normal value, that is, 1.0 pu. To simulate these conditions, the following two cases were investigated:

- Reference signal of 0.85 pu
- Reference signal of 1.15 pu

The results under abnormal situations of 14 and 30 bus systems were obtained by using the FRSE, SRSE and DSRSE methods. Pertinent results are shown in Table 7.21 for 0.80 pu reference signal and in Table 7.22 for 1.20 pu reference signal. Line flow estimation under unusual operating conditions for 30 bus system are also provided in Tables 7.23 and 7.24.

7.8 TEST RESULTS

The computational efficiency, convergence characteristics, solution accuracy and real-time monitoring ability of the proposed estimators have been examined by digital simulation studies on modified IEEE bus data systems. The system data for IEEE 14, 30, 57 and 107 bus are provided in Appendix - D. In the standard IEEE ac data system, some ac line is replaced by a dc line. Thus the standard ac data have been converted to link, mesh and mesh-link system. Also the viability of the proposed algorithms have been tested on mixed ac-dc system. The maximum number of iterations is fixed at 50.0.

The test results are provided in the following Tables 7.1-7.26 and Figs 7.1-7.9.

Table 7.1 Jacobian matrix [H] of a 3 busbar ac-dc system

	Δe_1	Δe_2	Δe_3	Δf_2	Δf_3	ΔVd_1
ΔP_1	6.24	-3.06	-3.06	-12.24	-12.24	0.00
ΔP_2	-2.94	3.62	0.00	11.84	0.00	0.00
ΔP_3	-3.06	0.00	2.20	0.00	12.66	0.00
ΔP_{12}	3.18	-3.06	0.00	-12.24	0.00	0.00
ΔV_1^2	2.08	0.00	0.00	0.00	0.00	0.00
$\Delta \theta_2$	-11.76	11.67	0.00	-2.26	0.00	0.00
$\Delta Z_3 ^2$	0.00	0.00	2.08	0.00	0.00	0.00
$\Delta \theta_{12}$	12.69	-12.24	0.00	3.06	0.00	0.00
ΔR_{11}	0.00	3.03	0.00	0.00	0.00	-2.70
ΔR_{12}	0.00	0.00	3.32	0.00	0.00	0.00
ΔR_{21}	0.00	-0.79	0.00	0.40	0.00	0.53
ΔR_{22}	0.00	0.00	0.85	0.00	-0.43	0.00
ΔR_{31}	0.00	0.00	0.00	0.00	0.00	-50.00
ΔR_{32}	0.00	0.00	0.00	0.00	0.00	50.00
ΔR_{41}	0.00	0.00	0.00	0.00	0.00	0.00
ΔR_{42}	0.00	0.00	0.00	0.00	0.00	0.00
ΔR_{51}	0.00	0.00	0.00	0.00	0.00	-66.00
ΔR_{61}	0.00	0.00	0.00	0.00	0.00	-50.00
ΔR_{71}	0.00	0.00	0.00	0.00	0.00	-0.53
ΔR_{82}	0.00	0.00	0.00	0.00	0.00	0.00
ΔR_{91}	0.00	0.00	0.00	0.00	0.00	0.00
ΔR_{92}	0.00	0.00	0.00	0.00	0.00	0.00
ΔR_{10-1}	0.00	0.00	0.00	0.00	0.00	0.00
ΔR_{11-1}	0.00	0.00	0.00	0.00	0.00	0.00
ΔR_{11-12}	0.00	0.00	0.00	0.00	0.00	0.00

	ΔVd_2	ΔId_1	ΔId_2	Δa_1	Δa_2	Δc_1
ΔP_1	0.00	0.00	0.00	0.00	0.00	0.00
ΔP_2	0.00	0.00	0.00	0.85	0.00	0.93
ΔP_3	0.00	0.00	0.00	0.00	-0.89	0.00
ΔP_{12}	0.00	0.00	0.00	0.00	0.00	0.00
ΔV_1^2	0.00	0.00	0.00	0.00	0.00	0.00
$\Delta \theta_2$	0.00	0.00	0.00	0.43	0.00	0.00
$\Delta Z_3 ^2$	0.00	0.00	0.00	0.00	0.00	0.00
$\Delta \theta_{12}$	0.00	0.00	0.00	0.00	0.00	0.00
ΔR_{11}	0.00	-0.26	0.00	3.26	0.00	0.00
ΔR_{12}	-2.63	0.00	0.18	0.00	3.45	0.00
ΔR_{21}	0.00	1.30	0.00	-0.85	0.00	-0.93
ΔR_{22}	-0.53	0.00	1.28	0.00	0.89	0.00
ΔR_{31}	50.00	1.00	0.00	0.00	0.00	0.00
ΔR_{32}	-50.00	0.00	1.00	0.00	0.00	0.00
ΔR_{41}	0.00	1.91	0.00	0.00	0.00	-1.71
ΔR_{42}	0.00	0.00	-1.91	0.00	0.00	0.00
ΔR_{51}	65.00	0.00	0.00	0.00	0.00	0.00
ΔR_{61}	50.00	0.00	0.00	0.00	0.00	0.00
ΔR_{71}	0.00	-1.30	0.00	0.00	0.00	0.00
ΔR_{82}	-1.00	0.00	0.00	0.00	0.00	0.00
ΔR_{91}	0.00	0.00	0.00	0.00	0.00	-1.71
ΔR_{92}	0.00	0.00	0.00	0.00	0.00	0.00
ΔR_{10-1}	0.00	0.00	0.00	-1.00	0.00	0.00
ΔR_{11-1}	0.00	0.00	0.00	0.00	0.00	0.00
ΔR_{11-12}	0.00	0.00	0.00	0.00	0.00	0.00

	Δc_2	Δd_1	Δd_2	$\Delta \cos \alpha_1$	$\Delta \cos \alpha_2$
ΔP_1	0.00	0.00	0.00	0.00	0.00
ΔP_2	0.00	0.00	0.00	0.00	0.00
ΔP_3	-1.00	0.00	0.00	0.00	0.00
ΔP_{12}	0.00	0.00	0.00	0.00	0.00
ΔV_1^2	0.00	0.00	0.00	0.00	0.00
$\Delta \theta_2$	0.00	0.93	0.00	0.00	0.00
$\Delta Z_3 ^2$	0.00	0.00	0.00	0.00	0.00
$\Delta \theta_{12}$	0.00	0.00	0.00	0.00	0.00
ΔR_{11}	0.00	0.00	0.00	3.08	0.00
ΔR_{12}	0.00	0.00	0.00	0.00	3.67
ΔR_{21}	0.00	0.00	0.00	0.00	0.00
ΔR_{22}	1.04	0.00	0.00	0.00	0.00
ΔR_{31}	0.00	0.00	0.00	0.00	0.00
ΔR_{32}	0.00	0.00	0.00	0.00	0.00
ΔR_{41}	0.00	-0.85	0.00	0.00	0.00
ΔR_{42}	-1.71	0.00	-0.85	0.00	0.00
ΔR_{51}	0.00	0.00	0.00	0.00	0.00
ΔR_{61}	0.00	0.00	0.00	0.00	0.00
ΔR_{71}	0.00	0.00	0.00	0.00	0.00
ΔR_{82}	0.00	0.00	0.00	0.00	0.00
ΔR_{91}	0.00	-0.85	0.00	0.00	0.00
ΔR_{92}	-1.71	0.00	-0.85	0.00	0.00
ΔR_{10-1}	0.00	0.00	0.00	0.00	0.00
ΔR_{11-1}	0.00	0.00	0.00	-1.00	0.00
ΔR_{11-12}	0.00	0.00	0.00	0.00	-1.00

Table 7.2 Gain matrix $[G] = [H]^T [W] [H]$ of a 3 busbar ac-dc system

	J=1	2	3	4	5	6
I = 1	.1043E+07	-.9761E+06	-.3885E+05	-.8493E+06	-.1659E+06	.0000E+00
2	-.9761E+06	.1046E+07	.1611E+05	.8021E+06	.6444E+05	-.8604E+05
3	-.3885E+05	.1611E+05	.4909E+06	.6444E+05	.8566E+05	.0000E+00
4	-.8493E+06	.8021E+06	.6444E+05	.3727E+07	.2578E+06	.2106E+04
5	-.1659E+06	.6444E+05	.8566E+05	.2578E+06	.4025E+06	.0000E+00
6	.0000E+00	-.8604E+05	.0000E+00	.2106E+04	.0000E+00	.4958E+09
7	.0000E+00	.0000E+00	-.9178E+05	.0000E+00	.2265E+04	-.4949E+09
8	.0000E+00	-.1815E+05	.0000E+00	.5166E+04	.0000E+00	-.4774E+06
9	.0000E+00	.0000E+00	.1677E+05	.0000E+00	-.5470E+04	.5000E+06
10	-.2289E+05	.1315E+06	.0000E+00	.5036E+05	.0000E+00	-.9251E+05
11	.2423E+04	.0000E+00	.1202E+06	.0000E+00	.1383E+05	.0000E+00
12	-.1501E+05	.2586E+05	.0000E+00	.5671E+05	.0000E+00	-.4929E+04
13	.2835E+04	.0000E+00	.6845E+04	.0000E+00	-.1618E+05	.0000E+00
14	-.1981E+05	.1965E+05	.0000E+00	-.3813E+04	.0000E+00	.0000E+00
15	.0000E+00	.0000E+00	.0000E+00	.0000E+00	.0000E+00	.0000E+00
16	.0000E+00	.9318E+05	.0000E+00	.0000E+00	.0000E+00	-.8309E+05
17	.0000E+00	.0000E+00	.1217E+06	.0000E+00	.0000E+00	.0000E+00

J = 7	8	9	10	11	12	
I = 1	.0000E+00	.0000E+00	.0000E+00	-.2289E+05	.2423E+04	-.1501E+05
2	.0000E+00	-.1815E+05	.0000E+00	.1315E+06	.0000E+00	.2586E+05
3	.9178E+05	.0000E+00	.1677E+05	.0000E+00	.1202E+06	.0000E+00
4	.0000E+00	.5166E+04	.0000E+00	.5036E+05	.0000E+00	.5671E+05
5	.2265E+04	.0000E+00	-.5470E+04	.0000E+00	-.1383E+05	.0000E+00
6	.4949E+09	-.4774E+06	.5000E+06	-.9251E+05	.0000E+00	.4929E+04
7	.4942E+09	.5000E+06	-.5114E+06	.0000E+00	-.9546E+05	.0000E+00
8	.5000E+06	.8563E+05	.0000E+00	-.1951E+05	.0000E+00	-.4480E+05
9	.5114E+06	.0000E+00	.6333E+05	.0000E+00	.1744E+05	.0000E+00
10	.0000E+00	-.1951E+05	.0000E+00	.2342E+06	.0000E+00	.1231E+05
11	-.9546E+05	.0000E+00	.1744E+05	.0000E+00	.1276E+06	.0000E+00
12	.0000E+00	-.4480E+05	.0000E+00	.1231E+05	.0000E+00	.4990E+06
13	-.5512E+04	.0000E+00	.4603E+05	.0000E+00	.1007E+05	.0000E+00
14	.0000E+00	-.1636E+05	.0000E+00	.7196E+03	.0000E+00	.2428E+06
15	.0000E+00	.0000E+00	.1636E+05	.0000E+00	.0000E+00	.0000E+00
16	.0000E+00	-.7935E+00	.0000E+00	.1002E+06	.0000E+00	.0000E+00
17	-.9657E+05	.0000E+00	.6455E+04	-.0000E+00	.1266E+06	.0000E+00

	J= 13	14	15	16	17
I= 1	.2835E+04	-.1981E+05	.0000E+00	.0000E+00	.0000E+00
2	.0000E+00	.1965E+05	.0000E+00	.9318E+05	.0000E+00
3	.6845E+04	.0000E+00	.0000E+00	.0000E+00	.1217E+06
4	.0000E+00	-.3813E+04	.0000E+00	.0000E+00	.0000E+00
5	-.1618E+05	.0000E+00	.0000E+00	.0000E+00	.0000E+00
6	.0000E+00	.0000E+00	.0000E+00	-.8309E+05	.0000E+00
7	-.5512E+04	.0000E+00	.0000E+00	.0000E+00	-.9657E+05
8	.0000E+00	-.1636E+05	.0000E+00	-.7935E+04	.0000E+00
9	.4603E+05	.0000E+00	.1636E+05	.0000E+00	.6455E+04
10	.0000E+00	.7196E+03	.0000E+00	.1002E+06	.0000E+00
11	.1007E+05	.0000E+00	.0000E+00	.0000E+00	.1266E+06
12	.0000E+00	.2428E+06	.0000E+00	.0000E+00	.0000E+00
13	.4974E+06	.0000E+00	.2428E+06	.0000E+00	.0000E+00
14	.0000E+00	.1230E+06	.0000E+00	.0000E+00	.0000E+00
15	.2428E+06	.0000E+00	.1214E+06	.0000E+00	.0000E+00
16	.0000E+00	.0000E+00	.0000E+00	.2069E+06	.0000E+00
17	.0000E+0	.0000E+00	.0000E+00	.0000E+00	.2505E+06

Table 7.3 State estimation results of 14 bus ac-dc link system

(a) AC state results

Bus No	Method							
	FRSE		SRSE		DSRSE		FDSE	
	e	f	e	f	e	f	e	f
1	1.05999	0.0000	1.05998	0.0000	1.06048	0.0000	1.06012	0.0000
2	1.04108	-0.09111	1.04105	-0.09114	1.04174	-0.09091	1.04125	-0.09110
3	0.98522	-0.2226	0.98519	-0.22273	0.98544	-0.22239	0.98529	-0.22245
4	0.98996	-0.17641	0.98994	-0.17647	0.99029	-0.17593	0.99012	-0.17612
5	0.98476	-0.14844	0.98475	-0.14849	0.98485	-0.14755	0.98480	-0.14785
6	1.03870	-0.26240	1.03869	-0.26251	1.03908	-0.26209	1.03891	-0.26226
7	1.02836	-0.24112	1.02833	-0.24121	1.02862	-0.24082	1.02842	-0.24098
8	1.06119	-0.24884	1.06116	-0.24891	1.06138	-0.24851	1.06125	-0.24867
9	1.01633	-0.26824	1.01630	-0.26834	1.01662	-0.26802	1.01642	-0.26814
10	1.01174	-0.27038	1.01171	-0.27049	1.01203	-0.27018	1.01188	-0.27025
11	1.02112	-0.26783	1.02109	-0.26795	1.02143	-0.26763	1.02123	-0.26772
12	1.01998	-0.27384	1.01977	-0.27397	1.01203	-0.27364	1.02001	-0.27375
13	1.01461	-0.27366	1.01459	-0.27379	1.01493	-0.27347	1.01473	-0.27358
14	0.99325	-0.28335	0.99321	-0.28347	0.99353	-0.28317	0.99336	-0.28328

(b) DC state results

Method		Variables						
		Vd	Id	a	θ	c	d	ϕ
FRSE	Conv.1	1.28380	0.48021	1.01264	11.78	0.57369	0.29505	
	Conv.2	1.27722	-0.47979	1.03842	22.39	0.53001	0.36766	
SRSE	Conv.1	1.28381	0.48021	1.01268	11.77	0.57366	0.29489	
	Conv.2	1.27723	-0.47980	1.03957	22.58	0.529191	0.36871	
FSRSE	Conv.1	1.28245	0.47731	1.01494	12.30	0.56304	0.30207	
	Conv.2	1.27587	-0.48090	1.04635	22.53	0.52974	0.36789	
FDSE	Conv.1	1.28310	0.48022	1.01265	11.57	-	-	19.5
	Conv.2	1.27725	-0.47998	1.03855	22.58	-	-	24.5

Table 7.4 State estimation results of 30 bus ac-dc link system

(a) AC system results

Bus No	Methods							
	FRSE		SRSE		DSRSE		FDSE	
	e	f	e	f	e	f	e	f
1	1.05025	0.0000	1.05828	0.0000	1.05027	0.0000	1.05045	0.00000
2	1.03288	-0.04915	1.03291	-0.04914	1.03289	-0.04915	1.03301	0.04972
3	1.03012	-0.8446	1.03013	-0.08443	1.03013	-0.08441	1.03024	-0.08435
4	1.02408	-0.10067	1.02408	-0.10064	1.02409	-0.10063	1.02419	-0.19957
5	1.99376	-0.15533	0.99375	-0.15528	0.99375	-0.15529	0.99379	-0.15392
6	1.01707	-0.11545	1.01705	-0.11540	1.01706	-0.11539	1.01724	-0.11527
7	0.99879	-0.14023	0.99878	-0.14018	0.99878	-0.14024	0.99886	-0.13954
8	1.01665	-0.11492	1.01660	-0.11485	1.01663	-0.11481	1.01718	-0.11486
9	1.03556	-0.14811	1.03557	-0.14805	1.03557	-0.14810	1.03504	-0.14792
10	1.02745	-0.18161	1.02746	-0.18155	1.02747	-0.18152	1.02691	-0.18147
11	1.08493	-0.11917	1.08494	-0.11911	1.08494	-0.11915	1.08375	-0.11893
12	1.03421	-0.16801	1.03424	-0.16795	1.03422	-0.16798	1.03378	-0.16786
13	1.07747	-0.15217	1.07750	-0.15210	1.07748	-0.15215	1.07688	-0.15196
14	1.01790	-0.18200	1.01792	-0.18194	1.01796	-0.18195	1.01741	-0.18185
15	1.01412	-0.18357	1.01414	-0.18351	1.01413	-0.18355	1.01360	-0.18342
16	1.02333	-0.17760	1.02335	-0.17754	1.02334	-0.17757	1.02285	-0.17748
17	1.02026	-0.18323	1.02027	-0.18137	1.02028	-0.18319	1.01973	-0.18309
18	1.00450	-0.19307	1.00452	-0.19301	1.00451	-0.19305	1.00392	-0.19292
19	1.00252	-0.19584	1.00254	-0.19578	1.00253	-0.19581	1.00192	-0.19570
20	1.00779	-0.19324	1.00781	-0.19317	1.00780	-0.19321	1.00720	-0.19309

21	1.01403	-0.18777	1.01404	-0.18771	1.01404	-0.18773	1.01343	-0.18763
22	1.01468	-0.18776	1.01469	-0.18770	1.01469	-0.18774	1.01408	-0.18763
23	1.00521	-0.19013	1.00523	-0.19006	1.00522	-0.19012	1.00460	-0.18997
24	1.00279	-0.19420	1.00280	-0.19413	1.00281	-0.19412	1.00212	-0.79406
25	1.00705	-0.19334	1.00705	-0.19327	1.00706	-0.19325	1.00634	-0.19326
26	0.98842	-0.19715	0.98842	-0.19709	0.98843	-0.19707	0.98752	-0.19701
27	1.01902	-0.18973	1.01901	0.18966	1.01902	-0.18963	1.01845	-0.18972
28	1.01156	-0.12213	1.01154	-0.12208	1.01155	-0.12205	1.01171	-0.12194
29	0.99567	-0.20701	0.99566	-0.20694	0.99568	-0.20685	0.99482	-0.20698
30	0.98141	-0.21945	0.98140	-0.21938	0.98142	-0.21945	0.98048	-0.21944

(b) DC state results

Methods	Variables						
	Vd	Id	a	θ	c	d	ϕ
FRSE	Conv.1	1.29953	0.44690	0.97432	8.173	0.56785	0.19610
	Conv.2	1.27843	-0.44698	1.03013	19.992	0.50789	0.32119
SRSE	Conv.1	1.29953	0.44691	0.97431	8.277	0.56783	0.19615
	Conv.2	1.27843	-0.44698	1.03085	19.992	0.50736	0.32151
FSRSE	Conv.1	1.29940	0.44757	0.97450	8.300	0.56937	0.19652
	Conv.2	1.27829	-0.44739	1.03766	19.994	0.50502	0.32534
FDSE	Conv.1	1.29953	0.44690	0.97432	8.174	-	- 16.900
	Conv.2	1.27843	-0.44698	1.03012	19.992	-	- 23.316

7.5 State estimation results of 57 bus ac-dc link system

(a) AC state results at some selected busbars

Bus No	Method							
	FRSE		SRSE		DSRSE		FDSE	
	e	f	e	f	e	f	e	f
1	1.03994	0.00000	1.03993	0.00000	0.03993	0.00000	0.03993	0.00000
5	0.96589	-0.14435	0.96587	-0.14441	0.96588	-0.14439	0.96586	-0.14437
10	0.96673	-0.19426	0.96671	-0.19429	0.96679	-0.19427	0.96676	-0.19425
15	0.98032	-0.12296	0.98030	-0.12298	0.98031	-0.12293	0.98032	-0.12294
20	0.93786	-0.22323	0.93783	-0.22327	0.93784	-0.22325	0.93786	-0.22323
25	0.93446	-0.30540	0.93443	-0.30548	0.93445	-0.30543	0.93442	-0.30541
30	0.91276	-0.30794	0.91272	-0.30802	0.91274	-0.30798	0.91272	-0.30796
35	0.93869	-0.23150	0.93863	0.23154	0.93866	-0.23152	0.93865	-0.23151
40	0.94611	-0.22901	0.94606	-0.22905	0.94608	-0.22903	0.94606	-0.22901
50	0.99582	-0.23617	0.99579	-0.23621	0.99581	0.23619	0.99579	-0.23617
55	1.01287	-0.19105	1.01283	-0.19108	1.01285	-0.19107	1.01284	-0.19105

(b) DC state results

Methods	Variables						
	V_d	I_d	a	θ	c	d	
FRSE Conv.1	1.29350	1.37998	1.06564	8.243	1.59810	0.94091	
Conv.2	1.27988	-1.38001	1.10968	20.05	1.45553	1.14948	
SRSE Conv.1	1.29350	1.37998	1.06560	8.254	1.5979	0.9409	
Conv.2	1.27984	-1.38001	1.10970	20.030	1.4552	1.1497	
DSRSE Conv.1	1.29352	1.37996	1.0657	8.466	1.5980	0.9409	
Conv.2	1.27986	-1.37998	1.1098	20.040	1.4552	1.14961	

Table 7.6 State estimation results of 107 bus ac-dc link system

(a) AC state results at some selected busbars

Bus No	Methods							
	FDSE		SRSE		DSRSE		FDSE	
	e	f	e	f	e	f	e	f
5	0.96876	0.028178	0.96887	0.28187	0.96883	0.28189	0.96881	0.28183
14	1.03482	-0.01231	1.03491	-0.01239	1.03497	-0.01237	1.03493	-0.01231
27	1.02871	0.00636	1.02859	0.00646	1.02867	0.00648	1.02861	0.00642
46	0.93742	-0.32414	0.93738	-0.32412	0.93732	-0.32405	0.93737	-0.32411
60	1.02461	-0.12243	1.02477	-0.12253	1.02478	-0.12257	1.02479	-0.12263
66	1.01207	0.22374	1.01199	0.22369	1.01191	0.22365	1.01190	0.22357
90	1.03188	0.11486	1.03181	0.11481	1.03176	0.11484	1.03167	0.11473
99	1.04717	-0.10227	1.04706	-0.10126	1.04701	-0.10217	1.04704	-0.10211
107	0.94667	-0.29042	0.94659	-0.29037	0.94651	-0.29032	0.94671	-0.29046

(b) DC state results

Method	Variables						
	V_d	I_d	a	θ	c	d	ϕ
FRSE	Conv.1	1.29873	3.37516	1.14530	3.35691	3.08738	20.50917
	Conv.2	1.28751	-3.37511	1.08153	3.56876	2.81729	20.0136
SRSE	Conv.1	1.29869	3.37503	1.14546	3.35331	3.08719	20.50906
	Conv.2	1.28757	-3.37510	1.08156	3.58419	2.81567	20.0037
FSRSE	Conv.1	1.29857	3.37511	1.14541	3.35671	3.04973	19.74971
	Conv.2	1.28746	-3.37503	1.08741	3.57103	2.79542	20.0016
FDSE	Conv.1	1.29862	3.37507	1.14544	19.918	-	- 37.06
	Conv.2	1.28748	-3.37514	1.08757	20.012	-	- 31.3

Table 7.7 State estimation results of 14 bus ac-dc mesh system

(a) AC state results

Bus No	Methods							
	FRSE		SRSE		DSRSE		FDSE	
	e	f	e	f	e	f	e	f
1	1.06019	0.0000	1.06023	0.0000	1.06032	0.0000	1.06024	0.0000
2	1.04227	-0.07845	1.04229	-0.07847	1.04244	-0.07842	1.04235	-0.07847
3	0.99538	-0.17108	0.99541	-0.17118	0.99572	-0.17101	0.99556	-0.17111
4	0.94748	-0.05228	0.94788	-0.05267	0.94775	-0.05155	0.94776	-0.05154
5	0.94830	-0.19004	0.94823	-0.19005	0.94842	-0.18995	0.94833	-0.18998
6	1.03645	-0.26551	1.03641	-0.26556	1.03662	-0.26456	1.03649	-0.26532
7	1.02245	-0.14699	1.02254	-0.14728	1.02257	-0.14528	1.02250	-0.14629
8	1.07903	-0.15514	1.07889	-0.15540	1.07901	-0.15344	1.07898	-0.15532
9	1.01534	-0.19109	1.01541	-0.19134	1.01552	-0.18962	1.01543	-0.19131

10	1.01137	-0.20767	1.01142	-0.20788	1.01165	-0.20688	1.01139	-0.20775
11	1.02053	-0.23728	1.02054	-0.23741	1.02095	-0.23624	1.02051	-0.23738
12	1.01697	-0.27140	1.01694	-0.27144	1.01710	-0.27095	1.01698	-0.27139
13	1.01312	-0.26552	1.01310	-0.26558	1.01325	-0.26512	1.01319	-0.26546
14	0.99262	-0.23733	0.99326	-0.23748	0.99277	-0.23648	0.99164	-0.23751

(b) DC State results

Methods	Variables							
	Vd	Id	a	θ	c	d	ϕ	
FRSE	Conv.1	1.28732	0.47784	1.05047	12.485	0.55107	0.33449	
	Conv.2	1.28876	0.76774	0.97014	10.456	0.94776	0.40230	
	Conv.3	1.27929	-1.24330	1.12614	22.530	1.44657	0.83776	
SRSE	Conv.1	1.28739	0.47785	1.05253	12.479	0.54965	0.33664	
	Conv.2	1.28883	0.76773	0.97015	10.452	0.94772	0.40212	
	Conv.3	1.27937	-1.24421	1.21640	22.586	1.44605	0.83863	
FRSE	Conv.1	1.28745	0.47787	1.05151	12.483	0.55081	0.33539	
	Conv.2	1.28889	0.76779	0.97011	11.440	0.94879	0.39998	
	Conv.3	1.27952	-1.24395	1.12661	22.578	1.44630	0.83762	
FDSE	Conv.1	1.28736	-1.47786	1.05161	12.482	-	-	19.5
	Conv.2	1.28879	0.76775	0.97012	10.455	-	-	19.0
	Conv.3	1.27932	-1.24426	1.12655	22.578	-	-	27.0

Table 7.8 State estimation results of 30 bus ac-dc mesh system

(a) AC system results

Bus No	Methods							
	FRSE		SRSE		DSRSE		FDSE	
	e	f	e	f	e	f	e	f
1	1.0506	1.0000	1.05065	0.0000	1.05080	0.0000	1.05062	0.0000
2	1.03325	-0.04890	1.03329	-0.04897	1.03355	-0.04885	1.03327	-0.04895
3	1.02980	-0.08432	1.02981	-0.08429	1.03008	-0.08412	1.02982	-0.08431
4	1.02360	-0.10040	1.02361	-0.10045	1.02388	-0.10025	1.02365	-0.10042
5	0.99629	-0.13978	0.99630	-0.13968	0.99637	-0.14021	0.99628	-0.13972
6	1.01616	-0.11515	1.01613	-0.11511	1.01629	-0.11495	1.01614	-0.11512
7	0.99436	-0.13862	0.99448	-0.13865	0.99478	-0.13885	0.99442	-0.13863
8	1.01640	-0.11490	1.01630	-0.11484	1.01624	-0.11465	1.01635	-0.11486
9	1.03526	-0.14793	1.03527	-0.14791	1.03556	-0.14698	1.03528	-0.14792
10	1.02716	-0.18149	1.02715	-0.18141	1.02735	-0.18079	1.02717	-0.18145
11	1.08527	-0.11912	1.08526	-0.11909	1.08576	-0.11845	1.08528	-0.11991
12	1.03433	-0.16796	1.03435	-0.16795	1.03439	-0.16798	1.03434	-0.16797
13	1.07813	-0.15218	1.07815	-0.15217	1.07781	-0.15219	1.07814	-0.15217
14	1.01798	-0.18198	1.01799	-0.18194	1.01801	-0.18198	1.01799	-0.18196
15	1.01414	-0.18351	1.01415	-0.18349	1.01425	-0.18345	1.01421	-0.18196
16	1.02327	-0.17750	1.02328	-0.17748	1.02338	-0.17736	1.02329	-0.17749
17	1.02003	-0.18308	1.02002	-0.18306	1.02028	-0.18275	1.02005	-0.18305
18	1.00437	-0.19297	1.00438	-0.19295	1.0045	-0.19268	1.00439	-0.19296
19	1.00239	-0.19576	1.00232	-0.19569	1.00285	-0.19521	1.00237	-0.19571

20	1.00754	-0.19311	1.00765	-0.19307	1.00796	-0.19275	1.00755	-0.19309
21	1.01378	-0.18762	1.01375	-0.18759	1.01397	-0.18657	1.01376	-0.18761
22	1.01446	-0.18764	1.01441	-0.18760	1.01456	-0.18674	1.01443	-0.18762
23	1.00520	-0.19010	1.00519	-0.19005	1.00521	-0.18995	1.00519	-0.19007
24	1.00270	-0.19441	1.00266	-0.19141	1.00296	-0.19311	1.00268	-0.19412
25	1.00710	-0.19339	1.00704	-0.19341	1.00755	-0.19275	1.00708	-0.19340
26	0.98862	-0.19733	0.98852	-0.19737	0.98952	-0.19632	0.98857	-0.19735
27	1.01910	-0.18972	1.01897	-0.18976	1.01985	-0.18857	1.01905	-0.18974
28	1.01090	-0.12195	1.01086	-0.12193	1.01101	-0.12168	1.01088	-0.12194
29	0.99598	-0.20718	0.99581	-0.20725	0.99721	-0.20621	0.99586	-0.20721
30	0.98176	-0.21964	0.98157	-0.21973	0.98311	-0.21871	0.98167	-0.21968

(b) DC state results

Methods	Variables							
	Vd	Id	a	θ	c	d	ϕ	
FRSE	Conv.1	1.29509	0.44310	0.97037	7.952	0.56353	0.19377	
	Conv.2	1.27789	-0.54445	1.03379	19.86	0.62201	0.38440	
	Conv.3	1.-28845	0.10033	0.98180	12.288	0.12371	0.05449	
SRSE	Conv.1	1.29510	0.44309	0.97036	7.957	0.56346	0.19395	
	Conv.2	1.27899	-0.54443	1.03380	19.858	0.62228	0.38363	
	Conv.3	1.28846	0.10036	0.98176	12.258	0.12462	0.05132	
DSRSE	Conv.1	1.29512	0.44312	0.97039	7.992	0.56396	0.19225	
	Conv.2	1.27902	-0.54424	1.03382	19.856	0.61991	0.38575	
	Conv.3	1.28851	0.10042	0.98182	12.329	0.12634	0.04566	
FDSE	Conv.1	1.29510	0.44311	0.97038	7.957	-	-	16.843
	Conv.2	1.27899	-0.54444	1.03380	19.864	-	-	24.00
	Conv.3	1.28848	0.10035	0.98180	12.303	-	-	13.8

Table 7.9 State estimation results of 57 bus ac-dc mesh system

(a) AC state results at some selected busbars

Bus No	Methods							
	FRSE		SRSE		DSRSE		FDSE	
	e	f	e	f	e	f	e	f
1	1.03989	0.00000	1.03991	0.00000	1.03992	0.00000	1.03990	0.00000
5	0.97253	-0.008645	0.97253	-0.08647	0.97258	-0.08635	0.97254	-0.08632
10	0.95982	-0.22163	0.95977	-0.22167	0.95979	-0.22159	0.95976	-0.22157
15	0.97899	-0.12454	0.97896	-0.12455	0.97898	-0.12449	0.97895	-0.12445
20	0.93521	-0.21143	0.93516	-0.21145	0.93519	-0.21142	0.93516	-0.21140
25	0.94041	-0.28390	0.94036	-0.28392	0.94039	-0.28375	0.94036	-0.28372
30	0.91742	-0.28890	0.91736	-0.28893	0.91738	-0.28879	0.91735	-0.28880
35	0.93514	-0.23494	0.93504	-0.23496	0.93508	-0.23486	0.93509	-0.23484
40	0.94187	-0.23347	0.94177	-0.23349	0.94181	-0.23342	0.94188	-0.23346
45	1.02109	-0.16840	1.02074	-0.16843	1.02081	-0.16833	1.02076	-0.16837
50	0.98892	-0.25274	0.98852	-0.25278	0.98872	-0.25252	0.98879	-0.25256
55	0.97654	-0.22524	0.99734	-0.22528	0.99754	-0.22525	0.99758	-0.22528

(b) DC state results

Methods	Variables						
	Vd	Id	a	θ	c	d	
FRSE	Conv.1	1.29000	1.38486	1.06474	8.483	1.70860	0.73478
	Conv.2	1.28013	-0.89024	1.08381	20.066	0.93927	0.73783
	Conv.3	1.27615	-0.49593	1.0454	17.997	0.59709	0.29435
SRSE	Conv.1	1.29000	1.38486	1.06473	8.486	1.70856	0.73479
	Conv.2	1.28013	-0.89024	1.08381	20.065	0.93920	0.73787
	Conv.3	1.27616	-0.49593	1.04541	17.996	0.59709	0.29411
DSRSE	Conv.1	1.2900	1.38485	1.0645	8.487	1.7096	0.7389
	Conv.2	1.28014	-0.89024	1.0839	20.064	0.9398	0.7389
	Conv.3	1.27617	-0.49594	1.0455	17.997	0.5979	0.2961

Table 7.10 True values, estimated values and percentage of error of 14 bus ac-dc link system using DSRSE

(a) AC state results

Bus No	e^t	\tilde{e}	$e\%$	f^t	\tilde{f}	$\in f\%$
1	1.0600	1.06048	0.0453	0.0000	0.0000	0.00000
2	1.0410	1.04174	0.0711	-0.9140	-0.9091	0.53610
3	0.9849	0.98544	0.05483	-0.2238	-0.33339	0.63000
4	0.9899	0.99029	0.0394	-0.1768	-0.17593	0.49208
5	0.9836	0.98485	0.1271	-0.1483	-0.14755	0.50573
6	1.0373	1.03908	0.17160	-0.2624	-0.26209	0.11814
7	1.0280	1.0286	0.0603	-0.2416	-0.24082	0.32284
8	1.0611	1.06138	0.20639	-0.2494	-0.24851	0.35685
9	1.0157	1.01662	0.0906	-0.2686	-0.26802	0.25307
10	1.0109	1.01203	0.11178	-0.2709	-0.27018	0.26578
11	1.0200	1.02143	0.14020	-0.2681	-0.26763	0.17530
12	1.0186	1.02031	0.16788	-0.2738	-0.27364	0.05843
13	1.0133	1.01493	0.16086	-0.2737	-0.27347	0.08403
14	0.9924	0.99353	0.113865	-0.2837	-0.28317	0.18681

(b) DC state results

Bus No	Vd^t	$\tilde{V}d$	$\in Vd\%$	Id^t	$\tilde{I}d$	$\in Id\%$	a^t	\tilde{a}	$\in a\%$
1	1.2860	1.2824	-0.2814	-0.4797	0.4773	-0.5107	1.0156	1.0149	-0.065
2	1.2795	1.2758	-0.2852	-0.4797	-0.4809	-0.2376	1.0352	1.0463	1.077

Bus No	c^t	\tilde{c}	$\in c\%$	d^t	\tilde{d}	$\in d\%$	α^t	$\tilde{\alpha}$	$\in \alpha\%$
1	0.5716	0.5630	-1.4940	0.3052	0.3020	-1.0386	12.5	12.30	-0.16
2	0.5332	0.5297	-0.6485	0.3683	0.3678	-0.1176	22.6	22.53	-0.31

Table 7.11 True values, Estimated Values and percentage of error of 14 bus ac-dc mesh system using DSRSE

(a) AC states results

Bus No	e^t	\tilde{e}	$e\%$	f^t	\tilde{f}	$\in f\%$
1	1.0600	1.06032	0.0302	0.0000	0.0000	0.00000
2	1.0420	1.04244	0.0422	-0.07862	-0.07842	0.25438
3	0.9953	0.99572	0.0422	-0.17190	-0.17101	0.51774
4	0.9466	0.94775	0.1215	-0.05212	-0.01535	1.09363
5	0.9486	0.94843	0.0179	-0.19058	-0.18995	0.33056
6	1.0364	1.03662	0.02122	-0.26607	-0.26456	0.56752
7	1.0220	1.02257	0.05577	-0.14706	-0.14528	0.21040
8	1.0789	1.0790	0.0120	-0.15524	-0.15344	1.15949
9	1.0149	1.01552	0.0611	-0.19127	-0.18962	0.86265
10	1.0109	1.01165	0.0742	-0.20802	-0.20688	0.54800
11	1.0203	1.02095	0.0637	-0.23772	-0.23624	0.62258
12	1.0169	1.01710	0.01966	-0.27192	-0.27095	0.35672
13	1.0130	1.01325	0.0247	-0.26604	-0.26512	0.34581
14	0.9925	0.99277	0.0247	-0.23773	-0.23648	0.52580

(b) DC state results

Bus No	Vd'	$\tilde{V}d$	$\in Vd\%$	Id'	$\tilde{I}d$	$\in Id\%$	a'	\tilde{a}	$\in a\%$
1	1.2875	1.2874	-0.0085	0.4792	0.4779	0.2712	1.0452	1.0515	0.6040
2	1.2888	1.8889	0.0007	0.7667	0.7677	0.1304	0.9660	0.9701	0.4240
3	1.2795	1.2793	0.0015	-1.2459	-1.2440	-0.1525	1.1230	1.1266	0.3214

Bus No	c'	\tilde{c}	$\in c\%$	d'	\tilde{d}	$\in d\%$	α'	$\tilde{\alpha}$	$\in \alpha\%$
1	0.5553	0.5508	-0.8085	0.3317	0.3353	1.1124	12.500	12.485	-0.120
2	0.9508	0.9487	-0.2114	0.4098	0.3998	-2.4377	10.546	10.44	-1.000
3	1.4532	1.4463	-0.4748	0.8480	0.8376	-1.2240	22.595	22.58	-0.066

Table 7.12 True values, estimated values and percentage of error of 30 bus ac-dc link system using DSRSE.

(a) AC state results

Bus No	e'	\tilde{e}	$e\%$	f'	\tilde{f}	$\in f\%$
1	1.5000	1.05045	0.04285	0.0000	0.0000	0.00000
2	1.03263	1.03301	0.03679	-0.0491	-0.04917	-0.14256
3	1.02998	1.03024	0.02524	-0.08432	-0.08432	0.00000
4	1.02395	1.02419	0.02344	-0.10051	-0.10051	0.00000
5	0.99382	0.99379	-0.00302	-0.15477	-0.15394	0.53628
6	1.01696	1.01724	0.02753	-0.11523	-0.11523	0.00000
7	0.99875	0.99886	0.01101	-0.13987	-0.13954	0.23593
8	1.01655	1.10718	0.06197	-0.1147	-0.11486	-0.1395
9	1.03544	1.03504	-0.03863	-0.14781	-0.14792	-0.07442

10	1.02732	1.02691	-0.04000	-0.1813	-0.18147	-0.09376
11	1.08481	1.08375	-0.0977	-0.11884	-0.11893	-0.07573
12	1.03425	1.03378	-0.04544	-0.16777	-0.16786	-0.05364
13	1.07764	1.07688	-0.07052	-0.15192	-0.15196	-0.02633
14	1.01793	1.01741	-0.05108	-0.18176	-0.18185	-0.04950
15	1.01414	1.01360	-0.05325	-0.18332	-0.18342	-0.05455
16	1.02332	1.02285	-0.04593	-0.17735	-0.17748	-0.0733
17	1.02018	1.01973	-0.04411	-0.18294	-0.18309	-0.0820
18	1.00449	1.00392	-0.0567	-0.19279	-0.19292	0.06743
19	1.00248	1.00192	-0.0917	-0.19555	-0.19570	-0.07670
20	1.00774	1.0072	-0.05358	-0.19294	-0.19309	-0.07774
22	1.01459	1.01408	-0.05026	-0.18747	-0.18763	-0.08535
23	1.00521	1.0046	-0.06068	-0.18987	-0.18997	-0.05266
24	1.00275	1.00212	-0.06287	-0.19394	-0.19406	-0.06187
25	1.00702	1.00634	-0.0675	-0.1931	-0.19326	-0.08286
26	0.98841	0.98752	-0.09004	-0.19693	-0.19701	-0.04062
27	1.01898	1.01845	-0.0520	-0.18949	-0.18972	-0.12140
28	1.01146	1.01171	0.0247	-0.12193	-0.12194	-0.02461
29	0.99564	0.99482	-0.08236	-0.20678	-0.20698	-0.09672
30	0.98139	0.98048	-0.0927	-0.21922	-0.21944	-0.10035

(b) DC state results

Bus No	Vd'	$\tilde{V}d$	$\in Vd\%$	Id'	$\tilde{I}d$	$\in Id\%$	a'	\tilde{a}	$\in a\%$
1	1.3006	1.2994	-0.0945	0.4476	0.4475	-0.0134	0.9729	0.9745	0.1645
2	1.2795	1.2782	-0.0945	-0.4476	-0.4469	-0.1452	1.0258	1.0305	0.4562

Bus No	c'	\tilde{c}	$\in c\%$	d'	\tilde{d}	$\in d\%$	α'	$\tilde{\alpha}$	$\in \alpha\%$
1	0.5699	0.5693	-0.9475	0.2018	0.1915	-2.655	8.499	8.30	-2.33
2	0.5115	0.5075	-0.7819	0.3224	0.3214	-0.2397	19.997	19.99	-0.015

Table 7.13 True values, estimated values and percentage of error of 57 bus ac-dc link system using DSRSE

(a) AC results at some selected busbar

Bus No	e'	\tilde{e}	$e\%$	f'	\tilde{f}	$\in f\%$
5	0.96566	0.96588	0.02278	-0.14508	-0.14439	0.47562
10	0.96692	0.96679	-0.01344	-0.19458	-0.19427	0.15932
15	0.98042	0.98030	0.0122	-0.12324	-0.12229	0.21907
20	0.93777	0.93784	0.00746	-0.22375	-0.22325	0.21124
25	0.93403	0.93445	0.0497	-0.30605	-0.30543	0.20263
30	0.91229	0.91247	0.0493	-0.30851	-0.30789	0.19775
35	0.93862	0.93866	0.00426	-0.24177	-0.23152	0.10786
40	0.94607	0.94608	0.00105	-0.22928	-0.22903	0.10492
45	1.02276	1.02267	-0.0088	-0.16634	-0.16609	0.1503
50	0.99595	0.99581	-0.0140	-0.23648	-0.23619	0.12263
55	1.01295	1.01283	-0.00098	-0.19150	-0.19170	0.22450

(b) DC state results

Bus No	Vd'	$\tilde{V}d$	$\epsilon Vd\%$	Id'	$\tilde{I}d$	$\epsilon Id\%$	a'	\tilde{a}	$\epsilon a\%$
1	1.2936	1.2935	-0.0124	1.3798	1.3799	0.0109	1.0619	1.0657	0.3578
2	1.2800	1.2798	-0.011	-1.3798	-1.3799	0.0123	1.1033	1.1098	0.5837

Bus No	c'	\tilde{c}	$\epsilon c\%$	d'	\tilde{d}	$\epsilon d\%$	α'	$\tilde{\alpha}$	$\epsilon \alpha\%$
1	1.6030	1.5980	0.3138	0.9500	0.9409	0.9620	8.501	8.466	-0.46
2	1.4633	1.4562	0.5542	1.1537	1.1496	0.3553	20.00	20.05	0.25

Table 7.14 Maximum and average percentage of error compared to true values

System studied	max %	aver %
14 bus DC link	1.494	0.412
14 bus DC mesh	2.437	0.248
30 bus DC link	2.545	0.365
30 bus DC mesh	4.727	0.285
57 bus DC link	0.962	0.316
57 bus DC mesh	3.458	0.274
107 bus DC link	3.264	0.243

Table 7.15 Computing time comparison of different methods

System Studied	FRSE		SRSE		DSRSE		FDSE	
	CPU time(s)	No. of itn.						
14 bus DC link	1.10	3	.52	4	.26	5	.34	6
14 bus DC mesh	1.10	3	.52	4	.26	5	.34	6
30 bus DC link	1.21	3	.58	4	.32	5	.40	6
30 bus DC mesh	1.21	3	.58	4	.32	5	.40	6
57 bus DC link	1.46	3	.62	4	.36	5	.46	6
57 bus DC mesh	1.46	3	.62	4	.36	5	.46	6
107 bus DC link	2.12	3	.78	4	.41	5	.61	6

Table 7.16 Percentage of saving in solution time with FRSE method as reference

System Studied	SRSE	DSRSE	FDSE
14 bus DC link	52.7	76.3	69.1
14 bus DC mesh	52.7	76.3	69.1
30 bus DC link	52.0	73.5	66.9
30 bus DC mesh	52.0	73.3	66.9
57 bus DC link	57.5	75.3	68.4
57 bus DC mesh	57.5	75.3	68.4
107 bus DC link	63.2	80.6	71.1

Table 7.17 Comparison of performance indices

System studied	J^0 (initial value)	J^* (final value)			
		FDSE	FRSE	SRSE	DSRSE
14 bus DC link	359520	4.11	4.27	4.56	4.80
14 bus DC mesh	1133228	4.98	5.30	7.37	8.40
30 bus DC link	128404	0.749	0.751	0.827	1.60
30 bus DC mesh	148541	2.21	2.43	2.45	2.90
57 bus DC link	2295107	0.81	0.81	0.82	0.83
57 bus DC mesh	1750831	8.91	9.11	9.11	9.21
107 bus DC link	2171638	21.63	25.78	26.07	28.32

Table 7.18 Comparison of performance indices using DSRSE method

System studied	J^*	J_E	J_M	R_{av}	R_{max}
14 bus DC link	4.80	0.201	0.634	0.470	0.768
14 bus DC mesh	8.40	0.458	0.384	0.544	1.150
30 bus DC link	1.60	0.190	0.147	0.147	0.340
30 bus DC mesh	2.90	0.225	0.184	0.567	1.354
57 bus DC link	0.83	0.058	0.122	0.248	0.563
57 bus DC mesh	9.21	0.064	0.142	0.425	1.278
107 bus DC link	28.32	0.126	0.168	0.277	1.154

Table 7.19 Missing data of 5 nodes, namely 2,3,4,5,6 for 14 bus dc link

(a) AC state results

Bus No	Methods					
	FRSE		SRSE		DSRSE	
	e	f	e	f	e	f
1	1.0600	0.0000	1.05993	0.0000	1.05998	0.00000
2	1.04101	-0.09134	1.04095	-0.09128	1.04098	-0.09130
3	0.98488	-0.22372	0.98539	-0.22249	0.98512	-0.22262
4	0.98994	-0.17682	0.98990	-0.17675	0.98998	-0.17670
5	0.98461	-0.14841	0.98459	-0.14868	0.98460	-0.14852
6	1.03846	-0.26228	1.03862	-0.26254	1.03852	-0.26232
7	1.02825	-0.24146	1.02825	-0.24133	1.02824	-0.21138
8	1.06115	-0.24923	1.06104	-0.24902	1.06103	-0.24915
9	1.01614	-0.26850	1.01622	-0.26840	1.01623	-0.26845
10	1.01151	-0.27062	1.01164	-0.27053	1.01163	-0.27055
11	1.02090	-0.26788	1.02103	-0.26798	1.02110	-0.26745
12	1.01982	-0.27366	1.01991	-0.27399	1.01998	-0.27395
13	1.01440	-0.27354	1.01453	-0.27381	1.01459	-0.27379
14	0.99304	-0.28341	0.99316	-0.28349	0.99320	-0.28345

(b) DC state results

Methods		Variables					
		Vd	Id	a	c	d	θ
FRSE	Conv.1	1.28377	0.48013	1.01267	0.57310	0.29618	12.35
	Conv.2	1.27720	-0.47992	1.0384	0.53052	0.36702	22.58
SRSE	Conv.1	1.28386	0.48016	1.01272	0.57339	0.29537	12.30
	Conv.2	1.27725	-0.48002	1.0391	0.53007	0.36755	22.60
DSRSE	Conv.1	1.28381	0.48011	1.0127	0.57325	0.29557	12.40
	Conv.2	1.27725	-0.47989	1.0389	0.53042	0.36718	22.58

Table 7.20 Missing data of 5 nodes, namely 1,4,9,12, 19 for 30 bus dc link

(a) AC state results

Bus No	Methods					
	FRSE		SRSE		DSRSE	
	e	f	e	f	e	f
1	1.05025	0.0000	1.05025	0.0000	1.05026	0.00000
2	1.03290	-0.04914	1.03291	-0.04908	1.03292	-0.04192
3	1.03011	-0.08461	1.03014	-0.08435	1.03015	-0.08451
4	1.02409	-0.10078	1.02410	-0.10055	1.02410	-0.10077
5	0.99374	-0.15534	0.99379	-0.15505	0.99384	-0.11554
6	1.01709	-0.11553	1.01708	-0.11530	1.01710	-0.11545
7	0.99879	-0.14028	0.99881	-0.14002	0.99889	-0.14015
8	1.01669	-0.11501	1.01663	-0.11475	1.01679	-0.11495
9	1.03556	-0.14819	1.03558	-0.14798	1.03566	-0.14811
10	1.02751	-0.18168	1.02748	-0.18147	1.02751	-0.18169

11	1.08479	-0.11924	1.08496	-0.11902	1.08481	-0.11914
12	1.03429	-0.16807	1.03423	-0.16788	1.03431	-0.16801
13	1.07759	-0.15222	1.07750	-0.15202	1.07761	-0.15215
14	1.01799	-0.18206	1.01793	-0.18186	1.01800	-0.18201
15	1.01420	-0.18364	1.01415	-0.18344	1.01425	-0.18352
16	1.02342	-0.17767	1.02338	-0.17747	1.02352	-0.17753
17	1.02034	-0.18331	1.02099	-0.18309	1.02038	-0.18321
18	1.00458	-0.19313	1.00454	-0.19293	1.00468	-0.19301
19	1.00260	-0.19590	1.00255	-0.19571	1.00270	-0.19582
20	1.00787	-0.19330	1.00782	-0.19310	1.00797	-0.19325
21	1.01411	-0.18785	1.01407	-0.18762	1.01421	-0.18972
22	1.01475	-0.18785	1.01471	-0.18761	1.04185	-0.18772
23	1.00529	-0.19020	1.00525	-0.18997	1.00539	-0.19015
24	1.00286	-0.19430	1.00283	-0.19404	1.00296	-0.19142
25	1.00707	-0.19350	1.00710	-0.19318	1.00717	-0.19333
26	0.98836	-0.19740	0.98847	-0.19696	0.98845	-0.19758
27	1.01904	-0.18988	1.01906	-0.18954	1.01914	-0.18967
28	1.01158	-0.12223	1.01157	-0.12198	1.01168	-0.12210
29	0.99569	-0.20716	0.99572	-0.20681	0.99575	-0.20709
30	0.98143	-0.21960	0.98147	-0.21924	0.98184	-0.21942

(b) DC state results

Methods		Variables					
		Vd	Id	a	c	d	θ
FRSE	Conv.1	1.29952	0.44671	0.97430	8.22	0.56650	8.22
	Conv.2	1.27842	-0.44697	1.03013	20.00	0.50793	20.00
SRSE	Conv.1	1.29953	0.44886	0.97431	8.32	0.56755	8.32
	Conv.2	1.27843	-0.44703	1.03085	19.99	0.50767	19.99
DSRSE	Conv.1	1.29954	0.44812	0.97435	8.32	0.56655	8.32
	Conv.2	1.27846	-0.44781	1.0300	19.99	0.50791	19.99

Table 7.21 State estimation results of 14 bus ac-dc mesh system under abnormal reference voltage (0.85)

(a) AC state results

Bus No	Methods					
	FRSE		SRSE		DSRSE	
	e	f	e	f	e	f
1	0.85000	0.0000	0.8500	0.0000	0.8500	0.0000
2	0.87987	-0.12172	0.87995	-0.12162	0.87991	-0.12168
3	0.82432	-0.23984	0.82462	-0.23964	0.82452	-0.23975
4	0.75847	-0.08297	0.75857	-0.08277	0.75851	-0.08287
5	0.71761	-0.24869	0.71771	-0.24859	0.71765	-0.24864
6	0.83268	-0.36588	0.83278	-0.36568	0.83272	-0.36575
7	0.82858	-0.20562	0.82867	-0.20542	0.82861	-0.20551
8	0.89910	-0.22366	0.89921	-0.22346	0.89914	-0.20551
9	0.80814	-0.25790	0.80825	-0.25778	0.80818	-0.25785
10	0.80266	-0.27980	0.80276	-0.27968	0.80267	-0.27972

11	0.81354	-0.32277	0.81363	-0.32257	0.81359	-0.32265
12	0.80744	-0.36803	0.80754	-0.36801	0.80749	-0.36802
13	0.80322	-0.35904	0.80334	-0.35902	0.80328	-0.35903
14	0.77750	-0.31470	0.77761	-0.31465	0.77758	-0.31468

(b) DC state results

Methods		Variables					
		Vd	Id	a	c	d	θ
FRSE	Conv.1	1.28756	0.47920	1.33152	0.50585	0.40364	12.45
	Conv.2	1.28888	0.76670	1.13639	0.92355	0.46814	10.59
	Conv.3	1.2795	-1.24590	1.39505	1.40539	0.92515	22.58
SRSE	Conv.1	1.28758	0.47919	1.33158	0.50600	0.40215	12.49
	Conv.2	1.28889	0.76668	1.13641	0.92400	0.45624	10.55
	Conv.3	1.27951	-1.24589	1.39507	1.41540	0.92415	22.60
DSRSE	Conv.1	1.28757	0.47920	1.33156	0.50595	0.40315	12.49
	Conv.2	1.28888	0.76669	1.13640	0.92365	0.45924	10.56
	Conv.3	1.27950	-1.24591	1.139506	1.40589	0.92485	22.58

Table 7.22 State estimation results of 30 bus ac-dc link system under abnormal reference voltage (1.15)

(a) AC state results

Bus No	Methods					
	FRSE		SRSE		DSRSE	
	e	f	e	f	e	f
1	1.1500	0.0000	1.1500	0.0000	1.1500	0.00000
2	1.18721	-0.06283	1.18756	-0.06261	1.18746	-0.06275
3	1.17155	-0.08698	1.17165	-0.08678	1.17158	-0.08688
4	1.17395	-0.10459	1.17403	-0.10439	1.17398	-0.10449
5	1.4681	-0.15081	1.14679	-0.15091	1.14680	-0.15088
6	1.17150	-0.11890	1.7149	-0.11892	1.17151	-0.11878
7	1.15415	-0.13964	1.15425	-0.13944	1.15421	-0.13954
8	1.17051	-0.11817	1.17062	-0.11807	1.17058	-0.11810
9	1.19951	-0.14836	1.19961	-0.14826	1.19957	-0.14828
10	1.19765	-0.17811	1.19785	-0.17807	1.19774	-0.17808
11	1.24892	-0.12337	1.24901	-0.12317	1.24895	-0.12325
12	1.19882	-0.16385	1.19892	-0.16365	1.19885	-0.16375
13	1.24252	-0.15007	1.24261	-0.15002	1.24258	-0.15005
14	1.18585	-0.17657	1.85853	0.17658	1.18575	-0.17665
15	1.18323	-0.17856	1.18321	-0.17866	1.18322	-0.17858
16	1.19150	-0.17345	1.19151	-0.17335	1.19152	-0.17331
17	1.19075	-0.17931	1.19085	-0.17921	1.19078	-0.17925
18	1.17832	-0.18758	1.17842	-0.18748	1.17838	-0.18751
19	1.17534	-0.19031	1.17585	-0.19011	1.17550	-0.19022

20	1.18012	-0.18811	1.18022	-0.18807	1.18018	-0.18109
21	1.18641	-0.18383	1.18652	-0.18362	1.18649	-0.18372
22	1.18700	-0.18384	1.18721	-0.18365	1.18715	-0.18373
23	1.17729	-0.18533	1.17741	-0.18524	1.17735	-0.18529
24	1.17734	-0.19010	1.17755	-0.19008	1.17742	-0.19009
25	1.18029	-0.18865	1.18068	-0.18855	1.18055	-0.18861
26	1.16451	-0.19244	1.16472	-0.19234	1.16462	-0.19239
27	1.18996	-0.18487	1.18999	-0.18465	1.18997	-0.18492
28	1.16734	-0.12495	1.16754	-0.12474	1.16745	-0.12481
29	1.17060	-0.20039	1.17072	-0.20029	1.17068	-0.20032
30	1.15887	-0.21149	1.15897	-0.21139	1.15890	-0.21142

(b) DC state results

Methods	Variables					
	Vd	Id	a	c	d	θ
FRSE Conv.1	1.30063	0.44763	0.84800	0.56883	0.20468	8.175
Conv.2	1.27950	-0.44763	0.89206	0.51911	0.30978	19.99
SRSE Conv.1	1.30065	0.44768	0.84850	0.56893	0.20455	8.19
Conv.2	1.27951	-0.44768	0.89210	0.51922	0.30968	20.00
DSRSE Conv.1	1.30064	0.44765	0.84825	0.56888	0.20462	8.20
Conv.2	1.27950	-0.44765	0.89208	0.51915	0.30971	19.99

Table 7.23 Power flow accuracy comparison of 30 bus ac-dc link system under abnormal reference voltage (0.85)

Line No	Bus No.		DSRLF		FRSE		FDSE	
	From	To	Pij(MW)	Qij(MVAR)	Pij(MW)	Qij(MVAR)	Pij(MW)	Qij(MVAR)
1	1	2	90.213	-1.347	90.195	-1.517	95.241	-2.897
2	1	3	47.678	-2.601	47.582	-2.845	47.564	-3.765
3	2	4	28.898	-7.789	28.908	-6.634	30.753	-8.543
4	3	4	44.431	-3.167	44.345	-3.545	44.751	-4.572
5	2	6	37.674	-7.109	37.812	-7.228	38.863	-9.492
6	4	6	38.784	2.105	38.537	2.367	35.947	3.842
7	5	7	-12.393	1.667	-12.342	1.634	-12.562	2.382
8	6	7	35.489	6.589	35.858	6.348	37.895	8.983
9	6	8	-0.784	0.910	-0.738	0.921	-1.983	1.692
10	6	9	14.672	-10.671	14.472	-10.553	14.593	-8.528
11	6	10	12.398	-3.389	12.225	-3.280	15.396	-5.278
12	9	11	-17.925	-22.514	-17.836	-22.717	-12.739	-14.483
13	9	10	32.599	3.139	32.814	3.236	34.563	5.237
14	4	12	26.148	-6.709	26.547	-6.528	25.458	-5.567
15	12	13	-16.920	-30.159	-16.916	-30.144	-11.672	-42.259
16	12	14	7.659	2.078	7.784	1.985	7.827	2.894
17	12	15	17.501	4.989	17.687	4.752	17.638	3.569
18	12	16	6.707	1.678	6.508	1.584	5.862	1.021
19	14	15	1.363	0.113	1.256	0.103	2.356	1.428
20	16	17	3.164	-0.202	3.165	-0.195	3.459	-0.456
21	15	18	5.601	0.928	5.648	0.926	7.860	0.129

22	18	19	2.418	-0.035	2.321	-0.039	4.567	-0.184
23	19	20	-7.086	-3.445	-7.085	-3.425	-7.432	-4.983
24	10	20	9.401	4.402	9.506	4.404	15.862	2.592
25	10	17	5.858	6.076	5.841	6.074	5.946	5.678
26	10	21	16.077	9.388	16.107	9.365	16.567	12.345
27	10	22	7.811	4.197	7.856	4.202	8.458	5.678
28	21	22	-1.583	-2.051	-1.587	-2.108	-2.783	-3.457
29	15	23	4.834	1.506	4.845	1.485	4.459	2.478
30	22	24	6.218	2.027	6.224	1.989	6.456	2.568
31	23	24	1.611	-0.145	1.612	-0.146	1.457	-0.219
32	24	25	0.921	-0.716	0.923	-0.719	0.789	-0.745
33	25	26	3.547	2.361	3.545	2.356	3.271	1.985
34	25	27	4.471	-3.088	4.428	-3.041	5.789	-4.896
35	27	28	17.769	5.392	17.756	5.385	18.567	7.592
36	27	29	6.185	1.666	6.182	1.664	7.459	2.156
37	27	30	7.085	1.652	7.051	1.658	7.248	2.346
38	29	30	3.701	0.605	3.712	0.614	3.568	0.765
39	8	28	4.224	-1.410	4.230	-1.413	4.327	-1.187
40	6	28	13.592	3.536	13.552	3.535	15.218	4.567

Table 7.24 Power flow accuracy comparison of 30 bus ac-dc link system under abnormal reference voltage (1.15)

Line No	Bus No.		DSRLF		FRSE		FDSE	
	From	To	P _{ij} (MW)	Q _{ij} (MVAR)	P _{ij} (MW)	Q _{ij} (MVAR)	P _{ij} (MW)	Q _{ij} (MVAR)
1	1	2	90.213	-1.347	90.185	-1.515	93.321	-2.786
2	1	3	47.678	-2.601	47.578	-2.848	42.761	-2.648
3	2	4	28.898	-7.789	28.906	-6.637	30.873	-7.842
4	3	4	44.431	-3.167	44.378	-3.548	43.784	-4.891
5	2	6	37.674	-7.109	37.822	-7.226	38.642	-9.463
6	4	6	38.784	2.105	38.541	2.166	37.941	2.982
7	5	7	-12.393	1.667	-12.341	1.635	-10.582	2.331
8	6	7	35.489	6.589	35.456	6.446	41.539	6.782
9	6	8	-0.784	0.910	-0.746	0.912	-1.021	0.931
10	6	9	14.672	-10.671	14.476	-10.558	15.961	-8.872
11	6	10	12.398	-3.389	12.234	-3.289	15.842	-3.457
12	9	11	-17.925	-22.514	-17.842	-22.623	-17.735	-22.48
13	9	10	32.599	3.139	32.578	3.212	34.673	3.281
14	4	12	26.148	-6.709	26.234	-6.526	31.980	-6.840
15	12	13	-16.920	-30.159	-16.918	-30.148	-16.672	-31.67
16	12	14	7.659	2.078	7.674	1.998	9.563	2.972
17	12	15	17.501	4.989	17.612	4.952	17.427	4.568
18	12	16	6.707	1.678	6.712	1.684	6.982	1.421
19	14	15	1.363	0.113	1.358	0.108	1.983	1.031
20	16	17	3.164	-0.202	3.168	-0.199	3.456	-0.254
21	15	18	5.601	0.928	5.644	0.927	5.793	0.679

22	18	19	2.418	-0.035	2.420	-0.037	3.784	-0.124
23	19	20	-7.086	-3.445	-7.089	-3.435	-10.784	-4.489
24	10	20	9.401	4.402	9.405	4.406	9.893	4.583
25	10	17	5.858	6.076	5.848	6.072	2.983	5.457
26	10	21	16.077	9.388	16.105	9.387	14.786	9.986
27	10	22	7.811	4.197	7.832	4.186	8.762	5.875
28	21	22	-1.583	-2.051	-1.582	-2.106	-2.453	-3.467
29	15	23	4.834	1.506	4.842	1.496	4.768	1.476
30	22	24	6.218	2.027	6.222	1.998	8.986	2.567
31	23	24	1.611	-0.145	1.615	-0.144	1.983	-0.243
32	24	25	0.921	-0.716	0.922	-0.717	0.897	-0.789
33	25	26	3.547	2.361	3.548	2.358	5.432	2.085
34	25	27	4.471	-3.088	4.445	-3.076	6.453	-3.459
35	27	28	17.769	5.392	17.762	5.393	18.563	6.962
36	27	29	6.185	1.666	6.181	1.661	9.831	1.546
37	27	30	7.085	1.652	7.082	1.656	9.642	1.344
38	29	30	3.701	0.605	3.710	0.610	3.934	0.734
39	8	28	4.224	-1.410	4.226	-1.412	5.378	-2.187
40	6	28	13.592	3.536	13.567	3.538	13.763	4.894

Table 7.25 Effect of increasing R/X ratio on convergence

System Studied	R/X ratio	FRSE	SRSE	DSRSE	FDSE
		No. of itn.	No. of itn.	No. of itn.	No. of itn.
14 Bus dc mesh	0.5 G-jB	3	4	5	6
	0.75G-jB	3	4	5	6
	1.0 G-jB	3	4	5	6
	1.25G-jB	3	4	5	7
	1.5 G-jB	3	4	5	8
	1.75G-jB	3	4	5	10
	2.0 G-jB	3	4	5	14
	2.25G-jB	4	4	5	20
	2.5 G-jB	4	4	5	28
	3.00G-jB	6	4	5	**
30 Bus dc mesh	0.5 G-jB	3	4	5	6
	0.75G-jB	3	4	5	6
	1.0 G-jB	3	4	5	6
	1.25G-jB	3	4	5	8
	1.5 G-jB	3	4	5	9
	1.75G-jB	3	4	5	12
	2.0 G-jB	4	4	5	18
	2.25G-jB	6	4	5	29
	2.5 G-jB	8	4	5	**
	3.00G-jB	8	4	5	**
57 Bus dc mesh	0.5 G-jB	3	4	5	6
	0.75G-jB	3	4	5	6
	1.0 G-jB	3	4	5	8
	1.25G-jB	3	4	5	12
	1.5 G-jB	3	4	5	18
	1.75G-jB	3	4	5	31
	2.0 G-jB	6	4	5	**
	2.25G-jB	8	4	5	**
	2.5 G-jB	10	4	5	**
	3.00G-jB	**	4	5	**

Table 7.26 Effect of convergence under different loading condition

System Studied	Load	FRSE	SRSE	DSRSE	FDSE
		No of itn.	No of itn.	No of itn.	No of itn.
14 Bus	P+jQ	3	4	5	6
dc mesh	0.2P+j.2Q	3	4	5	7
	0.5P+0.5Q	3	4	5	6
	1.5P+jQ	3	4	5	6
	P+1.5jQ	3	4	5	6
	1.5P+1.5jQ	3	4	5	6
	2.0P+jQ	3	4	5	7
	P+j2.0Q	3	4	5	7
	2.0P+j2.0Q	4	4	5	8
	P+j3.0Q	4	4	5	10
30 Bus	P+jQ	3	4	5	6
dc mesh	0.2P+j.2Q	3	4	5	8
	0.5P+0.5Q	3	4	5	6
	1.5P+jQ	3	4	5	6
	P+1.5jQ	3	4	5	6
	1.5P+1.5jQ	3	4	5	6
	2.0P+jQ	3	4	5	7
	P+j2.0Q	3	4	5	10
	2.0P+j2.0Q	4	4	5	12
	P+j3.0Q	4	4	5	14
57 Bus	P+jQ	3	4	5	6
dc mesh	0.2P+j.2Q	3	4	5	8
	0.5P+0.5Q	3	4	5	6
	1.5P+jQ	3	4	5	6
	P+1.5jQ	3	4	5	6
	1.5P+1.5jQ	3	4	5	6
	2.0P+jQ	3	4	5	8
	P+j2.0Q	3	4	5	15
	2.0P+j2.0Q	4	4	5	15
	P+j3.0Q	5	4	5	18

7.9 ANALYSIS OF SIMULATION RESULTS

Tables 7.1 and 7.2 show the size and structure of Jacobian and gain matrix of a simple 3 busbar ac-dc system. For the 3 busbar system one line between buses 1 and 2 is a dc line. There are no data provided for 3 busbar ac-dc system, because the algorithms has not been tested on 3 bus ac-dc system. These two tables are given to provide an overview of how the variables are arranged in constructing the Jacobian and gain matrix.

The states of 14, 30, 57 and 107 busbar networks were estimated using the FRSE, SRSE and DSRSE algorithms for both the link and mesh configurations. The results with the link configuration for the four systems are given in Tables 7.3, 7.4, 7.5 and 7.6. Similarly, the corresponding results with the mesh configuration for the first three systems are provided in Tables 7.7, 7.8 and 7.9. Results obtained from the FRSE serve to verify the accuracy of the solution. A comparison of the results obtained from the SRSE, DSRSE and FDSE with those obtained from the FRSE indicates that the new estimators perform satisfactorily. Earlier it has been mentioned that the state estimation results provided by the proposed methods are accurate and acceptable. A quantitative assessment of the accuracies is provided in Tables 7.10, 7.11, 7.12 and 7.13. In some cases the results obtained from the DSRSE is only provided in this chapter in order to avoid the repeated results. The maximum percentage of errors in 'e' and 'f' for 14 busbar system are very small. Among the dc system variables the maximum errors are the real and imaginary components of the transformer secondary side current and the values are 1.5 percent for the real part and 1.04 percent for the imaginary part. The overall maximum average percentage errors for

different systems are exhibited in Table 7.14. From the table it is observed that the maximum error are not much far away from the average value. Also the average error in the different system is very small. A closer examination of the errors suggest that the results obtained from the proposed methods are acceptable.

Table 7.15 shows the number of iterations and solution time comparison of different methods. It appears from the table that the number of iterations required by FRSE becomes less as compared to the other methods. However, the number of iteration is not the important factor currently, the most important factor being the computer memory and how fast one can get the solution. Though FRSE converges within 3 iterations, but the solution time for the higher bus system is relatively large. On the other hand, both the solution time and the number of iterations for DSRSE is better than the FDSE. The DSRSE is shown to be superior than the SRSE. Its time per iterations and total solution time are less than those for the SRSE. The gain matrices both in the SRSE and DSRSE remain constant. However, the size of the gain matrix in the DSRSE is smaller than that in the SRSE. This accounts for smaller computation time. Though SRSE takes some times to converge in comparison to FDSE, however the number of iteration is less.

Table 7.16 provides the saving in solution time as compared to other methods with FRSE method taken as reference. From the table it is observed that SRSE and DSRSE exhibits a good amount of saving in solution time. For example, a saving in solution time of about 73.3 and 75.3 percent is possible on 30 and 57 busbar system with the DSRSE method. Also, it is observed that the savings in solution time of 107 bus system by

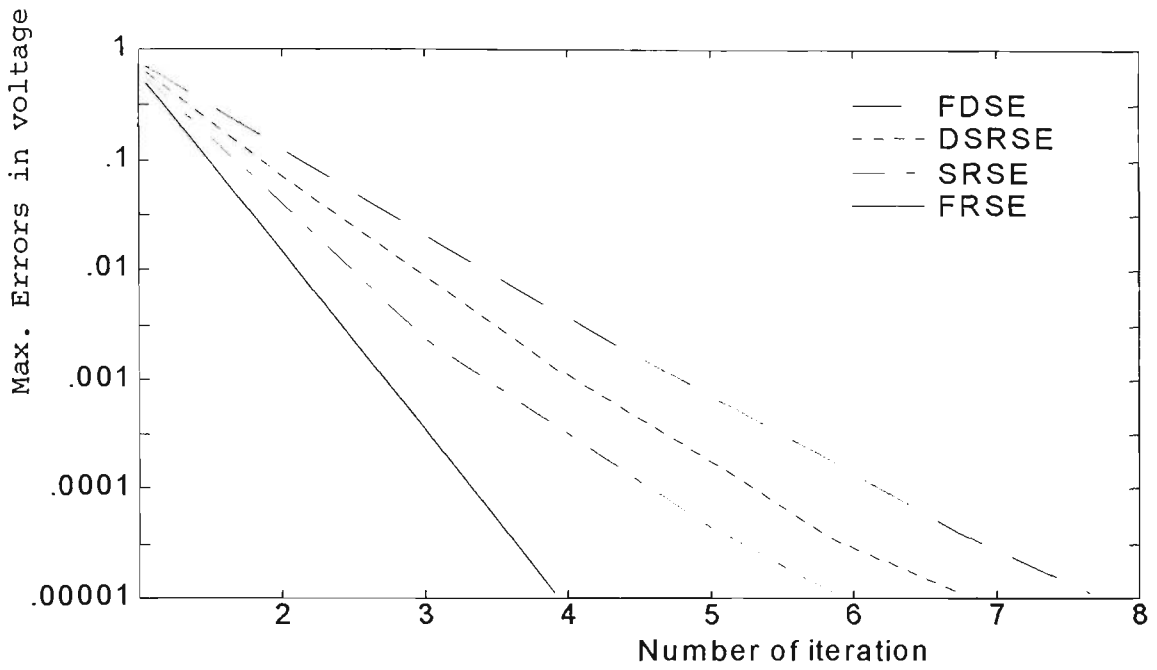


Fig.7.1 Convergence characteristics of 14 bus system with dc link

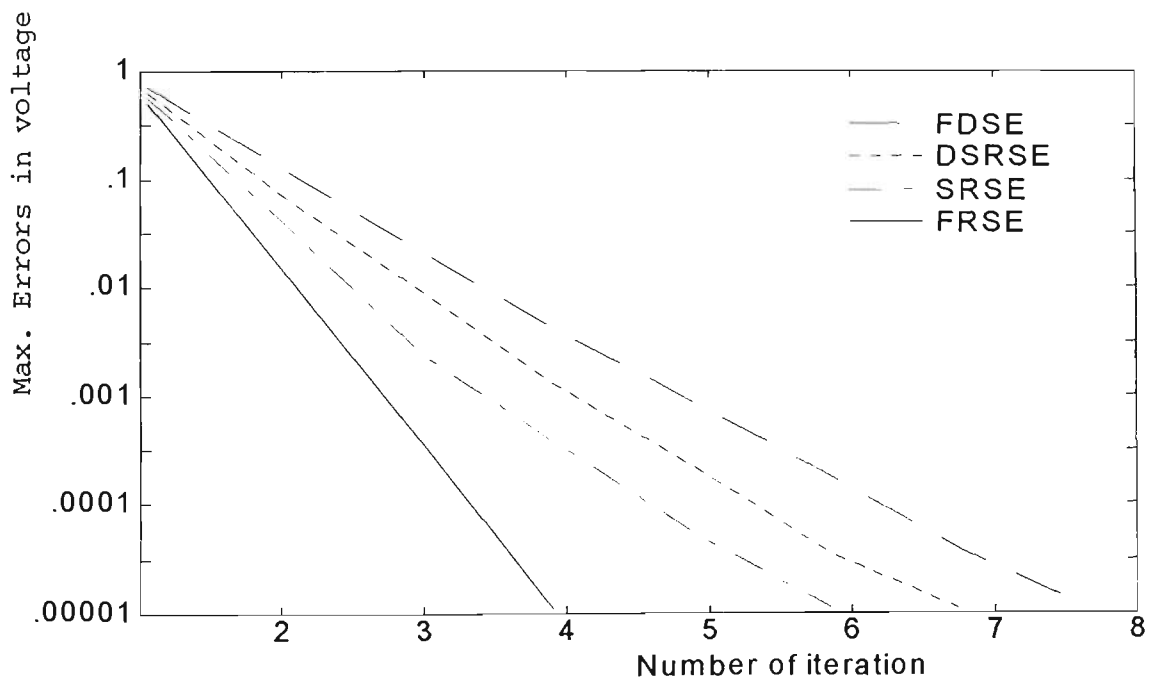


Fig.7.2 Convergence characteristics of 14 bus system with dc mesh

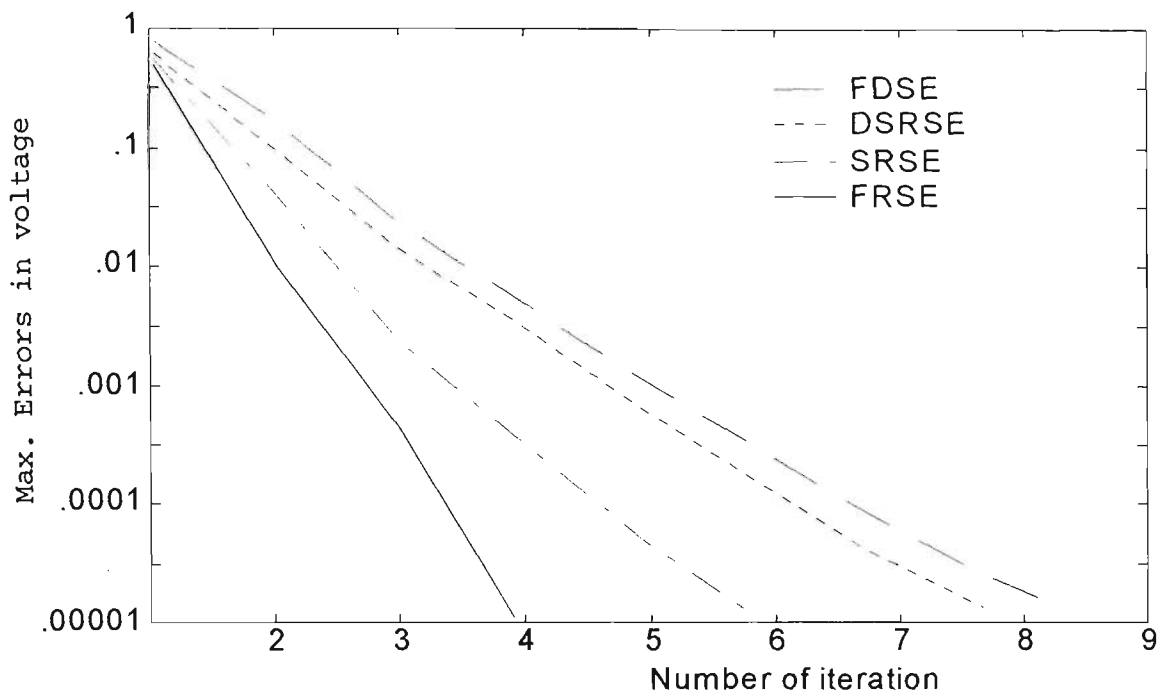


Fig.7.3 Convergence characteristics of 14 bus system with dc mesh-link

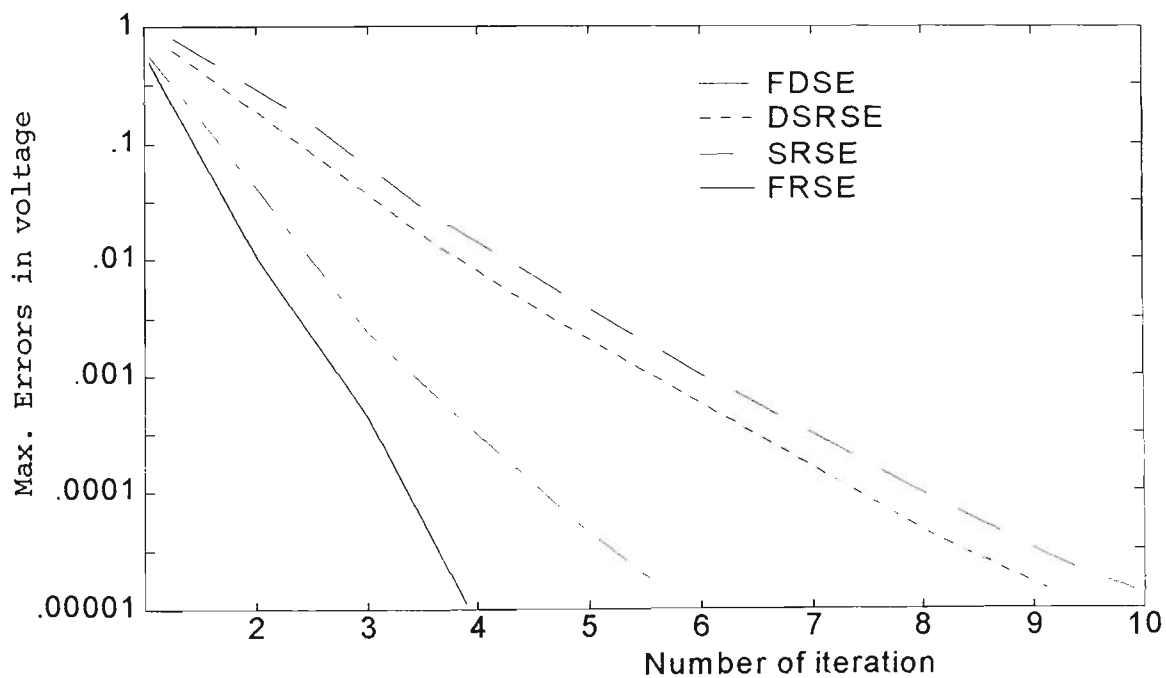


Fig. 7.4 Convergence characteristics of 30 bus system with dc link

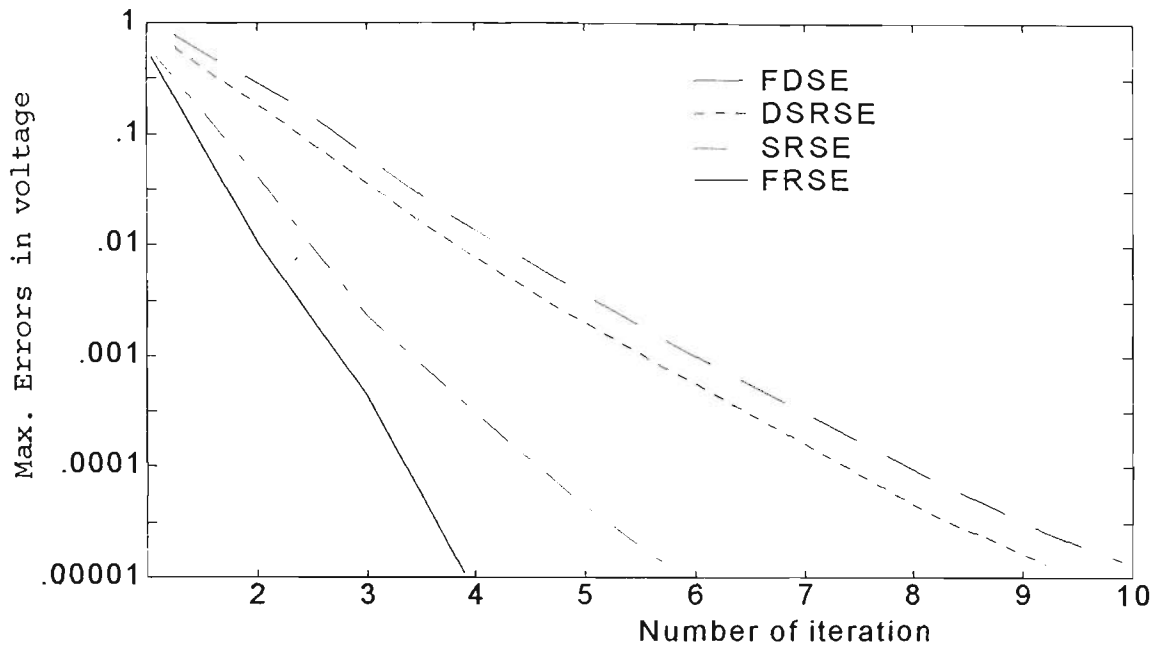


Fig. 7.5 Convergence characteristics of 30 bus system with dc mesh

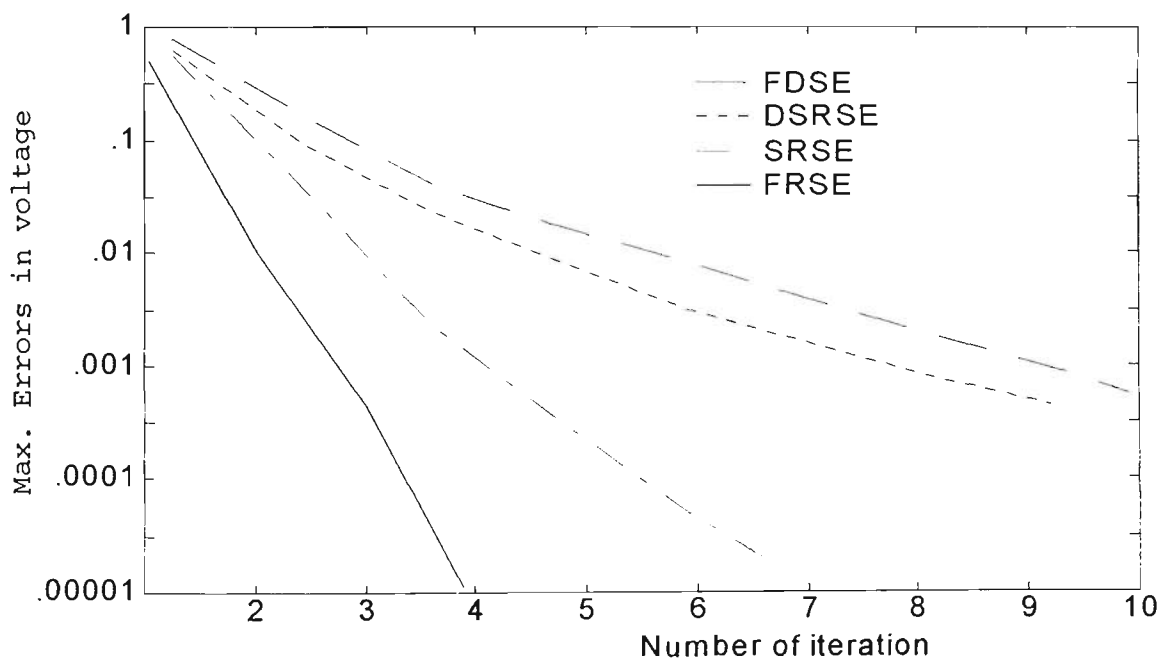


Fig.7.6 Convergence characteristics of 30 bus system with dc mesh-link

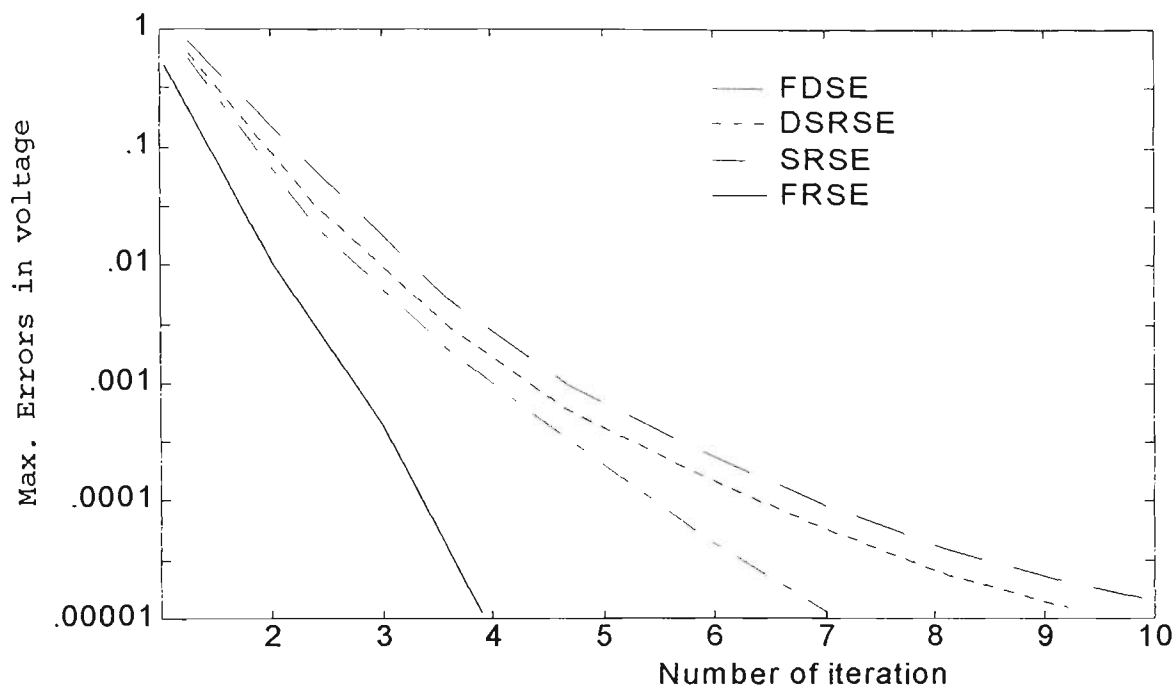


Fig. 7.7 Convergence characteristics of 57 bus system with dc link

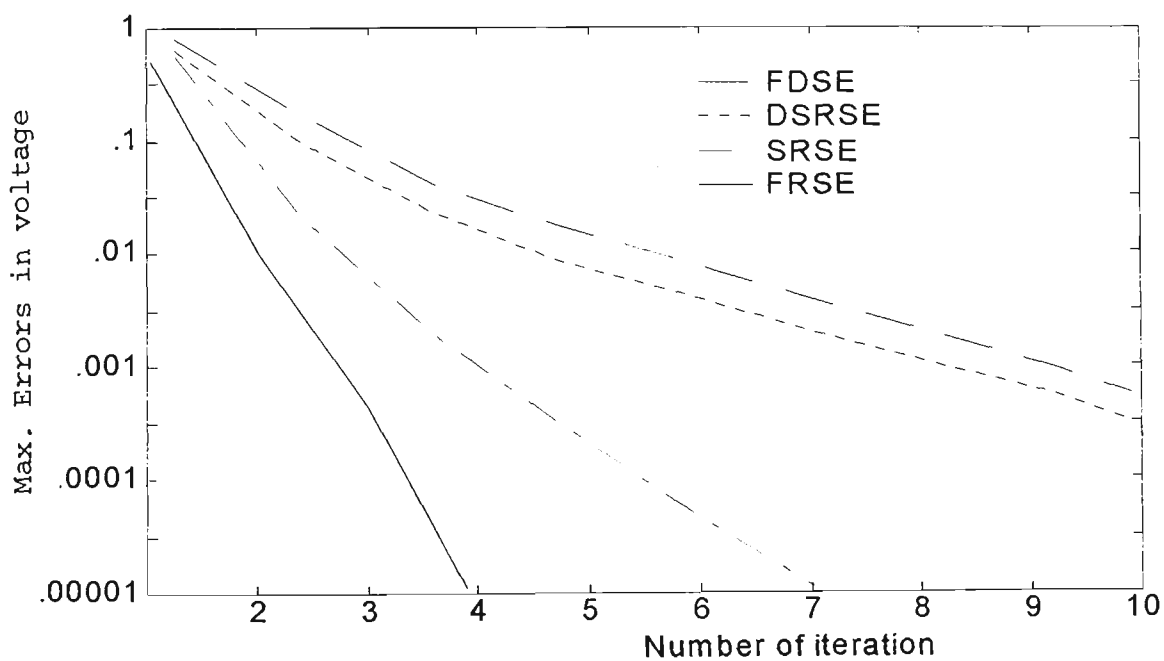


Fig. 7.8 Convergence characteristics of 57 bus system with dc mesh

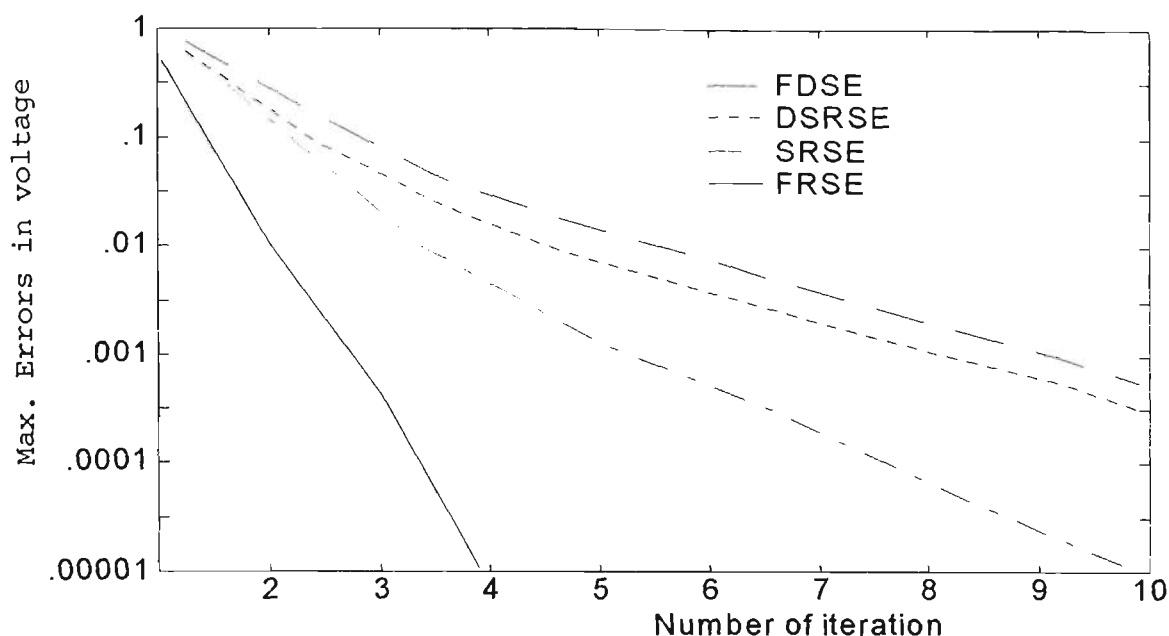


Fig. 7.9 Convergence characteristics of 57 bus system with dc mesh-link

the SRSE, DSRSE and FDSE are 63.2, 80.6 and 71.1 percent respectively. It may be concluded that for higher bus system the DSRSE possess an excellent saving in solution time.

Figs 7.1-7.9 indicate the relative convergence behaviour of different methods. These figures show that the SRSE method takes few more iterations than FRSE method but less iterations than the DSRSE method. Therefore, from the convergence point of view, the SRSE is slower than the FRSE and DSRSE is slower than SRSE. The convergence of the DSRSE and FDSE are similar. It is well known that the convergence of the WLSE is quadratic [93]. The mathematical model of FRSE is same as the mathematical model of WLSE in rectangular co-ordinate, so the convergence

characteristic of FRSE is similar to that of WLSE. In the WLSE approach, the state vector is updated in each iteration. In contrast, whilst considering second order approach, the error vectors are updated. In addition, the constant gain matrix is used in the iterative scheme. These factors may be attributed to the slower convergence of the second order method. The DSRSE is a decoupled version of the SRSE. This decoupling may be responsible for further deterioration in the convergence rate. Although the convergence rate of SRSE is slower than the FRSE, yet its times per iteration as well as the total solution time are much less. This is attributed to the fact that the gain matrix remains constant in the iterative solution. As a result, total number of mathematical operations is much less compared to that in FRSE.

The performance characteristic of the state estimator is also assessed in terms of the performance index. Tables 7.17 and 7.18 illustrate the convergence behaviour of the proposed methods on 14, 30, 57 and 107 busbar in terms of the performance index. The convergence properties are comparable and acceptable. From Table 7.18 it is also observed that the value of J_E is less than the value of J_M which indicates that the filtering process works effectively. The value of average and maximum weighted residual are small which indicates that the estimated value is very close to the true value.

A state estimator is a data processing algorithm for converting telemetered readings and topological information, including redundant measurements into an estimate of the power system's state. During the estimation process if some data are lost for any reasons, for example due to communication

failure, till the proposed algorithms estimate correctly the system states. Tables 7.19 and 7.20 confirms this.

During normal operating conditions FD state estimator provides accurate results and exhibits excellent convergence pattern [93]. However, on well conditioned system, in rare cases, unusual operating mode may occur. During the restoration period following an emergency or in the circumstances of unusual plant outages the system voltage may vary within ± 20 percent. Tables 7.21 and 7.22 indicate the proposed methods provide accurate solutions when the metered reference voltage is either too low or too high. On the other hand FDSE sometimes provide erroneous results when metered reference voltage is either too low or too high. Tables 7.23 and 7.24 confirms this. The reason for faulty solutions could be due to the fact that the decoupling assumptions are not valid at voltage much vary from 1 pu.

FDSE is based upon certain decoupling assumptions. The decoupling principle is weakened when the transmission lines have high R/X ratio. Table 7.25 indicates that the proposed algorithms perform well for high value of R/X ratio. SRSE and DSRSE possess an excellent convergence rate when the system has high value of R/X ratio, FRSE fail to converge for large system when R/X ratio is abnormally high. From the table it appears that the convergence rate of FRSE is much superior than the SRSE and DSRSE, however the solution time is relatively large. On the other hand FDSE sometimes produces oscillatory convergence and the oscillatory nature increases as the value of R/X ratio increases. Also the FDSE fail to converge when the R/X ratio exceeds certain limit and it also depends upon

the system. For example, FDSE diverge when the R/X ratios exceeds 3.0 for 14 bus, 2.5 for 30 bus and 2.0 for 57 bus system. Most important things which are observed in the table is that FRSE either converges within 10 iteration otherwise it diverges, it cannot produce oscillatory convergence like FDSE. Moreover, in case of SRSE and DSRSE the convergence rate is independent on the system size.

The convergence rate is also influenced by the system loading. Some of the algorithms does not perform well under heavy loading condition. Also during heavy loading condition the angle difference between the two adjacent nodes may not be neglected. Table 7.26 shows the effect of different loading upon convergence. From the table it may be concluded that the convergence rates of the proposed algorithms are independent upon the system loading. However, FDSE sometime produces oscillatory convergence with very low value of underloading condition as well as overloading condition.

7.10 CONCLUSIONS

Three estimators for assessing the state of ac-dc power systems have been tested and the test results are provided in this chapter. The results provided by FDSE is just for comparison purpose. The new method has significant practical importance as it is capable of providing the reliable system state even during unusual operating conditions. Under normal operating conditions, the performance characteristics, viz., accuracy and convergence rate of the proposed estimators are nearly similar and are comparable to FDSE. However, in terms of computational speed only DSRSE is

comparable to FDSE. On well behaved networks, under unusual operating conditions, such as due to sharp deviation of the metered reference bus voltage (which may occur due to loss of large generation or loads or transmission line outages), the proposed estimators still retains its convergence behaviour and provides a reliable solution, whereas FDSE deteriorates its convergence rate and also gives erroneous result. For ill-conditioned networks the SRSE and DSRSE gives an efficient and reliable solution as it does for well behaved power systems under all operating modes, unlike the FDSE which produces oscillatory convergence and generally diverges. However, for higher bus system with abnormal high value of R/X ratio the FRSE fail to converge, but it does not produce oscillatory convergence. Also the proposed estimators are able to provide a reliable estimate even when some system data are missing. Thus, due to the ability to perform accurately, efficiently and reliably on well as well as ill-conditioned power systems under all operating modes, the proposed estimators are seen to be practically viable and preferred alternative analytical tool for real time monitoring for ac-dc power systems.

PART - III

GENERAL CONCLUSIONS

Chapter 8

GENERAL CONCLUSIONS AND SUGGESTIONS FOR FUTURE WORK

8.1 CONCLUSIONS

A simple, efficient and flexible algorithms for the load flow and static state estimator of interconnected ac-dc system are presented. The methods are based on a sequential approach and yield optimum results. The algorithms are capable of handling two terminal as well as multi-terminal dc networks. By applying sparsity technique for ac-dc interconnected system makes the algorithms suitable for on-line computation for large scale ac or ac-dc systems.

First and second order ac-dc load flow and state estimation algorithms have been developed and experimented in this thesis. Digital simulation studies on a number of tests as well as real power systems indicate that second order algorithms is not only far superior to the first order one, but its performance even sometimes better than the fast decoupled (FD) load flow and FD state estimation methods. The performance characteristics of the second order algorithms are comparable to those of the FD load flow and FD state estimation methods on well-conditioned networks, however characteristics are superior on ill-conditioned ones. Even more significantly, second order

algorithms perform well under heavy loading conditioned networks, whereas first order method takes few more iteration and FD method encounters convergence problem. Further, the second order methods, inspite of being exact and faster than the first order method, is not superior against the most popular FD load flow and FD state estimator methods in terms of computational efficiency. For the past several years the FD load flow and FD state estimator methods have been acknowledged in the power industry to be superior to other load flow and state estimation methods as far as computational speed and storage requirements are concerned. However, on closer examination, it is recognised that amongst the second order methods the computer storage and the computational efficiency of the decoupled second order rectangular co-ordinate ac-dc load flow (DSRLF) and decoupled second order rectangular co-ordinate ac-dc state estimator (DSRSE) are comparable to those of fast decoupled ac-dc load flow (FDLF) and fast decoupled ac-dc state estimator (FDSE) methods. The principal difference between the DSRLF and DSRSE methods with second order rectangular co-ordinate ac-dc load flow (SRLF) and second order rectangular co-ordinate ac-dc state estimator (SRSE) methods is that the former are the parent version of latter one. The first order rectangular co-ordinate ac-dc load flow (FRLF) is basically the modified form of Newton-Raphson load flow (NRLF) and first order rectangular co-ordinate ac-dc state estimator (FRSE) is also the modified form of weighted least square state estimator (WLSE).

Load flow: Three new methods, namely FRLF, SRLF and DSRLF are developed and presented in Chapters 2 and 3 for the load flow study of the

ac-dc power systems. The methods are based on the rectangular co-ordinate formulation of the ac-dc system performance equations.

The FRLF method is basically the Newton-Raphson (NR) formulation in the rectangular co-ordinate for the load flow solution of the ac-dc systems. Therefore, its characteristics are similar to those of the NR formulation in the polar co-ordinate. A Taylor series expansion of the ac equations in the rectangular form terminates after the second order derivatives. Likewise, four of the six equations per converter also terminate after the second order derivatives. Two equations per converter have derivatives higher than the second order terms. Omission of the terms beyond the second order of these equations and inclusion of full Taylor series of the remaining equations' results in the SRLF method. A reorganisation of the SRLF mathematical model without introducing any approximation results in a faster version, called the DSRLF method.

The following outstanding features characterising the proposed methods have been identified on the basis of various simulation studies conducted on several ac-dc power systems:

- The computer storage requirements for the FRLF and SRLF methods are comparable.
- The computer storage needed for the DSRLF and FDLF methods are comparable. However, they are nearly half that for the FRLF and SRLF method.
- The solution time requirement for the SRLF method is less than that for the FRLF method but more than that for the

DSRLF and FDLF methods. However, the computational efficiencies of the DSRLF and FDLF methods are comparable. It is found that the computing time of DSRLF is better than FDLF method.

- The convergence characteristic of FRLF method is quadratic. This is found to be linear in case of SRLF and DSRLF methods. Though these methods take more sub-iterations than the FRLF method, but the solution time is much less. The convergence rate of the SRLF method seems to be superior to that of the DSRLF and FDLF methods. However, the convergence rate of DSRLF and FDLF methods are comparable.
- The solution times of DSRLF and FDLF methods are comparable. Though DSRLF method takes few more time in first iterations, however the total solution time is less than the FDLF method.
- The proposed methods are found to be valid under different control conditions on converters. It is more stable as well.
- On well behaved systems all the methods exhibit excellent convergence pattern. However, on ill-conditioned system FDLF method produces oscillatory convergence and some times fail to converge. Whereas, the proposed methods provide good convergence pattern on ill-conditioned systems.
- Under heavy loaded condition systems, the proposed algorithms are found to be more reliable and provide

excellent convergence pattern, whereas FDLF method some time take a few more iterations to converge.

In conclusion, the SRLF is decidedly superior to the FRLF method. Also the DSRLF method is superior to the SRLF method but comparable to the FDLF method.

Thus, because of their ability to perform accurately, efficiently and reliably under all operating modes and different converter control specifications the proposed methods are seen to be practically viable.

State estimation : Three new algorithms for state estimation of ac-dc power systems have been developed and presented in this thesis. The performance equations of the ac system, dc system and interface system are formulated in the rectangular co-ordinates. The first algorithm is based on the first order derivatives of the Taylor series, and is basically the WLSE in rectangular co-ordinates. The complete Taylor series expansion of the performance equations indicate that the series terminates after the second order derivatives for all but four equations per converter. In an ac-dc system there are only a few converters, thus the number of equations containing third and higher order derivatives are extremely small as compared to the total number of equations. A scheme of using both the first and second order derivatives for all the equations result in an exact mathematical model. An algorithm based on this model is developed and named SRSE. Decoupling of the real power, reactive power and dc system equations of the SRSE mathematical model results in an improved version, called the DSRSE. Decoupling is done not by zeroing the off diagonal submatrices of

the Jacobian and gain matrices but as a two step procedure. Also, there is no approximation introduced while decoupling.

The characteristics of the new methods are ascertained by digital simulation studies on several ac-dc power systems. The proposed algorithms are found to have the following outstanding features which are summarised below:

- The size and structure of the mathematical models of the WLSE and FRSE are comparable. Their convergence characteristics are quadratic.
- The size and structure of the mathematical model of the SRSE are similar to those of the FRSE, but unlike in the FRSE the gain matrix of the SRSE remains constant. This is because the SRSE is based on a complete Taylor series expansion of the performance equations, subject to the approximation outlined above.
- The size and structure of the mathematical model of the DSRSE are very much different from those of the FRSE and SRSE. The size of the gain matrix in the DSRSE is less than half of that in the FRSE and SRSE.
- The convergence characteristics of the SRSE are inferior to those of the FRSE and require a few more iterations to provide a solution with the comparable accuracy.
- The DSRSE requires a few more iterations than the SRSE. The poor convergence could be attributed to the constant gain matrix and decoupling of the equations in the solution scheme.

- In the iterative solution, the total computational burden for the SRSE is less than that for the FRSE, but more than that for the DSRSE. This is attributed to the fact that though the SRSE and DSRSE require more iterations, they involve less mathematical operations as the gain matrix is neither calculated nor factorised in each iteration. Further, in the DSRSE the size of the gain matrix is much smaller as compared to that of the SRSE.
- Computationally the DSRSE is much superior to the SRSE which in turn is superior to the FRSE.
- Results obtained from the SRSE and DSRSE methods are accurate and in good agreement with those obtained from the FRSE. Also, these methods are as stable as the WLSE and FRSE.
- The new methods perform satisfactorily not only under normal operating conditions but even under abnormal ones when some data are missing and reference signal is much different from unity.
- The proposed methods perform well under ill-conditioned networks, whereas FDSE produces oscillatory convergence and some time fail to converge.
- The algorithms also converge under loaded conditioned networks, however, in some heavily loading conditioned networks FDSE take few more iterations to converge.

From the above discussion it be may concluded that, the proposed method not only performs satisfactorily but they are fast, accurate and stable. Thus

the proposed methods can faithfully be applied to solve power system state estimation problems.

8.2 FUTURE WORK

The work reported in this thesis involve the formulation, development and simulation of ac-dc load flow and ac-dc state estimation as applied to electrical power systems. The following aspects relating to future research are outlined below:

- In actual ac-dc converter model there are ten variables, out of ten variables only minimum number of variables have been used. This is sufficient to represent the converter model. The minimum number of variable is chosen in order to reduce the program complexity. Use of all the variables may be the subject of future study.
- When the ac and dc equations are expressed in Taylor series, all the ac equations in the rectangular form terminate after the second order derivatives. Also the four equations of the converter terminate after the second order derivatives. Only two converter equations have terms upto six order derivatives. In this study, the equations which contained the terms beyond the second order are neglected in order to reduce the algorithmic complexity. Taking the full Taylor series of the two converter equations in the mathematical model, similar studies can be undertaken.

- In developing the mathematical models the converter and transformer losses are neglected. This may produce some errors in the solution. Incorporating these features in the mathematical model may also be of considerable research interest.
- In the development of the algorithms it is assumed that converter terminal busbar voltages are balanced and sinusoidal in nature. Also the converter operation is perfectly balanced. The study can be extended to unbalanced system as well.
- Algorithms for the three phase load flow for the ac-dc system may be developed in a similar manner.
- Contingency study is one of the important part of power system operation and planning which is not included in this study. This may also be a subject for future study.
- The algorithms are suitable for balanced high and low voltage distribution system. Further investigation may be carried out on unbalanced radial distribution system.
- The proposed models can be solved by using linear programming techniques in order to make it more faster. Future studies in this connection would be very useful.

REFERENCES

- [1] Ward, J.B. and Hale, H.W., "*Digital simulation of power flow problems*", AIEE Trans. PAS Vol. 77, June 1956, pp. 298-404.
- [2] Clair, R.E., and Stagg, G.W., "*Experience in computation of load flow studies using high speed computers*", AIEE Trans. Vol. 77, pt. III, 1958, pp. 1275- 1282.
- [3] Jordan, E.M., "*Rapidly converging digital load flow*", AIEE Trans. Vol. 76, pt. III, 1957, pp. 1433-1438.
- [4] Hale, H.W. and Goodrich, R.W., "*Digital computation of power flow some new aspects*", AIEE Trans. Vol. 78, pt III, 1959, pp. 919-924.
- [5] Glimn, A.F. and Stagg, G.W., "*Automatic calculation of load flows*", AIEE Trans. PAS Vol. 76, Oct. 1957, pp. 817-828.
- [6] Brown, H.E. and Tinney, W.F., "*Digital solution for large power networks*", AIEE Trans. Vol. 76, pt. III, 1957, pp. 347-355.
- [7] Stott, B., "*Review of load flow calculation methods*", Proc IEEE Vol. 62, July 1974, pp. 916-926.
- [8] Tinney, W.F. and Hart, C.E., "*Power flow solution by Newton's method*", IEEE Trans. PAS Vol. 86, Nov. 1967, pp. 1449-1456.
- [9] Tinney, W.F. and Walker, J.W., "*Direct solution of sparse network equations by ordered elimination*", Proc IEEE, Vol. 55, Nov. 1967, pp. 1801-1809.
- [10] Stott, B. and Alsac, O., "*Fast decoupled load flow* ", IEEE Trans. PAS, Vol. 93, May/June 1974, pp. 859-869.

- [11] Roy, L., "*Exact second order load flow*", Proc. of 6th PSCC, Darmstadt, West Germany, Aug. 21-25, 1978, pp. 314-320.
- [12] Iwamoto, S. and Tamura, Y., "*A fast load flow method retaining nonlinearity*", IEEE Trans. PAS Vol. 97, Sept/Oct. 1978. pp. 1586-1599.
- [13] Lo, K.L. and Mahmoud, Y.M., "*A decoupled linear programming technique for power system state estimation*", IEEE Trans. 1986, Vol. PWRS-1, pp. 154-160.
- [14] El-Hawary, M.E. and Wellon, O.K., "*The alfa modified quasi second order Newton Raphson method for load flow solution in rectangular form*", IEEE Trans. PAS, Vol. 101, Jan. 1982, pp. 854-866.
- [15] Rao, P.S.N., Rao, K.S.P. and Nanda, J., "*A novel hybrid load flow method*", IEEE Trans. PAS Vol. 100, Jan. 1981, pp. 303- 308.
- [16] Krishnaparandhama, T., Elangovan, S., Kuppurajulu, A. and Sankarn-aryanan, V., "*Fast power flow solution by the method of reduction and restoration*", Proc. IEE, Vol. 127, pt. C, No. 2, March 1980, pp. 90-93.
- [17] Horigome, T. and Ito, N., "*Digital computer method for the calculation of power flow in an ac-dc interconnected power system*", Proc. IEE, 1964, pt. C, No. 6, pp. 1137-1144.
- [18] Gavrilovic, A. and Taylor, D.G., "*The calculation of the regulation characteristics of dc transmission systems*", IEEE Trans. PAS Vol. 83, March 1964, pp. 215-223.
- [19] Hingorani, N.G. and Mountford, J.D., "*Simulation of hvdc systems in ac load flow analysis by digital computers*", Proc. IEE, Vol. 113, pt. C, No. 9, Sept. 1966, pp. 1541- 1546.

- [20] Barker, I.E. and Carre, B.A., "*Load flow calculation for systems containing hvdc links in hvdc transmission*", Proc. IEE, Vol. 113, pt. C, No.1, March 1966, pp. 115-118
- [21] Brever, G.D. and Young, D.C., "*Studies of large ac-dc systems on the digital computer*", IEEE Trans. PAS, Vol. 85, Nov. 1966, pp. 1107-1116.
- [22] Sato, H. and Arrillaga, J., "*Improved load flow techniques for integrated ac-dc systems*", Proc. IEE, pt. C, No. 4, 1969, pp. 525-532.
- [23] Sheble, J.R. and Heydt, G.T., "*Power flow studies for systems with hvdc transmission*", Proc. Power Industry Computer Applications, 1975, pp. 223-228.
- [24] Braunagel, D.A., Kraft, L.A. and Whysong, J.L., "*Inclusion of dc converter and transmission equations directly in a Newton power flow*", IEEE Trans. PAS Vol. 95, Jan/Feb 1976, pp.76- 88.
- [25] Arrillaga, J. and Bodger, P., "*Integration of hvdc links with fast decoupled load flow solutions*", Proc IEE, Vol. 124, No. 5, pt. C, 1977, pp. 453-468.
- [26] Arrillaga, J., Bodger, P. and Harker, B.J., "*FDLF algorithm for ac-dc systems*", IEEE paper A 78, 555-5, PES Summer meeting Los Angeles, July 1978, pp. 16-21.
- [27] Arrillaga, J., Harker, B.J. and Turner, K.S., "*Clarifying an ambiguity in recent ac-dc load flow formulations*", Proc. IEE, Vol. 127, pt. C, Sept. 1980, pp. 324-329.
- [28] Reeve, J., Fahmy, G. and Stott, B., "*Versatile load flow method form multiterminal hvdc systems*", IEEE Trans. PAS, Vol. 96, 1977, pp. 925-933.

- [29] El-Marsafawy, M. and Mathur, R.M., "*A new technique for load flow solution of integrated multiterminal ac-dc systems*", IEEE Trans. PAS, Vol. 99, Jan/Feb 1980, pp. 246-255.
- [30] Fudeh, A.M. and Ong, C.M., "*A simple and efficient ac-dc load flow method for multiterminal dc systems*", IEEE Trans. PAS, Vol. 100, Nov. 1981, pp. 4389-4396.
- [31] Ong, P.S. and Hamzel-nejad, A., "*A general purpose multiterminal dc load flow*", IEEE Trans. PAS, Vol. 100, July 1981, pp. 3166-3374.
- [32] Mehseredjian, C., Lefbvre, S. and Mukhedkar, D., "*A multiterminal hvdc load flow with flexible control specifications*", IEEE Trans. PAS, April 1986, pp. 272-282.
- [33] El-Marsafwy, M., "*Accurate simulation of computation overlap effects in an hvdc terminal model for power flow studies*", Elec. power system research 13 (1987), pp. 185-189.
- [34] Wu, F.F., "*Theoretical study of the convergence of the fast decoupled load flow*", IEEE Trans. PAS, Vol. 96, Jan/Feb. 1977, pp. 268-275.
- [35] Abou El-Ela, A.A., "*A non-iterative and exact linearization load flow technique for circuit contingency effects in power systems*", Journal of Electr. power system, 1990, pp. 213-218.
- [36] Tripathy, S.C. and Prasad, D.G., Malik, O.P., "*Load flow solution for ill conditioned power system by quadratically convergent Newton like method*", IEEE Trans. PAS, Vol. 101, Nov/Dec. 1982, pp. 3648-3657.
- [37] Deckmann, S., Monticelli, A., Stott, B. and Alsac, O., "*Numerical testing of power system load flow equivalents*", IEEE Trans. PAS, Vol. 99, No. 6, Nov/Dec. 1980, pp. 2292-2300.

- [38] Deckmann, S., Pizzolante, A., Monticelli, A. and Alsac, O., "*Studies on power system load flow equivalencing*", IEEE Trans. PAS, Vol. 99, Nov/Dec. 1980, pp. 2301-2310.
- [39] Arillaga, J. and Bodger, P., "*AC-DC load flow with realistic representation of the converter plant*", Proc. IEE, Vol. 125, pt. C, No. 1, 1978, pp. 41-46.
- [40] Rao, P.S.N., Rao, K.S. and Nanda, J., "*An exact fast load flow method including second order terms in rectangular coordinates*", IEEE Trans. PAS, Vol. 101, Sept. 1982, pp. 3261-3268.
- [41] Roy, L. and Rao, N.D., "*Real time monitoring of power systems using fast second method*", Proc. IEE, Vol. 130, No.3, pt. C, May 1983, pp. 103-110.
- [42] Keyhani, A., "*Study of fast decoupled load algorithms with substantially reduced memory requirements*", Electric power system research 9, 1985, pp. 1-9.
- [43] Hubbi, W., "*The mismatch theorem and second order load flow algorithms*", Proc. IEE, Vol. 132, No. 4, pt. C, July 1985, pp. 189-194.
- [44] Duraiswamy, P., Sadasivam, G., Khan, M.A. and Jegatheesan, R., "*An efficient power flow algorithm for integrated ac-dc systems*", Proc. 9th National system conference Allahabad, Dec. 1985, pp. 210-215.
- [45] Nanda, J., Bijwe, P.R. and Kothari, D.P., "*Second order decoupled load flow*", Electric machines and power systems, Vol. 12, 1987, pp. 301-312.
- [46] Nanda, J., Kothari, D.P. and Srivastava, S.C., "*Some important observations on fast decoupled load flow algorithm*", Proc. IEEE Vol. 75, May 1987, pp. 732-733.

- [47] Nanda, J., Kothari, D.P. and Srivastava, S.C., "*A novel second order fast decoupled load flow method in polar coordinates*", *Electric machines and power systems*, Vol. 14, 1988, pp. 339- 351.
- [48] Sanghavi, G.S. and Banerjee, S.K., "*Load flow analysis of integrated ac-dc power systems*", *Proc. IEEE 4th International Conference, Bombay, Nov. 1989*, pp.746-751.
- [49] Dopazo, J.F., Klitin, O.A., Stagg, G.W. and Slyck, L.S.V., "*State calculation of power systems from line flow measurements*", *IEEE Trans. PAS*, Vol. 89, Sept/Oct. 1970, pp. 1698-1708.
- [50] Smith, O.J.M., "*Power system state estimation*", *IEEE Trans. PAS*, Vol. 89, March 1970, pp. 363-379.
- [51] Schweppe, F.C. and Wildes, J., "*Power system static state estimation*", *IEEE Trans. PAS*, Vol. 89, Jan. 1970, pp. 120- 135.
- [52] Larson, R.E., Tinney, W.F. and Peschon, J., "*State estimation in power systems part I : Theory and feasibility*", *IEEE Trans. PAS*, Vol. 89, Mar. 1970, pp. 345-352.
- [53] Dopazo, J.F., Klitin, O.A. and Van Slyck, L.S., "*State calculation of power systems from line flow measurements, Part II*", *IEEE Trans. PAS*, Vol. 91, Jan/Feb. 1972, pp. 145-151.
- [54] Schweppe, F.C. and Handschin, E.J., "*Static state estimation in electric power systems*", *Proc. IEEE*, Vol. 62, July 1974, pp. 972-983.
- [55] Rao, N.D. and Tripathy, S.C., "*A variable step size decoupled state estimator*", *IEEE Trans. PAS*, Vol. 98, March/April 1979, pp. 436-443.
- [56] Rao, N.D. and Tripathy, S.C., "*Power system static state estimation by the Levenberg Marquardt algorithm*", *IEEE Trans. PAS*, Vol. 99, 1980, pp. 695-702.

- [57] Wang, J.W. and Quintana, V.H., "*A decoupled orthogonal row processing algorithm for power system state estimation*", IEEE Trans. PAS, Vol. 103, Aug. 1984, pp. 2337-2344.
- [58] Ramarao, K.A. and Muralikrishna, G., "*A new robust algorithm for estimating the state of a power system*", Electric machine and power systems, Vol. 16, 1989, pp. 431-439.
- [59] Horisberger, H.P., Richard, J.C. and Rossier, C., "*A fast decoupled static state estimator for electric power systems*", IEEE Trans. PAS, Vol. 95, Jan/Feb. 1976, pp. 208-215.
- [60] Garcia, A., Monticelli, A. and Abreu, P., "*Fast decoupled state estimation and bad data processing*", IEEE Trans. PAS, Vol. 98, Sept./Oct. 1979, pp. 1645-1652.
- [61] Allemong, L., Radu, L. and Sasson, A.M., "*A fast and reliable state estimation algorithm for AEP's new control center*", IEEE Trans. PAS, Vol. 101, April 1982, pp.933-944.
- [62] Sirisena, H.R. and Brown, E.P.M., "*Convergence analysis of weighted least square and fast decoupled weighted least square state estimation*", Electric power and energy systems, Vol. 6, 1984, pp. 74-78.
- [63] Jegatheesan, R. and Duraiswamy, K., "*AC multiterminal dc power system state estimation : A sequential approach*", Electric machine and power systems, Vol. 12, 1987, pp. 27-42.
- [64] Handschin, E., Schweppe, F.C., Kohlas, J. and Fletcher, A., "*Bad data analysis for power system state estimation*", IEEE Trans. PAS, Vol. 94, March/April 1975, pp. 329-337.
- [65] Lo, K.L., Ong, P.S., Mc coll, R.D., Moffat, A.M., and Sulley, J.L., "*Development of a static state estimator*", IEEE Trans. PAS, Vol. 102, Aug. 1983, pp. 2492-2500.

- [66] Nian-de, X., Shi-yang, W. and Er-king, Y., "*An application of estimation, identification approach of multiple bad data in power system state estimation*", IEEE Trans. PAS, Vol. 103, Feb. 1984, pp. 225-234.
- [67] Zhuang, F. and Balasubramaniam, R., "*Bad data suppression in power system state estimation with a variable quadratic constant criterion*", IEEE Trans. PAS, Vol. 104, April 1985, pp. 857-863.
- [68] Monticelli, A. and Garcia, A., "*Reliable bad data processing for real time state estimation*", IEEE Trans. PAS, Vol. 102, May 1983, pp. 1126-1139.
- [69] Masiello, R.D. and Schweppe, F.C., "*A tracking static state estimator*", IEEE Trans. PAS, Vol. 90, March/April 1971, pp.1025-1033.
- [70] Falcao, D.M., Cooke, P.A. and Brammeler, A., "*Power system tracking state estimator and bad data processing*", IEEE Trans. PAS, Vol. 101, Feb. 1982, pp. 325-333.
- [71] Rao, N.D., and Roy, L., "*Tracking state estimation in power system through SRLF with bad data analysis and data compression*", Proc. AMSE, International Conference in Modelling and Simulation, Dec. 1985, pp. 27-32.
- [72] Kotiuga, W.W, "*Development of a least absolute value power system tracking state estimation*", IEEE Trans. PAS, Vol. 104, May 1985, pp. 1160-1166.
- [73] Debs, A.S., and Larson, R.E., "*A dynamic estimator for tracking the state of a power system*", IEEE Trans. PAS, Vol. 89, Sept./Oct. 1970, pp. 1670-1678.
- [74] Leita da Silva, A.M., Docoutto Filho, M.B. and Cantera, J.M.C., "*An efficient dynamic state estimation algorithm including bad data*

processing", IEEE Trans, PAS, Vol. PWR-1, Nov. 1987, pp. 1050-1058.

- [75] Keyhani, A. and A. Abur, "*Comparative study of polar and Cartesian coordinate algorithm for power system state estimation problems*", Proc. IEE, Vol. 132, No. 3, pt. C, May 1985, pp. 132-138.
- [76] Holten, L., Gjelskid, A., Aam, S. and Wu, F. F., "*Comparison of different methods for state estimation*", IEEE Trans. PAS, Vol. PERS-3, Nov. 1988, pp. 1798- 1806.
- [77] Sirisena, H.R. and Brown, E.P.M., "*Inclusion of hvdc links in ac power system state estimation*", Proc. IEE, Vol. 128, pt. C, May 1981, pp. 147-154.
- [78] Glover, J.D. and Sheikoleslami, M., "*State estimation of interconnected hvdc/ac systems*", IEEE Trans. PAS, Vol. 102, June 1983, pp. 1805-1810.
- [79] Leita da Silva, A.M., Prada, R.B. and Falcao, D.M., "*State estimation for integrated multiterminal dc/ac systems*", IEEE Trans. PAS, Vol. 104, Sept. 1985, pp. 2349-2355.
- [80] Arafeh, S.A. and Chinzinger, R., "*Estimation algorithms for large scale power systems*", IEEE Trans. PAS, Vol. 98, Nov./Dec. 1979, pp. 1968-1977.
- [81] Rao, N.D. and Roy, L., "*A Cartesian coordinate algorithm for power system state estimation*", IEEE Trans. PAS, Vol. 102, May 1983, pp. 1070-1082.
- [82] Srinivasan, N., Rao, K.S.P. and Indulkar, C.S., "*Some new algorithms for state estimation in power system*", IEEE Trans. PAS, Vol. 103, May 1984, pp. 982-998.

- [83] Bijwe, P.R., "*Comparison of first order and second order state estimators*", Electric machine and power systems, Vol. 12, 1987, pp. 433-444.
- [84] Tripathy, S.C., Chauhan, D.S. and Durga Prasad, G., "*State estimation algorithm for illconditioned power systems by Newton's method*", Electric power and energy systems, Vol. 9, April 1987, pp. 113-116.
- [85] Abbasy, N.H. and Shahidehpour, S.M., "*Application of nonlinear programming in power system state estimation*", Electric Power System Research, 1987, pp. 41-50.
- [86] Hegi, M., Bahman, N., Stott, G. and Libb, G., "*Control of the Quebec New England multiterminal hvdc system*", CIGRE 1988, paper 14-04, pp. 35-41.
- [87] Stott, B., "*Load flow solution for ac and integrated ac-dc power system*", Ph.D. thesis, Victoria University of Manchester, 1971.
- [88] Rao, K.S.P., Roy, L. and Rao, N.D., "*A fast exact second order load flow method for larger power systems*", Proc. Large Engineering Systems, No.4, June 1982, pp. 35-41.
- [89] Cory, B.J., Ekwue, A.O. and Johnson, R.B.I., "*Comparative Analysis of the convergence characteristics of second order load flow methods*", International journal of Electric power and energy systems, Oct. 1990, pp. 251-256.
- [90] Ghonem, H., Arini, M. El. and Rumpel, D., "*On an exact decoupled load flow*", *ibid*, Vol. 13, No. 1, 1991, pp. 28-32.
- [91] De Silva, J.R. and Arnold, C.P., "*A simple improvement to sequential ac/dc power flow algorithms*", Int. J. of Electric power and energy systems, Vol. 12, 1990, pp. 219-221.

- [92] Monticelli, A. and Garcia, A., "*Fast decoupled state estimators*", IEEE Trans. PAS, Vol. 5, May 1990, pp. 556-564.
- [93] Do Coutto, M.B., Leite da Silva, A.M. and Falcao, D.M., "*Bibliography on power system state estimation (1968-1989)*", *ibid*, Vol. 5, No. 3, August 1990, pp. 950-961.
- [94] Laughton, M.A., "*A note on some questions in the load flow solution*", Proc. PSCC, London, 1963, paper 2.15, pp. 45-50.
- [95] Arrillaga, J., and Arnold, C.P., "*Computer Analysis of Power Systems*", John Wiley and Sons Ltd., England, 1990.
- [96] Haque, M.H., "*Novel decoupled load flow method*", Proc. IEE, Vol. 140, No. 3, pt. C, No. 3, May 1993, pp. 199-205.
- [97] Nanda, J., Bijwe, P.R., Henry, J. and Raju, V.B., "*General purpose fast decoupled power flow*", Proc. IEE, Vol. 139, pt. C, No.2, March 1992, pp. 87-92.
- [98] Habiballah, I.O. and Quintana, V.H., "*Exact decoupled rectangular coordinate state estimation with efficient data structure management*", IEEE Trans. PAS, Vol. 7, Feb. 1992, pp. 45-53.
- [99] Abou El-Ela, A.A., "*Fast and accurate technique for power system state estimation*", Proc. IEE, Vol. 139, pt. C, No.1, Jan. 1992, pp. 7-12.
- [100] Sachdev, M.S. and Medicherla, T.K.P., "*A second order load flow technique*", IEEE Trans. PAS, Vol. 96, Jan/Feb. 1975, pp. 189-197.
- [101] Monticelli, A., Garcia, A. and Saavedra, O.R., "*Fast decoupled load flow: hypothesis, derivations and testing*", IEEE Trans. PS, Vol. 5, 1990, pp. 1425-1431.

APPENDIX - A

PER UNIT SYSTEM

For all ac and interface dc system quantities a per unit (p.u.) system is used. This enables the use of comparable convergence tolerance for both ac and dc quantities as well as avoids the translation from p.u. to actual quantities and vice versa. Common power and voltage base quantities are used for both ac and dc quantities.

A.1 AC Per Unit System (base quantities)

$$(\text{VA base}) \text{ ac} = \text{MVA}_b = \text{MVA (3 phase power)}$$

$$(\text{V base}) \text{ ac} = V_b = \text{kV (line to line)}$$

$$(\text{I base}) \text{ ac} = I_b = (\text{MVA}_b / \sqrt{3} V_b) 10^3 = \text{A}$$

$$(\text{Z base}) \text{ ac} = Z_b = (V_b^2 (\text{kV}) / \text{MVA}_b) = \text{ohm}$$

A.2 DC Per Unit System (base quantities)

$$(\text{VA base}) \text{ dc} = \text{MVA}_b = \text{MVA}$$

$$(\text{V base}) \text{ dc} = V_b = \text{kV}$$

$$(\text{I base}) \text{ dc} = \sqrt{3} I_b = \text{A}$$

$$(\text{Z base}) \text{ dc} = Z_b = \text{ohm.}$$

APPENDIX - B

FIRST AND SECOND ORDER DERIVATIVES OF THE PERFORMANCE EQUATIONS

The elements of the Jacobian matrix (first order derivatives) and the second order derivatives for the ac network, interface and dc system equations are derived as shown below.

The ac, dc and interface system equations are recalled from Chapter 2 and 3 and are rewritten here for completeness and easy reference.

$$P_p = \sum_{q=1}^{Nac} \{e_p (e_q G_{pq} + f_q B_{pq}) + f_p (f_q G_{pq} - e_q B_{pq})\} + a_i S_i (e_p c_i - f_p d_i)$$

$$P_{ij} = e_i \{G_{ij} (e_j - e_i) + f_j B_{ij}\} + f_i \{G_{ij} (f_j - f_i) - e_j B_{ij}\} + (e_i^2 + f_i^2) G'_{ij}$$

$$Q_p = \sum_{q=1}^{Nac} \{f_p (e_q G_{pq} + f_q B_{pq}) - e_p (f_q G_{pq} - e_q B_{pq})\} + a_i t_i (e_p c_i + f_p d_i)$$

$$Q_{ij} = f_i \{G_{ij} e_j + B_{ij} (f_j - f_i)\} - e_i \{G_{ij} f_j - B_{ij} (e_j - e_i)\} + (e_i^2 + f_i^2) B'_{ij}$$

$$(V_p)^2 = e_p^2 + f_p^2$$

$$R_{1i} = (k_1 a_i \cos \alpha_i)^2 (e_p^2 + f_p^2) - (V d_i + S_i k_2 X c_i I d_i)^2$$

$$R_{2i} = V d_i I d_i - S_i a_i (e_p c_i - f_p d_i)$$

$$R_{3i} = Id_i - \sum_{j=1}^{Ndc} Gdc_{ij} Vd_j$$

$$R_{4i} = (k_1 Id_i)^2 - (c_i^2 + d_i^2)$$

$$R_{5i} = Pd_{ij}^m - Vd_i Gdc_{ij} (Vd_j - Vd_i)$$

$$R_{6i} = Id_{ij}^m - Gdc_{ij} (Vd_j - Vd_i)$$

$$R_{7i} = Pd_i^m - Vd_i Id_i$$

$$R_{8i} = Vd_i^m - Vd_i$$

$$R_{9i} = (k_1 Id^m)^2 - (c_i^2 + d_i^2)$$

$$R_{10i} = a_i^m - a_i$$

$$R_{11i} = \cos \alpha_i^m - \cos \alpha_i$$

The first order derivatives for the system performance equations presented above are derived in details as follows:

$$\frac{\partial P_P}{\partial e_P} = 2e_P G_{PP} + \sum_{\substack{q=1 \\ q \neq P}}^{Nac} (e_q G_{Pq} + f_q B_{Pq}) + S_i a_i c_i$$

$$\frac{\partial P_P}{\partial f_P} = 2f_P G_{PP} + \sum_{\substack{q=1 \\ q \neq P}}^{Nac} (f_q G_{Pq} - e_q B_{Pq}) - S_i a_i d_i$$

$$\frac{\partial P_P}{\partial e_q} = e_P G_{Pq} - f_P B_{Pq}$$

$$\frac{\partial P_P}{\partial f_q} = e_P B_{Pq} + f_P G_{Pq}$$

$$\frac{\partial P_{ij}}{\partial e_i} = G_{ij} (e_j - 2e_i) + B_{ij} f_j + 2e_i G'_{ij}$$

$$\frac{\partial P_{ij}}{\partial f_i} = G_{ij} (f_j - 2f_i) + B_{ij} e_j + 2f_i G'_{ij}$$

$$\frac{\partial P_{ij}}{\partial e_j} = e_i G_{ij} - f_j B_{ij}$$

$$\frac{\partial P_{ij}}{\partial f_j} = f_i G_{ij} + e_i B_{ij}$$

$$\frac{\partial Q_P}{\partial e_P} = 2e_P B_{PP} - \sum_{\substack{q=1 \\ q \neq P}}^{Nac} (f_q G_{Pq} - e_q B_{Pq}) + t_i a_i c_i$$

$$\frac{\partial Q_P}{\partial f_P} = 2f_P B_{PP} + \sum_{\substack{q=1 \\ q \neq P}}^{Nac} (e_q G_{Pq} + f_q B_{Pq}) + t_i a_i d_i$$

$$\frac{\partial Q_P}{\partial e_q} = e_P B_{Pq} + f_P G_{Pq}$$

$$\frac{\partial Q_P}{\partial f_q} = -e_P G_{Pq} + f_P B_{Pq}$$

$$\frac{\partial |V_P|^2}{\partial e_P} = 2e_P$$

$$\frac{\partial |V_P|^2}{\partial f_P} = 2f_P$$

$$\frac{\partial Q_{ij}}{\partial e_i} = B_{ij} (e_j - 2e_i) - G_{ij} f_j + 2e_i B'_{ij}$$

$$\frac{\partial Q_{ij}}{\partial f_i} = B_{ij} (f_j - 2f_i) + G_{ij} e_j + 2f_i B'_{ij}$$

$$\frac{\partial Q_{ij}}{\partial e_j} = f_i G_{ij} - e_i B_{ij}$$

$$\frac{\partial Q_{ij}}{\partial f_j} = -e_i G_{ij} + f_j B_{ij}$$

$$\frac{\partial P_P}{\partial a_i} = S_i (e_P c_i - f_P d_i)$$

$$\frac{\partial P_P}{\partial c_i} = S_i a_i e_P$$

$$\frac{\partial P_P}{\partial d_i} = -S_i a_i f_P$$

$$\frac{\partial Q_P}{\partial a_i} = t_i (f_P c_i + e_P d_i)$$

$$\frac{\partial Q_P}{\partial c_i} = t_i a_i e_P$$

$$\frac{\partial Q_P}{\partial d_i} = -a_i t_i f_P$$

$$\frac{\partial R_{1i}}{\partial e_P} = 2e_P (k_1 a_i \cos \alpha_i)^2$$

$$\frac{\partial R_{1i}}{\partial f_P} = 2f_P (k_1 a_i \cos \alpha_i)^2$$

$$\frac{\partial R_{1i}}{\partial Vd_i} = -2Vd_i - 2S_i k_2 Xc_i Id_i$$

$$\frac{\partial R_{1i}}{\partial Id_i} = -2Id_i (k_2 S_i Xc_i)^2 - 2S_i k_2 Xc_i Vd_i$$

$$\frac{\partial R_{1i}}{\partial a_i} = 2a_i (k_1 \cos \alpha_i)^2 (e_P^2 + f_P^2)$$

$$\frac{\partial R_{1i}}{\partial \cos \alpha_i} = 2 \cos \alpha_i (k_1 a_i)^2 (e_P^2 + f_P^2)$$

$$\frac{\partial R_{2i}}{\partial e_P} = -S_i a_i c_i$$

$$\frac{\partial R_{2i}}{\partial f_P} = S_i a_i d_i$$

$$\frac{\partial R_{2i}}{\partial Vd_i} = Id_i$$

$$\frac{\partial R_{2i}}{\partial Id_i} = Vd_i$$

$$\frac{\partial R_{2i}}{\partial a_i} = -S_i (e_P c_i - f_P d_i)$$

$$\frac{\partial R_{2i}}{\partial c_i} = -S_i a_i e_P$$

$$\frac{\partial R_{2i}}{\partial d_i} = S_i a_i f_P$$

$$\frac{\partial R_{3i}}{\partial Vd_i} = -Gdc_{ii}$$

$$\frac{\partial R_{3i}}{\partial Vd_j} = -Gdc_{ij}$$

$$\frac{\partial R_{3i}}{\partial Id_i} = 1$$

$$\frac{\partial R_{4i}}{\partial Id_i} = 2k_1^2 Id_i$$

$$\frac{\partial R_{4i}}{\partial c_i} = -2c_i$$

$$\frac{\partial R_{4i}}{\partial d_i} = -2d_i$$

$$\frac{\partial R_{5i}}{\partial Vd_i} = Gdc_{ij} (2Vd_i - Vd_j)$$

$$\frac{\partial R_{5i}}{\partial Vd_j} = -Gdc_{ij} Vd_i$$

$$\frac{\partial R_{6i}}{\partial Vd_i} = Gdc_{ij}$$

$$\frac{\partial R_{6i}}{\partial Vd_j} = -Gdc_{ij}$$

$$\frac{\partial R_{7i}}{\partial Vd_i} = -Id_i$$

$$\frac{\partial R_{7i}}{\partial Id_i} = -Vd_i$$

$$\frac{\partial R_{8i}}{\partial Vd_i} = -1$$

$$\frac{\partial R_{9i}}{\partial c_i} = -2c_i$$

$$\frac{\partial R_{9i}}{\partial d_i} = -2d_i$$

$$\frac{\partial R_{10i}}{\partial a_i} = -1$$

$$\frac{\partial R_{11i}}{\partial \cos \alpha_i} = -1$$

Rest of the terms are zero.

The second order derivatives of the performance equations are presented as:

$$\begin{aligned}
 \frac{\partial^2 P_P}{\partial e_p^2} &= 2G_{PP} = \frac{\partial^2 P_P}{\partial f_P^2} \\
 \frac{\partial^2 P_P}{\partial e_p \partial e_q} &= G_{Pq} = \frac{\partial^2 P_P}{\partial f_P \partial f_q} = \frac{\partial^2 Q_P}{\partial e_q \partial f_P} \\
 \frac{\partial^2 Q_P}{\partial e_p^2} &= \frac{\partial^2 Q_P}{\partial f_P^2} = 2B_{PP} \\
 \frac{\partial^2 P_P}{\partial e_p \partial f_q} &= \frac{\partial^2 Q_P}{\partial e_p \partial e_q} = \frac{\partial^2 Q_P}{\partial f_P \partial f_q} = B_{Pq} \\
 \frac{\partial^2 P_P}{\partial e_q \partial f_P} &= -B_{Pq} \\
 \frac{\partial^2 Q_P}{\partial e_p \partial f_q} &= -G_{Pq} \\
 \frac{\partial^2 P_P}{\partial e_p \partial f_P} &= \frac{\partial^2 P_P}{\partial e_q \partial f_q} = \frac{\partial^2 P_P}{\partial e_q \partial e_q} = \frac{\partial^2 P_P}{\partial f_q \partial f_q} = 0 \\
 \frac{\partial^2 Q_P}{\partial e_p \partial f_P} &= \frac{\partial^2 Q_P}{\partial e_q \partial f_q} = \frac{\partial^2 Q_P}{\partial e_q \partial e_q} = \frac{\partial^2 Q_P}{\partial f_q \partial f_q} = 0 \\
 \frac{\partial^2 P_{ij}}{\partial e_i^2} &= -2G_{ij} \\
 \frac{\partial^2 P_{ij}}{\partial e_i \partial e_j} &= G_{ij} = \frac{\partial^2 P_{ij}}{\partial f_i \partial f_j} \\
 \frac{\partial^2 P_{ij}}{\partial e_i \partial f_j} &= B_{ij} = -\frac{\partial^2 P_{ij}}{\partial f_i \partial e_j} \\
 \frac{\partial^2 P_P}{\partial e_p \partial c_i} &= S_i a_i \\
 \frac{\partial^2 P_P}{\partial e_p \partial a_i} &= S_i c_i \\
 \frac{\partial^2 P_P}{\partial f_P \partial d_i} &= -S_i a_i \\
 \frac{\partial^2 P_P}{\partial f_P \partial a_i} &= -S_i d_i \\
 \frac{\partial^2 P_P}{\partial a_i \partial c_i} &= S_i e_p
 \end{aligned}$$

$$\begin{aligned} \frac{\partial^2 P_p}{\partial a_i \partial d_i} &= -S_i f_p \\ \frac{\partial^2 Q_p}{\partial f_p \partial a_i} &= t_i c_i \\ \frac{\partial^2 Q_p}{\partial e_p \partial a_i} &= t_i d_i \\ \frac{\partial^2 Q_p}{\partial e_p \partial c_i} &= t_i a_i \\ \frac{\partial^2 Q_p}{\partial a_p \partial c_i} &= t_i e_p \\ \frac{\partial^2 Q_p}{\partial f_p \partial d_i} &= -t_i a_i \\ \frac{\partial^2 Q_p}{\partial a_p \partial d_i} &= -t_i f_p \\ \frac{\partial R_{1i}}{\partial e_p^2} &= 2(k_1 a_i \cos \alpha_i)^2 \\ \frac{\partial R_{1i}}{\partial f_p^2} &= 2(k_1 a_i \cos \alpha_i)^2 \\ \frac{\partial R_{1i}}{\partial e_p \partial a_i} &= 4a_i e_p (k_1 \cos \alpha_i)^2 \\ \frac{\partial^2 R_{1i}}{\partial f_p \partial a_i} &= 4a_i f_p (k_1 \cos \alpha_i)^2 \\ \frac{\partial^2 R_{1i}}{\partial Id_i^2} &= -2(k_2 S_i Xc_i)^2 \\ \frac{\partial^2 R_{1i}}{\partial Vd_i \partial Id_i} &= -2k_2 Xc_i S_i \\ \frac{\partial^2 R_{1i}}{\partial Vd_i^2} &= -2 \\ \frac{\partial^2 R_{1i}}{\partial a_i^2} &= 2k_1^2 (e_p^2 + f_p^2) \cos^2 \alpha_i \\ \frac{\partial^2 R_{1i}}{\partial a_i \partial \cos \alpha_i} &= 4a_i \cos \alpha_i \{k_1^2 (e_p^2 + f_p^2)\} \\ \frac{\partial^2 R_{1i}}{\partial \cos^2 \alpha_i} &= 2(k_1^2 a_i) (e_p^2 + f_p^2) \\ \frac{\partial^2 R_{1i}}{\partial e_p \partial \cos \alpha_i} &= 4(K_1 a_i)^2 (\cos \alpha_i) e_p \end{aligned}$$

$$\frac{\partial^2 R_{1i}}{\partial f_p \partial \cos \alpha_i} = 4(K_1 a_i)^2 (\cos \alpha_i) f_p$$

$$\frac{\partial^2 R_{2i}}{\partial V d_i \partial I d_i} = 1$$

$$\frac{\partial^2 R_{2i}}{\partial e_p \partial a_i} = -S_i c_i$$

$$\frac{\partial^2 R_{2i}}{\partial f_p \partial a_i} = S_i d_i$$

$$\frac{\partial^2 R_{2i}}{\partial e_p \partial c_i} = -S_i a_i$$

$$\frac{\partial^2 R_{2i}}{\partial a_i \partial c_i} = -S_i e_p$$

$$\frac{\partial^2 R_{2i}}{\partial f_p \partial d_i} = S_i a_i$$

$$\frac{\partial^2 R_{2i}}{\partial a_i \partial d_i} = S_i f_p$$

$$\frac{\partial^2 R_{4i}}{\partial I d_i^2} = 2k_1^2$$

$$\frac{\partial^2 R_{4i}}{\partial c_i^2} = -2$$

$$\frac{\partial^2 R_{4i}}{\partial d_i^2} = -2$$

$$\frac{\partial^2 R_{5i}}{\partial V d_i^2} = 2Gdc_{ij}$$

$$\frac{\partial^2 R_{5i}}{\partial V d_i \partial V d_j} = -Gdc_{ij}$$

$$\frac{\partial^2 R_{7i}}{\partial V d_i \partial I d_i} = -1$$

$$\frac{\partial^2 R_{9i}}{\partial c_i^2} = -2$$

$$\frac{\partial^2 R_{9i}}{\partial d_i^2} = -2.$$

Rest of all other terms are zero.

APPENDIX - C

BENEFITS OF RECTANGULAR CO-ORDINATES FORMULATION AND BASIC MATHEMATICAL MODEL FOR AC SYSTEM

PART - I : LOAD FLOW

C.1 FIRST ORDER MODEL

The nodal performance equations of the real and reactive powers in the polar co-ordinate form at busbars 'P' are

$$P_p = \sum_{q=1}^n V_p V_q \{G_{pq} \cos(\delta_p - \delta_q) + B_{pq} \sin(\delta_p - \delta_q)\} \quad (1)$$

$$Q_p = \sum_{q=1}^n V_p V_q \{G_{pq} \sin(\delta_p - \delta_q) - B_{pq} \cos(\delta_p - \delta_q)\} \quad (2)$$

Similarly the above equations in the rectangular co-ordinate form are

$$P_p = \sum_{q=1}^{Nac} \{e_p (e_q G_{pq} + f_q B_{pq}) + f_p (f_q G_{pq} - e_q B_{pq})\} \quad (3)$$

and

$$Q_p = \sum_{q=1}^{Nac} \{f_p (e_q G_{pq} + f_q B_{pq}) - e_p (f_q G_{pq} - e_q B_{pq})\} \quad (4)$$

The NR iterative mathematical model relating mismatch and error vector corresponding to equations (1) and (2) in concise form is

$$\begin{bmatrix} \Delta P \\ \Delta Q \end{bmatrix}^{(k)} = [J]^{(k)} \begin{bmatrix} \Delta \delta \\ \Delta V \end{bmatrix}^{(k+1)} \quad (5)$$

Similarly, the same model based on equations (3) and (4) is

$$\begin{bmatrix} \Delta P \\ \Delta Q \end{bmatrix}^{(k)} = [J]^{(k)} \begin{bmatrix} \Delta e \\ \Delta f \end{bmatrix}^{(k+1)} \quad (6)$$

The expressions of $[J]$ in equations (5) and (6) are not the same.

Equations (5) and (6) are based on the first order derivatives of P_p and Q_p in the Taylor series. The second and other higher order terms which are not zero are omitted.

C.1.1 Main Features of First Order Model

- ◆ The NR method characterised by the first order model both in the polar and rectangular forms is reliable, and yields accurate results on well-conditioned systems. However, the method is not fast due to repetitive calculations of Jacobian, especially on large size systems.
- ◆ The number of iterations for the convergence is more or less same in both the polar and rectangular versions.
- ◆ The rectangular coordinate formulation does not involve trigonometric function evaluation, and is thus faster than the polar version, However, this advantage is offset due to one more equation for each P-V busbar.

- ◆ Exploitation of the inherent loose coupling between P- δ and Q-V models in polar formulation leads to a very fast solution method known as fast decoupled load flow. However, the oscillating convergence is observed on the ill-conditioned and heavy loading condition networks. At times, it leads to erroneous solution as well.

C.2 SECOND ORDER MODEL

C.2.1 Second Order Model in Polar Form

In, 1977 Sachdev *et al.* [100] proposed a second order load flow algorithm in the polar form. In this formulation, the first and second order terms of the Taylor series were used and other higher order derivatives ignored although they were not zero. This second order model involves sine and cosine term like its first order counterpart. As, such, when compared with the NR and FD load flow methods it does not offer any advantage from the point of view of either memory or computing time.

C.2.2 Second Order Model in Rectangular Form

In 1978 Iwamoto *et al.* [12] and Roy [11] working concurrently and independently proposed the second order (SO) load flow method in rectangular co-ordinate form. The fact that the rectangular co-ordinate formulation of power equations are quadratic in e and f lead to an exact Taylor series of these equations. The third and other higher order derivatives are zero. The mathematical model is:

$$\begin{aligned}
 \begin{bmatrix} \Delta P_p \\ \Delta Q_p \end{bmatrix} &= \begin{bmatrix} J_1 & J_2 \\ J_3 & J_4 \end{bmatrix} \begin{bmatrix} \Delta e_q \\ \Delta f_q \end{bmatrix} + \begin{bmatrix} H_1 & H_2 \\ H_3 & H_4 \end{bmatrix} \begin{bmatrix} \Delta e_p & \Delta e_q \\ \Delta f_p & \Delta f_q \end{bmatrix} \\
 &+ \begin{bmatrix} H_5 & H_6 \\ H_7 & H_8 \end{bmatrix} \begin{bmatrix} \Delta e_p & \Delta e_q \\ \Delta f_p & \Delta f_q \end{bmatrix} \quad (7)
 \end{aligned}$$

Where the Jacobian matrix J is partitioned into four blocks and the second order derivatives H are partitioned into eight blocks. H can be explicitly expressed in terms of G and B .

$$H_1(i, j) = (G_{ij}; \quad j = 1, 2, \dots, n-1)$$

$$H_2(i, j) = (G_{ij}; \quad j = 1, 2, \dots, n-1)$$

$$H_3(i, j) = (B_{ij}; \quad j = 1, 2, \dots, n-1)$$

$$H_4(i, j) = (B_{ij}; \quad j = 1, 2, \dots, n-1)$$

$$H_5(i, j) = (-B_{ij}; \quad j = 1, 2, \dots, n-1, \quad j=i, \quad -B_{ii} = 0)$$

$$H_6(i, j) = (B_{ij}; \quad j = 1, 2, \dots, n-1, \quad j=i, \quad B_{ii} = 0)$$

$$H_7(i, j) = (G_{ij}; \quad j = 1, 2, \dots, n-1, \quad j=i, \quad G_{ii} = 0)$$

$$H_8(i, j) = (G_{ij}; \quad j = 1, 2, \dots, n-1, \quad j=i, \quad -G_{ii} = 0)$$

In all the above cases $i = 1, 2, \dots, n-1$.

Equation (7) in an iterative scheme is

$$\begin{bmatrix} \Delta P'_p \\ \Delta Q'_p \end{bmatrix}^{(k)} = \begin{bmatrix} J_1 & J_2 \\ J_3 & J_4 \end{bmatrix}^{(0)} \begin{bmatrix} \Delta e_q \\ \Delta f_q \end{bmatrix}^{(k+1)} \quad (8)$$

where

$$\Delta P'_p = \Delta P_p - S_p \quad (9)$$

$$\Delta Q'_p = \Delta P_q - S_q \quad (10)$$

and

$$S_p = (\Delta e_p H_1 + \Delta f_p H_5) \Delta e_q + (\Delta f_p H_2 + \Delta e_p H_6) \Delta f_q \quad (11)$$

$$S_q = (\Delta e_p H_3 + \Delta f_p H_7) \Delta e_q + (\Delta f_p H_4 + \Delta e_p H_8) \Delta f_q \quad (12)$$

It may be noted that the second order derivatives given by matrix H involve elements of the nodal admittance matrix and hence are constant. Also, the model is exact.

C.2.3 Main Features of Second Order Model

- ◆ The mathematical model represented by equation (7) is based on the exact Taylor series expansion. Also the initial estimate e^0, f^0 remain constant in the iterative scheme based on equation (7). Consequently the Jacobian matrix J and residuals ΔP and ΔQ which are functions of e^0, f^0 also remain constant in the iterative scheme. Only $\Delta P', \Delta Q'$ change in the iterative scheme because, they are the function of Δe and Δf . It is interesting to note that in this model the Jacobian matrix becomes constant in the iterative scheme without incorporating any assumptions. Also, only the error vector Δe and Δf is updated and not the state vector e and f .
- ◆ As the second order derivatives are constant and functions of admittance matrix, no additional memory is required to

store them. The size and structure of the Jacobian matrix is similar to the jacobian matrix in the NR method.

- ◆ The Jacobian matrix remains constant in the iterative solution. It is calculated once only using the initial estimate value.
- ◆ ΔP and ΔQ are also calculated once only using the initial estimate state, and remains constant in the iterative solution.
- ◆ The second order method is found to be faster than the conventional NR methods, and requires comparable computer memory.
- ◆ The method is more reliable and provides solution for a number of heavy loading and ill-conditioned systems for which the FD load flow method fails. The second order load flow offers the opportunity to perform very fast multiple case solutions as the Jacobian is only triangularised once during a solution process.
- ◆ The limitation of the second order method is that the convergence is considerably slower than the quadratic convergence of the NR approach. Further, the second order method inspite of being exact and faster than the NR method, does not perform well against the most popular FD method in terms of computational efficiency.

C.2.4 Decoupled Second Order Load Flow Model

The second order load flow model is given by equation (8). A reorganisation of this equation provides two sets of exact matrix equations (without introducing any approximation):

$$\Delta P_p^* = J_2 \Delta f_q \quad (13)$$

$$\Delta Q_p^* = J_3 \Delta e_q \quad (14)$$

where

$$\Delta P_p^* = \Delta P_p' - J_1 \Delta e_q$$

$$\Delta Q_p^* = \Delta Q_p' - J_4 \Delta f_q$$

In an iterative scheme it is

$$J_2 \Delta f_q^{(k+1)} = \Delta P_p^{*(k)} \quad (15)$$

$$J_3 \Delta e_q^{(k+1)} = \Delta Q_p^{*(k)} \quad (16)$$

Equations (15) and (16) characterise the decoupled second order (DSO) model. They are solved sequentially and iteratively until changes in Δe_p and Δf_q or ΔP_p^* and ΔQ_p^* are less than the specified tolerances.

C.2.5 Main Features of Decoupled Second Order Load Flow Model

The following outstanding features characterising the decoupled second order load flow method have been identified in comparison with the performance of the NR, SO and FD methods.

- ◆ Under normal operating conditions, with no system over loading and ill-conditioning, the performance of the DSO and FD methods are comparable in all respects, viz., accuracy, computational time, memory and convergence rate. The saving in solution time by the decoupled second order method is far better than SO method making the method more faster.

- ◆ On well behaved systems, under abnormal operating conditions which could conceivably occur due to loss of large generating units or heavily loaded lines, the decoupled second order model still retains its nearly linear convergence behaviour and provides a reliable and accurate solution, where as FD method not only suffers a significant deterioration in convergence rate but also gives an erroneous solution.
- ◆ For all ill-conditioned and heavily loaded networks the fast second order method performs as efficiently and reliable as it does for well behaved power systems, unlike the FD method which generally diverges. In addition, its computational requirements are significantly less due to better convergence characteristics which could be attributed to the exact formulation of the model.

Because of its ability to perform accurately, efficiently and reliable on well behaved, as well as, ill-conditioned and heavily loaded power systems, the fast second order method is seen to be practically viable and preferred alternative analytical tool for the load flow solution of power systems.

PART - II : STATE ESTIMATION

C.3. FIRST ORDER MODEL

C.3.1 Weighted Least Square State Estimator

Several methods of static state estimation in power systems are available in the literature. Of them weighted least square (WLS) approach has gained wide spread application. In the WLS approach the state of a power system is estimated using the following mathematical model in an iterative scheme [51]:

$$\Delta X^{(k+1)} = [H^T (X)^k W H (X)^k]^{-1} [H^T (X)^k W] [Z - h(X)^k] \quad (17)$$

where

- Z = (m x 1) vector of measurements
- $h(X)$ = non-linear function of state vector (X)
- X = (n x 1) vector of system variables
- H = Jacobian matrix
- $H^T W H$ = Information matrix
- W = Weighting inverse matrix
- m = Number of measurements
- n = Number of state variables
- K = Iteration count
- $\Delta X^{(k+1)}$ = $X^{(k+1)} - X^{(k)}$

Equation (17) is solved iteratively until ΔX is less than a pre-specified tolerance. Though the method is reliable, but the computer memory and

time requirements are relatively large. In order to reduce the computation time and memory requirements, the $P-\delta$ and $Q-V$ decoupling is used in the FD load flow and applied to the WLS power system state estimation problem.

C.3.2. Fast Decoupled State Estimator

Applying active-reactive decoupling and other simplifying assumptions of the FD load flow, the recursive relationship of equation (17) is modified to two sets of decoupled equations

$$I_{P\delta} \Delta \delta^{(k+1)} = [H_1^T H_3^T W] \Delta Z \quad (18)$$

$$I_{QV} \Delta V^{(k+1)} = [H_2^T H_4^T W] \Delta Z \quad (19)$$

where

δ, V = nodal voltage angles and modulus respectively.

$$H(X) = H(V, \delta) = \begin{bmatrix} H_1 & H_2 \\ H_3 & H_4 \end{bmatrix}$$

$$I_{P\delta} = H_1^T W_1 H_1$$

$$I_{QV} = H_4^T W_2 H_4$$

$$\Delta Z = Z - h(\delta, V)$$

$$\Delta \delta^{(k+1)} = \delta^{(k+1)} - \delta^k$$

$$\Delta V^{(k+1)} = V^{(k+1)} - V^k$$

$$W = [W_1^T : W_2^T]^T$$

In equations (18) and (19) $I_{P\delta}$ and I_{QV} are calculated at $V = 1$ pu and $\delta = 0$ (flat voltage) and contain elements of the network nodal admittance matrix,

and hence remain constant in the iterative scheme. The fast decoupled state estimator is thus computationally very efficient and seems to enjoy wide acceptance as a result. However, based on the underlying simplifying assumptions contained in the fast decoupled load flow, a number of limitations of the latter has cropped up in the former. The simplifying assumptions, including the approximations that $V = 1$ and $\delta = 0$ are justified during normal operating conditions when the metered reference voltage is near nominal. However, during the restoration period following an emergency, or in circumstances of unusual plant outages, the system voltage may not be near nominal, and then the above assumptions may lead to erroneous results. Also, during heavy loading conditions, the angle difference between the adjacent nodes may not be small, and this would introduce additional errors in the results.

C.4 SECOND ORDER MODEL

In rectangular co-ordinate version the nodal and line flow equations are completely expressible in the Taylor series. The series contains terms upto the second order derivatives only, results in an estimator, named here as second order state estimator (SOSE).

C.4.1 Second Order State Estimator

The non-linear equation relating the measurement and the state vector is

$$Z = h(X) + v \quad (20)$$

The measurement vector Z consists of node injections and line flows. The equations in the rectangular co-ordinates for the real and reactive powers at

the bus 'p' are given by equations (3) and (4). The line flow equations for the real and reactive powers in a line i-j are

$$P_{ij} = e_i \{G_{ij}(e_j - e_i) + f_i B_{ij}\} + f_i \{G_{ij}(f_j - f_i) - e_j B_{ij}\} + (e_i^2 + f_i^2) G'_{ij} \quad (21)$$

$$P_{ij} = f_i \{G_{ij} e_j + B_{ij}(f_j - f_i)\} - e_i \{G_{ij} f_j - B_{ij}(e_j - e_i)\} + (e_i^2 + f_i^2) B'_{ij} \quad (22)$$

where

$$Y'_{ij} = G'_{ij} + j B'_{ij} = \frac{1}{2} X \quad (\text{line charging admittance for line i-j})$$

The node injections and line flow equations correspond to $h(X)$ in equation (20). From the Taylor series expansion of $h(X)$ around a nominal point X^0 , one can write:

$$h(X) = h(X^0) + H(X^0) \Delta X + \frac{1}{2} L(G, B) \Delta X^2 \quad (23)$$

where $H(X^0)$ is the Jacobian matrix whose elements are evaluated at (X^0) . $L(G, B)$ is the second order derivative and involves only the elements of the nodal admittance matrix G and B . It is noteworthy that in equation (23) no terms beyond the second order derivatives exist because $h(X)$ is quadratic in e and f .

To minimise the performance index $J(X) = [Z - h(X)]^T W [Z - h(X)]$, the state vector X must satisfy the non-linear equation

$$\frac{\partial J}{\partial X} \Big|_{x=\bar{x}} = -2 H(X)^T W [Z - h(X)] = 0 \quad (24)$$

Substituting equation (23) in equation (24) one can write

$$[H(X^0)^T W H(X^0)] \Delta X = [H(X^0)^T W] [Z - h(X^0) - \frac{1}{2} L(G, B) \Delta X^2] \quad (25)$$

And in concise form it is

$$G \Delta X = K \left[\Delta Z - \frac{1}{2} L \Delta X^2 \right] = K \Delta Z' \quad (26)$$

where

$$G = H(X^0)^T W H(X^0)$$

$$K = H(X^0)^T W$$

$$\Delta Z = Z - h(X^0)$$

$$\Delta Z' = \Delta Z - \frac{1}{2} L \Delta X^2$$

Although equation (23) is exact, ΔX obtained from equation (25) does not provide a solution in one iteration because $h(X)$ is non-linear. ΔX is updated in an iterative cycle using the iterative model; i.e.

$$\Delta X^{(k+1)} = [G^{-1} K]^0 \left[\Delta Z - \frac{1}{2} S(\Delta X^k)^2 \right] \quad (27)$$

until

$$|\Delta X^{k+1} - \Delta X^k| \leq \varepsilon ; \varepsilon \text{ is a prespecified tolerance.}$$

C.4.2 Main Features of Second Order State Estimator

Since equations (23) and (26) are based on a complete Taylor series with no approximation or truncation, the initial estimate $X^0(e^0, f^0)$ and consequently $H(X^0)$ and ΔZ which are functions of e^0, f^0 remain constant in the iterative model. As a result, matrices G and K remains constant and are evaluated only once at the beginning of the iterative cycle. Only $\Delta Z'$ and ΔX changes during iterative process. That is, the measurement error vector $[\Delta Z - \frac{1}{2} L(\Delta X^k)^2]$ which is updated in each iteration, the state vector $[e, f]$ remains constant at initial estimate value

$[e^0, f^0]$ during the iterative process. The desirable feature of second order model is that it is exact, and uses constant Jacobian and information matrices, making the method several time faster than the basic WLS estimator, while keeping the memory requirement comparable.

The second order state estimator, inspite of being exact and faster than the basic WLS estimator, does not stack up well against the most popular FD state estimator in terms of computational efficiency. Consequently, a faster version of the exact second order state estimator known as decoupled second order (DSO) state estimator has been developed.

C.4.3 Decoupled Second Order State Estimator

Let

Z_a = Set of active line power flow and injection measurements.

Z_r = Set of reactive power flow injection and voltage magnitude measurements.

Accordingly, the change in the state and measurement vectors can be expressed as

$$\Delta X = \begin{bmatrix} \Delta X_a \\ \Delta X_r \end{bmatrix} = \begin{bmatrix} \Delta e \\ \Delta f \end{bmatrix} \quad (28)$$

$$\Delta X = \begin{bmatrix} \Delta Z_a \\ \Delta Z_r \end{bmatrix} = \begin{bmatrix} \Delta P \\ \Delta Q \end{bmatrix} \quad (29)$$

With the above definition, equation (26) can be written in the partitioned form, which is as follow:

$$\begin{bmatrix} G_1 & G_2 \\ G_3 & G_4 \end{bmatrix} \begin{bmatrix} \Delta X_a \\ \Delta X_r \end{bmatrix} = \begin{bmatrix} K_1 & K_2 \\ K_3 & K_4 \end{bmatrix} \left\{ \begin{bmatrix} \Delta Z_a \\ \Delta Z_r \end{bmatrix} - \begin{bmatrix} L_1 & L_2 \\ L_3 & L_4 \end{bmatrix} \begin{bmatrix} \Delta X_a^2 \\ \Delta X_r^2 \end{bmatrix} \right\} \quad (30)$$

where G, K and L are partitioned into four blocks. Again equation (30) can be written in the partitioned form

$$G_1 \Delta X_a^{(k+1)} = [K_1 \ K_2] \begin{bmatrix} \Delta Z'_a \\ \Delta Z'_r \end{bmatrix} - G_2 \Delta X_r^{(k)} \quad (31)$$

$$G_4 \Delta X_r^{(k+1)} = [K_3 \ K_4] \begin{bmatrix} \Delta Z'_a \\ \Delta Z'_r \end{bmatrix} - G_3 \Delta X_a^{(k)} \quad (32)$$

where

$$\Delta Z'_a = \Delta Z_a - L_1 (\Delta X_a^k)^2 - L_2 (\Delta X_r^k)^2$$

$$\Delta Z'_r = \Delta Z_r - L_3 (\Delta X_a^k)^2 - L_4 (\Delta X_r^k)^2$$

k = iteration count.

Equations (31) and (32) are solved iteratively sequentially until convergence with the specified accuracy is achieved.

C. 4. 4 Main Features of DSO State Estimator

The set of equations given by (31) and (32) constitute the decoupled second order state estimator. As the solution algorithm has been developed from the exact second order state estimator model without involving any major approximation, the version is also an exact model. Consequently, the

matrices G_1 and G_2 are constant. They are computed using the initial estimated nodal voltages and factorised only once.

It may be recalled that the FD state estimator consists of two coefficient matrices I_{ps} and I_{qv} ; each equal in size to one fourth of the full information matrix H^TWH . Similarly, each of G_1 and G_4 is also equal to one fourth of H^TWH in size. Further, K_1 and H_1 are equal in size. However, K_1 is calculated once only and remain constant in the iterative scheme. In contrast to the FD state estimator, H_1 is computed in each iteration, otherwise the accuracy of the solution is degraded as the objective function is then not actually minimised. G_2 and G_3 in the DSO estimator involve elements of the nodal admittance matrix, known as X^0 (initial state) and weighting matrix W . As these matrices are available in the computer core, G_2 and G_3 are computed in each iteration and not stored explicitly in the matrix form. This avoids the need for extra computer storage but increases the computational time. This additional time is offset by the time needed to compute H_1 in the FD approach. L_i ($i=1,2,\dots,n$) involve elements of the nodal admittance matrix, and hence are constant and do not require additional storage. Also, ΔZ_a and ΔZ_r are constant as they are computed at the initial estimated state. On the other hand, ΔZ in the FD state estimator is computed in each iteration. Thus, the mathematical operations required to compute $\Delta Z'$ in the DSO estimator and ΔZ in the FD state estimator are comparable.

From the above comparative estimates, it is evident that the memory and unit time requirements of the DSO state estimator and FD state estimator are of the same order. Besides, the DSO state estimator while retaining the

theoretical merit of involving no approximation makes it either comparable or decidedly superior to the FD state estimator depending upon the operating modes and network characteristics in terms of the presence of an ill-conditioning.

APPENDIX - D

SYSTEM DATA

D.1 SYSTEM DATA FOR 14 BUS SYSTEM

Number of lines = 20

Number of transformers = 3

Number of shunt capacitor = 1

Table D.1.1 : Bus Data

Bus No.	Generation		Load		P-V bus
	P(pu)	Q(pu)	P(pu)	Q(pu)	V(pu)
1	0.00000	0.00000	0.00000	0.00000	1.06000
2	0.40000	0.42400	0.21700	0.12700	1.04500
3	0.00000	0.23400	0.94200	0.19000	1.01000
4	0.00000	0.00000	0.47800	0.03900	
5	0.00000	0.00000	0.07600	0.01600	
6	0.00000	0.12200	0.11200	0.07500	1.07000
7	0.00000	0.00000	0.00000	0.00000	
8	0.00000	0.17400	0.00000	0.00000	1.09000
9	0.00000	0.00000	0.29500	0.16600	
10	0.00000	0.00000	0.09200	0.05800	
11	0.00000	0.00000	0.03500	0.01800	
12	0.00000	0.00000	0.06100	0.01600	
13	0.00000	0.00000	0.13500	0.05800	
14	0.00000	0.00000	0.14900	0.05000	

Table D.1.2 : Line Data

Sl No	From bus	To bus	R	X	Y'/2
			(pu)	(pu)	(pu)
1	1	2	0.01938	0.05917	0.02640
2	1	5	0.05403	0.22304	0.02460
3	2	3	0.04699	0.19797	0.02190
4	2	4	0.05811	0.17632	0.01870
5	2	5	0.05695	0.17388	0.01700
6	3	4	0.06701	0.17103	0.01730
7	4	5	0.01335	0.04211	0.00640
8	4	7	0.00000	0.20912	0.00000
9	4	9	0.00000	0.55618	0.00000
10	5	6	0.00000	0.25202	0.00000
11	6	11	0.09498	0.19890	0.00000
12	6	12	0.12291	0.25581	0.00000
13	6	13	0.06615	0.13027	0.00000
14	7	8	0.00000	0.17615	0.00000
15	7	9	0.00000	0.11001	0.00000
16	9	10	0.03181	0.08450	0.00000
17	9	14	0.12711	0.27038	0.00000
18	10	11	0.08205	0.19207	0.00000
19	12	13	0.22092	0.19988	0.00000
20	13	14	0.17093	0.34802	0.00000

Table D.1.3 : Transformer Data

Trans. No.	Between buses		Tap position
1	4	7	0.97800
2	4	9	0.96900
3	5	6	0.93200

Table D.1.4 : Shunt Capacitor Data

Sl. No	Bus No.	Susceptance (pu)
1	9	0.19000

Table D.1.5 : DC Link System

Number of dc buses = 2

Number of dc line = 1

Table D.1.5.1 : Bus Data

dc bus No.	ac bus No.	Si	Vd	Id	Pd	atap	alpha	Xc
1	5	1	-	-	0.61700	-	12.500	0.1
2	4	-1	1.27950	-	-	-	22.600	.04

Table D.1.5.2 : Line Data

Sl No	Between buses		Rdc (pu)
1	1	2	0.01370

Table D.1.6 : DC Mesh System

Number of dc buses = 3

Number of dc lines = 3

Table D.1.6.1 : Bus Data

dc bus No.	ac bus No.	Si	Vd	Id	Pd	atap	alpha	Xc
1	5	1	-	-	.61700	-	12.5000	0.1
2	2	1	-	.76670	-	-	10.550	.07
3	4	-1	1.2795	-	-	-	22.600	.04

Table D.1.6.2 : Line Data

Sl No	Between buses		Rdc (pu)
1	1	2	0.01370
2	1	3	0.01400
3	2	3	0.01400

Table D.1.7 : DC Mesh-Link System

Number of dc buses = 5

Number of dc lines = 4

Table D.1.7.1 : Bus Data

dc bus No.	ac bus No.	Si	Vd	Id	Pd	atap	alpha	Xc
1	5	1	-	-	.61700	-	12.500	0.1
2	2	1	-	.76670	-	-	10.550	.07
3	4	-1	1.27950	-	-	-	22.600	.04
4	9	1	-	-	.32620	-	10.000	0.1
5	10	-1	-	-.27200	-	-	20.000	.07

Table D.1.7.2 : Line Data

Sl No	Between buses		Rdc (pu)
1	1	2	0.01370
2	1	3	0.01400
3	2	3	0.01400
4	4	5	0.03181

D.2 SYSTEM DATA FOR 30 BUS SYSTEM

Number of lines = 41

Number of transformers = 4

Number of shunt capacitors = 2

Table D.2.1 : Bus Data

Bus No.	Generation		Load		P-V bus
	P(pu)	Q(pu)	P(pu)	Q(pu)	V(pu)
1	0.00000	0.00000	0.00000	0.000000	1.05000
2	0.57560	0.02470	0.21700	0.12700	1.03380
3	0.00000	0.00000	0.02400	0.01200	
4	0.00000	0.00000	0.07600	0.01600	
5	0.24560	0.22570	0.94200	0.19000	1.00580
6	0.00000	0.00000	0.00000	0.00000	
7	0.00000	0.00000	0.22800	0.10900	
8	0.35000	0.34840	0.30000	0.30000	1.02300
9	0.00000	0.00000	0.00000	0.00000	
10	0.00000	0.00000	0.05800	0.02000	
11	0.17930	0.30780	0.00000	0.00000	1.09130
12	0.00000	0.00000	0.11200	0.07500	
13	0.16910	0.37830	0.00000	0.00000	1.08880
14	0.00000	0.00000	0.06200	0.01600	
15	0.00000	0.00000	0.08200	0.02500	
16	0.00000	0.00000	0.03500	0.01800	

17	0.00000	0.00000	0.09000	0.05800
18	0.00000	0.00000	0.03200	0.00900
19	0.00000	0.00000	0.09500	0.03400
20	0.00000	0.00000	0.02200	0.00700
21	0.00000	0.00000	0.17500	0.11200
22	0.00000	0.00000	0.00000	0.00000
23	0.00000	0.00000	0.03200	0.01600
24	0.00000	0.00000	0.08700	0.06700
25	0.00000	0.00000	0.00000	0.00000
26	0.00000	0.00000	0.03500	0.02300
27	0.00000	0.00000	0.00000	0.00000
28	0.00000	0.00000	0.00000	0.00000
29	0.00000	0.00000	0.02400	0.00900
30	0.00000	0.00000	0.10600	0.01900

Table D.2.2 : Line Data

Sl No	From bus	To bus	R (pu)	X (pu)	Y'/2 (pu)
1	1	2	0.01920	0.05750	0.02640
2	1	3	0.04520	0.18520	0.02040
3	2	4	0.05700	0.17370	0.01840
4	3	4	0.01420	0.03790	0.00420
5	2	5	0.04720	0.19830	0.02090
6	2	6	0.05810	0.17630	0.01870

7	4	6	0.01190	0.04140	0.00450
8	7	7	0.04600	0.11600	0.01020
9	6	7	0.02670	0.08200	0.00850
10	6	8	0.01200	0.04200	0.00450
11	6	9	0.00000	0.20800	0.00000
12	6	10	0.00000	0.55600	0.00000
13	9	11	0.00000	0.20800	0.00000
14	9	10	0.00000	0.11000	0.00000
15	4	12	0.00000	0.25600	0.00000
16	12	13	0.00000	0.14000	0.00000
17	12	14	0.12310	0.25590	0.00000
18	12	15	0.06620	0.13040	0.00000
19	12	16	0.09450	0.19870	0.00000
20	14	15	0.22100	0.19970	0.00000
21	16	17	0.08240	0.19320	0.00000
22	15	18	0.10700	0.21850	0.00000
23	18	19	0.06390	0.12920	0.00000
24	19	20	0.03400	0.06800	0.00000
25	10	20	0.09360	0.20900	0.00000
26	10	17	0.03240	0.08450	0.00000
27	10	21	0.03480	0.07490	0.00000
28	10	22	0.07270	0.14990	0.00000
29	21	22	0.01160	0.02360	0.00000
30	15	23	0.10000	0.20200	0.00000

31	22	24	0.11500	0.17900	0.00000
32	23	24	0.13200	0.2700	0.00000
33	24	25	0.18850	0.32920	0.00000
34	25	26	0.25440	0.38000	0.00000
35	25	27	0.10930	0.20870	0.00000
36	27	28	0.00000	0.39600	0.00000
37	27	29	0.21980	0.42530	0.00000
38	27	30	0.32020	0.60270	0.00000
39	29	30	0.23990	0.45330	0.00000
40	8	28	0.06360	0.20000	0.02140
41	6	28	0.01690	0.05990	0.00650

Table D.2.3 : Transformer Data

Trans. No.	Between buses	Tap position
1	6 9	1.01550
2	6 10	0.96290
3	4 12	1.01290
4	28 27	0.95810

Table D.2.4 : Shunt Capacitor Data

Sl. No	Bus No.	Susceptance (pu)
1	10	0.19000
2	24	0.04000

Table D.2.5 : DC link System

Number of dc buses = 2

Number of dc line = 1

Table D.2.5.1 : Bus Data

dc bus No.	ac bus No.	Si	Vd	Id	Pd	atap	alpha	Xc
1	2	1	-	-	0.58220	-	8.5000	0.1
1	5	-1	1.2795	-	-	-	20.0000	0.07

Table D.2.5.2 : Line Data

Sl No	Between buses	Rdc (pu)
1	1 2	0.04720

Table D.2.6 : DC Mesh System

Number of dc buses = 3

Number of dc lines = 3

Table D.2.6.1 : Bus Data

dc bus No.	ac bus No.	Si	Vd	Id	Pd	atap	alpha	Xc
1	2	1	-	-	0.58220	-	8.50	0.1
2	5	-1	1.2795	-	-	-	20.00	.07
3	7	1	-	-	0.13000	-	12.50	.07

Table D.2.6.2 : Line Data

Sl No	Between buses		Rdc (pu)
1	1	2	0.04720
2	1	3	0.06620
3	2	3	0.04600

Table D.2.7 : DC Mesh-Link System

Number of dc buses = 5

Number of dc lines = 4

Table D.2.7.1 : Bus Data

dc bus No.	ac bus No.	Si	Vd	Id	Pd	atap	alpha	Xc
1	2	1	-	-	0.58220	-	8.50	0.1
2	5	-1	1.27950	-	-	-	20.00	.07
3	7	1	-	0.10086	-	-	12.50	.07
4	15	1	-	-	0.05660	-	10.00	0.1
5	18	-1	-	-0.0470	-	-	22.00	.07

Table D.2.7.2 : Line Data

Sl No	Between buses		Rdc (pu)
1	1	2	0.04720
2	1	3	0.06620
3	2	3	0.04600
4	4	5	0.10700

D.3 SYSTEM DATA FOR 57 BUS SYSTEM

Number of lines = 80

Number of transformers = 17

Number of shunt capacitors = 3

Table D.3.1 : Bus Data

Bus No.	Generation		Load		P-V bus
	P(pu)	Q(pu)	P(pu)	Q(pu)	V(pu)
1	0.00000	0.00000	0.00000	0.00000	1.04000
2	0.00000	-.00800	0.03000	0.88000	1.01000
3	0.40000	-.01000	0.00000	0.00000	
5	0.00000	0.00000	0.13000	0.04000	
6	0.00000	0.00800	0.75000	0.02000	0.98000
7	0.00000	0.00000	0.00000	0.00000	
8	4.50000	0.62100	1.50000	0.22000	1.00500
9	0.00000	0.02200	1.21000	0.26000	0.98000
10	0.00000	0.00000	0.05000	0.02000	
11	0.00000	0.00000	0.00000	0.00000	
12	3.10000	1.28500	3.77000	0.24000	1.01500
13	0.00000	0.00000	0.18000	0.02300	
14	0.00000	0.00000	0.10500	0.05300	
15	0.00000	0.00000	0.22000	0.05000	
16	0.00000	0.00000	0.43000	0.03000	
17	0.00000	0.00000	0.42000	0.08000	
18	0.00000	0.00000	0.27200	0.09800	

19	0.00000	0.00000	0.03300	0.00600
20	0.00000	0.00000	0.02300	0.01000
21	0.00000	0.00000	0.00000	0.00000
22	0.00000	0.00000	0.00000	0.00000
23	0.00000	0.00000	0.06300	0.02100
24	0.00000	0.00000	0.00000	0.00000
25	0.00000	0.00000	0.06300	0.03200
26	0.00000	0.00000	0.00000	0.00000
27	0.00000	0.00000	0.09300	0.00500
28	0.00000	0.00000	0.04600	0.02300
29	0.00000	0.00000	0.17000	0.02600
30	0.00000	0.00000	0.03600	0.01800
31	0.00000	0.00000	0.05800	0.02900
32	0.00000	0.00000	0.01600	0.00800
33	0.00000	0.00000	0.03800	0.01900
34	0.00000	0.00000	0.00000	0.00000
35	0.00000	0.00000	0.06000	0.03000
36	0.00000	0.00000	0.00000	0.00000
37	0.00000	0.00000	0.00000	0.00000
38	0.00000	0.00000	0.14000	0.07000
39	0.00000	0.00000	0.00000	0.00000
40	0.00000	0.00000	0.00000	0.00000
41	0.00000	0.00000	0.06300	0.03000
42	0.00000	0.00000	0.07100	0.04000

43	0.00000	0.00000	0.02000	0.01000
44	0.00000	0.00000	0.12000	0.01800
45	0.00000	0.00000	0.00000	0.00000
46	0.00000	0.00000	0.00000	0.00000
47	0.00000	0.00000	0.29700	0.11600
48	0.00000	0.00000	0.00000	0.00000
49	0.00000	0.00000	0.18000	0.08500
50	0.00000	0.00000	0.21000	0.10500
51	0.00000	0.00000	0.18000	0.05300
52	0.00000	0.00000	0.04900	0.02200
53	0.00000	0.00000	0.20000	0.10000
54	0.00000	0.00000	0.04100	0.01400
55	0.00000	0.00000	0.06800	0.03400
56	0.00000	0.00000	0.07600	0.02200
57	0.00000	0.00000	0.06700	0.02000

Table D.3.2 : Line Data

Sl No	From bus	To bus	R	X	Y'/2
			(pu)	(pu)	(pu)
1	1	2	0.00830	0.02800	0.06450
2	2	3	0.02980	0.08500	0.04090
3	3	4	0.01120	0.03660	0.01900
4	4	5	0.06250	0.13200	0.01290
5	4	6	0.04300	0.14800	0.01740
6	6	7	0.02000	0.10200	0.01380
7	6	8	0.03390	0.17300	0.02350
8	8	9	0.00990	0.05050	0.02740
9	9	10	0.03690	0.16790	0.02200
10	9	11	0.02580	0.08480	0.01090
11	9	12	0.06480	0.29500	0.03860
12	9	13	0.04810	0.15800	0.02030
13	13	14	0.01320	0.04340	0.00550
14	23	15	0.02690	0.08690	0.01150
15	1	15	0.01780	0.09100	0.04940
16	1	16	0.04540	0.20600	0.02730
17	1	17	0.02380	0.10800	0.01430
18	3	15	0.01620	0.05300	0.02720
19	4	18	0.00000	0.55500	0.00000
20	4	18	0.00000	0.43000	0.00000
21	5	6	0.03020	0.06410	0.00620

22	7	8	0.01390	0.07120	0.00970
23	10	12	0.02770	0.12620	0.01640
24	11	13	0.02230	0.07320	0.00940
25	12	13	0.01780	0.05800	0.03020
26	12	16	0.01800	0.08130	0.01080
27	12	17	0.03970	0.17900	0.02380
28	14	15	0.01710	0.05470	0.00740
29	18	19	0.46100	0.68500	0.00000
30	19	20	0.28300	0.43400	0.00000
31	20	21	0.00000	0.77670	0.00000
32	21	22	0.07360	0.11700	0.00000
33	22	23	0.00990	0.01520	0.00000
34	23	24	0.16600	0.25600	0.00420
35	24	25	0.00000	1.18200	0.00000
36	24	25	0.00000	1.23000	0.00000
37	24	26	0.00000	0.04730	0.00000
38	26	27	0.16500	0.25400	0.00000
39	27	28	0.06180	0.09540	0.00000
40	28	29	0.04180	0.05870	0.00000
41	7	29	0.00000	0.06480	0.00000
42	25	30	0.13500	0.20200	0.00000
43	30	31	0.32600	0.49700	0.00000
44	31	32	0.50700	0.75500	0.00000
45	32	33	0.03920	0.03600	0.00000

46	32	34	0.00000	0.95300	0.00000
47	34	35	0.05200	0.07800	0.00160
48	35	36	0.04300	0.05370	0.00080
49	36	37	0.02900	0.03660	0.00000
50	37	38	0.06510	0.10090	0.00100
51	37	39	0.02390	0.03790	0.00000
52	36	40	0.03000	0.04660	0.00000
53	22	38	0.01920	0.02950	0.00000
54	11	41	0.00000	0.74900	0.00000
55	41	42	0.20700	0.35200	0.00000
56	41	43	0.00000	0.41200	0.00000
57	38	44	0.02890	0.05850	0.00100
58	15	45	0.00000	0.10420	0.00000
59	14	46	0.00000	0.07350	0.00000
60	46	47	0.02300	0.06800	0.00160
61	47	48	0.01820	0.02330	0.00000
62	48	49	0.08340	0.12900	0.00240
63	49	50	0.08010	0.12800	0.00000
64	50	51	0.13860	0.22000	0.00000
65	10	51	0.00000	0.07120	0.00000
66	13	49	0.00000	0.19100	0.00000
67	29	52	0.14420	0.18700	0.00000
68	52	53	0.07620	0.09840	0.00000

69	53	54	0.18780	0.23200	0.00000
70	54	55	0.17320	0.22650	0.00000
71	11	43	0.00000	0.15300	0.00000
72	44	45	0.06240	0.12420	0.00200
73	40	56	0.00000	1.19500	0.00000
74	41	56	0.55300	0.54900	0.00000
75	42	56	0.21250	0.35300	0.00000
76	39	57	0.00000	1.35500	0.00000
77	56	57	0.17400	0.26000	0.00000
78	38	49	0.11500	0.17700	0.00300
79	38	48	0.03120	0.04820	0.00000
80	9	55	0.00000	0.12050	0.00000

Table D.3.3 : Transformer Data

Trans. No.	Between buses		Tap position
1	4	18	0.97000
2	4	18	0.97800
3	7	29	0.96700
4	9	55	0.94000
5	10	51	0.93000
6	11	41	0.95500
7	11	43	0.95800
8	13	49	0.89500

11	21	20	1.04300
12	24	25	1.00000
13	24	25	1.00000
14	24	26	1.04300
15	34	32	0.97500
16	39	57	0.98000
17	40	56	0.95800

Table D.3.4 : Shunt Capacitance Data

Sl. No	Bus No.	Susceptance (pu)
1	18	0.10000
2	25	0.05900
3	53	0.06300

Table D.3.5 : DC link System

Number of dc buses = 2

Number of dc line = 1

Table D.2.5.1 : Bus Data

dc bus No.	ac bus No.	Si	Vd	Id	Pd	atap	alpha	Xc
1	8	1	-	-	1.78500	-	8.5000	0.1
2	9	-1	1.28000	-	-	-	20.0000	.07

Table D.3.5.2 : Line Data

Sl No	Between buses		Rdc (pu)
1	1	2	0.00990

Table D.3.6 : DC Mesh System

Number of dc buses = 3

Number of dc lines = 3

Table D.3.6.1 : Bus Data

dc bus No.	ac bus No.	Si	Vd	Id	Pd	atap	alpha	Xc
1	8	1	-	-	1.78500	-	8.50	0.1
2	9	-1	1.2800	-	-	-	20.00	.07
3	6	1	1.27600	-	-	-	18.50	.07

Table D.3.6.2 : Line Data

Sl No	Between buses		Rdc (pu)
1	1	2	0.00990
2	1	3	0.03390
3	2	3	0.04390

Table D.3.7 : DC Mesh-Link System

Number of dc buses = 5

Number of dc lines = 4

Table D.3.7.1 : Bus Data

dc bus No.	ac bus No.	Si	Vd	Id	Pd	atap	alpha	Xc
1	8	1	-	-	1.78500	-	8.50	0.1
2	9	-1	1.28000	-	-	-	20.00	.07
3	6	-1	-	-.49530	-	-	18.00	.07
4	45	1	-	-	0.36420	-	10.00	0.1
5	44	-1	-	-.3080	-	-	20.00	.07

Table D.3.7.2 : Line Data

Sl No	Between buses	Rdc (pu)
1	1 2	0.00990
2	1 3	0.03390
3	2 3	0.04390
4	4 5	0.06240

D.4 : SYSTEM DATA FOR 107 BUS SYSTEM

Number of lines = 174

Number of transformers = 22

Number of shunt capacitor = 0

Table D.4.1 : Bus data

Bus No.	Generation		Load		P-V bus
	P(pu)	Q(pu)	P(pu)	Q(pu)	V(pu)
1	0.00000	0.00000	0.00000	0.00000	1.04500
2	0.00000	0.00000	0.00000	0.00000	1.01200
3	0.00000	0.00000	0.00000	0.00000	1.05000
4	0.35000	0.00000	0.00000	0.00000	1.04800
5	2.00000	0.00000	0.00000	0.00000	1.00900
6	1.00000	0.00000	0.00000	0.00000	1.04800
7	0.55000	0.00000	0.00000	0.00000	0.04000
8	1.60000	0.00000	0.00000	0.00000	0.99000
9	2.00000	0.00000	0.00000	0.00000	1.04000
10	3.25000	0.00000	0.00000	0.00000	0.99200
11	3.25000	0.00000	0.00000	0.00000	1.02000
12	5.50000	0.00000	0.00000	0.00000	1.02000
13	0.55000	0.00000	0.00000	0.00000	0.04800
14	1.60000	0.00000	0.00000	0.00000	1.03500
15	1.80000	0.00000	0.00000	0.00000	1.04000
16	0.00000	0.00000	0.00000	0.00000	1.05000
17	0.00000	0.00000	0.00000	0.00000	1.00000

18	0.00000	0.00000	0.00000	0.00000	1.00000
19	0.00000	0.00000	0.00000	0.00000	1.00000
20	0.00000	0.00000	0.10000	0.07000	1.00000
21	0.00000	0.00000	0.34000	0.25000	1.00000
22	0.00000	0.00000	0.00000	0.00000	1.00000
23	0.00000	0.00000	0.24000	0.18000	1.00000
24	0.00000	0.00000	0.00000	0.00000	1.00000
25	0.00000	0.00000	0.00000	0.00000	1.00000
26	0.00000	0.00000	0.11000	0.08000	1.00000
27	0.00000	0.00000	0.15000	0.13000	1.00000
28	0.00000	0.00000	0.40000	0.10000	1.00000
29	0.00000	0.00000	0.00000	0.00000	1.00000
30	0.00000	0.00000	0.13000	0.10000	1.00000
31	0.00000	0.00000	0.00000	0.00000	1.00000
32	0.00000	0.00000	1.72000	1.18000	1.00000
33	0.00000	0.00000	0.00000	0.00000	1.00000
34	0.00000	0.00000	0.00000	3.00000	1.00000
35	0.00000	0.00000	0.63000	0.47000	1.00000
36	0.00000	0.00000	0.00000	0.00000	1.00000
37	0.00000	0.00000	0.29000	0.22500	1.00000
38	0.00000	0.00000	0.23000	0.18000	1.00000
39	0.00000	0.00000	0.00000	0.00000	1.00000
40	0.00000	0.00000	0.58000	0.51000	1.00000
41	0.00000	0.00000	0.14000	0.05000	1.00000

42	0.00000	0.00000	0.28000	0.20000	1.00000
43	0.00000	0.00000	0.42000	0.29500	1.00000
44	0.00000	0.00000	0.48000	0.27000	1.00000
45	0.00000	0.00000	0.05000	0.04000	1.00000
46	0.00000	0.00000	0.23000	0.15000	1.00000
47	0.00000	0.00000	0.24000	0.21000	1.00000
48	0.00000	0.00000	0.10000	0.09000	1.00000
49	0.00000	0.00000	0.48000	0.31500	1.00000
50	0.00000	0.00000	1.39000	-.03000	1.00000
51	0.00000	0.00000	0.14000	0.11000	1.00000
52	0.00000	0.00000	0.12000	0.09000	1.00000
53	0.00000	0.00000	0.00000	0.00000	1.00000
54	0.00000	0.00000	0.00000	0.00000	1.00000
55	0.00000	0.00000	0.00000	0.50000	1.00000
56	0.00000	0.00000	0.00000	0.00000	1.00000
57	0.00000	0.00000	0.00000	0.00000	1.00000
58	0.00000	0.00000	1.14000	0.58500	1.00000
59	0.00000	0.00000	0.33000	0.27500	1.00000
60	0.00000	0.00000	0.00000	0.00000	1.03200
61	0.00000	0.00000	0.00000	0.00000	1.00000
62	0.00000	0.00000	0.19000	0.07000	1.00000
63	0.00000	0.00000	0.18000	0.04000	1.00000
64	0.00000	0.00000	0.59000	0.42000	1.00000

65	0.00000	0.00000	3.50000	0.50000	1.00000
66	0.00000	0.00000	0.00000	0.00000	1.00000
67	0.00000	0.00000	0.15000	0.11000	1.00000
68	0.00000	0.00000	2.00000	1.38000	1.00000
69	0.00000	0.00000	0.00000	0.00000	1.00000
70	0.00000	0.00000	0.00000	0.00000	1.00000
71	0.00000	0.00000	0.00000	0.00000	1.00000
72	0.00000	0.00000	0.14000	0.05000	1.00000
73	0.00000	0.00000	0.14000	0.10000	1.00000
74	0.00000	0.00000	0.07000	0.06000	1.00000
75	0.00000	0.00000	0.17000	0.15000	1.00000
76	0.00000	0.00000	0.22000	0.08000	1.00000
77	0.00000	0.00000	0.13000	0.10000	1.00000
78	0.00000	0.00000	0.76000	0.21000	1.00000
79	0.00000	0.00000	0.00000	0.00000	1.00000
80	0.00000	0.00000	0.39000	-.01000	1.00000
81	0.00000	0.00000	0.00000	0.00000	1.00000
82	0.00000	0.00000	0.13000	0.10000	1.00000
83	0.00000	0.00000	0.37000	0.12000	1.00000
84	0.00000	0.00000	0.00000	0.00000	1.00000
85	0.00000	0.00000	0.19000	0.15000	1.00000
86	0.00000	0.00000	0.13000	0.10000	1.00000
87	0.00000	0.00000	0.05000	0.04000	1.00000
88	0.00000	0.00000	0.47000	0.10000	1.00000

89	0.00000	0.00000	0.09000	0.03000	1.00000
90	0.00000	0.00000	0.10000	0.07000	1.00000
91	0.00000	0.00000	0.27000	-0.01500	1.00000
92	0.00000	0.00000	0.00000	0.00000	1.00000
93	0.00000	0.00000	0.20000	0.17000	1.00000
94	0.00000	0.00000	0.60000	0.17000	1.00000
95	0.00000	0.00000	0.24000	0.17000	1.00000
96	0.00000	0.00000	0.15000	0.11000	1.00000
97	0.00000	0.00000	0.15000	0.11000	1.00000
98	0.00000	0.00000	0.23000	0.17000	1.00000
99	0.00000	0.00000	0.08000	0.06000	1.05200
100	0.00000	0.00000	0.00000	0.50000	1.00000
101	0.00000	0.00000	0.09000	0.07000	1.00000
102	0.00000	0.00000	0.14000	0.12000	1.00000
103	0.00000	0.00000	0.17000	0.03000	1.00000
104	0.00000	0.00000	0.74000	-0.57000	1.00000
105	0.00000	0.00000	0.10000	0.09000	1.00000
106	0.00000	0.00000	0.38000	-0.03000	1.00000
107	0.00000	0.00000	0.00000	0.00000	1.00000

Table D.4.2 : Line Data

Sl No	From bus	To bus	R	X	Y ² /2
			(pu)	(pu)	(pu)
1	4	21	0.00010	0.17900	0.00000
2	5	22	0.00010	0.04600	0.00000
3	21	22	0.00010	0.05000	0.00000
4	28	29	0.00010	0.05570	0.00000
5	24	40	0.00010	0.05260	0.00000
6	33	34	0.00010	0.01940	0.00000
7	30	31	0.00010	0.03320	0.00000
8	38	39	0.00010	0.05470	0.00000
9	6	51	0.00010	0.06030	0.00000
10	54	58	0.00010	0.02750	0.00000
11	59	60	0.00010	0.05640	0.00000
12	7	66	0.00010	0.13140	0.00000
13	8	68	0.00010	0.04200	0.00000
14	9	68	0.00010	0.04830	0.00000
15	10	71	0.00010	0.03100	0.00000
16	11	70	0.00010	0.03100	0.00000
17	70	71	0.00010	0.02590	0.00000
18	12	69	0.00010	0.02090	0.00000
19	66	68	0.00010	0.05020	0.00000
20	80	81	0.00010	0.05820	0.00000
21	78	79	0.00010	0.05450	0.00000

22	13	84	0.00010	0.10000	0.00000
23	91	92	0.00010	0.06940	0.00000
24	14	99	0.00010	0.05550	0.00000
25	15	99	0.00010	0.05600	0.00000
26	1	100	0.00010	0.02940	0.00000
27	99	100	0.00010	0.02370	0.00000
28	98	99	0.00010	0.05000	0.00000
29	106	107	0.00010	0.05520	0.00000
30	18	36	0.00010	0.04800	0.00000
31	18	35	0.00010	0.00620	0.00000
32	16	18	0.00010	0.13520	0.00000
33	19	61	0.00010	0.03120	0.00000
34	19	64	0.00010	0.00300	0.00000
35	3	19	0.00010	0.08740	0.00000
36	32	33	0.00010	0.01210	0.00000
37	50	53	0.00010	0.03420	0.00000
38	17	55	0.00010	0.02180	0.00000
39	17	54	0.00010	0.00200	0.00000
40	2	17	0.00010	0.04960	0.00000
41	20	106	0.04324	0.10721	0.01184
42	21	42	0.06624	0.16423	0.01814
43	22	61	0.03099	0.15536	0.13136
44	22	61	0.03099	0.15536	0.13136
45	22	71	0.02329	0.11672	0.09869

46	22	71	0.02329	0.11672	0.09869
47	23	46	0.07930	0.15600	0.01528
48	24	33	0.03903	0.19564	0.16541
49	24	33	0.03903	0.19564	0.16541
50	26	91	0.04600	0.11405	0.01260
51	27	90	0.12880	0.31934	0.03528
52	27	90	0.12880	0.31934	0.03528
53	25	101	0.08832	0.21898	0.02419
54	28	58	0.05888	0.14598	0.01613
55	28	58	0.05888	0.14598	0.01613
56	29	54	0.01049	0.05261	0.04448
57	29	79	0.01837	0.09206	0.07784
58	29	79	0.01837	0.09206	0.07784
59	29	107	0.01968	0.09864	0.08340
60	31	33	0.02028	0.11261	0.09522
61	32	37	0.11040	0.27372	0.03024
62	32	88	0.02208	0.05474	0.00605
63	32	88	0.02400	0.05953	0.00658
64	32	102	0.05888	0.14598	0.01613
65	34	100	0.00750	0.07500	1.05000
66	34	65	0.00296	0.02960	0.41440
67	23	35	0.07930	0.15600	0.01528
68	35	59	0.08280	0.20529	0.02268

69	35	75	0.02576	0.06487	0.00706
70	36	39	0.02198	0.11015	0.09313
71	36	39	0.02198	0.11015	0.09313
72	38	85	0.11040	0.27372	0.03024
73	38	85	0.11040	0.27372	0.03024
74	39	53	0.04084	0.20468	0.17306
75	39	53	0.04084	0.20468	0.17306
76	44	94	0.06992	0.17336	0.01915
77	44	94	0.06992	0.17336	0.01915
78	28	41	0.04858	0.12044	0.01331
79	28	41	0.04858	0.12044	0.01331
80	41	67	0.05796	0.14370	0.01588
81	43	98	0.07360	0.18248	0.02016
82	43	98	0.07360	0.18248	0.02016
83	49	96	0.06164	0.15283	0.01688
84	45	50	0.07084	0.17564	0.01940
85	46	47	0.00736	0.01825	0.00202
86	48	89	0.03680	0.09124	0.01008
87	51	103	0.07084	0.17564	0.01940
88	51	106	0.17664	0.43795	0.04838
89	52	82	0.04140	0.10265	0.01134
90	54	92	0.01706	0.08549	0.07228
91	54	92	0.01706	0.08549	0.07228
92	54	107	0.00836	0.04192	0.03545

93	56	57	0.01380	0.03422	0.00378
94	56	57	0.01380	0.03422	0.00378
95	57	106	0.04692	0.11633	0.01285
96	57	106	0.04692	0.11633	0.01285
98	48	58	0.06532	0.16195	0.01798
99	56	58	0.00920	0.02281	0.00252
100	56	58	0.00920	0.02281	0.00252
101	58	87	0.02162	0.05360	0.00592
102	58	87	0.02162	0.05360	0.00592
103	59	86	0.05520	0.13686	0.01512
104	29	60	0.03116	0.15618	0.13205
105	29	60	0.03116	0.15618	0.13205
106	36	60	0.01476	0.07398	0.06255
107	36	60	0.01476	0.07398	0.06255
108	60	99	0.01180	0.05918	0.05004
109	60	99	0.01180	0.05918	0.05004
110	60	61	0.03673	0.18412	0.15568
111	60	61	0.03673	0.18412	0.15568
112	25	64	0.02484	0.06158	0.00680
113	25	64	0.02484	0.06158	0.00680
114	49	64	0.08280	0.20529	0.02268
115	49	64	0.08280	0.20529	0.02268
116	62	76	0.04600	0.11405	0.01260

117	63	72	0.05612	0.13914	0.01537
118	73	74	0.02944	0.07299	0.00806
119	73	74	0.02944	0.07299	0.00806
120	44	66	0.03680	0.09124	0.01008
121	44	66	0.03680	0.09124	0.01008
122	64	73	0.08648	0.21441	0.02368
123	64	73	0.08648	0.21441	0.02368
124	63	67	0.05980	0.14826	0.01638
125	37	66	0.06808	0.16879	0.01864
126	37	66	0.06808	0.16879	0.01864
127	42	66	0.09660	0.23950	0.02646
128	31	68	0.00769	0.04274	0.03614
129	33	68	0.02797	0.15535	0.13135
130	68	71	0.00053	0.00295	0.00250
131	68	71	0.00053	0.00295	0.00250
132	34	69	0.00380	0.00380	0.53200
133	34	69	0.00380	0.00380	0.53200
134	34	70	0.00398	0.03980	0.55720
135	69	70	0.00014	0.00140	0.01960
136	72	89	0.05060	0.12545	0.01386
137	59	75	0.05704	0.14142	0.01562
138	76	83	0.04232	0.10492	0.01159
139	21	77	0.14996	0.37180	0.04107
140	21	77	0.14996	0.37180	0.04107

141	80	91	0.03588	0.08895	0.00982
142	64	82	0.06440	0.15967	0.01764
143	51	83	0.07084	0.17563	0.01940
144	41	78	0.05428	0.13457	0.01486
145	41	78	0.05428	0.13457	0.01486
146	45	85	0.07084	0.17563	0.01940
147	50	85	0.11868	0.29424	0.03250
148	52	86	0.04784	0.11861	0.01310
149	32	90	0.01472	0.03649	0.00404
150	32	90	0.01472	0.03649	0.00404
151	62	91	0.02760	0.06843	0.00756
152	93	104	0.04692	0.11633	0.01285
253	74	104	0.05796	0.14370	0.01587
254	74	104	0.05796	0.14370	0.01587
155	38	96	0.06164	0.15282	0.01688
156	55	100	0.00521	0.05216	0.73024
157	27	101	0.08004	0.19844	0.02192
158	27	101	0.08004	0.19844	0.02192
159	43	101	0.07084	0.17563	0.01940
160	43	101	0.07084	0.17563	0.01940
161	84	101	0.07084	0.17563	0.01940
162	84	101	0.07084	0.17563	0.01940
163	95	97	0.04140	0.10264	0.01134

164	35	95	0.09200	0.22810	0.02520
165	30	102	0.02760	0.06843	0.00756
166	30	102	0.02760	0.06843	0.00756
167	37	102	0.05152	0.12773	0.01411
168	102	105	0.01196	0.02965	0.00327
169	20	103	0.06256	0.15510	0.01713
170	26	106	0.04600	0.14050	0.01260
171	46	106	0.04880	0.09600	0.00940
172	80	106	0.05060	0.12545	0.01386
173	97	106	0.06624	0.16423	0.01814
174	81	107	0.00852	0.04274	0.03614

Table D.4.3 : Transformer Data

Trans. No.	Between buses	Tap position	
1	22	5	1.04500
2	28	29	1.05000
3	40	24	1.05000
4	38	39	1.05000
5	58	54	1.05000
6	59	60	1.05000
7	68	8	1.10000
8	68	9	1.04500
9	71	10	1.09100

10	70	11	1.05000
11	69	12	1.05000
12	78	79	1.05000
13	84	13	1.01250
14	91	92	1.05000
15	99	14	1.04500
16	99	15	1.04500
17	100	1	1.02500
18	106	107	1.05000
19	18	36	1.05000
20	19	61	1.05000
21	32	33	1.04400
22	50	53	1.05000

Table D.4.4 : DC link System

Number of dc buses = 2

Number of dc line = 1

Table D.4.4.1 : Bus Data

dc bus No.	ac bus No.	Si	Vd	Id	Pd	atap	alpha	Xc
1	99	1	-	-	4.3830	1.1455	-	0.07
2	60	-1	-	-3.375	-	-	20.00	.04

Table D.4.4.2 : Line Data

Sl No	Between buses	Rdc (pu)
1	1 2	0.00330

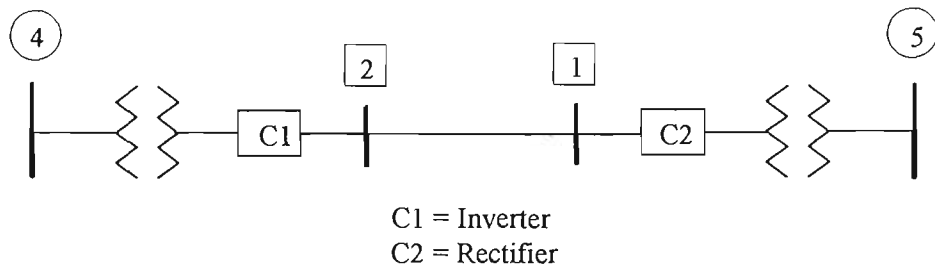


Fig. E.1.1 14 bus dc link system

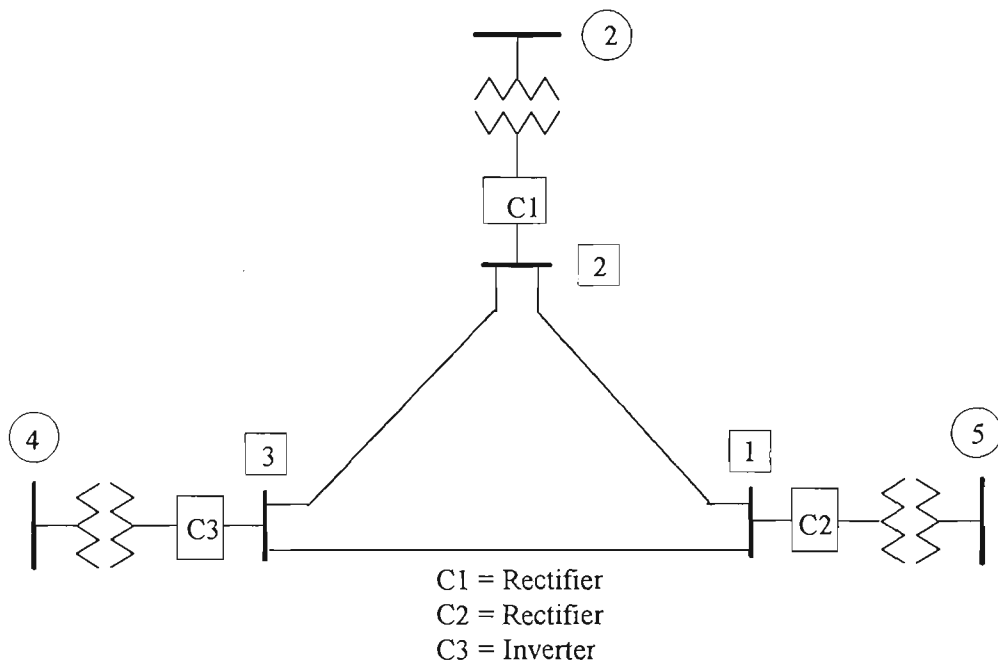
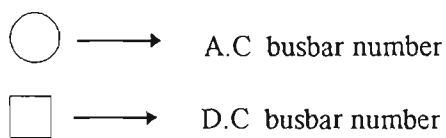


Fig. E.1.2 14 bus dc mesh system



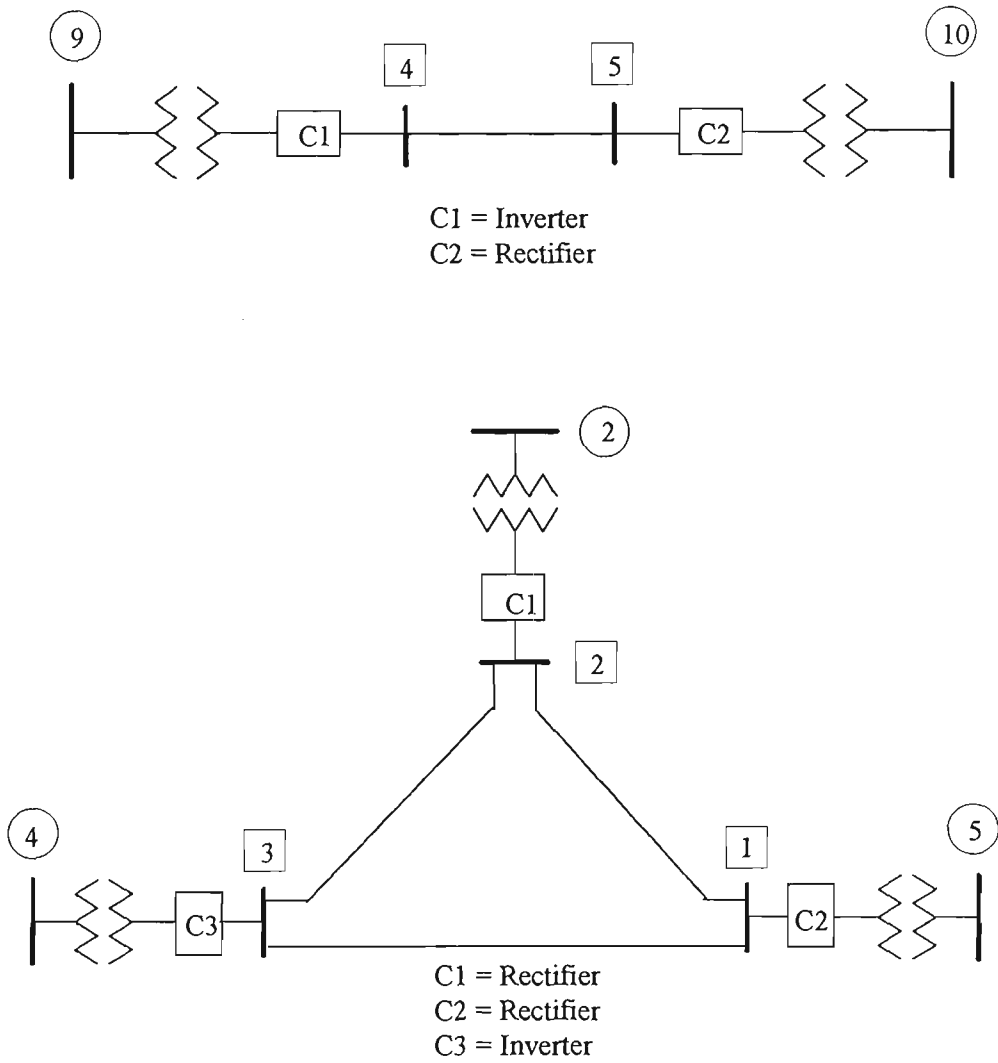
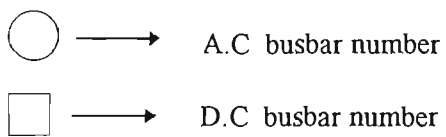


Fig. E.1.3 14 bus dc link-mesh system



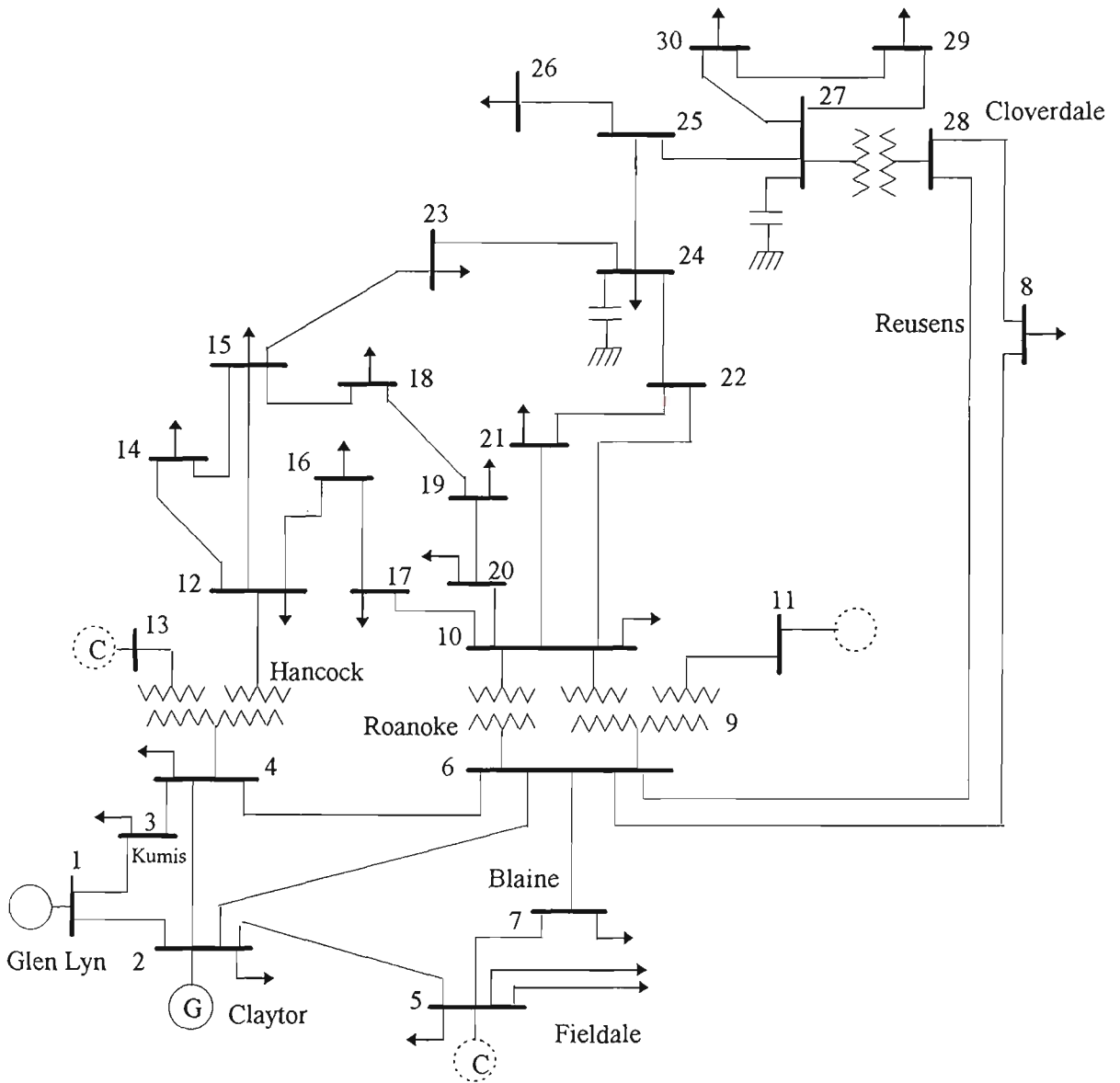
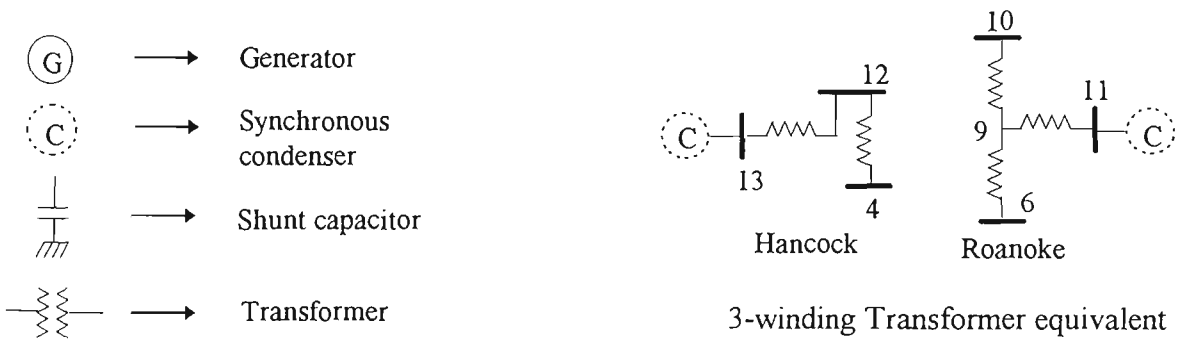


Fig. E.2 IEEE 30 bus system



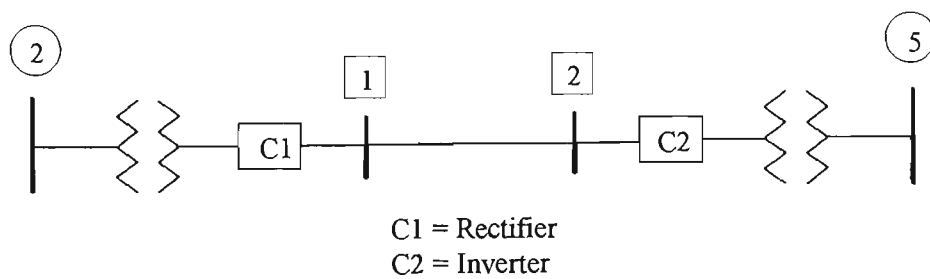


Fig. E.2.1 30 bus dc link system

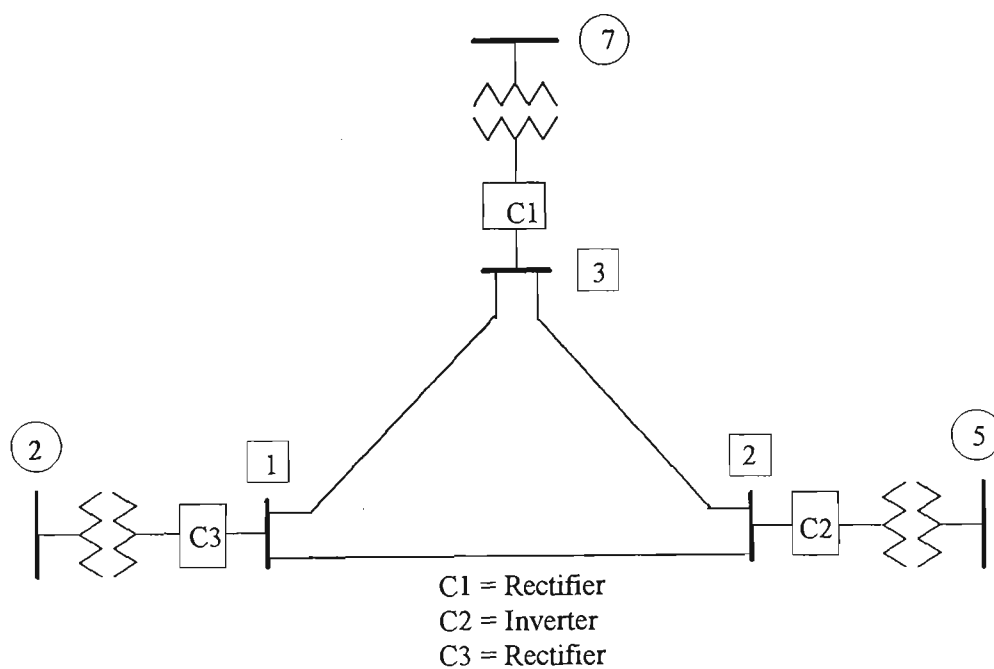
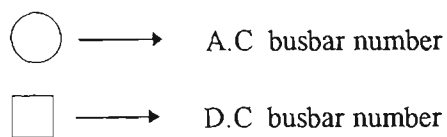


Fig. E.2.2 30 bus dc mesh system



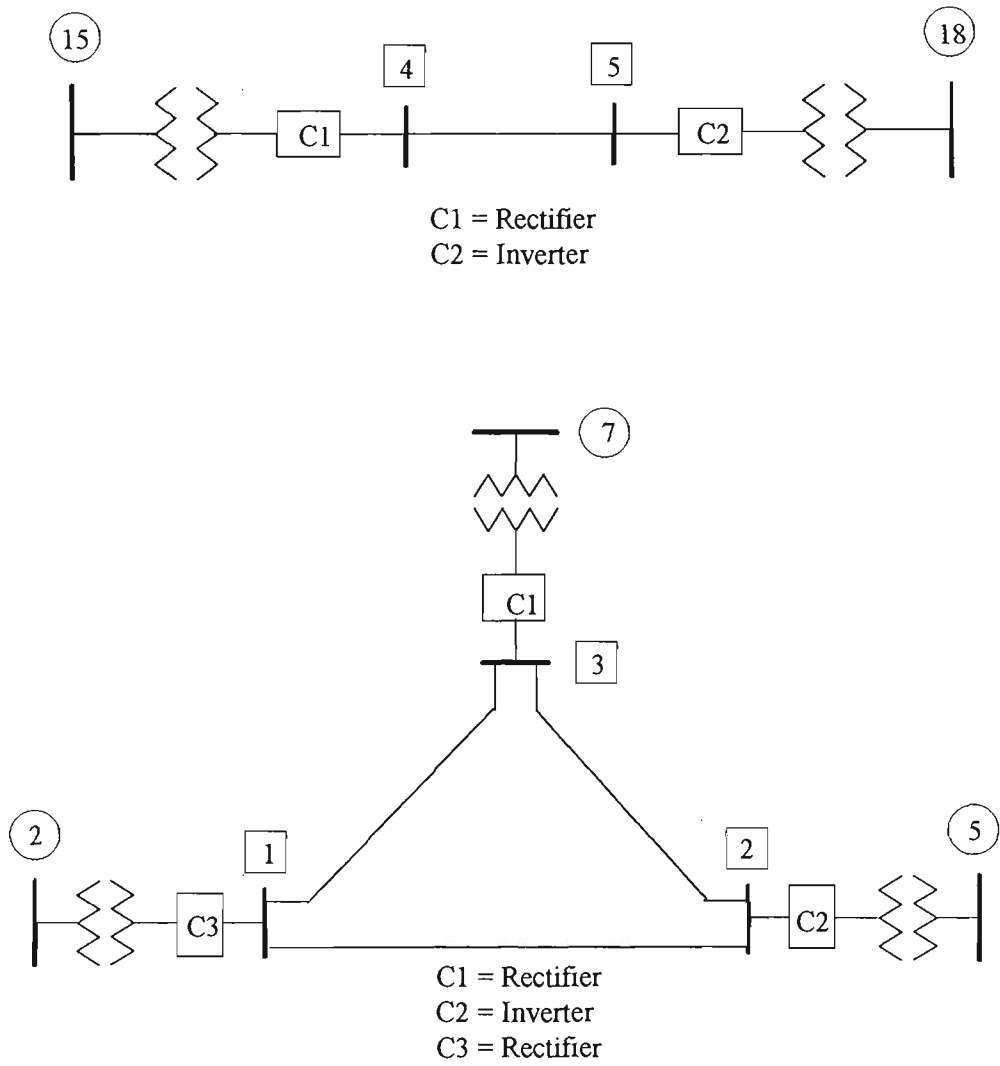
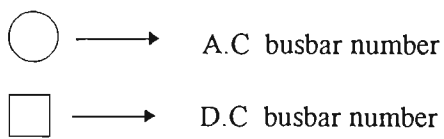


Fig. E.2.3 30 bus dc link-mesh system



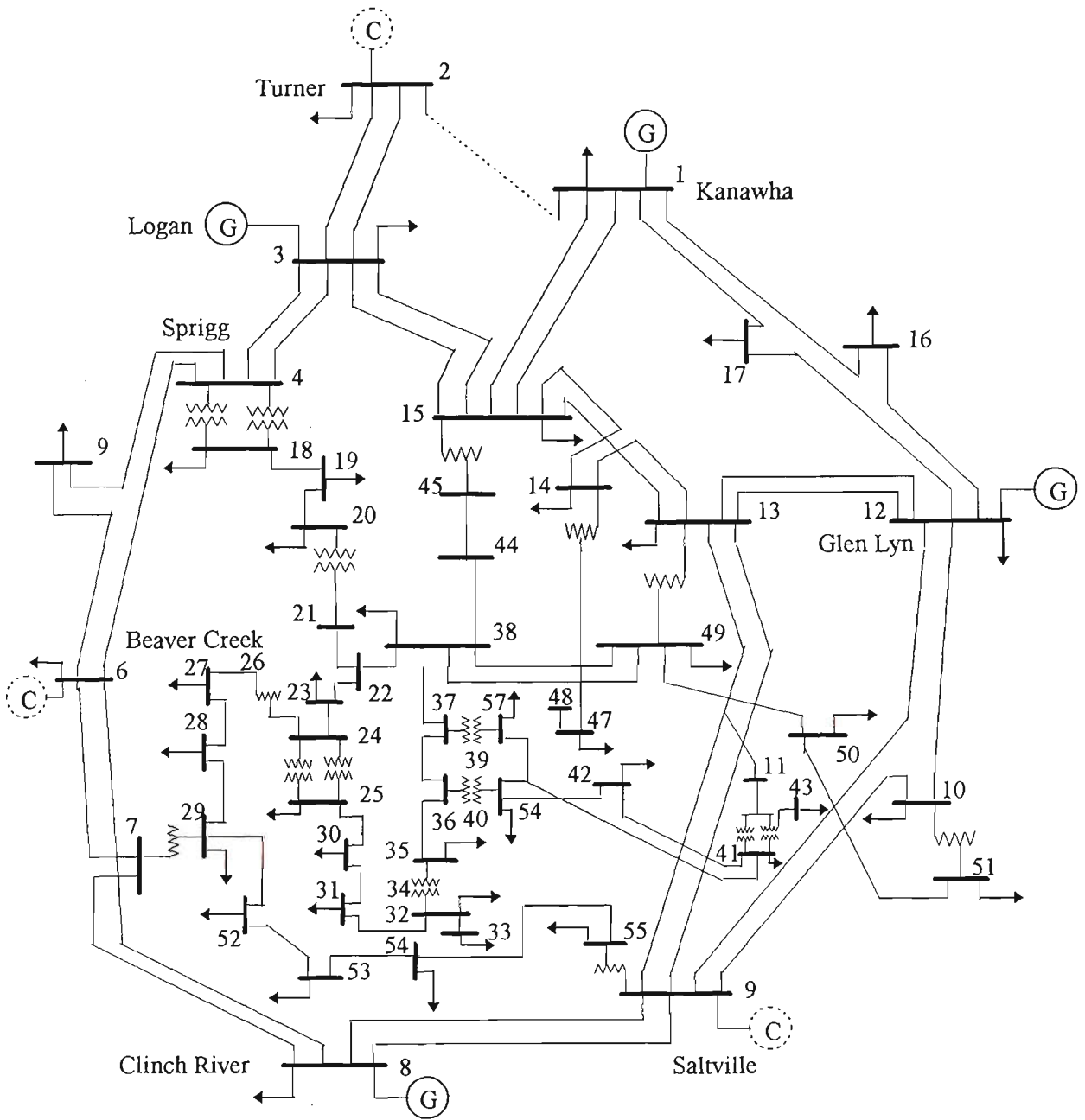
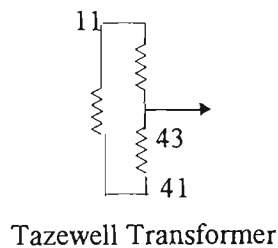
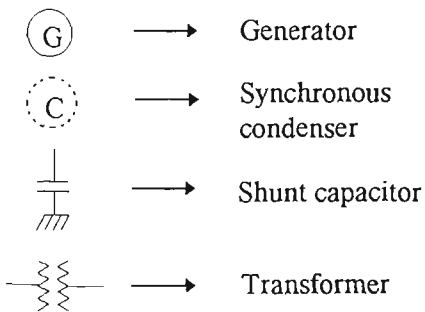


Fig. E.3 IEEE 57 bus system



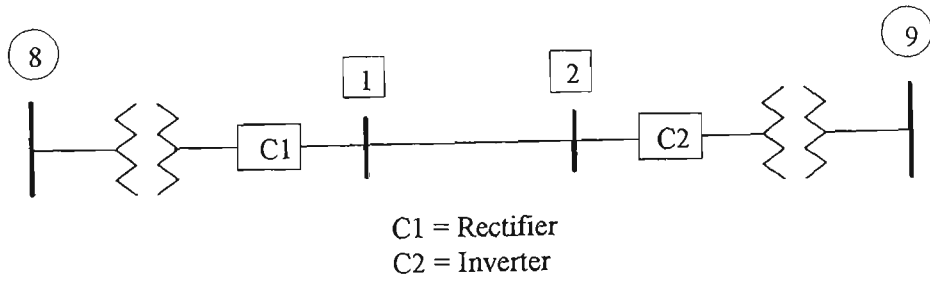


Fig. E.3.1 57 bus dc link system

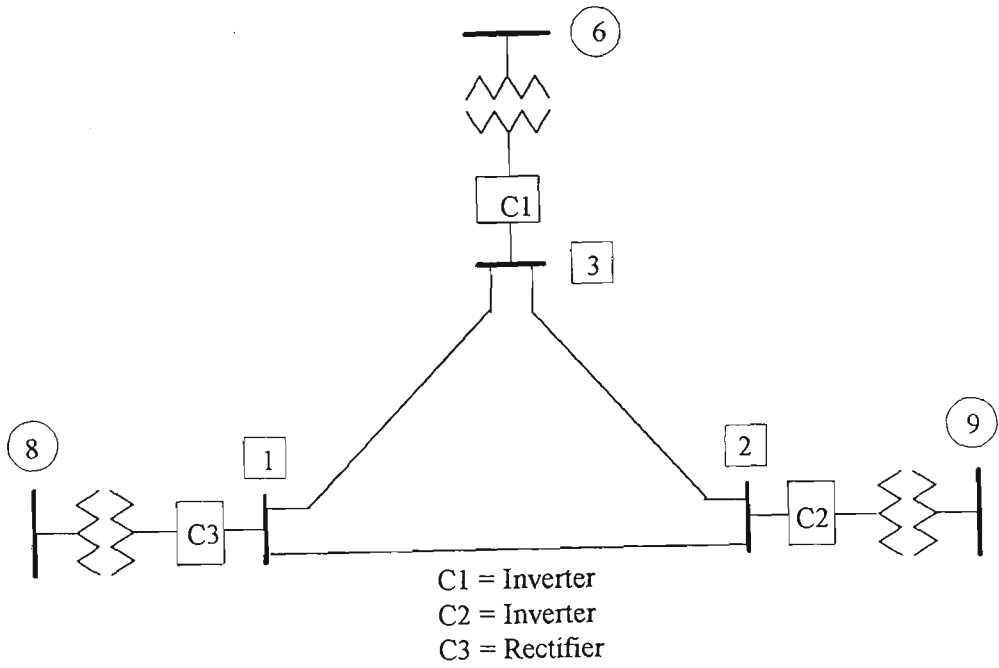
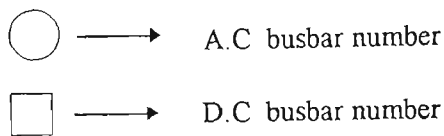


Fig. E.3.2 57 bus dc mesh system



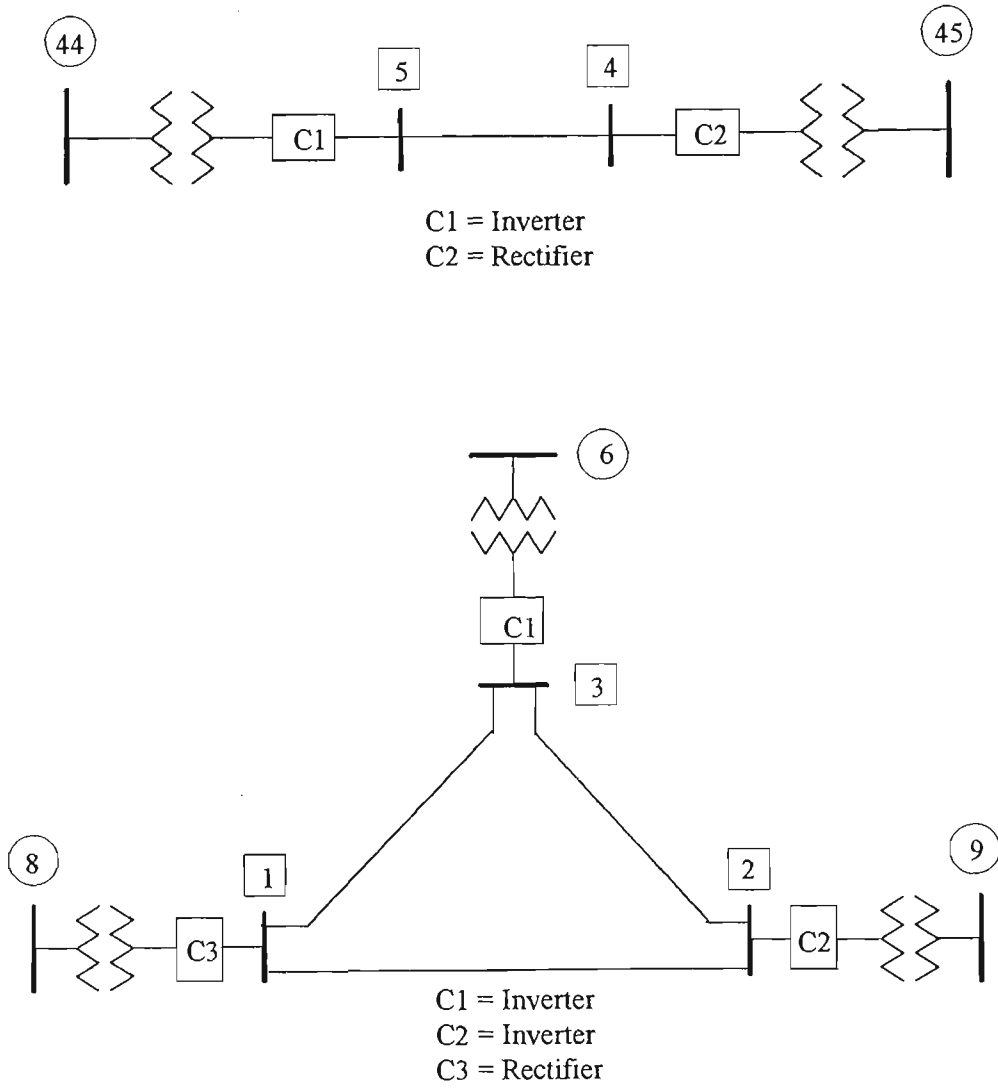
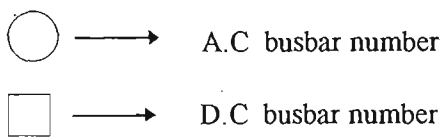


Fig. E.3.3 57 bus dc link-mesh system



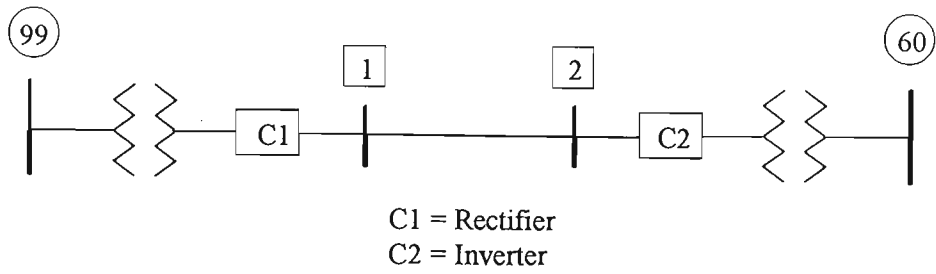


Fig. E.4.1 107 bus dc link system

APPENDIX - F

LOAD FLOW AND LINE FLOW SOLUTIONS OF DIFFERENT BUS SYSTEM

Table F.1 Load Flow Solution of 14 Bus System with DC Link

(a) AC voltage Profile

Bus No	Methods							
	FRLF		SRLF		DSRLF		FDLF	
	e	f	e	f	e	f	e	f
1	1.0600	0.0000	1.0600	0.0000	1.0600	0.0000	1.0600	0.00000
2	1.04099	-0.09142	1.04099	-0.09142	1.04099	-0.09142	1.04100	-0.09134
3	0.98488	-0.22385	0.98488	-0.22384	0.98488	-0.22384	0.98491	-0.22372
4	0.98985	-0.17683	0.98992	-0.17686	0.98990	-0.17686	0.98996	-0.17666
5	0.98357	-0.14829	0.98358	-0.14829	0.98363	-0.14831	0.98365	-0.14820
6	1.03733	-0.26237	1.03735	-0.26235	1.03734	-0.26237	1.03741	-0.26208
7	1.02800	-0.24161	1.02805	-0.24163	1.02802	-0.24163	1.02814	-0.24128
8	1.06109	-0.24939	1.06108	-0.24940	1.06108	-0.24940	1.06117	-0.24904
9	1.01570	-0.26874	1.01576	-0.26876	1.01572	-0.26876	1.01587	-0.26835
10	1.01089	-0.27089	1.01095	-0.27091	1.01090	-0.27091	1.01114	-0.27040
11	1.02001	-0.26808	1.02005	-0.26807	1.02001	-0.26809	1.02016	-0.26769
12	1.01862	-0.27382	1.01867	-0.27379	1.01881	-0.27363	1.01873	-0.27358
13	1.01329	-0.27371	1.01333	-0.27368	1.01322	-0.27379	1.01337	-0.27339
14	0.99240	-0.28372	0.99245	-0.28373	0.99237	-0.28376	0.99254	-0.28337

(b) DC Results

Methods	Variables						
	Vd	Id	a	θ	c	d	ϕ
FRLF Conv.1	1.28607	0.47976	1.01557	12.498	0.57166	0.30525	
Conv.2	1.27950	-0.47976	1.03522	22.597	0.53323	0.36834	
SRLF Conv.1	1.28607	0.47976	1.02097	12.498	0.56870	0.30360	
Conv.2	1.27950	-0.47976	1.04090	22.597	0.53093	0.36566	
FSLF Conv.1	1.28607	0.47976	1.02038	12.497	0.56906	0.30292	
Conv.2	1.27950	-0.47976	1.04007	22.597	0.53087	0.36575	
FDLF Conv.1	1.28607	0.47976	1.0155	12.50	-	-	19.484
Conv.2	1.27950	-0.47976	1.0352	22.55	-	-	24.468

Table F.2 Load Flow Solution of 30 Bus System with DC Link

(a) AC Voltage Profile

Bus No	Methods							
	FRLF		SRLF		DSRLF		FDLF	
	e	f	e	f	e	f	e	f
1	1.05000	0.00000	1.05000	0.00000	1.05000	0.00000	1.05000	0.00000
2	1.03263	-.04910	1.03263	-.04910	1.03263	-.04910	1.03263	-.04910
3	1.02998	-.08432	1.02997	-.08432	1.02998	-.0843	1.02998	-.08432
4	1.02395	-.10051	1.02395	-.10051	1.02395	-.10051	1.02395	-.10051
5	.99382	-.15477	.99382	-.15477	.99382	-.15477	.99382	-.15478
6	1.01696	-.11523	1.01696	-.11523	1.01696	-.11523	1.01696	-.11523
7	.99875	-.13987	.99875	-.13987	.99875	-.13987	.99875	-.13987

8.	1.01655	-.11470	1.01655	-.11470	1.01655	- 11470	1.01655	-.11470
9	1.03544	-.14782	1.03545	-.14781	1.03544	-.14781	1.03544	-.14782
10	1.02731	-.18130	1.02732	-.18129	1.02732	-.18130	1.02731	-.18130
11	1.08481	-.11884	1.08481	-.11884	1.08481	-.11884	1.08481	-.11885
12	1.03425	-.16778	1.03424	-.16779	1.03424	-.16778	1.03425	-.16778
13	1.07764	-.15192	1.07764	-.15194	1.07764	-.15193	1.07764	-.15193
14	1.01793	-.18176	1.01772	-.18206	1.01789	-.18179	1.01793	- 18176
15	1.01414	-.18332	1.01421	-.18322	1.01415	-.18331	1.01414	-.18332
16	1.02332	-.17735	1.02332	-.17735	1.02332	-.17735	1.02332	-.17735
17	1.02018	-.18295	1.02019	-.18294	1.02018	-.18294	1.02018	-.18295
18	1.00449	-.19279	1.00454	-.19272	1.00449	-.19278	1.00449	-.19279
19	1.00248	-.19555	1.00252	-.19550	1.00249	-.19554	1.00248	-.19555
20	1.00774	-.19295	1.00776	-.19291	1.00774	-.19294	1.00774	-.19295
21	1.01393	-.18748	1.01394	-.18746	1.01393	-.18747	1.01393	-.18748
22	1.01458	-.18747	1.01459	-.18746	1.01458	-.18747	1.01458	-.18747
23	1.00521	-.18987	1.00527	-.18979	1.00522	-.18986	1.00521	-.18987
24	1.00275	-.19394	1.00278	-.19389	1.00275	-.19393	1.00275	-.19394
25	1.00702	-.19310	1.00703	-.19308	1.00702	-.19310	1.00702	-.19310
26	0.98841	-.19693	.98843	-.19689	.98841	-.19692	.98841	-.19693
27	1.01898	-.18949	1.01898	-.18948	1.01898	-.18949	1.01897	-.18949
28	1.01146	-.12192	1.01146	-.12191	1.01146	-.12191	1.01146	-.12192
29	.99564	-.20678	.99565	-.20677	.99564	-.20678	.99564	-.20678
30	.98139	-.21923	.98139	-.21921	.98139	-.219Z2	.98138	-.21922

(b) DC Results

Methods		Variables						
		Vd	Id	a	θ	c	d	ϕ
FRLF	Conv.1	1.30063	.44763	.97290	8.499	.56991	.20188	
	Conv.2	1.27950	-.44763	1.02587	19.997	.51156	.32241	
SRLF	Conv.1	1.30063	.44762	.97778	8.499	.56711	.20055	
	Conv.2	1.27950	-.44762	1.03138	19.997	.50911	.32032	
DSRLF	Conv.1	1.30063	.44763	.97780	8.499	.56705	.20076	
	Conv.2	1.27950	-.44763	1.03078	19.997	.50924	.32010	
FDLF	Conv.1	1.30063	.44763	.97290	8.499	-	-	16.753
	Conv.2	1.27950	-.44763	1.02587	19.997	-	-	23.329

Table F.3 Load Flow Solution of 57 Bus System with DC Link

(a) AC Voltage Profile at Selected Busbars

Sl No	Bus No	Methods					
		FRLF		SRLF		DSRLF	
		e	f	e	f	e	f
1	1	1.0400	0.0000	1.0400	0.0000	1.0400	0.00000
2	10	0.96692	-0.19458	0.96692	-0.19458	0.96692	-0.19459
3	20	0.93777	-0.22374	0.93777	-0.22374	0.93779	-0.22372
4	30	0.91229	-0.30857	0.91233	-0.30852	0.91229	-0.30858
5	40	0.94607	-0.22928	0.94607	-0.22927	0.94608	-0.22927
6	50	0.99595	-0.23648	0.99595	-0.23648	0.99598	-0.23643
7	57	0.92622	-0.27480	0.92624	-0.27478	0.92623	-0.27479

(b) DC Results

Methods		Variables						
		Vd	Id	a	θ	c	d	ϕ .
FRLF	Conv.1	1.29366	1.37981	1.0619	8.499	1.60303	0.95005	
	Conv.2	1.2800	-1.37981	1.10338	19.997	1.46331	1.15370	
SRLF	Conv.1	1.29366	1.37981	1.06736	8.499	1.59532	0.94476	
	Conv.2	1.28000	-1.37981	1.11019	19.997	1.45975	1.14307	
DSRLF	Conv.1	1.29366	1.37981	1.06712	8.499	1.59527	0.94481	
	Conv.2	1.28000	-1.37981	1.10785	19.997	1.45804	1.14526	
FDLF	Conv.1	1.30063	.44763	.97290	8.499	-	-	17.234
	Conv.2	1.27950	-.44763	1.02587	19.997	-	-	2.418

Table F.4 Load Flow Solution of 107 Bus System with DC Link

a) AC Voltage Profile at Selected Busbars

Bus No	Method							
	FRLF		SRLF		DSRLF		FDLF	
	e	f	e	f	e	f	e	f
1	1.04500	0.0000	1.04500	0.0000	1.04500	0.0000	1.04500	0.0000
8	0.93186	0.33428	0.93183	0.33425	0.93185	0.33428	0.93184	0.33434
11	0.94780	0.37693	0.94777	0.37690	0.94779	0.37694	0.94777	0.37700
23	0.94055	-0.29536	0.94055	-0.29527	0.94056	-0.29525	0.94053	-0.29533
28	0.97815	-0.32685	0.97815	-0.32685	0.97815	-0.32683	0.97812	-0.32692
35	0.99262	-0.25471	0.99262	-0.25472	0.99263	-0.25469	0.99260	-0.25478
41	0.95525	-0.34656	0.95525	-0.34657	0.95524	-0.34655	0.95521	-0.34664
50	0.91481	-0.46428	0.91480	-0.46426	0.91480	-0.46430	0.91471	-0.46438

56	0.96911	-0.32453	0.96911	-0.32453	0.96910	-0.32451	0.96907	-0.32460
60	0.99720	-0.05670	0.99719	-0.05671	0.99719	-0.05669	1.02469	-0.12262
66	1.01198	0.22365	1.01196	0.22363	1.01198	0.22367	1.01197	0.22369
71	1.01812	0.28812	1.01809	0.28809	1.01812	0.28814	1.01810	0.28817
75	0.99652	-0.23910	0.99652	-0.23911	0.99652	-0.23908	0.99649	-0.23916
94	0.95506	0.12171	0.95504	0.12169	0.95505	0.12173	0.95504	0.12173
99	1.04703	-0.10219	1.04703	-0.10220	1.04703	-0.10215	1.04702	-0.10222
102	1.01250	0.18458	1.01248	0.18456	1.01250	0.18461	1.01249	0.18462
107	0.94653	-0.2903	0.94654	-0.29031	0.94653	-0.29030	0.94651	-0.29038

(b) DC Results

Methods	Variables						
	Vd	Id	a	θ	c	d	ϕ
FRLF Conv.1	1.29867	3.37500	1.14550	20.50920	3.35321	3.087121	
Conv.2	1.28753	-3.37500	1.08154	20.000	3.58414	2.815720	
SRLF Conv.1	1.29867	3.37500	1.14550	19.74871	3.35679	3.04940	
Conv.2	1.28753	-3.37500	1.08744	20.0000	3.57189	2.79442	
DSRLF Conv.1	1.29867	3.37500	1.14550	19.69944	3.35695	3.04938	
Conv.2	1.28753	-3.37500	1.08656	20.0000	3.56806	2.79929	
FDLF Conv.1	1.29867	3.37500	1.14550	20.50902	-	-	37.06120
Conv.2	1.28753	-3.37500	1.08154	20.0000	-	-	31.33220

Table F.5 Load Flow Solution of 14 Bus System with DC Mesh

(a) AC Voltage Profile

Bus No	Method							
	FRLF		SRLF		DSRLF		FDLF	
	e	f	e	f	e	f	e	f
1	1.06000	0.00000	1.06000	0.00000	1.06000	0.00000	1.06000	0.00000
2	1.04204	-0.07862	1.04204	-0.07862	1.04204	-0.07862	1.04204	-0.07857
3	0.99526	-0.17192	0.99527	-0.17190	0.99526	-0.17190	0.99530	-0.17170
4	0.94660	-0.05212	0.94667	-0.05214	0.94667	-0.05213	0.94669	-0.05175
5	0.94864	-0.19058	0.94845	-0.19053	0.94903	-0.19067	0.94868	-0.19039
6	1.03639	-0.26607	1.03641	-0.26605	1.03640	-0.26606	1.03650	-0.26565
7	1.02200	-0.14706	1.02203	-0.14707	1.02202	-0.14706	1.02215	-0.14653
8	1.07889	-0.15524	1.07889	-0.15525	1.07889	-0.15525	1.07900	-0.15469
9	1.01493	-0.19127	1.01497	-0.19128	1.01495	-0.19128	1.01514	-0.19069
10	1.01094	-0.20802	1.01098	-0.20802	1.01096	-0.20802	1.01116	-0.20734
11	1.02029	-0.23772	1.02032	-0.23771	1.02030	-0.23772	1.02050	-0.23720
12	1.01688	-0.27192	1.01692	-0.27190	1.01710	-0.27208	1.01707	-0.27155
13	1.01303	-0.26604	1.01307	-0.26600	1.01295	-0.26594	1.01317	-0.26557
14	0.99247	-0.23773	0.99251	-0.23773	0.99244	-0.23770	0.99265	-0.23721

(b) DC Results

Methods	Variables						
	Vd	Id	a	θ	c	d	ϕ .
FRLF Conv.1	1.28756	0.47920	1.04513	12.498	0.55568	0.33170	
Conv.2	1.28888	0.76670	0.96593	10.548	0.95084	0.40985	
Conv.3	1.27950	-1.24590	1.12275	22.597	1.45324	0.84801	
SRLF Conv.1	1.28756	0.47920	1.05224	12.498	0.55217	0.33129	
Conv.2	1.28888	0.76670	0.97074	10.548	0.94623	0.40751	
Conv.3	1.27950	-1.24590	1.12844	22.597	1.44647	0.84294	
DSRLF Conv.1	1.28756	0.47920	1.04823	12.498	0.55444	0.32744	
Conv.2	1.28888	0.76670	0.97083	10.548	0.94603	0.40795	
Conv.3	1.27950	-1.24590	1.12814	22.597	1.44621	0.84339	
FDLF Conv.1	1.28756	0.4792	1.0451	12.50	-	-	19.472
Conv.2	1.28888	0.7667	0.9659	10.55	-	-	19.003
Conv.3	1.27950	-1.2458	1.1227	22.60	-	-	27.110

Table F.6 Load Flow Solution of 30 Bus System with DC Mesh

(a) AC Voltage Profile

Bus No	Methods							
	FRLF		SRLF		DSRLF		FDLF	
	e	f	e	f	e	f	e	f
1	1.05000	0.00000	1.05000	0.00000	1.05000	0.00000	1.05000	0.00000
2	1.03264	-.04904	1.03264	-.04904	1.03264	-.04904	1.03264	-.04904
3	1.02946	-.08403	1.02947	-.08403	1.02946	-.08402	1.02947	-.08403
4	1.02334	-.10015	1.02334	-.10015	1.02334	-.10013	1.02334	-.10015
5	.99633	-.13767	.99633	-.13767	.99634	-.13764	.99633	-.13767
6	1.01605	-.11470	1.01605	-.11471	1.01605	-.11469	1.01605	-.11471
7	.99445	-.13768	.99446	-.13769	.99444	-.13765	.99447	-.13769
8	1.01657	-.11456	1.01657	-.11456	1.01657	-.11455	1.01657	-.11456
9	1.03499	-.14738	1.03499	-.14738	1.03499	-.14736	1.03499	-.14738
10	1.02683	-.18088	1.02684	-.18088	1.02685	-.18087	1.02683	-.18088
11	1.08485	.11844	1.08485	.11844	1.08486	.11843	1.08485	.11844
12	1.03396	-.16749	1.03397	-.16749	1.03396	-.16747	1.03396	-.16750
13	1.07768	-.15168	1.07768	-.15168	1.07768	-.15165	1.07768	-.15168
14	1.01762	-.18147	1.01762	-.18147	1.01734	-.18127	1.01758	-.18151
15	1.01380	-.18301	1.01380	-.18301	1.01390	-.18306	1.01381	-.18300
16	1.02295	-.17701	1.02296	-.17701	1.02296	-.17700	1.02296	-.17701
17	1.01973	-.18255	1.01974	-.18256	1.01974	-.18254	1.01973	-.18255
18	1.00409	-.19245	1.00409	-.19245	1.00416	-.19248	1.00410	-.19244
19	1.00206	-.19519	1.00206	-.19519	1.00211	-.19521	1.00206	-.19519
20	1.00730	-.19257	1.00730	-.19257	1.00734	-.19258	1.00730	-.19257

21	1.01344	-.18707	1.01345	-.18707	1.01346	-.18706	1.01345	-.18707
22	1.01410	-.18707	1.01410	-.18707	1.01411	-.18706	1.01410	-.18707
23	1.00480	-.18953	1.00481	-.18953	1.00488	-.18956	1.00482	-.18952
24	1.00225	-.19356	1.00226	-.19356	1.00230	-.19357	1.00226	-.19355
25	1.00644	-.19269	1.00644	-.19269	1.00646	-.19269	1.00644	-.19269
26	.98781	-.19653	.98782	-.19653	.98785	-.19653	.98782	-.19652
27	1.01834	-.18906	1.01835	-.18906	1.01835	-.18905	1.01834	-.18906
28	1.01077	-.12148	1.01077	-.12148	1.01077	-.12146	1.01077	-.12148
29	.99499	-.20637	.99500	-.20637	.99500	-.20636	.99499	-.20637
30	.98073	-.21882	.98074	-.21883	.98074	-.21881	.98073	-.21883

(b) DC Results

Methods	Variables						
	Vd	Id	a	θ	c	d	ϕ
FRLF Conv.1	1.29580	.44930	.96952	8.499	.57188	.20301	
Conv.2	1.27950	-.55016	1.03124	19.997	.63089	.39243	
Conv.3	1.28892	.10086	.97885	12.498	.12655	.05058	
SRLF Conv.1	1.29580	.44930	.97438	8.499	.56908	.20174	
Conv.2	1.27950	-.55016	1.03672	19.997	.62783	.39032	
Conv.3	1.28892	.10086	.98365	12.498	.12594	.05013	
DSRLF Conv.1	1.29580	.44930	.97440	8.499	.56901	.20194	
Conv.2	1.27950	-.55016	1.03619	19.997	.62795	.39011	
Conv.3	1.28892	.10086	.98395	12.498	.12586	.05032	

FDLF Conv.1	1.29580	.44930	.96952	8.499	-	-	16.798
Conv.2	1.27950	-.55015	1.03124	19.997	-	-	24.012
Conv.3	1.28892	.10085	.97883	12.498	-	-	13.778

Table F.7 Load Flow Solution of 57 Bus System with DC Mesh

(a) AC Voltage Profile at Selected Busbars

Bus No	Method							
	FRLF		SRLF		DSRLF		FDLF	
	e	f	e	f	e	f	e	f
1	1.0400	0.00000	1.0400	0.0000	1.0400	0.0000	1.0400	0.0000
10	0.95989	-0.22247	0.95989	-0.22247	0.95991	-0.22244	0.95982	-0.22242
20	0.93514	-0.21215	0.93514	-0.21215	0.93517	-0.21213	0.93516	-0.21216
30	0.91710	-0.28978	0.91710	-0.28978	0.91723	-0.28979	0.91728	-.028976
40	0.94176	-0.23411	0.94176	-0.23411	0.94180	-0.23409	0.94180	-.023406
50	0.98859	0.25351	0.98859	0.25351	0.98861	0.25349	0.98857	0.25346
57	0.92274	-0.28953	0.92274	-0.28953	0.92278	-0.28951	0.92275	-0.28952

(b) DC Results

Methods	Variables						
	Vd	Id	a	θ	c	d	ϕ
FRLF Conv.1	1.28970	1.38404	1.05925	8.499	1.71508	0.74306	
Conv.2	1.28000	-0.88877	1.07699	19.997	0.94163	0.74430	
Conv.3	1.27600	-0.49527	1.04005	17.998	0.59842	0.29897	
SRLF Conv.1	1.28970	1.38404	1.06473	8.499	1.70660	0.73912	
Conv.2	1.28000	-0.88877	1.08423	19.997	0.94083	0.73546	
Conv.3	1.27600	-0.49527	1.04536	17.998	0.59509	0.29795	
DSRLF Conv.1	1.28970	1.38404	1.06445	8.499	1.70684	0.73856	
Conv.2	1.28000	-0.88877	1.08105	19.997	0.93885	0.73821	
Conv.3	1.27600	-0.49527	1.04518	17.998	0.59553	0.29708	

Table F.8 Load Flow Solution of 14 Bus System with DC Mesh-Link

(a) AC Voltage Profile

Bus No	Methods							
	FRLF		SRLF		DSRLF		FDLF	
	e	f	e	f	e	f	e	f
1	1.06000	0.00000	1.06000	0.00000	1.06000	0.00000	1.06000	0.00000
2	1.04176	-0.08227	1.04175	-0.08229	1.04176	0.08226	1.04176	0.08223
3	0.99263	-0.18650	0.99261	-0.18662	0.99264	-0.18647	0.99265	-0.1864
5	0.95292	-0.18163	0.95273	-0.18163	0.95323	-0.18173	0.95310	-0.18133
6	1.04131	-0.24610	1.04131	-0.24614	1.04130	-0.24615	1.04148	-0.24541
7	0.99773	-0.17283	0.99734	-0.17251	0.99763	-0.17279	0.99778	-0.17260

8	1.07401	-0.18604	1.07404	-0.18584	1.07401	-0.18602	1.07405	-0.18579
9	0.97480	-0.21902	0.97443	-0.21879	0.97454	-0.21896	0.97476	-0.21874
10	1.01637	-0.12536	1.01644	-0.12544	1.01613	-0.12526	1.01676	-0.12401
11	1.02620	-0.18576	1.02623	-0.18582	1.02607	-0.18573	1.02651	-0.18474
12	1.01909	-0.25609	1.01906	-0.25611	1.01924	-0.25595	1.01928	-0.25546
13	1.01093	-0.25287	1.01087	-0.25286	1.01081	-0.25297	1.01110	-0.25228
14	0.96803	-0.24747	0.96780	-0.24734	0.96784	-0.24748	0.96817	-0.24707

(b) DC Results

Methods	Variables						
	Vd	Id	a	θ	c	d	ϕ
FRLF Conv.1	1.28756	0.47920	1.04245	12.498	0.55894	0.32618	
Conv.2	1.28888	0.76670	0.96593	10.548	0.94941	0.41318	
Conv.3	1.27950	-1.24590	1.14168	22.597	1.43792	0.87374	
Conv.4	1.19926	0.27200	0.92208	9.998	0.32404	0.17301	
Conv.5	1.19061	-0.27200	0.93013	19.998	0.32041	0.17965	
SRLF Conv.1	1.28756	0.47920	1.04928	12.498	0.55547	0.32570	
Conv.2	1.28888	0.76670	0.97074	10.548	0.94481	0.41076	
Conv.3	1.27950	-1.24590	1.14896	22.597	1.42964	0.87101	
Conv.4	1.19926	0.27200	0.92595	9.998	0.32267	0.17168	
Conv.5	1.19061	-0.27200	0.93425	19.997	0.31889	0.17859	
DSRLF Conv.1	1.28756	0.47920	1.04591	12.498	0.55740	0.32239	
Conv.2	1.28888	0.76670	0.97084	10.548	0.94460	0.41125	
Conv.3	1.27950	-1.24590	1.14694	22.597	1.43140	0.86816	

Conv.4	1.19926	0.27200	0.92853	9.998	0.32136	0.17411	
Conv.5	1.19061	-0.27200	0.93560	19.997	0.31854	0.17922	
FDLF Conv.1	1.28756	0.47920	1.0425	12.50	-	-	19.472
Conv.2	1.28888	0.76670	0.9659	10.55	-	-	19.001
Conv.3	1.27950	-1.24590	1.1415	22.59	-	-	27.110
Conv.4	1.19080	0.2720	0.9155	10.01	-	-	15.465
Conv.5	1.18215	-0.27200	0.9236	19.998	-	-	22.259

Table F.9 Load Flow Solution of 30 Bus System with DC Mesh-Link.

(a) AC Voltage Profile

Bus No	Methods							
	FRLF		SRLF		DSRLF		FDLF	
	e	f	e	f	e	f	e	f
1	1.05000	0.00000	1.05000	0.00000	1.05000	0.00000	1.05000	0.00000
2	1.03263	-.04907	1.03264	-.04906	1.03264	-.04906	1.03263	-.04908
3	1.02916	-.08399	1.02918	-.08397	1.02918	-.08397	1.02917	-.08400
4	1.02297	-.10009	1.02299	-.10008	1.02299	-.10008	1.02298	-.10011
5	0.99632	-.13777	0.99633	-.13769	0.99633	-.13769	0.00632	-.13779
6	1.01566	-.11459	1.01568	-.11457	1.01568	-.11457	1.01566	-.11461
7	0.99422	-.13765	0.99426	-.13761	0.99426	-.13761	0.99423	-.13768
8	1.01656	-.11461	1.01656	-.11458	1.01656	-.11458	1.01656	-.11463
9	1.03305	-.14683	1.03308	-.14681	1.03308	-.14681	1.03305	-.14688
10	1.02302	-.18000	1.02307	-.17998	1.02307	-.17998	1.02302	-.18006
11	1.08489	-.11810	1.08489	-.11807	1.08489	-.11807	1.08488	-.11814

12	1.03268	-.16782	1.03294	-.16782	1.03294	-.16782	1.03288	-.16782
13	1.07761	-.15271	1.07761	-.15261	1.07761	-.15261	1.07761	-.15216
14	1.01626	-.18174	1.01639	-.18175	1.01639	-.18175	1.01634	-.18170
15	1.01224	-.18312	1.01240	-.18317	1.01240	-.18317	1.01227	-.18312
16	1.02070	-.17681	1.02077	-.17679	1.02077	-.17679	1.02071	-.17683
17	1.01637	-.18187	1.01643	-.18185	1.01643	-.18185	1.01637	-.18192
18	0.98849	-.18335	0.98853	-.18332	0.98853	-.18332	0.98847	-.18358
19	.99009	-.18891	.99014	-.18889	.99014	-.18889	.99007	-.18860
20	0.99731	-.18771	0.99736	-.18769	0.99736	-.18769	0.99730	-.18786
21	1.00980	-.18628	1.00985	-.18626	1.00985	-.18626	1.00980	-.18634
22	1.01052	-.18630	1.01057	-.18628	1.01057	-.18628	1.01053	-.18636
23	1.00273	-.18944	1.00285	-.18948	1.00285	-.18948	1.00275	-.18946
24	0.99950	-.19321	0.99957	-.19321	0.99957	-.19321	0.99951	-.19325
25	1.00449	-.19265	1.00455	-.19264	1.00455	-.19264	1.00450	-.19269
26	0.98583	-.19649	0.98589	-.19647	0.98589	-.19647	0.98584	-.19653
27	1.01693	-.18919	1.01697	-.18917	1.01697	-.18917	1.01693	-.18923
28	1.01035	-.12139	1.01036	-.12137	1.01036	-.12137	1.01035	-.12141
29	0.99354	-.20651	0.99358	-.20649	0.99358	-.20649	0.99354	-.20655
30	0.97925	-.21898	0.97929	-.21895	0.97929	-.21895	0.97962	-.21902

(b) DC Results

Methods	Variables							
	Vd	Id	a	θ	c	d	ϕ .	
FRLF	Conv.1	1.29580	.44930	.96952	8.499	.57188	.20302	
	Conv.2	1.27950	-.55016	1.03124	19.997	.63085	.39252	
	Conv.3	1.28892	.10086	.97907	12.498	.12654	.05057	
	Conv.4	1.20426	.04700	.88352	9.998	.05909	.02323	
	Conv.5	1.19923	-.04700	.95513	21.997	.05330	.03448	
SRLF	Conv.1	1.29577	.44930	.97429	8.499	.56925	.20175	
	Conv.2	1.27950	-.55029	1.03673	19.997	.62791	.39017	
	Conv.3	1.28891	.10080	.98398	12.498	.12592	.05017	
	Conv.4	1.20422	.04700	.88603	9.998	.05895	.02285	
	Conv.5	1.19919	-.04700	.95939	21.999	.05302	.03431	
DSRLF	Conv.1	1.29577	.44835	.97429	8.499	.56905	.20174	
	Conv.2	1.27950	-.55029	1.03619	19.998	.62789	.39020	
	Conv.3	1.28891	.10080	.98398	12.498	.12591	.05016	
	Conv.4	1.20422	.04700	.88603	9.998	.05851	.02375	
	Conv.5	1.19919	-.04700	.96039	21.999	.05298	.03431	
FDLF	Conv.1	1.29580	.44930	.96952	8.499	-	-	16.798
	Conv.2	1.27950	-.55016	1.03124	19.997	-	-	24.012
	Conv.3	1.28892	.10086	.97906	12.498	-	-	13.778
	Conv.4	1.19664	.04700	.87793	9.998	-	-	11.147
	Conv.5	1.19161	-.04700	.94907	21.997	-	-	22.367

Table F.10 Load Flow Solution of 57 Bus System with DC Mesh-Link

(a) AC Voltage Profile at Selected Busbars

Sl No	Bus No	Methods							
		FRLF		SRLF		DSRLF		FDLF	
		e	f	e	f	e	f	e	f
1	1	1.0400	0.0000	1.04000	0.00000	1.04000	0.00000	1.04000	0.0000
2	10	0.95801	-0.22383	0.95800	-0.22383	0.95788	-0.22422	0.95786	-0.2242
3	20	0.92620	-0.20793	0.92616	-0.20790	0.92606	-0.20819	0.92604	-0.20817
4	30	0.90303	-0.28739	0.90295	-0.28736	0.90276	-0.28771	0.90277	-0.28773
5	40	0.92710	-0.22996	0.92702	-0.22992	0.92687	-0.23024	0.92684	-0.23020
6	50	0.98062	-0.25322	0.98058	-0.25321	0.98043	-0.25352	0.98040	-0.25354
7	57	0.91271	-0.28619	0.91267	-0.28616	0.91250	-0.28654	0.91247	-0.28652

(b) DC Results

Methods	Variables						
	Vd	Id	a	θ	c	d	ϕ
FRLF Conv.1	1.28970	1.38404	1.05925	8.499	1.71435	0.74475	
Conv.2	1.28000	-0.88874	1.07699	19.997	0.94033	0.74590	
Conv.3	1.27600	-0.49530	1.04005	17.998	0.59824	0.29921	
Conv.4	1.18247	0.30800	0.89536	9.998	0.37580	0.17828	
Conv.5	1.16325	-0.30800	0.94107	19.997	0.34360	0.23442	
SRLF Conv.1	1.28970	1.38404	1.06473	8.499	1.70587	0.74081	
Conv.2	1.28000	-0.88874	1.08426	19.997	0.94221	0.74280	
Conv.3	1.27600	-0.49530	1.04536	17.998	0.59519	0.29783	
Conv.4	1.18247	0.30800	0.89849	9.998	0.37450	0.17618	
Conv.5	1.16325	-0.30800	0.94542	19.997	0.34137	0.23400	

DSRLF Conv.1	1.28970	1.38404	1.06443	8.499	1.70531	0.74173
Conv.2	1.28000	-0.88874	1.08107	19.997	0.93982	0.75219
Conv.3	1.27600	-0.49530	1.04520	17.998	0.59522	0.29778
Conv.4	1.18247	0.30800	0.90147	9.998	0.37297	0.17938
Conv.5	1.16325	-0.30800	0.94667	19.997	0.34141	0.23399

Table F.11 Line Flow of 14 Bus System with DC Link

Line No	Bus No.		DSRLF	
	From	To	Pij (MW)	Qij(MVAR)
1	1	2	157.981	020.663
2	1	5	074.882	015.389
3	2	3	073.627	003.522
4	2	4	055.539	000.388
5	2	5	042.750	015.489
6	3	4	022.919	010.473
7	4	7	028.055	-24.052
8	4	9	016.034	-0 7.757
9	5	6	044.373	-29.690
10	6	11	007.512	004.693
11	6	12	007.737	002.641
12	6	13	017.915	007.805
13	7	8	000.001	-20.361
14	7	9	028.057	005.542
15	9	10	005.282	003.112

16	9	14	009.317	002.897
17	10	11	003.929	-02.717
18	12	13	001.787	000.852
19	13	14	005.752	002.459

Table F.12 Line Flow of 30 Bus System with DC Link

Line No	Bus No.		DSRLF	
	From	To	Pij(MW)	Qij(MVAR)
1	1	2	090.198	-1.316
2	1	3	047.732	-2.545
3	2	4	028.909	-7.745
4	3	4	044.398	-3.145
5	2	6	037.512	-7.025
6	4	6	038.839	02.067
7	5	7	-12.366	01.639
8	6	7	035.576	06.656
9	6	8	-00.778	00.901
10	6	9	014.681	-10.676
11	6	10	012.328	-3.390
12	9	11	-17.930	-22.515
13	9	10	032.611	03.147
14	4	12	026.159	-6.669
15	12	13	-16.911	-30.164
16	12	14	007.664	02.083

17	12	15	017.497	04.992
18	12	16	006.709	01.682
19	14	15	001.366	00.112
20	16	17	003.168	-0.204
21	15	18	005.653	00.930
22	18	19	002.420	-0.037
23	19	20	-07.084	-3.444
24	10	20	009.397	04.394
25	10	17	005.861	06.077
26	10	21	016.075	09.390
27	10	22	007.805	04.191
28	21	22	-01.586	-2.049
29	15	23	004.836	01.503
30	22	24	006.215	02.024
31	23	24	001.612	-0.146
32	24	25	000.922	-0.718
33	25	26	003.544	02.363
34	25	27	004.469	-3.090
35	27	28	017.774	05.394
36	27	29	006.187	01.663
37	27	30	007.088	01.655
38	29	30	003.703	00.604
39	8	28	004.222	-1.412
40	6	28	13.596	3.534

Table F.13 Line Flow of 57 Bus System with DC Link

Line No	Bus No.		DSRLF	
	From	To	P _{ij} (MW)	Q _{ij} (MVAR)
1	1	2	101.874	75.056
2	2	3	097.562	-4.585
3	3	4	060.430	-8.255
4	4	5	013.894	-4.471
5	4	6	014.297	-5.127
6	6	7	-17.706	-1.730
7	6	8	-42.338	-6.609
8	9	10	017.488	-9.320
9	9	11	013.408	01.708
10	9	12	002.841	-15.913
11	9	13	002.805	-2.179
12	13	14	-09.946	22.164
13	13	15	-48.460	04.757
14	1	15	148.458	33.716
15	1	16	078.920	-0.867
16	1	17	093.015	03.938
17	3	15	033.364	-18.251
18	4	18	031.811	-7.051
19	4	18	031.811	-7.051
20	5	6	000.758	-6.278
21	7	8	-77.640	-12.479
22	10	12	-17.355	-20.101

23	11	13	-09.463	-4.446
24	12	13	-00.531	60.161
25	12	16	-33.096	08.699
26	12	17	-48.164	09.048
27	14	15	-68.479	-9.655
28	18	19	004.609	01.376
29	19	20	001.202	00.618
30	20	21	-01.101	-5.325
31	21	22	-01.103	-0.402
32	22	23	009.732	03.105
33	23	24	003.434	00.986
34	24	25	013.850	03.347
35	24	25	013.850	03.347
36	24	26	-10.450	81.942
37	26	27	-10.455	-1.602
38	27	28	-19.955	-2.411
39	28	29	-24.766	-5.121
40	7	29	059.856	-39.67
41	25	30	007.550	04.623
42	30	31	003.841	02.658
43	31	32	-02.038	-0.358
44	32	33	003.584	02.029
45	32	34	-07.471	-0.673

46	34	35	-07.477	-3.791
47	35	36	-13.510	-6.556
48	36	37	-17.049	-10.559
49	37	38	-21.036	-13.584
50	37	39	003.837	02.879
51	36	40	003.445	04.022
52	22	38	-10.836	-3.509
53	11	41	009.204	-2.856
54	41	42	008.899	03.020
55	41	43	-11.617	-2.778
56	38	44	-24.252	05.309
57	15	45	037.251	-47.061
58	14	46	047.908	-130.843
59	46	47	047.953	25.354
60	47	48	16.933	12.449
61	48	49	000.078	-7.363
62	49	50	009.565	04.548
63	50	51	-11.445	-6.103
64	10	51	029.698	-98.168
65	13	49	032.497	-32.114
66	29	52	017.701	02.651
67	52	53	012.371	-0.143
68	53	54	-07.677	-4.384
69	54	55	-11.938	-5.975

70	11	43	013.616	-23.708
71	44	45	-36.424	03.363
72	40	56	003.424	00.380
73	41	56	005.617	-0.539
74	42	56	001.616	-1.292
75	39	57	003.832	01.383
76	56	57	002.883	-0.537
77	38	49	-04.697	-10.638
78	38	48	-17.353	-19.253
79	39	55	019.087	-43.822

Table F.14 Line Flow of 107 Bus System with DC Link

(line flows of selected lines only)

Line No	Bus No.		DSRLF	
	From	To	P _{ij} (MW)	Q _{ij} (MVAR)
1	28	29	-0.91341	-0.17311
2	30	31	-0.71552	-0.19545
3	10	71	03.24972	-0.27401
4	11	70	3.24970	-0.14698
5	80	81	-0.34185	00.13124
6	91	92	-0.59354	00.48870
7	106	107	-0.55852	00.73864
8	27	90	-0.60922	-0.13932
9	25	101	-0.36914	-0.07258

10	29	79	00.76897	00.06570
11	29	79	00.76897	00.05700
12	34	100	03.35951	-1.33564
13	34	65	03.53507	-0.02153
14	48	89	00.24038	00.01474
15	52	82	-0.10599	00.02351
16	54	107	00.63215	-0.03610
17	60	99	-0.90060	-0.56255
18	60	99	-0.90060	-0.56255
19	49	64	-0.83135	-0.09764
20	34	69	-5.71179	-1.24227
21	34	69	-5.71179	-1.24227
22	74	104	00.97527	-0.38572

Table F.15 Line Flow of 14 Bus System with DC Mesh

Line No	Bus No.		DSRLF	
	From	To	Pij(MW)	Qij(MVAR)
1	1	2	136.711	-15.566
2	1	5	097.660	026.319
3	2	3	052.942	005.959
4	3	4	-42.494	055.199
5	4	7	042.021	-37.298
6	4	9	023.781	-13.339

7	5	6	023.367	-41.422
8	6	11	-05.534	014.822
9	6	12	006.434	004.106
10	6	13	011.277	012.953
11	7	8	000.000	-33.675
12	7	9	042.020	000.663
13	9	10	018.740	-06.052
14	9	14	017.562	-03.093
15	10	11	009.424	-12.159
16	12	13	000.314	002.601
17	13	14	-02.1466	009.180

Table F.16 Line Flow of 30 Bus System with DC Mesh

Line No	Bus No.		DSRLF	
	From	To	P _{ij} (MW)	Q _{ij} (MVAR)
1	1	2	90.098	-1.287
2	1	3	47.642	-2.235
3	2	4	28.872	-7.359
4	3	4	44.311	-2.822
5	2	6	37.452	-6.450
6	4	6	38.720	02.909
7	5	7	00.754	00.285
8	6	7	35.401	11.127
9	6	8	-00.771	-01.469

10	6	9	014.688	-10.884
11	6	10	012.329	-03.464
12	9	11	-17.930	-22.764
13	9	10	032.619	003.185
14	4	12	026.163	-06.795
15	12	13	-16.910	-30.390
16	12	14	007.589	001.986
17	12	15	017.563	005.124
18	12	16	006.711	001.737
19	14	15	001.522	000.216
20	16	17	003.169	-00.150
21	15	18	005.642	000.942
22	18	19	002.409	-00.245
23	19	20	-07.095	-03.432
24	10	20	009.406	004.380
25	10	17	005.860	006.023
26	10	21	016.082	009.391
27	10	22	007.809	004.192
28	21	22	-01.529	-20.048
29	15	23	004.831	001.524
30	22	24	006.234	002.034
31	23	24	001.607	-00.125
32	24	25	-00.917	-00.701

33	25	26	003.546	002.365
34	25	27	-04.461	-03.071
35	27	28	-17.764	005.399
36	27	29	006.187	001.663
37	27	30	007.088	001.655
38	29	30	003.703	000.604
39	8	28	004.230	-01.035
40	6	28	013.578	003.142

Table F.17 Line Flow of 57 Bus System with DC Mesh

Line No	Bus No.		DSRLF	
	From	To	Pij(MW)	Qij(MVAR)
1	1	2	089.619	078.437
2	2	3	085.443	-01.376
3	3	4	019.893	004.689
4	4	5	-02.728	002.982
5	4	6	-10.509	001.698
6	6	7	-38.204	003.417
7	7	8	-119.511	-01.850
8	9	10	007.279	-06.765
9	9	11	-03.677	007.435
10	9	12	-06.073	-13.978
11	9	13	-13.490	003.565
12	13	14	-25.019	027.897

13	13	15	-64.351	010.806
14	1	15	150.712	034.809
15	1	16	086.119	-00.870
16	1	17	100.221	003.956
17	3	15	062.409	-24.161
18	4	18	033.084	-07.152
19	4	18	033.084	-07.152
20	5	6	-15.738	001.432
21	10	12	-24.265	-19.165
22	11	13	-24.709	001.040
23	12	13	-03.222	062.718
24	12	16	-39.700	011.398
25	12	17	-54.770	011.729
26	14	15	-81.630	-05.388
27	18	19	005.884	001.069
28	19	20	002.419	000.226
29	20	21	000.102	-05.683
30	21	22	000.102	-00.805
31	22	23	002.074	007.823
32	23	24	-04.232	005.718
33	24	25	014.769	003.244
34	24	25	014.769	003.244
35	24	26	-19.106	086.459

36	26	27	-19.091	003.021
37	27	28	-29.066	001.495
38	28	29	-34.208	-01.622
39	7	29	081.020	-46.347
40	25	30	008.469	004.357
41	30	31	004.743	002.369
42	31	32	-01.156	-00.681
43	32	33	003.807	001.898
44	32	34	-06.574	-01.003
45	34	35	-06.574	-03.985
46	35	36	-12.605	-06.717
47	36	37	-17.147	-10.439
48	37	38	-21.820	-13.236
49	37	39	004.549	002.621
50	36	40	004.448	003.750
51	22	38	-01.973	-08.628
52	11	41	008.424	-02.707
53	41	42	007.987	003.157
54	41	43	-10.587	-03.087
55	38	44	-24.960	005.132
56	15	45	37.989	-46.623
57	14	46	045.924	-129.315
58	46	47	045.913	026.522
59	47	48	015.635	013.557

60	48	49	003.157	-08.880
61	49	50	012.795	002.351
62	50	51	-08.331	-08.342
63	10	51	026.522	-95.846
64	13	49	028.950	-30.916
65	29	52	029.303	-02.774
66	52	53	023.191	-06.525
67	53	54	002.733	-11.118
68	54	55	-01.630	-12.867
69	11	43	012.589	-23.493
70	44	45	-37.144	003.168
71	40	56	004.437	000.126
72	41	56	004.724	-00.142
73	42	56	000.734	-01.104
74	39	57	004.542	001.135
75	56	57	002.166	-00.228
76	38	49	-01.074	-12.486
77	38	48	-12.211	-22.021
78	9	55	008.727	-37.015

Table F.18 Line Flow of 14 Bus System with DC Mesh-link

Line No	Bus No.		DSRLF	
	From	To	Pij(MW)	Qij(MVAR)
1	1	2	142.659	-11.086
2	1	5	093.263	031.097
3	2	3	058.971	009.962
4	3	4	-36.465	065.492
5	4	7	045.433	-34.359
6	4	9	025.489	-09.680
7	5	6	019.394	-40.859
8	6	11	-18.016	023.946
9	6	12	008.086	004.134
10	6	13	018.119	013.827
11	7	8	000.000	-44.424
12	7	9	045.432	013.465
13	9	14	009.041	-04.074
14	10	11	022.955	-18.963
15	12	13	002.098	002.349
16	13	14	002.190	009.768

Table F.19 Line Flow of 30 Bus System with DC Mesh-Link

Line No	Bus No.		DSRLF	
	From	To	Pij (MW)	Qij(MVAR)
1	1	2	90.137	004.523
2	1	3	47.660	002.429
3	2	4	29.090	-03.229
4	3	4	44.401	-01.771
5	2	6	37.648	-02.240
6	4	6	38.695	003.938
7	5	7	01.033	002.499
8	6	7	35.602	012.661
9	6	8	-00.644	-01.491
10	6	9	14.568	-10.110
11	6	10	12.257	-02.798
12	9	11	-17.930	-23.717
13	9	10	32.498	004.982
14	4	12	26.326	-06.521
15	12	13	-16.910	-31.122
16	12	14	07.683	002.074
17	12	15	17.538	005.452
18	12	16	06.816	002.323
19	14	15	01.455	000.326
20	16	17	03.271	000.428
21	18	19	02.400	-03.205
22	19	20	-7.110	-06.625

23	10	20	09.470	007.670
24	10	17	05.757	005.440
25	10	21	15.985	009.125
26	10	22	07.744	004.019
27	21	22	-1.624	-02.310
28	15	23	04.915	001.764
29	22	24	06.070	001.601
30	23	24	01.669	000.112
31	24	25	- 0.989	-00.916
32	25	26	03.544	002.366
33	25	27	-4.530	-03.288
34	27	28	-17.844	005.146
35	27	29	06.187	001.663
36	27	30	07.088	001.656
37	29	30	03.703	000.604
38	8	28	04.750	003.598
39	6	28	13.789	004.525

Table F.20 Line Flow of 57 Bus System with DC Mesh-Link

Line No	Bus No.		DSRLF	
	From	To	Pij (MW)	Qij(MVAR)
1	1	2	090.101	078.304
2	2	3	085.918	-01.497
3	3	4	020.432	005.033
4	4	5	-02.572	002.828
5	4	6	-10.266	001.505
6	6	7	-37.743	004.016
7	7	8	-119.325	-02.954
8	9	10	007.410	-05.899
9	9	11	-03.833	010.081
10	9	12	-06.285	-13.934
11	9	13	-13.753	005.713
12	13	14	025.067	031.698
13	13	15	-64.848	012.125
14	1	15	150.378	039.631
15	1	16	086.705	-00.857
16	1	17	100.807	003.971
17	3	15	062.359	-16.308
18	4	18	033.192	-06.461
19	4	18	033.192	-06.461
20	5	6	-15.603	001.257
21	10	12	-24.913	-20.180
22	11	13	-25.045	002.572

23	12	13	-002.988	068.470
24	12	16	-040.240	011.623
25	12	17	-55.300	011.950
26	14	15	-82.225	-06.353
27	18	19	005.994	001.689
28	19	20	002.514	000.821
29	20	21	000.190	-04.993
30	21	22	000.192	-00.213
31	22	23	001.803	006.471
32	23	24	-04.503	004.350
33	24	25	014.798	003.564
34	24	25	014.797	003.564
35	24	26	-19.310	082.742
36	26	27	-19.373	001.286
37	27	28	-29.372	-00.296
38	28	29	-34.533	-03.475
39	7	29	081.219	-44.536
40	25	30	008.497	004.468
41	30	31	004.762	002.467
42	31	32	-01.146	-00.593
43	32	33	003.813	001.928
44	32	34	-06.566	-00.989
45	34	35	-06.567	-03.915

46	35	36	-12.604	-06.694
47	36	37	-17.100	-09.820
48	37	38	-21.703	-12.163
49	37	39	004.481	002.208
50	36	40	004.399	003.143
51	22	38	-01.612	-06.683
52	11	41	008.482	-02.221
53	41	42	008.001	003.651
54	41	44	-23.580	017.028
56	15	45	036.414	-33.593
57	14	46	046.336	-123.01
58	46	47	046.425	030.957
59	47	48	016.057	017.790
60	48	49	002.895	-10.751
61	49	50	012.081	000.638
62	50	51	-09.041	-10.060
63	10	51	027.208	-93.591
64	13	49	028.933	026.719
65	29	52	029.225	-02.794
66	52	53	023.110	-06.579
67	53	54	002.642	-11.337
68	54	55	-01.732	-13.078
69	11	43	012.648	-22.749
70	40	56	004.388	-00.370

71	41	56	004.854	000.357
72	42	56	000.733	-00.630
73	39	57	004.47	000.760
74	56	57	002.238	000.167
75	38	49	-01.413	-15.401
76	38	48	-12.765	-27.931
77	9	55	008.804	-36.832
